The Influence of Fire Retardant Additives on the Properties of HIPS and PBT

By

SIMON ELLIOTT

A Doctoral Thesis Submitted in Partial Fulfilment of the Requirement for the award of Doctor of Philosophy of Loughborough University

October 2002

Supervised by J.F. Harper

Sponsored by Great Lakes Chemical Corporation and Loughborough University

Acknowledgments

Throughout the three years of my PhD there have been many people how have provided either emotional of practical help or in some cases both. I would like to take this opportunity to thank my family, friends and colleagues.

First of all I would like to think my family, in particular my parents and sister who have given me so much support and with out whom I would not have been able to finish, or possible even start.

I would also like to thank my academic supervisor John Harper, who has spent many hours correcting and improving my reports and work, which has helped improve my report writing skills, and the over all quality of my thesis.

There have been many other staff, in particular the technicians in IPTME who have been a great help in completing my thesis, and I would like to thank them all. I would like particular to mention Andy, who saved me much time with his ability to fix and require equipment in the pilot plant.

Lastly and by no means least, I would like to thank my friends from both from IPTME and at Loughborough that have made my day-to-day life so much fun.

Abstract

Halogen compounds and antimony based synergists are used at low loading levels in many polymers systems to impart high levels of flame retardancy. This study used a range of brominated flame retardants (BFR) and the most commonly used synergist for halogen based flame retardance, antimony trioxide (Sb_2O_3), to investigate the effects on mechanical and physical properties of flame retardants in HIPS and PBT. The polymers used were High Impact Polystyrene (HIPS) and Polybutylene Terephthalate (PBT). Initially each of the additives was used individually, before being combined to study the effect of the complete package. This was achieved by producing a series of compounds using a twin screw extruder, and then an injection moulder to produce impact, tensile and fracture toughness specimens. The compounds were also analysed using rheological testing and thermal analysis. Also the effects of Stereon impact modifier and Fyrebloc masterbatches were determined in HIPS.

The results showed that the impact performance of HIPS and PBT was reduced as the loading level of both the BFR and Sb_2O_3 increased. Impact performance was also affected by Sb_2O_3 particle size, with the smallest particles causing the greatest reduction in impact properties. The addition of FR additives significantly reduced the ability of both HIPS and PBT to plastically deform, whilst having little or no effect on elastic deformation. None of the FR additives used were melt blendable in either HIPS or PBT as claimed by the manufacturers. Using back scattered SEM analysis it was shown that twin screw extrusion provided adequate mixing to break down any agglomerates or aggrogates present. Dispersion of the FR additives was good.

The addition of FR additives to both HIPS and PBT caused a reduction in their tensile strain at break. As the loading level increased so did the reductions. For the PBT compounds a transitions from ductile to brittle failure occurred with loading level. This transition was not seen in the HIPS compounds. The results indicated that the use of Fyrebloc masterbatches aided dispersion when added directly at the injection moulding stage in HIPS compounds.

Fyrebloc masterbatches caused less reduction in impact performance than direct powder additions. Both the BFR and Sb_2O_3 caused greater reductions in properties including impact and tensile strain at break in PBT than HIPS. For impact properties, typically at loading levels of ≈30wt.% FR additive, reductions of 80% were seen for PBT and 65% for HIPS

TEM analysis of stained HIPS samples revealed that both the BFR and Sb_2O_3 additives, located in the PS main phases of HIPS compounds. The morphology of the Stereon changed, from small discreet particles to a continuous phase within the PS, as the loading level increased. There appeared to be no blending between the Stereon impact modifier and the primary rubber phase.

Contents Page

List of Tables

List of Graphs

List of Plates

1.0 Introduction

Approximately 5000 people die as a direct result of fire each year in the EU [1,2] and many more are burned and/or injured by its effect. The financial costs are also huge, as it is estimated that within the EU about 0.65% of the gross domestic product is lost to fire related causes.

Technologies, such as high-pressure water jets and social development such as dedicated fire services, have reduced the risk of large-scale fires that destroy or ruin whole towns and cities during peacetime. However, small scale accidental fires can still cause death injury and loss of life. The primary methods for reducing these risks is to make products that are used in high risk environments, such as building, cars and other enclosed areas, from materials that will not ignite and burn with such vigour. This can be achieved by a multitude of methods, but the most common is the use of flame retardants additives and coating, or the use of non-flammable materials such as metal or glass.

1.1 The Need for Flame Retardant Polymers

The majority of polymers will both ignite and burn with ease, which means they pose considerable risk to both life and property [2]. This combined with an increase in the amount of polymers being used, and increased use of them in applications such as building and cars interior, and electronic and electrical products means that there is an increased risk of fires caused or aided by polymers [3-6]. In many applications alternative material cannot be used or are impractical due to either cost or properties. For these products the use of flame retardant to reduce the flammability of polymers is the most common flame retardant method. The majority of flame retardants are chemical based materials that are added either during production or along with other additives during a separate compounding stage. There are many flame retardants that can be used in polymers, which have varying efficiency at any given loading level.

Use of flame retardant polymers improves fire safety [7-9]. Full and small scale testing shows that the use of flame retardant additives significantly decreases ease of ignition and increases time to ignition, and flame spread once ignited [10,1], for products containing flame retardant additives compared to non-flame retardant equivalents. There are environmental concerns over the use of many flame retardants [9,11], which is starting to lead to both the development of other chemical based flame retardants, and the long term possibility of non-chemical based flame retardants, such as expanded carbon, surface coatings and product design changes [7].

1.2 High Impact Polystyrene (HIPS)

HIPS was the first commercially developed and marketed rubber toughened polymer, with the first grades sold during the 1940's [13]. HIPS has a two phase structure, which primarily consists of a polystyrene matrix with between 5-15% [13,14] dispersed rubber. The amount of rubber used depends on the final properties required and the cost, the majority of rubber currently used is polybutadiene. The main reason for the addition of the rubber is to increase the impact properties of polystyrene, although others properties are affected.

HIPS finds application where its good impact properties, ease of moulding and low cost are required, commonly injection moulded housing for electronic and electrical appliances and other such containers. One of the largest markets for HIPS is backs of TV [7,10,14,15], which pose a significant fire risk, from both internal and external ignition sources. Current EU legislation does not require the use of flame retardant grades of material for TV backs, high levels of flame retardancy are required in both Japan and the USA [10,15].

Figure 1.1 shows how the number of TV set fires has fluxuated from 1985 to 1995. The decrease up to the early 1990's is due to increased use of flame retardants, and changes in TV design. The increase during the late 1990's is due to manufacturers using less flame retardants in their TV enclosures, due to legalisation changes, caused by concerns about the environmental impact of certain flame retardants. The most common method of flame retarding HIPS is the use of bromine compounds using antimony synergists, as these can be used at low loading levels and produce high levels of flame retardancy.
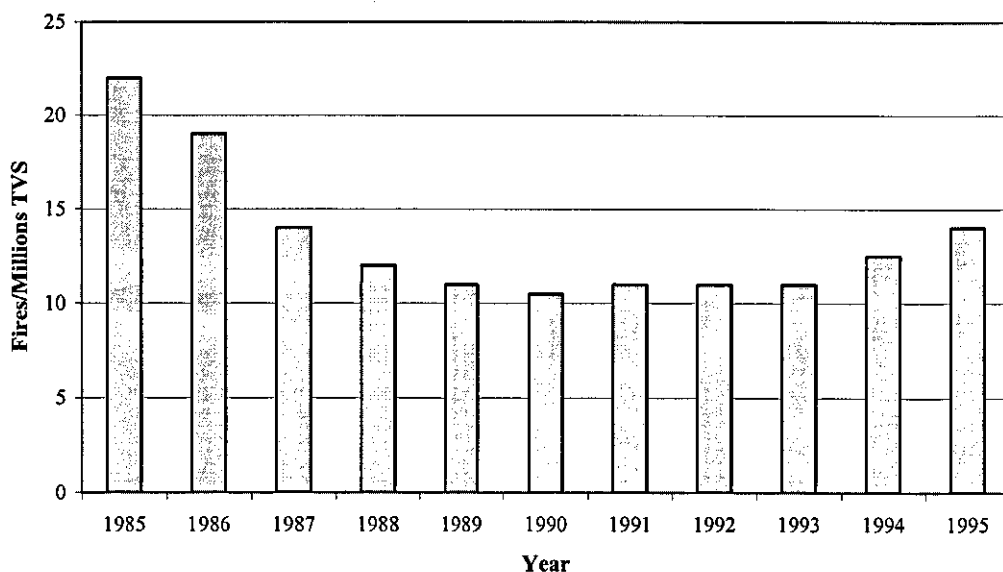
Figure 1.1, Number of TV Set Fires in the UK per Million TVs, [2]

1.3 Polybutylene Terephthalate (PBT)

Polybutylene Terephthalate (PBT) was developed as an alternative to PET for injection moulding [17,18]. There was extensive work to create new grades when the original patent for PET ran out in the early seventies. The biggest market for PBT is for short glass fibre reinforced grades and blends [19], but there is also a substantial market for non-reinforced halogen/antimony based flame retarded grades. These formulations are normally used for small electrical contacts and connectors, where the ability to obtain intricate mouldings, combined with good electrical and flammability properties, are desirable.

GE plastics are the single largest producer of PBT resin in the world, accounting for around 30% of total world production. There are numerous other manufactures such as Polyplastics and Dupont. As demand increases especially in Europe, it is expected that new production sites will be build. However due to the similarities with PET it will be possible to use PET production sites to manufacture PBT resin. Table 1.1 [18] indicates the number of products and capacities for all grades of PBT worldwide for 1994. From this table 1.1 it can be seen that the USA and the Far East have the biggest markets for PBT, whilst the Far East has the largest number of end uses.

Region	No. Of Producers	Capacities (ktons)
USA	3	125-130
Western Europe	9	75-100
Far East	13	125

Table 1.1, Number of Producers and Approximate Capacities for PBT

Table 1.2 summarises [18] the amount of PBT used for particular applications in the three biggest markets. From this table the biggest markets in Western Europe and Japan are the electrical and electronic sectors, whilst the biggest market in the USA is the automotive industry. The vast majority of PBT used, about 70-75%, is reinforced or filled, with about 7% being for monofilament/film applications. The majority of the rest is unfilled resin used for injection moulding applications where its properties make it desirable.

Application	Region (all units in percentage)			
	USA	Europe	Japan	World
Transportation	36	32	39	36
Electrical/electronic	27	43	46	37
Appliances	26	12	15	5
Machinery and other	31	13		22

Table 1.2, Consumption of PBT and PET Resins for Engineering Purposes by Major Region and End Use.

1.4 Bromine Compounds

Bromine compounds are the most commonly used halogen for flame retarding polymers [2,7]. Bromine Flame Retardants (BFR) have a large number of uses, although 50% of their applications are in electronics and electrical equipment such as TV and computer outer housing and printed circuit boards where their use helps to prevent or reduce risk from short circuits or over heating [7].

There are approximately 75 BFRs, which make up a family of compounds whose only common point is their source element, bromine. Bromine is a natural element widely found in nature, primarily in seawater, salt lakes and the earth. Concerns have been raised over the effect of some BFRs on human health and the environment, although the mainstream view indicates that only a small number of the currently available compounds are a significant risk to human health and the environment.

Greatlakes Chemical Corporation is a company that produces Bromine compounds for use as BFR, and other specialist additives. They acquired Anzon in 1997, which had formally been part of Cooksons. Greatlakes now produces around 50 bromine and 10 antimony based compounds.

1.5 Antimony Trioxide (Sb_2O_3)

Antimony trioxide (Sb_2O_3) is found in the earths crust naturally, but this is not used in polymers due to low purity and quality of the material [20]. The majority of Sb_2O_3 used is man-made from either raw antimony metal or natural occurring Sb_2O_3. There are other antimony based compounds that are used such as antimony pentoxide and sodium antimonate although Sb_2O_3 is the most wildly used because it has a high antimony content and low manufacturing costs compared to other types available.

Antimony trioxide is not considered to be a flame retardant in its own right and a suitable halogen must be present for a flame retardant effect to be obtained, this will normally be a BRF, although chlorinated waxes or other halogens are sometimes used. It is used because high levels of flame retardancy and low loading levels can be achieved compared to BFR alone. Antimony trioxide is considered to be carcinogenic material, this only applies to it when in powder form and once compounded into a polymer the risks become negligiable. There is currently a EU risk assessment of Sb_2O_3 with the results due for publication in 2003 [7].

1.6 The Burning Process

Although every fire is a unique process, the majority of fires can be broken down into several stages, these are initiation, development, and extinction. These are shown diagrammatically against time in Figure 1.1. During the ignition stage a suitable source such as cigarette, or electrical short circuit, ignites combustible matter. The material burns generating heat, which creates a loop increasing both the heat and the amount of flammable gas being produced. The ignition of these gases causes a fast or even explosive spread of the fire over a wide area, this phonenonmon is called flashover. At this stage the fire is considered to be fully developed, and will spread to any other flammable material in close proximity to it, continuing to spread if left to do so. The temperatures can reach 1000°C or higher, and during this stage is considered to have peaked. Once all possible material has been consumed by the fire, it will start to decline and will eventually each a point where there is insufficient fuel for it to continue, this is the final stage.

There are three separate elements required for a fire, these are fuel, heat and air. Figure 1.3 shows how these different elements are linked. Material such as polymers and wood will both ignite and burn with ease unless modified in some way. To stop flammable materials from burning the removal of one or more of these elements is required. The majority of flame retardants work using this method. Polymers like others material burn as described in this section.
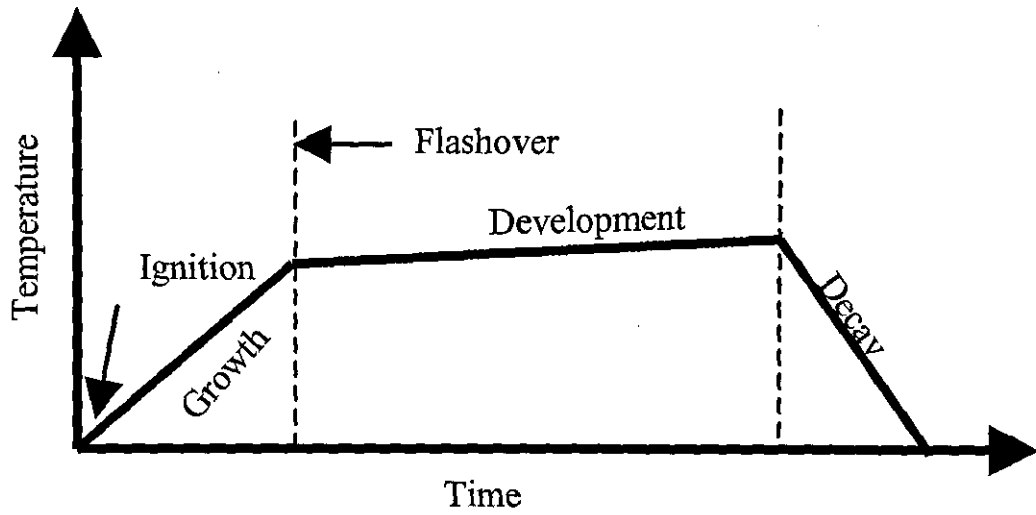
Figure 1.2, Common Stages of a Fire [21]
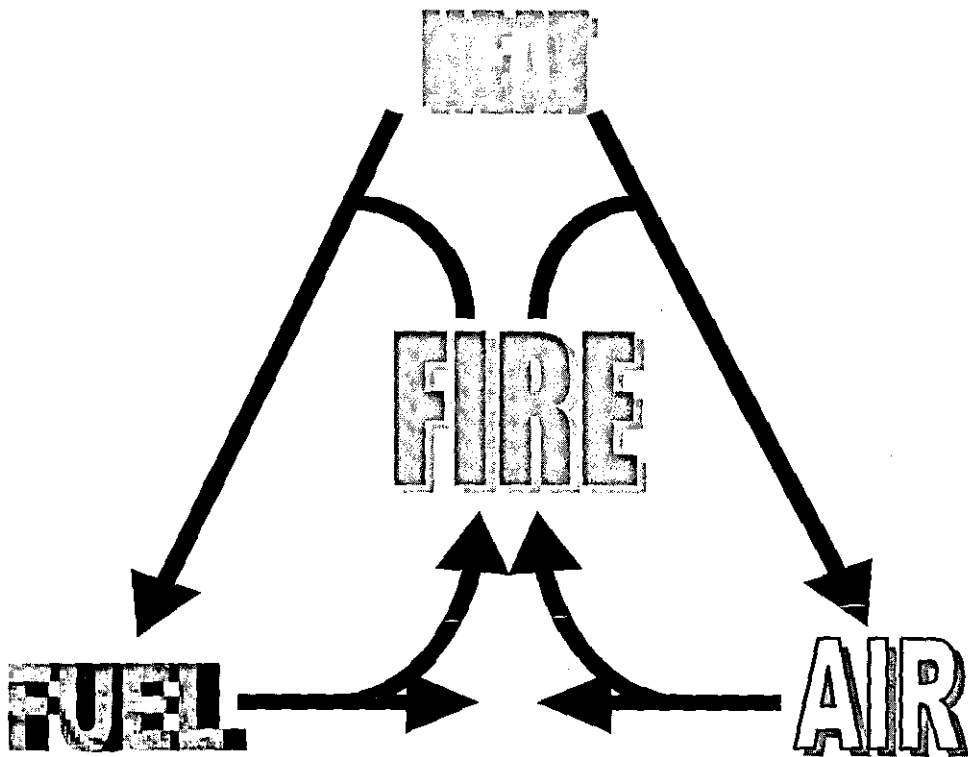
Figure 1.3, Relationship between Heat, Fuel and Air in a Fire.

1.7 Aims and Objectives

The primary aim of this study was to investigate the effects on mechanical and physical properties of the most commonly used flame retardants in HIPS and PBT. For both polymers mechanical properties are of great importance and flame retardant additives can affect these. The most commonly used flame retardants for both polymers are bromine based (BFR) using antimony synergists to increase the flame retardant affect and reduce the total filler loading level required. This work looked at each of the additives used individually, before combining them to study the effect of the complete package.

To achieve this aim a series of objectives were set. These were: -

- To develop an understanding of the influence of the material variables on the processing and characterisation equipment to be used for the work. This was done to gain an understanding of the equipment to be used and to allow a standard series of setting and parameters to be used where possible throughout the remaining work.

- To produce a series of compounds in both HIPS and PBT, using twin screw extrusion, containing initially only BFRs and Sb_2O_3, and finally fully FR formulations containing both. This was to allow the effect of the FR and other additives to be determined both individually and then together in both HIPS and PBT.

- To characterise the extruded compounds using capillary rheometry to determine the effect of the fillers on the melt properties of the compounds and thus to identify the affects of the additives on the processing of the polymers.

- Where relevant to determine the effect of the FR additives on the molecule weight and molecule weight distribution of the polymers used.

- To determine the mechanical properties of the compounds using injection moulded specimens. In particular to determine the impact properties, fracture toughness (K_C), and tensile properties such as Young's modulus, maximum stress and strain at break for both HIPS and PBT compounds.

- To determine the flame retardancy of the unfilled polymers and those compounds containing relevant BFR and Sb_2O_3 combinations. This was to

evaluate the influence of flame retardant loading level and the effect of any additives present, such as impact modifiers and carrier waxes.

- To examine fracture surfaces to determine the effect of the additives on the fracture type and mechanism, and also the dispersion and any agglomeration of the additives.

- To compare the different effects that the various additives had on the mechanical and physical properties of the two polymers.

2.0 Literature Review

2.1 High Impact Polystyrene (HIPS)

2.1.1 Production

The most common method of large scale HIPS production is by grafting a suitable rubber to styrene. This is achieved by dissolving a suitable rubber most often polybutadiene into styrene monomer, then, depending on the final rubber content required in the polymer, 5 to 15% rubber is used. This creates a solution with a small volume of PS in styrene, in a continuous phase of polybutadiene in styrene. Polymerisation of the styrene is then initiated by increasing the temperature of the solution. The whole process is conducted in a nitrogen atmosphere, and constantly stirred. At between 8 to 14% polymerisation, a phase inversion starts, the volume of the polystyrene increases to a point where a solution of PS in styrene becomes the main phase and the polybutadiene in styrene becomes the dispersed phase.

One characteristic of the phase inversion process is the formation of multiple emulsions. These are formed as the new dispersed phase (polybutadiene in styrene) still contains remnants of the original dispersed phase (PS in styrene). This causes the formation of rubber structure discussed in the next section. After the phase inversion the remaining styrene is polymerised, this is normally by a mass polymerisation method, although suspension polymerisation is sometimes used, the lack of stirring can cause an undesirable structure of the rubber phase that affects final properties.

It is also possible to produce HIPS by mechanical blending a suitable rubber with PS. The blending can be carried out using a range of different equipment such as batch or continuous kneaders, heated two roll mills or twin screw extruders. The processing is normally carried out at a temperature of 200°C, high shear is needed to disperse the rubber in the PS matrix. This process will give rubber morphology of irregular shapes particles with a size range of 2-5µm. This process is rarely used commercially to produce HIPS, but is often used to modifier the final properties of the HIPS.

Styrene homoplymer are used to produce grades with intermediate impact properties [22], or polystyrene-block-polybutadiene-block-polystyrene often called SBS triblock copolymers to increase impact properties, or to maintain properties when additives such as flame retardants are incorporated [23].

2.1.2 Structure

To obtain significant impact improvements over PS, the rubber present must form a separate phase [13,24], if it is completely compatible in the PS the effect of the rubber will be similar to that of a plastiser and the correct range of properties will not be attained [24,25]. If the rubber phase is entirely incompatible impact improvements will not occur. Bonding is required between the rubber and PS matrix, as otherwise on application of an impact load the rubber phase will act in a similar manor to small rigid particles, being ripped out of the matrix forming large voids, inferring no improvements of properties over unmodified PS. To obtain a tough polymer a strong bound between the rubber and plastic is undesirable, other considerations e.g. inter-particle spacing being constant [26]. For rubber toughened polymers van der Waal forces will create enough adhesion between the rubber and matrix, to increases the toughness of the PS. Wu [26] investigated the effect of particle size and rubber particle matrix adhesion on impact properties of rubber toughened Nylon 66. The work showed that for toughening to accrue, the rubber phase should not detach from the matrix, and that the amount of adhesion should be in the region of the tear strength of the rubber.

A rubber must be chosen that is partially compatible with the PS matrix to obtain the best overall range of properties. The morphology of the rubber phase is critical in determining the properties of the final HIPS polymer [13, 26-28]. In the case of HIPS, relatively larger rubber particles (1 to 5 μm) are desirable as these give the optimal range of properties at a given rubber content. Wu [26] found that there was a transition from brittle to ductile at a critical rubber particle size, at constant adhesion. When the rubber volume was increased the critical particle size also increased.

It is common for commercial grades of HIPS to have rubber phases with PS inclusion in them [22]. This is primarily sought as it allows a lower weight of rubber to create a larger surface volume. This does not have the same effect as solid rubber phases but will reduce the overall amount of rubber needed. Athene [25] conducted work using HIPS with solid rubber particles and with PS inclusions, the solid particles gave lower toughness, which was attributed to the solid rubber particles promoting void formation as well as crazing, which lowered toughness.

HIPS is a two-phase polymer and as such has a more complex microstructure than other mono phase polymers. Fig 2.1 illustrates the main aspects of the HIPS structure. There are many methods for examining the microstructure of HIPS but one of the most useful is staining with Osmium Tetroxide [29]. This turns the rubber phase black, whilst the styrene main phase appears grey. Any fillers present will be seen as dark black areas. By taking thin sectioned samples it is possible to use TEM, this allows fine details to be seen in the samples, such as fillers present and the morphology of the rubber phase.

Fillers such as Sb_2O_3 Polybutadiene

Polystyrene matrix
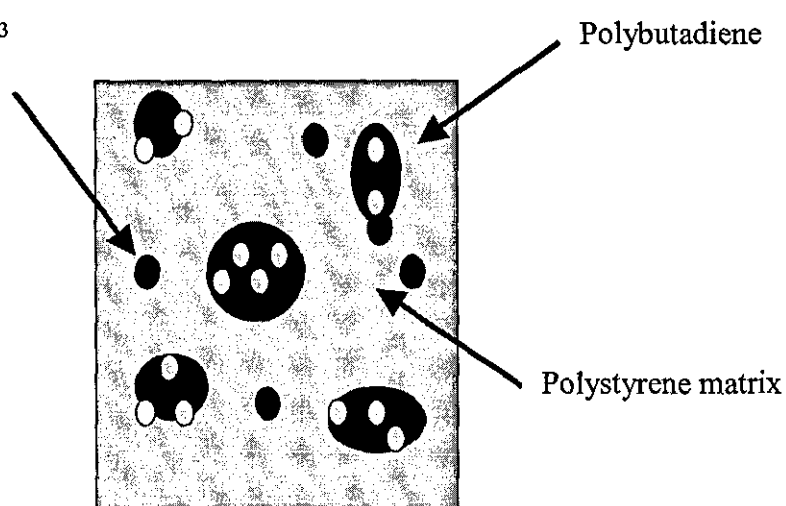
Fig. 2.1, Diagram of HIPS structure, when stained with Osmium Tetroxide

2.1.3 Properties

The main reason for the addition of rubber to PS is to increase the impact properties, although many other properties are affected, both positively and negatively [13,24]. Several properties such as electrical and chemical resistance, thermal properties, resistance to humidity, good processability and low shrinkage in moulds are not changed from unmodified PS [13,22], this is because these properties are governed by the PS matrix and not any rubber present. For flammability properties such as ease of ignition and burn rate there will be no difference between PS and HIPS (these are very low for non-flamed retardant grades), although smoke production will increase as the amount of rubber is increased in the PS.

Table 2.1 lists the major mechanical properties of both PS and HIPS. From this table it is possible to identify the effects of the rubber phase on the properties of (PS).

Property	PS	HIPS
Tensile modulus (GN/m^2)	3.5	1.6
Tensile strength at yield (MN/m^2)	Does not	17.5
Tensile elongation at yield (%)	Yield	2
Tensile strength at break (MN/m^2)	54	21
Tensile elongation at break (%)	2.1	40
Notched Izod impact strength (J/cm)	1.0	4.5

Table 2.1, Mechanical properties of PS and HIPS

The addition of a rubber phase also increases the toughness of PS at low strain rates, such as those used in tensile or flexural testing. Fig. 2.2 shows typical stress strain curves for PS and HIPS. From Fig. 2.2 it can be seen that both PS and HIPS under go an elastic region where the relationship between stress and strain are linear. PS fails at this stage, although maximum stress and stiffness values are slightly higher than for HIPS. HIPS undergoes an upper yield and then lower yield point, after which the stress slowly increases with strain up to final failure. During the upper yield region of the curve HIPS starts to stress whiten and craze formation occurs.

By calculating the area under the stress/strain curves, energy to failure can be obtained. The values for HIPS are significantly higher than for PS, indicating a high toughness. The decrease in stiffness can have consequences for products made from HIPS and can lead to the use of products with thicker walled sections.

Some disadvantages of HIPS compared to PS have already been discussed in the previous section, but there are several more that may need to be considered, these include a low resistance to environmental stress cracking in the present of surface active substances, and a deterioration of their ageing resistance [13,22,24].
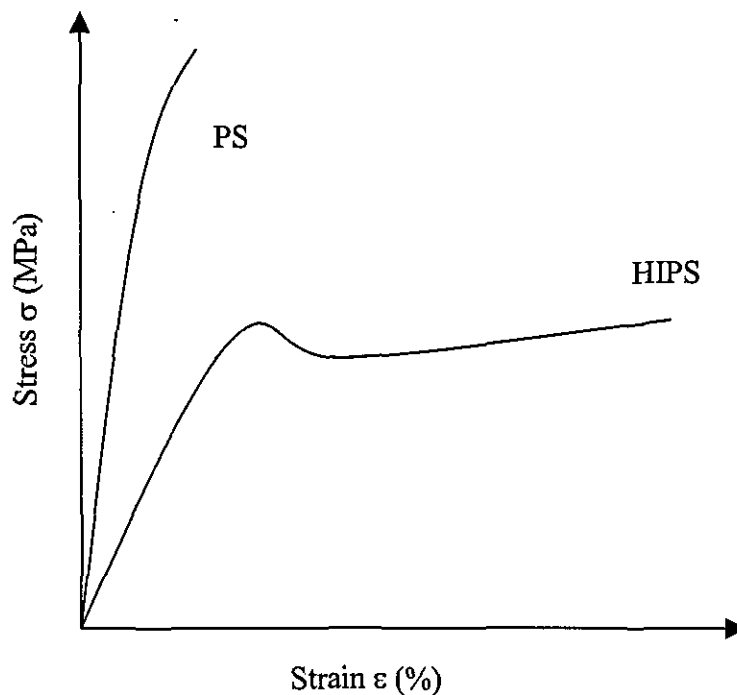
Fig. 2.2, Stress Strain Curves for PS and HIPS

2.1.4 Crazes

The method by which a small amount of rubber can change the properties of the polymer from a brittle glassy material to one that has considerably impact properties, is due to the separate rubber phase allowing the formation of a large number of microscopic crazes in the surrounding PS matrix [24,29,30,31,41]. Crazes are not cracks, but are small regions, where the material inside undergoes plastic deformation forming fibrils, between which voids are formed [32]. Fibrils are only a few molecules thick and in the case of HIPS consist of PS. They are highly oriented in the direction of the applied stress and span the craze stopping it from opening any further. Also as they are highly oriented they can withstand a large load before failure.

Crazes will initiate at the site of maximum stress, which will primarily be at the interface, at equatorial regions on the rubber particles in respect to the applied stress [13,32,33]. When the stress is applied a substantial amount of the energy involved is consumed in the initiation and growth of many small crazes. This energy can therefore not be used to initiate and grow true cracks that will lead to catastrophic fracture of the sample at lower applied energies. After formation of the crazes the rubber particles present will share the applied load with the matrix, this deforms the rubber particles from spherical to elliptical shape, it is these elliptical shaped particles that are normally viewed under microscopic analysis.

As well as craze initiation, craze termination is just as important. If the crazes formed in the very early stages of failure are allowed to develop into cracks then a more brittle failure similar to that of unmodified PS will be seen [22,24]. Craze growth will terminate when the stress at the tip decreases to below a critical value necessary for continued growth or when it encounters an obstacle such as a rubber particle of significant size. This means that the inter-particle distance of the rubber particles is also important for craze termination and toughness enhancement. If the distance is too large the crazes will be less likely to terminate, which will lead to them developing into cracks.

The inter-particle distance, required for toughening, is a material property of the matrix and independent of rubber volume fraction and particle size [26,34]. It is also a critical factor affecting impact properties of rubber reinforced polymers [33]. There are several reasons for this, firstly particles need to be close enough for craze termination, to stop them developing into normal cracks. Matsuo [33] conducted work using PS with two rubber balls, with varying distance between them. The results showed that by increasing the distance between the rubber balls the lower was the stress required to start craze formation, up to an applied stress of 2000 psi, after which the results levelled of. Also the results showed that the closer together the rubber particles were, the increased likelihood of stable craze development and termination. These two factors mean that a compromise must be made for the inter-particle distance of rubber particles in PS for optimum properties.

The crazes present in the transformed region have a different refractive index to the surrounding material, which allows the crazes to be visible to the naked eye, this effect is normally referred to as stress whitening [35]. Unlike many other rubber toughened polymers such as ABS there is little evidence that shear band formation takes place, it is because craze formation dominates failure.

2.1.5 Processing and Applications

There are many methods that can be used for processing and shaping both PS and HIPS. The main method for compounding additive into HIPS is twin screw extrusion, Single screw extruders are also used, primarily for production of sheet from 0.3 to 2mm thick. For extrusion, temperatures in the range of 160 to 230°C are normally used with an increasing temperature gradient along the barrel. The majority of shaping and moulding is conducted by injection moulding. Around 65% [24] is used for injection moulding, using similar temperatures to that for extrusion, 170 to 240°C, with mould temperatures from 40 to 65°C. It is not uncommon to use a chilled mould at 10°C. Other methods such as blow moulding and thermoforming are also used for moulding and shaping HIPS.

HIPS finds application in many ways, but the biggest use is in plastic housing and packing such as those used for electronic products like TVs and packaging such as cups and bottles for yoghurt and butter [24]. There are also markets in refrigerator and freezer components, in the construction industry for decorative tiles, consumer goods such as hangers and camping equipment. It is generally used in these applications due to its good impact performance and the ability to form large and/or complex injection moulded parts, as well as cost performance against other polymers such as ABS

Almost the entire use for flame retardant HIPS is the backs of TV's housing and the relatively new market of housings for other computer components. The level of flame retardancy required for the backs of TV and other similar components varies depending on the part of the world. Current EU legislation does not require the need for flame retardant additives, but the US and Japanese markets require that products obtain the UL94 part three V0 classification. The most common method of flame retardancy for HIPS is the use of BFR and antimony based systergists [36-37]

2.2 Polybutylene Terephthalate (PBT)

2.2.1 Production

PBT is polymerised in a two-stage process, Transesterification followed by Polycondensation [17,18]. The first stage produces bishydroxybutyl terephthalate (bis-HBT) by transesterification of methyl terephthalate (DMT) with 1,4-butanediol. During this process the temperature is increased from 150°C to 210°C, at a pressure slightly lower than atmospheric. The methanol formed is then distilled off whilst the 1,4-butanediol is refluxed. The most common catalysts for this stage are organotitanium or organotin compounds such as tetrabutyl titanate. The component parts and the reaction are shown in Fig. 2.3.
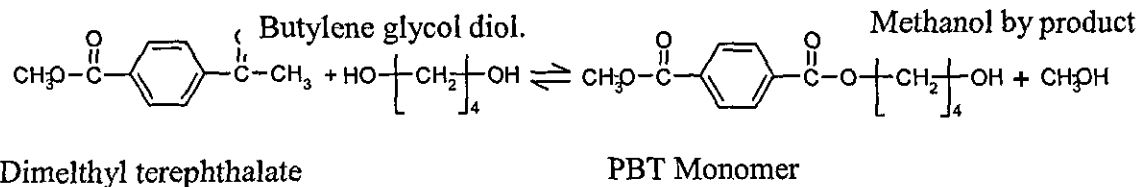
Fig. 2.3, Component Parts and Reaction to Form PBT Monomer.

The second stage is carried out at temperatures of 250 to 260°C and under full vacuum. This change in conditions allows the pre-polymer, formed in the first reactions, to further polymerise. Similar catalysts are used for this stage as for the previous stage.

This process can be used to produce PBT in both batch and continuous processes. The method used depends on whether a range of different grades need to be made, in which case the batch method will be used, or whether a single grade needs to be made, in which case the continuous process is used.

2.2.2 Properties

Properties of PBT are often controlled by the morphology of the material [17]. PBT is classified as a semi-crystalline material with a T_g of around 40°C and T_m of about 240°C. PBT is normally around 35% crystalline but the addition of nucleating agents, such as talc, can increases this to between 40 and 45%, and levels of up to 60% are obtainable.

PBT has excellent strength, rigidity, toughness, dimensional stability, and chemical resistance [17,22]. One of its major disadvantages is its ease of ignition. This problem is further amplified by the fact that one of the major uses for PBT is small electrical connector, which need to pass flammability tests such as UL94.

The main reason for the choice of PBT is that it has a very high crystallization rate, which, when combined with a high mould temperature, means there is little or no need for nucleating agents. Also PBT has good electrical insulating properties and gives a good surface finish after moulding.

Mechanical properties of PBT are largely controlled by the presence of glass fibre reinforcement, but the presence of fillers or additives such as flame retardants, can also have a significant effect on properties, even of glass fibre reinforced grades [18,22]. The inclusion of glass fibres increases stiffness, strength and impact resistance but decreases elongations to break. Most mineral fillers such as bromine/antimony mixes make the compound more brittle, but they can be considered as stiffening rather than re-forcing agents.

PBT has a LOI value of 23 and fails UL94 vertical burn tests if no additives are present. Flame retardant additives are often added to PBT for application in the electronic and electrical sector [17]. The most common type of flame retardants used are halogen-based systems using an antimony synergist. These fillers have several advantages over others for use in PBT. They can be used at low loading levels (typical 16wt%), and give high levels of flame retardancy (UL94 vertical burn 1.6mm samples V0). To prevent blooming, and degradation of the bromine compounds, two methods are used [38]. The addition of an anti-oxidant at low loading (0.1wt.%), such as Greatlakes PP18, or the use of additives that are stable at the high processing temperatures.

2.2.3 Processing and Applications

Compounds based on PBT are normally compounded using a twin-screw extruder. This method can be used for fillers and additives such as antioxidants and flame-retardants and glass fibre reinforcement. Before any form of compounding or other process at elevated temperature takes place, the PBT granules must be dried to avoid hydrolysis of the ester bonds, which can cause huge drops in molecular weight if not controlled. Drying conditions for a typical GE grade involve 2-4 hours at 110-120°C [39].

Injection moulding is often used for shaping PBT due to the nature of the final parts and relative ease of injection moulding PBT. Optimum melt temperatures vary between 240°C for unfilled material, to 270°C for highly glass filled material. End products with good properties can be obtained by controlling the mould temperature, in a range from 30 to 120°C, which will affect the final morphology. This will also reduce the affect of mould shrinkage. Single screw extruders are often used to produce either PBT sheet or more commonly pipe. Similar processing condition and precautions are used for single screw extrusion as have already been detailed for twin screw extrusion.

PBT can be broken down into four main classes, each of these uses PBT with different fillers, or other reinforcement. The main classes are [17,18,22], unfilled PBT, glass fibre reinforced, impact modified and flame retardant grades. Unfilled PBT is often used for injection moulding and extrusion. It finds uses in applications such as gears and household appliances where good dimensional stability and chemical resistance are needed. Glass fibre reinforced grades are commonly used in the automotive industry where its heat resistance, combined with oil and petrol resistance, make it possible to use close to the engine of the car.

Impact-modified grades fall into two sub groups. The first is for use as automotive covers, due to its high impact strength, good dimensional stability and chemical resistance. The other is a glass fibre, rubber impact modified grade. These have improved elongation to break, which allows them to be used to make snap fit assembly easier. Applications include such items as lighting and electrical components. Flame retardant grades are a large market for PBT and most of it is used in the electronics and electrical industry. Components and contacts are made from PBT due to its good dimensional stability and electrical resistance. A large portion of the flame retardant market is based on glass fibre filled PBT, as the addition of the FR above reduces many mechanical properties of PBT.

2.3 Halogens and Antimony Synergists

2.3.1 Bromine Compounds

Initial work on flame retardants concentrated on chlorinated compounds for use in thermoplastic materials. More recently bromine compounds have been developed and are still under development.

Bromine compounds are the most common commercial halogens used for flame retardants in polymers as they have the best range of properties for producing a flame retardant effect (see section 2.7). The largest single market for brominated flame retardants (BFR) is electrical equipment (more than 50% of their application). These included outer housing and internal applications such as printed circuit boards, 96% of which use some form of flame retardant. BFR are also used in cable compounds to prevent fires,

There are approximately 75 bromine compounds available for use as flame retardants in polymers. These compounds all have different properties, characteristics and performance. The choice of which to use in a polymer will normally be governed by end use application and the final properties required, not just flame retardancy, but effects on mechanical properties, processing, physicals and cost of the compound.

2.3.2 Antimony Trioxide

Antimony trioxide is the most commonly used antimony compound as it has the highest Sb content (83.53%) of any antimony oxide. Naturally occurring Sb_2O_3 is not used in polymers, as manufactured material has more consistence properties such as purity, colour and particle size [20]. Impurities present in the metal ores will however still be present in the final material. Table 2.2 below [20,40] lists the type and the level of impurities present in a common grade of Sb_2O_3.

Impurity	Amount present as a percentage of Sb_2O_3
Arsenic	0.15
Iron	0.003
Lead	0.05
Acidity (H_4SO_4)	0.01

Table 2.2, Impurities present in a standard polymer grade of Sb_2O_3.

There are several production methods for Sb_2O_3 the method that is used depends on the quality of the final product required and the starting material (pure metal or sulphide ore). Methods of Sb_2O_3 production include furnace and chemical precipitation. The most common method is the furnace route as it is the most cost efficient route.

2.3.3 Antimony Trioxide Properties

At temperatures up to 570 °C, Sb_2O_3 is found as the mineral Senarmontite, but at temperatures above 570 °C it changes form to exits as Valentinte, many grades of Sb_2O_3 contain significant amounts of Valentinte in them at room temperature due to the slow conversion rate from Valentinte to Senaromonite. Table 2.3 below [20,40] lists the main properties of the two crystal forms of Sb_2O_3.

Crystal form	Cubic	Rhombic
Name	Senaromonite	Valentinte
Specific gravity	5.2	5.67
Melting point °C	656	656
Refractive index	2.087	2.18, 2.35

Table 2.3, Properties of the Two Crystal Forms of Sb_2O_3

Sb_2O_3 is amphoteric and will therefore react with both acids and alkalines to form salts, this is used in several processes to form various antimony based materials. Sb_2O_3 has a quoted melting temperature of 656 °C and boils at 1555 °C. Other properties of Sb_2O_3 such as tint strength and pigmenting power will be governed by the particle size of the Sb_2O_3 and it is common for manufactures to produced Sb_2O_3 in a range of particle sizes from 0.5 to $13\mu m$ [42,45].

2.3.4 Environmental and Health Concerns

There are environmental and health concerns about both bromine and antimony compounds. Many environmental organisations such as Greenpeace and WWF are actively trying to stop the use of all chemical based flame retardants in polymers with a particular emphasis on BFR. Although other FR additives are available few are as effective as BFR using Sb_2O_3 synergists, at low loading levels, in providing high levels of flame retaradncy [43], which is a critical factor for many applications. This factor will mean the continued use of many BFR and Sb_2O_3 until a direct alternative can be found or legislation is changed to ban all BRR and/or Sb_2O_3, either directly or indirectly.

There are currently two BFR that have had action taken against then by the EU, these are pentabromodiphenyl ether (penta-BDE) and polybrominatedbiphenyls (PBB). Penta-BDE is being phased out of production by 2003, and both production and marketing of PBBS was stopped by industry, voluntarily in 2000. There are also other BFR that are being investigated, these are octa-BDE and deca-BDE, which could be restricted in electrical and electronic applications by 2007. The use of both deca-DPE and octa-BDE, which are the most common BFR used in electrical and electronics housing applications, will be reviewed in 2002 to allow for an EU risk assessment on these products. Preliminary conclusions indicate that there is no need for a reduction of theses BFR.

2.3.5 Recycling of BFR and Sb$_2$O$_3$ Containing Polymers

The ability to be able to cost effectively recycle polymers is of concern for manufacture of polymer products. Recycling of thermoplastics normally falls into two groups, either energy recovery, or mechanically ground and then used along with virgin polymer in a new product. Research work done using a variety of polymers and BFR has shown that high efficiency rates can be reached for energy recovery and that increases in harmful substances are reduced [7]. Studies have also shown that electrical housings containing recycled brominated flame retardant polymers give better recycling properties than other polymers systems. The majority of new photocopiers contain recycled flame retardant ABS, which helps meet the EU eco-label system.

Other less direct legislation will also affect the possible use of BFR. The draft EU directive on Waste Electrical & Electronic Equipment (WEEE) will place the responsibility of end use recycling on the product manufactures. BFR and Sb$_2$O$_3$ will not be banned or restricted but polymers containing BFR and Sb$_2$O$_3$ will need to be separated prior to recycling. It is believed that this will be conducted on a national scale as part of a larger collection and separation process [7]. Both energy and mechanical recovery methods of recycling are used for polymers containing BFR. Several authors have reported that polymers containing BFR maintain mechanical properties after several mechanical grinding and re-processing operations [7,45]. The eventual content and the implications of the WEEE directive are currently unclear and only time will tell what the effect will be on the use of BFR and Sb$_2$O$_3$.

2.3.6 Effect of Bromine Compounds on Polymer Properties

Depending on the grade being used BFR can either be melt blendable, or remain as a secondary particulate phase after processing. This fact alone means that the effect of BFR on the mechanical properties of polymers can vary hugely depending on the grade being used. Other factors such as molecule weight, chemical compatibility and particle size and morphology will affect the final mechanical properties of BFR filled polymers.

It is uncommon for BFR to be used without an antimony compound present to achieve a flame retardant effect. Therefore there has been little published work on the effect of BFR alone on mechanical properties of polymers.

Owen [46] investigated four commonly used BFR in ABS at loading level of 18 and 24 wt.%. The BFR used were octabromodiphenyl oxide (OBDPO), 1,2-bis(tribromophenoxy) Ethane (BTBPE), poly-dibromostyrene (PDBS80) and tetrabromabisphenol A (TBBA). All the materials were melt blendable with the ABS, although all the BFR affected mechanical properties. As the loading level increased, the impact strength decreased, and the flexural modulus increased for all the BFR. The effect of OBDPO and BTBPE were similar, reducing impact strength by approximately 20% at both loading levels, whilst marginally increasing flexural modulus. Both PDBS80 and TBBA significantly reduced the impact properties of ABS, by 60% and 80%, but greater increases in flexural modulus were seen. These effects were primarily attributed to the degree of compatibility and melt blendablity of the BFR and dilution of the rubber content of the ABS. The BFR which remained as separate phases gave significantly lower impact strength and acted to stiffen the ABS

Seddon [47] used several bromine compounds in ABS at approximately 20wt.%. The BFR used were TBBT, BTBPE, DBDPO and a grade of DBDPO, which had undergone particle size reduction. As with Owen impact strength was observed to decrease with the addition of all of the BFR whilst small increases in flexural modulus were observed. Unlike the other bromine compounds the DBDPO is non-melt blendable in ABS, which is the main reason it gave lower impact results compared to others. The effects on the flexural modulus were attributed to effects on molecular weight of the ABS, and the DBDPO particles being more rigid than the ABS matrix.

2.3.7 Effect of Sb$_2$O$_3$ On Polymer Properties

As Sb$_2$O$_3$ is only ever used at loading levels of up to 5wt.% to provide a flame retardant effect in polymers, the majority of work has concentred on these loading levels. It is common for manufactures to produce Sb$_2$O$_3$ in a range of particle sizes. At consistent loading levels the particle size of Sb$_2$O$_3$ can affect several polymers properties but particularly impact, where others such as tensile properties are often unaffected.

Owen [46] and Seddon [47] used Sb$_2$O$_3$ with varying particle size in ABS resin. The results showed that impact properties were sensitive to changes in particle size but that flexural strength and Young's modulus were not. Both sets of work indicated that Sb$_2$O$_3$ with the smallest particle size gave the highest impact energies when added to filled compounds. This was attributed to the smallest particle sized material creating smaller sites of stress concentration during failure, therefore causing smaller reductions in impact properties.

White [49], used Sb$_2$O$_3$ with a variety of particle sizes in UPVC, HIPS and ABS. For the ABS and HIPS compounds, all grades caused reductions in impact properties, with the smallest sized Sb$_2$O$_3$ having the smallest effect. For the PVC compounds the largest particle sized Sb$_2$O$_3$ had a reinforcing effect on the impact properties. This was attributed to the surface area characteristics of these grades allowing them to act as impact modifiers, in a similar way to CaCO$_3$.

2.3.8 Combined Effect of BFR and Sb$_2$O$_3$

Many authors have investigated the combined effect of BFR and Sb$_2$O$_3$ on polymers properties, including HIPS and PBT. Loading level used have been those needed to achieve a high level of flame retardancy (such as UL94 V0 rating), typically 10-20wt.% depending on the polymer. As with the previous section the main effect of these additives is on impact properties, with little change in others properties such as tensile strength .

Owen [46] and Seddon [47] used the same grades of BFR and Sb_2O_3 as discussed in previous sections at loading levels of 20wt.% BFR and 4wt.% Sb_2O_3 to achieve compounds with a high level of flame retardancy. The results indicated that, depending on the BFR and Sb_2O_3 combination, the failure was either the same as when the two were added separately, or dependant mainly on the BFR present, as this had a higher loading level. For those compounds containing OBDPO and BTBPE (which separately had recorded higher impact values) the impact properties were determined by both the BFR and Sb_2O_3, whilst for those containing TBBA and PDBS80 impact values were predominately determined by the BFR, with the Sb_2O_3 having less effect on both impact value and fracture mechanisms. All of the compounds containing both BFR and Sb_2O_3 gave significantly better flame retardancy results than unfilled ABS, most having a UL94 V0 rating.

Pettigrew [45], used a variety of ethylene bis(tetrabromophthalimide) (ETBT) based BFR, and two grades of TBBA and DBDPO, with Sb_2O_3 synergist, in 30wt.% glass filled PBT. Formulations were compounded using a Bulcher System 40 twin screw extruder and test specimens were injection moulded. The results showed that all of the compounds had lower tensile strength than the glass filled PBT, and that there was little differences between the grades of BFR. Even though the grade of PBT was glass filled, differences were seen in the impact testing results. As with tensile strength all grades gave lower results than glass filled PBT. The compounds containing ETBT gave the highest results with the others slightly lower. The differences seen were attributed to the differences in compatibility of the various BFR.

Smith [50] studied the effect of melt blendable impact modifiers on the impact performance of FR PBT using polypenta-bromobenzyl acrylate BFR and Sb_2O_3 synergist in PBT. The results showed that the addition of the FR reduced the impact performance of the PBT, which was caused by a change in the failure mechanism of the PBT matrix from ductile to brittle. The impact properties were increased linearly by the addition of the impact modifier, up to a loading level of 20wt%. This was caused by the impact modifier increasing the base impact performance of the PBT resin. A Teflon based anti drip-agent was required to maintain a UL94 V0 rating.

Although this caused a small drop in impact properties the flame retardancy of the impact modified formulations containing the anti dip-agent were the same as those with the BFR and Sb_2O_3.

2.4 Fillers and Additives

Fillers and additives have been used almost as long as polymers. Early fillers were developed and used for stabilisation of polymer during processing and to increase properties of moulded products during use. Without the development of suitable fillers and additives it is unlikely that polymers would be the successful materials they are today.

2.4.1 Definition of Fillers and Additives

The terms fillers and additives are often used interchangeably, although there are clear definitions in the literature for both. The term fillers generally refers to low cost materials that are primarily used to reduce the cost of the polymer compound by bulking it out as the filler material being used is cheaper than the base polymer [51]. These are normally mineral materials such as talc, chalk and clay. Fillers can affect properties such as stiffness, impact properties, melt viscosity and electrical resistance, and these effects can either be either advantages or disadvantages depending on the polymer, filler and the end use application [52]. There has been much work developing mutli-function fillers that will improve other properties or effect one or more properties. Similar work has looked at the addition of surface coating to the filler. The benefits of surface coating can be significant when compared to additives, as the total surface area is greater.

Additives refer to materials added to polymers to achieve one or more increases in properties, this may be increased impact resistance, tensile strength or flame retardancy. The addition of additives also affect other properties negatively so the choice of filler and its effect on all properties must be considered. Many additives are manufactured with a variety of particle sizes, shape and purity. These factors, along with compatibility with the polymer, and temperature stability, must be considered when choosing an additive. Types of additives are discussed further in section 2.4.2.

2.4.2 Types of Additives

Additives can be subdivided into several groups, depending on their primary use in the polymers. Additives that influence flame retardantcy and impact modifiers, are discussed in greater detail in later sections so will be left out here. The rest of this section will outline some the additives types that are commonly used in polymers today.

Processing aids, are required for some polymers to increase the ease and compatibility of the polymer to be processed and shaped, they are sometimes called lubricants. The majority of thermoplastics are heated before being moulded in some way, such as injection moulding, blow moulding or extrusion. The ease with which a polymer can be processed depends on its physical and chemical properties, such as melt viscosity and resistance to heat, water and oxidation, during processing. The majority of processing aids are liquid at the processing temperature and are normally considered to act as lubricants. There are many methods by which processing aids affect polymers during processing and moulding, they can act internally forming films around individual particles allowing better mixing, or allowing the particles to adhere during melting with greater ease, reducing melt viscosity [48]. For certain polymers such as PVC, external lubricants are used, they work by forming a film between the polymer melt and mould surface allowing better flow of the melt into the mould [48].

Antioxidants and heat stabilizers are often required in polymers to reduce or prevent degradation of polymers during compounding or shaping [53,54]. Most polymers are processed at a temperature over 180°C and up to 300°C. Also there are applications where polymers will be at elevated temperatures for long periods of time where heat stabilisers may need to be used. Attack by oxygen is the main source of degradation of polymer products. This can occur both during processing where elevated temperatures accelerate the effect, but also during the lifetime of the product. Other factor such as sunlight, heat, ozone, water and mechanical stress can increase the degradation. Antioxidants are therefore used to reduce these effects, both during processing, and throughout the lifetime of the polymer product.

Pigments are used to modify or change the colour of plastic parts and are mainly of design and commercial importance [54,55]. Generally only small amounts of pigments are required to achieve a significant colour change. There are many reasons why pigments may need to be used in polymers, such as colour matching with other parts used in the product, such as car interiors, fashion or marketing reasons. Products being used for storage of medical or foodstuff, may requires special pigmenting to reduce the effect of UV radiation [55]. Controls on machinery or equipment are often different colours to allow easy identification. Many fillers or additives used for other reasons, can also have pigmenting effects on polymers, which are often undesirable, as they will require the addition of pigments or an increase in the total amount of pigment that will be required to obtain the correct colour. Two of the most commonly used pigments to make polymers opaque are carbon black and titanium dioxide. Carbon black absorbs light, whereas titanium dioxide with a high refractive index scatters light producing a high level of whiteness and brightness [55].

2.4.3 Agglomeration and Aggregates

Agglomeration and aggregates are terms used interchangeably, although they do have there own meaning. Both are terms used to describe groups of primary particles that have formed a single larger particle. The main difference between agglomerates and aggregates is that agglomerates have strong bonds between the particles, which can be difficult to break down during processing. Aggregates are loosely bonded particles with weak bonds between them, which can be broken down during processing. During mixing and compounding of polymers it is therefore agglomerates that are of greatest interest as these are less likely to break down during compounding. It is also possible that during processing agglomerates can be formed, as inorganic solids are poorly wetted by polymer melts, which causes individual particles to form aggregates or agglomerates [56].

As inorganic powders decrease in size the effect of gravity acting on them rapidly decreases. This decrease is significant. As particle diameter decreases the effect of gravity decreases by the third power. As particles get smaller in size the surface area increases, which means the attractive forces between then increases.

As particles decrease in size the attractive force acting between them increases by the first or second power of the diameter. This effect is greatest for sub micron particles. The formation of agglomerates in the polymer will reduce the effectiveness of the filler in modifying the polymer properties [56]. They also increase the viscosity of the polymer melt and can reduce the amount of filler that can be added to the polymer.

2.4.4 Dispersion

For the majority of fillers and additives it is essential that they are well dispersed throughout the polymer with no agglomerates or aggregates present, if not they may not perform their job adequately, or cause detrimental effects on other polymer properties. Dispersion can be described as the distribution, of and wetting out of, the particles by a polymer or suitable carrier. Dispersability can also describe the ease with which particle agglomerates can be reduced to an acceptable size, in a continuous medium [16].

Bad dispersion can also affect mechanical properties, such as, impact, tensile strength and strain at break [57]. Poor wetting by the polymer melt or inadequate shear during processing normally causes bad dispersion of the fillers and additives. Good dispersion can be achieved by a long time in the high shear area of the mixer, although excessive mixing can cause degradation of the polymer. The objective of most mixing is to reduce the degree of agglomeration, while maximizing the degree of particle dispersion in the polymer [54,56]. Polymer mixing and dispersion can be broken down into three sections.

Firstly initial wetting of the particulate by the polymer melt, which is aided if the compatibility of the solid and liquid phases are high. Secondly rupture of the agglomerates is accomplished by exposing the mixture to high stress and shear during processing and break down of the agglomerates will occur when the external stress exceeds the forces holding the individual particles together. The last stage involves intimate wetting of the particles, when normally air present at the particle surface, will be replaced. This can be more difficult with smaller particles as they have a greater surface area.

2.5 Effects of Fillers and Additives on Polymer Properties

2.5.1 Impact

The addition of fillers generally decreases the impact resistance of polymers [46,47,66]. Predicting the impact performance of filled polymers is difficult, as final impact properties are dependent on the polymer/filler system being studied. There are several reasons for this, including interaction between the polymer and fillers, such as bonding and crack iniation/termination. Impact properties are also dependent on the test conditions used, such as specimen geometry, impact velocity and temperature. The high-speed nature of an impact test means it is more sensitive to the fillers present, their size, morphology and loading level.

Unlike other properties, such as tensile strength and strain at break, no theoretical equations exit to actually predict impact performance of filled polymers [47,60]. It is however possible to modify equations for tensile strength and strain at break, from low speed tensile tests, to determine the energy required to break a sample [58]. Thus experimental methods, such as pendulum and falling weight, are commonly used methods to determine impact properties of polymers.

There are many mechanisms by which the fillers may reduce impact properties. Many fillers, after processing or mixing, remain within the polymer matrix as a separate phase. When a load is applied these fillers act as points of stress concentration, which will allow the formation of cracks, which will increase the likelihood of premature failure of the polymer.

It is also possible that rigid particles can reinforce the polymer matrix increasing impact properties. If the particles are considered to act as stress concentrators they will divert cracks towards themselves, which will increase the total surface area of the crack, and the total crack length. This will cause energy to be dissipated that will increase the total energy needed for a catastrophic crack to be formed and propagate. Cracks will be diverted from one stress concentration to another, and this will increase the total distance propagated by the crack during fracture.

Also depending on the inter-particle distance it is possible to stop them reaching a critical length which will lead to failure. The voids formed by the particles may also act as crack stoppers or blunters, which will have a similar effect to that described above. Both of these mechanisms are often difficult to obtain within a polymer/filler system and are therefore overshadowed by other detrimental effects, which will reduce the impact properties of filled polymers.

2.5.1.1 Loading Level

Many authors have reported that increasing loading levels of uncoated fillers decreases the impact resistance of polymers [46,47,59,60]. Increasing amounts of filler induce more effects such as void and crack formation as discussed in previous sections. Which increasing amounts of filler are added to the polymers, the filler will start to dominate the failure mechanism of the composite. Normally the fillers will induce an increasingly more brittle failure within the polymer, with only small or no plastic deformation, and less tendency to yield. This cannot only be attributed to increasing amounts of crack and void formation but dilution of the polymer by a much more brittle but stiff material. Fillers are often used at loading level of greater than 60wt.%. At these loading levels it may be more appropriate to consider that the composite properties are dominated by the fillers properties. At these very high loading levels dispersion and agglomeration break down are increasingly difficult to obtain.

Raymond [66] compounded magnesium hydroxide ($Mg(OH)_2$) in MDPE, at loading levels of 0 to 60wt.%. Impact testing was conducted using a Type 5 IFWI machine set up for Charpy tests using Izod dimmension bars. The results showed that for uncoated $Mg(OH)_2$ both values at peak and failure decreased. The steepest reduction in impact strength occurred at the lower loading levels. Whilst increasing amounts of filler did decrease still further the impact properties, the reductions were smaller than for lower loading levels.

2.5.1.2 Particle Size

Filler particle size can affect impact properties of polymers and this has been reported by many authors [46,47,63,109,113,]. For the majority of filled polymer systems, decreasing the particle size leads to less detrimental effects on impact properties. Particles act in similar ways during impact testing affecting properties, as discussed earlier in the section. Although the high speed nature of an impact test means that they are more sensitive to fillers present, their size and morphology.

If fillers or additives with a large particle size are compared to ones with a smaller size, there will be fewer particles with a total smaller surface area. The larger particles act as greater stress concentrators and leave bigger voids, due to their greater size, and these are more likely to cause failure at lower impact energies. The state of dispersion of the filler, can affect impact properties of polymers. It the filler is so poorly dispersed as to have aggregates or agglomerates present, then these will affect the impact properties of the polymer.

Hutley [61,62] compounded a series of polypropylene compounds with a range of limestone fillers with different particle sizes and particle size distribution. Impact testing was conducted using a falling weight impact test machine. The results showed that varying the particle size and particle size distribution of limestone varied impact results and changed the mode of failure. Generally the coarser the particle the greater the reduction in impact results. Also the mode of failure changed from ductile to brittle.

Miyata [63] investigated the effects of a series of magnesium hydroxide samples with varying particle and crystal size. A surface coating of sodium stearate was applied to each grade of magnesium hydroxide, before compounding using a twin screw extruder and injection moulding test samples. Izod impact tests showed that there was an increase in impact properties up to 30wt% filler, after this the impact results decreased with increasing loading level. The results also showed that the particles with the smaller particle size gave the highest results at constant loading levels.

2.5.1.3 Polymer Filler Adhesion

A major factor affecting the impact properties of filled polymer systems is the level of bonding between the polymer and filler. It is these interactions that make predicting impact properties more difficult than other properties. Many fillers used in polymers are incompatible with the polymer they are incorporated into and the amount of bonding between the polymer and filler is minimal.

There have been many studies investigating the effect of modifying the surface of the fillers. This can make them more compatible with the polymer thus allowing some degree of bonding or coupling between the filler and polymer. Other surface coatings reduce the free surface energy of the fillers or act as internal lubricants, which can aid filler dispersion. One of the most common chemicals used in this way is stearic acid, although many others exit such as behenic acid and decanoic acid. These surface coatings showed the best results when relatively higher loading levels of fillers were used, as the amount of interface area between the polymer and the filler was increased.

Raymond [66], found that $Mg(OH)_2$ with a surface coating of 6% stearic acid gave increased impact properties at a variety of loading levels compared to uncoated $Mg(OH)_2$. The increased impact values for coated $Mg(OH)_2$ were attributed to better dispersion of the filler within the polymer matrix, which meant less agglomerates were present to form large points of stress concentration which would lead to the formation of significant voids.

Fu [64] used both uncoated and phosphate coated calcium carbonate in HDPE. The amount of phosphate added was 1.5wt% of $CaCO_3$, and the $CaCO_3$ was compounded into the HDPE using a two roll mill. Impact testing revealed that the addition of uncoated $CaCO_3$ reduced impact properties substantially as compared with unfilled HDPE, whilst the coated $CaCO_3$ increased impact values. The increased impact properties were attributed to better dispersion and adhesion of the $CaCO_3$ in the HDPE.

The better dispersion increased the number and amount of interaction between crazes formed during fracture. These factors meant that the HDPE changed from having a brittle failure when filled with uncoated $CaCO_3$ to a more ductile failure for phosphate coated material.

2.5.1.4 Rubber Impact Modifiers

The method of rubber toughening of PS is discussed in section 2.1. Many authors have investigated the effect of changing the rubber content of rubber modified PS. Rink [65] investigated the effect of increasing the rubber content in ABS for both unnotched and notched samples. Instrumented Izod impact test machine was used. The results showed that increasing the rubber content increased both peak and failure energy up to a limit of 25 wt.%. After this point the peak and failure energy for the unnotched samples started to decrease whilst the notched samples remained at constant values. The initial increase was attributed to the fact that more rubber particles allowed both more craze initiation and termination. At the higher loading levels it was suggested that as the number of rubber particles increased, the stress fields around them started to increase, which raised the stress in the surrounding polymer matrix. This required less energy to be applied for failure to happen within the ABS.

Bouton [23] investigated the effect of two grades of butadiene-styrene multi-block impact modifiers, which had different molecular weights and styrene contents, when added to FR HIPS, containing Sb_2O_3 and bromine. The Sb_2O_3 and bromine only compounds had significantly lower impact properties that the compounds containing 10 and 20 wt. % impact modifier with Sb_2O_3 and bromine. The results showed that the impact modifier with higher molecular weight and lower styrene content gave the highest impact improvements, although there was a significant increase in the melt viscosity of these compounds.

2.5.2 Fracture Toughness

Little literature seems to have been published on the effects of fillers on the fracture toughness of particulate filled polymers. Although more has been published on the effects of polymer alterations such as the addition of rubber and changes in molecular weight [67-69]. It is not unfair however, to assume that the filler will have similar effects to those described for impact testing of compounds containing modifiers. The majority of K_C and G_C calculations are made from raw data obtained from either instrumented impact testing, or slow speed three point bend tests, where in each case a load deflection curve is obtained for the sample.

Bramuzzo [59] used $CaCO_3$, talc and glass spheres, at varying loading levels, and $CaCO_3$ at varying particle size and shape in polypropylene. Loading levels from 0 to 0.3 volume fraction were studied. The fracture toughness of the compounds was determined by linear elastic fracture mechanics (LEMF), with maximum load values obtained from an instrument impact test machine. The results showed that the particle size and shape did not affect the K_{IC}, although increasing loading level did increase the values for $CaCO_3$, The glass spheres decreased K_{IC} values. This was attributed to the large particle size not conferring any toughness benefits. For G_{IC} both the glass spheres and $CaCO_3$ gave improvements with increased loading levels, but the values for talc filled compounds were unchanged. The variation between fillers was accounted for by the change in morphology and shape of the fillers used.

Friedrich [70] used silicon oxide (SiO_2) in polypropylene at various levels. The fillers were incorporated using a heated two-roll mill, with loading levels of between 10 and 50wt% filler. Fracture toughness testing was conducted using compact tension, notched samples, with the notch sharpened using a razor blade. The results showed that with loading levels up to 10wt% the values of fracture toughness K_C remained unchanged, above this loading level the values rapidly decreased. This large decrease was attributed to the polymer matrix (which was assumed to carry the load) not being a continuous phase at the higher loading levels, and the filler particles only being separated by a thin isolated region of polymer.

2.5.3 Tensile

The effect of fillers on tensile properties depends on the exact properties being considered. Generally properties such as strain at break are reduced [30,70,71] whilst properties such as tensile strength and Young's modulus are increased with increasing loading level of filler [58, 60,70,71]. Although, as with many other properties of filled polymer systems, there are exceptions. The shape and loading level of the filler, as well as the properties of the matrix, will determine whether the filler will reinforce or reduce properties [73-76, 107]. An example of a filler morphology or aspect ratio effecting polymer properties, is that glass fibres are well known for reinforcement of many polymers but glass spheres will generally reduce properties [73].

There are many reasons for the effect of fillers on these properties. For example the fact that fillers and additives have different properties compared to the polymer they are being used in. Most rigid particles, as their name indicates, have much higher tensile strength and higher flexural modulus than the polymers they are incorporated into. The effect of this is to make the compound more brittle. Also fillers and additives can interact with the polymer they are being used in, this effect will be influenced by the particle size and loading level of the filler being used [77,78].

Many authors [46,52,79] have suggested that the tensile strength of filled polymers lie between an upper and lower boundary, the upper boundary indicating a situation were perfect adhesion between the polymer and filler exit and the lower boundary were no adhesion exits, as shown in Fig. 2.4. In practice the tensile strength of a polymer/filler composite lies somewhere in between the two. The actual strength will therefore depend on the degree of interaction between the filler and polymer, the higher the level of interaction, the better the tensile strength.

Miyata [63], showed that tensile properties were affected by the particle size of the filler, loading level and crystal size. Tensile and flexural strength decreased with increasing $Mg(OH)_2$ content. The $Mg(OH)_2$ with the smallest particle size had the smallest reduction. Flexural modulus increased with increasing $Mg(OH)_2$ content, with the small particle sized material giving the best results.
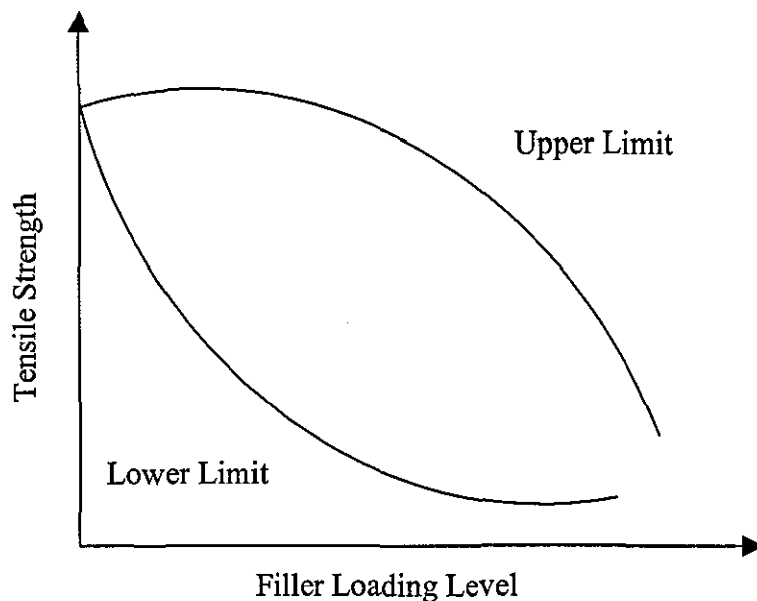
Fig. 2.4, Effect of Filler Loading Level and Adhesion on the Tensile Strength of
Filled Polymer Systems.

Trotignon [80,81] investigated the effect of low concentrations of various fillers on
the mechanical properties of polypropylene. Three fillers were used with different
morphologies, mica, talc and wollastonite. Loading levels were between 0.5wt.% and
5wt.%. Tensile testing showed no change in elastic or yield properties for the filled
compounds. This was attributed to the crystalline region of the polymer controlling
these properties, which was unaffected by the addition of the fillers at low loading
level. All filled polymers exhibited increases in ultimate strength of up to 50%.
Increasing the loading level did not increase these values further. It was suggested
that a transition in failure type was the reason for this large increase in ultimate stress,
the small number of particles inducing a changing crack formation.

Sumita [82] investigated the effect of ultra-fine particles on polypropylene. A variety
of particle sizes and loading levels were used and their affect on yield stress studied.
The results indicated that both loading level and particle size of fillers affect tensile
properties. At a given filler content the stress decreased with filler size, and
increasing loading levels slightly improved yield stress values.

2.5.4 Crystallinity

Only a small number of polymers are able to crystallise. There are many factors affecting whether a polymer can crystallise and how crystalline it will become. Some of these are cooling rate, chain structure, side groups, molecule weight, and the presence of nucleating agents. It has been shown that the level and type of crystal structure in a polymer can affect many properties such as tensile strength, fracture toughness, impact strength and flame retardantcy, although other work has shown crystallinity to have no effect on mechanical and/or other properties [66].

The effect that crystallinity has on a polymer system depends on both the polymer and the filler. Generally fillers increase the crystallinity of polymers, which can affect the final properties of the compound [61,65]. Authors have suggested that fillers increase the crystallinity by acting as nucleating agents, allowing crystallisation to start from more points [61,62,83], which will create a larger number of small crystalline regions.

Mitsuishi [83], used a range of $CaCO_3$ at increasing loading levels and a range of particle sizes, in polypropylene. The compounds were formulated using a two roll mill before DSC analysis was conducted to determine the crystallization temperature. This temperature was found to be dependent on both the particle size and the volume fraction of the $CaCO_3$. Increasing the loading level and decreasing the particle size raised the crystallization temperature. These affects were attributed in varying degrees to the interaction between the polymer and $CaCO_3$. This was further supported by considering the available surface areas of the filler, which increased crystallization temperature.

2.6 Flame Retardant Mechanisms for Polymers

2.6.1 How Polymers Burn

As already stated there are three main requirements for a fire, these are heat, fuel and oxygen. The relationship between these was shown in Fig. 1.2. Each fire is an individual occurrence, although the majority of fires can be divided into several distinct stages, which have already been discussed in section 1.6, they are also shown diagrammatically in Fig. 1.2. Flame retardant additives can only act in the ignition and growth stages of a fire, after this conventional fire fighting methods must be employed.

2.6.2 Flame Retardant Mechanisms For Polymers

There are three primary methods of flame retarding polymers, but all use the same basic principle; the inhibition or suppression of one or more of the fundamental requirements, heat, fuel and oxygen. Dependent on their type, flame retardants can act chemically or physically, and in either the condensed (sometimes called the solid phase), liquid or gas phase.

There are many methods by which flame retardants can operate physically to influence the combustion process. Firstly by cooling. Materials that decompose endothermically during combustion will cool the substrate to a temperature below that required from combustion, examples of this type of flame retardant are Alumina Trihydrate (ATH) and Magnesium Hydroxide ($Mg(OH)_2$) [66,84]. ATH is the most widely used flame retardant, due to its low cost and ease of incorporation into plastics [84]. It breaks down in the temperature range 180°C to 200°C, via an endothermic reaction to aluminium oxide as shown in Equation 2.1. During this break down it also releases water vapour.

$$2Al(OH)_3 \xrightarrow{\Delta} Al_2O_3 + 3H_2O - 298KJ/mol \quad \textbf{Equation} \quad \textbf{2.1}$$
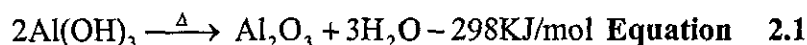
Within the combustion zone the reaction shown in Equation 2.1 triggers several processes, which affect the combustion process, primarily the endothermic nature of the reaction will cool the process, allowing less pyrolysis products to be formed. Magnesium Hydroxide ($Mg(OH)_2$) works in a similar way to ATH but decomposition occurs at the much higher temperatures of 320°C to 450°C, absorbing around 1450J/g of heat [66]. Its main benefit is its ability to be processed at a higher temperature increasing the range of polymers it can be used in.

Flame retardants can also form a protective layer, or coating, on the flammable substrate. This can take the form of either a solid or gaseous layer, and will provide a barrier between the substrate and the gaseous phases. Flame retardantancy is achieved in several ways. Smaller quantities of pyrolysis gases are evolved, the oxygen needed for combustion is reduced, and heat flow within the process is impeded. Zinc borate operates as shown in Equation 2.2, this reaction happens over a temperature range of 130°C to 270°C [84]. This forms a glass like non-flammable coating on the polymer. Also as can be seen from Equation 2.2, there is a dehydration action, which promotes char formation on the polymer. The two actions reduce attack on the polymer substrate by both oxygen and heat.

$$2H_3BO_3 \xrightarrow{-2H_2O} 2HBO_2 \xrightarrow{-H_2O} B_2O_3 \qquad \textbf{Equation 2.2}$$
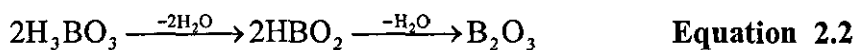
Phosphorous based flame retardants also work by promoting char formation. The FR is converted by thermal decomposition to phosphoric acid, which in the condensed phase extracts water from the area of the substrate undergoing pyrolysis to cause charring.

ATH discussed above can also work by this method. Water vapour formed in Equation 2.1 dilutes the gas phase forming an oxygen displacing protective layer over the polymer substarte, also the ATH, together with char products formed, will form a protective insulating layer on the polymer surface.

The last method is by the dilution of the flammable gases by inert ones. This is primarily achieved by the use of additives that are inert, or give off inert gases during the combustion process. Alumina trihydrate discussed earlier and calcium carbonate are examples of this method. Calcium carbonate's (chalk) only flame retardant action is by dilution. It is normally incorporated into polymers at loading levels of up to 80wt%. The amount of polymer available per unit volume of the compound is significantly reduced, conferring some degree of flame retardancy. As calcium carbonate does not break down below 900°C it cannot have any other effect over the combustion temperature range of polymers ($\approx$150 to 400 °C).

Flame retardants that act chemically primarily operate in the solid and gas phase. In the gas phase the flame retardant reacts with the high energy $O^\bullet$ and $OH^\bullet$ groups formed during chain branching, to leave less active groups. Antimony and halogen based flame retardants discussed in more detail in section 2.6.3 are the best known example of this type of flame retardant. In the solid phase flame retardants can act chemically in two ways. Firstly by causing excessive melt and flow of the polymer in the flame region, which removes the fuel from the fire. Secondly, some flame retardants promote carbon formation on the polymer surface. This layer forms a barrier between the polymer and the fire.

The majority of commercially available flame retardants work by using several of the methods described above. Flame retardants for polymers are often sub divided into two groups, reactive and additive flame retardants [84, 85]. Reactive flame retardants are chemically built into the polymer molecule along with the starting components. They are generally more efficient than additive flame retardants, but their cost is also greater. The most common use is in thermosets such as polyesters, epoxy resins and polyurethane's as they can easily be incorporated into the structure during manufacture.

Additive flame retardants are added into the plastic at any stage from polymerisation, to final compounding and shaping. They are most commonly used in thermoplastics. If compatible with the polymer they are being used in, they tend to act like plasticisers, if not they are treated as an additive. The development of high molecular weight compounds has meant that they are more stable in the polymer, which allows the compound to maintain its flame retardancy for longer [84].

2.6.3 The Flame Retardant Action of Halogens

All halogen elements will act as flame retardants for polymers, although their effectiveness increases in the order F<<Cl<Br<I [46,47]. But fluorine and iodine are not used in practise because they do not interfere with the combustion process at the right stage. Fluorine is too strongly bound to carbon and cannot become a radical interceptor in the gas phase, whilst iodine is so loosely attached to carbon that it will break off at such low energies that other properties, such as UV stability, will be affected.

Bromine and chlorine are the primary halogen elements used. This is because they react with the polymer burning process at the right stage to produce the best effect. Of these two, bromine is the most commonly used, as it is the most effective of them [43]. Although all halogens produce different levels of flame retardancy based on their bond strength to carbon, they all work as a flame retardant in the same way, interfering and replacing high-energy free radicals in the gas phase. These are formed by chain branching as shown in Equations 2..3 and 2.5.

$$H^\bullet + O_2 \rightarrow OH^\bullet + O^\bullet \quad \textbf{Equation 2.3}$$

$$O^\bullet + H_2 \rightarrow OH^\bullet + H^\bullet \quad \textbf{Equation 2.4}$$
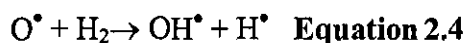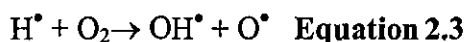
The flame retardant will first break down, and then react to form hydrogen halides as shown in Equations 2.5 and 2.6

$$RX \rightarrow R^{\bullet} + X^{\bullet} \qquad \textbf{Equation 2.5}$$

Where X is either Cl or Br

$$X^{\bullet} + RH \rightarrow R^{\bullet} + HX \qquad \textbf{Equation 2.6}$$

These will then interfere with the radical chain mechanism as shown in Equations 2.7 and 2.8.

$$HX + H^{\bullet} \rightarrow H_2 + X^{\bullet} \qquad \textbf{Equation 2.7}$$
$$HX + OH^{\bullet} \rightarrow H_2O + X^{\bullet} \qquad \textbf{Equation 2.8}$$
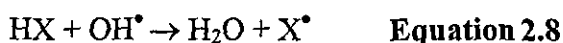
The high energy $H^{\bullet}$ and $OH^{\bullet}$ radicals are removed by reactions with HX and replaced with lower energy X radicals. The flame retardant effect is therefore produced by the HX particles. Reacting with hydrocarbons, as shown in Equation 2.9 they can regenerate the hydrogen halide used in the reaction.

$$X^{\bullet} + RH \rightarrow R^{\bullet} + HX \qquad \textbf{Equation 2.9}$$
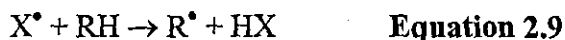
Halogen compounds also have other methods by which they can exhibit flame retardant effects. The hydrogen halides formed in Equation 2.6 are non-flammable and can therefore form a non-combustible protective layer on the condensed phases, interfering or stopping, the combustion process. It is also thought that these reactions can lead to char formation, where the char acts as a physical insulation barrier preventing oxygen attack. In the solid phase, accelerated break down of the polymer by the flame, can lead to large amounts of polymer flow, resulting in withdrawal of the fuel for the fire from the pyrolysis zone.

2.6.4 Flame Retardant Action of Antimony Trioxide

Antimony trioxide exhibits little or no flame retardant effect when added to polymers on its own. When combined at low loading levels with a suitable halogen compound it produces a significant synergistic effect [86], compared to similar levels of halogen only. There is no entirely agreed method of how the Sb_2O_3 works as a flame retardant but it is believed that the most important mechanism takes place in the gas phase, and effects the radical chain mechanism. Equations 2.10 to 2.13, show the current most accepted method [21].

$$Sb_2O_3 + 2HX \xrightarrow{\approx 250^\circ C} 2SbOX + H_2O \qquad \text{Equation 2.10}$$

$$5SbOX \xrightarrow{245-280^\circ C} Sb_4O_5X_2 + SbX_3 \uparrow \qquad \text{Equation 2.11}$$

$$4Sb_4O_5X_2 \xrightarrow{410-475^\circ C} 5Sb_3O_4X + SbX_3 \uparrow \qquad \text{Equation 2.12}$$

$$3Sb_3O_4X \xrightarrow{475-565^\circ C} 4Sb_2O_3 + SbX_3 \uparrow \qquad \text{Equation 2.13}$$
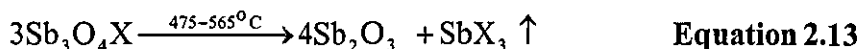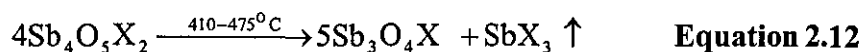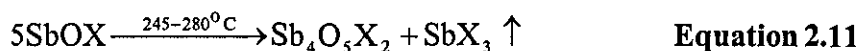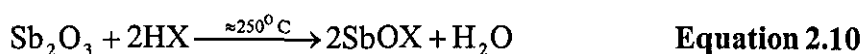
As a result of the reactions 2.11 to 2.13, SbX_3 is given off over a temperature range of 245°C to 565°C. The SbX_3 acts as the flame retardant, in a similar method as for the HX formed in Equation 2.9. The SbX_3 is produced over a significant temperature range, which corresponds to the temperature seen in the pyrolysis zone of the fire. Also each step in the process detailed above is endothermic, removing heat from the fire.

The SbX_3 will also break down to form HX, which will operate as detailed in Equations. 2.7 and 2.8. The formation of HX from SbX_3 is shown below.

$$SbX_3 + H^\bullet \rightarrow SbX_2 + HX \qquad \textbf{Equation 2.14}$$

$$SbX_2 + H^\bullet \rightarrow SbX + HX \qquad \textbf{Equation 2.15}$$

$$SbX + H^\bullet \rightarrow Sb + HX \qquad \textbf{Equation 2.16}$$

This allows HX to be formed over a larger temperature range than if just a halogen were used.

3.0 Experimental Detail

This chapter details the experiments and methods used in this work to produce and characterise the formulations. The majority of the work was carried out in the laboratories of IPTME, although additive content and particle sizing was measured by Greatlakes at their site at West Lafayette in the USA, and the molecular weight determination was conducted at RAPRA. The work can be divided into three sections, firstly an outline of the materials, secondly the manufacture of the compounds, and lastly the characterisation of the compounds produced.

3.1 Materials Used

3.1.1 HIPS

As the biggest market for flame retarded HIPS is in the USA, an American grade of HIPS was used throughout this work, the grade was Huntsman HCC-333, supplied by Ashland Inc. It is a commonly used flame retarded grade and is recommended by Greatlakes for use with their flame retardants. The exact rubber content of this grade is not known,, although due to it being classified as a high impact grade, it is likely to be between 8 and 12 wt.%. The processing conditions used in this work are discussed latter in this section.

3.1.2 PBT

The grade of PBT used was Valox 305F manufactured by GE plastics, which contained no glass filler and which is normally used for injection moulding applications, and is often flame retarded. A full list of the manufactures properties are given in [39], and the processing condition used in this work are discussed later in this section.

3.1.3 Bromine Compounds

A total of four bromine compounds have been used in this work, Greatlakes Chemical Corporation supplied all these materials. A decabromodiphenyl oxide (DE83R^{TM}) was the primary bromine compound used in HIPS, this is because it has a high bromine content (83%) and low cost, which makes it one of the most cost efficient flame retardants available. The other three bromine compounds were mainly used in PBT, they are all proprietary grades of phenoxy-terminated carbonate oilgomer of tetrabromobisphenol A. Table 3.1 lists the bromine content of each compound and their quoted melting temperatures.

Compound	Bromine Content (wt.%)	Melting Range (°C)
BC52	51.3	180-210
BC52HP	53.9	210-240
BC58	58.7	200-230

Table 3.1, Properties of Tetrabromobisphenol A Bromine Compounds

3.1.4 Antimony Trioxide

In total five different grades of Sb_2O_3 have been used in this study. These have all been supplied by Greatlakes Chemical Corporation, and have a range of particle size. Table 3.2 lists the average particle size, Sb_2O_3 content and other impurities of the five Sb_2O_3 compounds used.

Grade	Sb_2O_3 (%)	Arsenic (%)	Iron (%)	Lead (%)	Particle Size (μm)
Azub ® (contains 15% wax)	82.7	0.05	0.001	0.12	0.08
MicrofineAO5 Antimony Oxide	99.7	0.05	0.001	0.12	0.5
Timonox Red Star ®	99.7	0.15	0.003	0.05	1.25
TruTint ® 50	99.7	0.05	0.0001	0.12	2.5
Timonox RT	99.5	0.1	0.01	0.2	10

Table 3.2, Properties of Sb_2O_3 compounds Used

Timonox ® Red Star (RS) is the most commonly used grades of Sb_2O_3 out of the five, used in industry. It is a furnace produced grade. The is primarily due to its relative cheapness compared to the other grades, although its intermediate particle size will often lead to a reduction in mechanical properties and a high pigmentation effect. Microfine ® AO5 can be manufactured using one of two methods. Firstly a direct furnace process using different conditions which form a smaller particle size or secondly by simply collecting the fine particles from the RS grade. AO5 is used where the low particle size will have less effect on the mechanical properties.

Trutint 50, (TT) has a larger particle size than the previous grades discussed, it is used in industry to reduce the pigmenting effect of the Sb_2O_3, and as with the previous grades it is a furnace produced product. Reduced Tint (RT) has the largest particle size of all grades used, unlike other grades it is chemically precipitated and no longer marketed or manufactured by Greatlakes. The last grade is an experimental grade and has the smallest particle size of any used, this is achieved by wet milling RS, and attaching the Sb_2O_3 particle to a wax carrier to allow a fine dispersion within the final polymer

3.1.5 Other Materials

There have been a range of other additives used in this work, the biggest group are the Fyrebloc materials, which were supplied by Greatlakes Chemical Corporation. These are masterbatches of BFR and Sb_2O_3 in a carrier resin, for the majority of Fyrebloc materials the carry was polyethylene tetrastearate wax. (PETS), although HIPS has also been used. RS was the grade of Sb_2O_3 used in all Fyrebloc materials. Table 3.3 lists the Fyrebloc material and their composition. They were supplied in a pellet form and the materials that used PETS wax as a binder had a tendency to break up upon handling and processing.

Fyrebloc	Carrier		BFR		Wt. % Sb$_2$O$_3$
	Type	Wt.%	Type	Wt.%	
210	PETS	10	DE83R	72	18
211	PETS	10	DE83R	67.5	22.5
510	PETS	10	BC52	63.5	26.5
2DB-370S3	HIPS	30	DE83R	52.5	17.5

Table 3.3, Fyrebloc Materials, and Their Compositions

Stereon 840 is a styrene-butadiene impact modifier made by the Firestone Synthetic Rubber & Latex Company, primarily for use in flame retardant HIPS to reduce the effect of the flame retardant additives on impact properties [23]. It has a butadiene content of 57% and the remaining amount is styrene. Typically, only small amounts are added (around 4% [23,122]), but increasing the loading level will increase the impact properties still further [23].

PP18 is an antioxidant produced by Greatlakes for use in a wide range of polymer systems. It was added to all PBT compounds including the unfilled material, at a loading level of 0.1wt%. The reason for adding it was to help prevent degradation to both the PBT and the bromine compounds during processing. Its effects on mechanical properties are minimal, due to the low loading level, and a melting point of 50°C which should mean that it completely melt blended during compounding.

3.2 Analysis of Powders

3.2.1 Particle Size Analysis

Particle size analysis was conducted on the majority of the bromine and Sb$_2$O$_3$ powders. The measurements were made in West Lafayette USA using a Hordia LA-900 laser particle sizing machine. The powders were dispersed in an aqueous solution before the measurements were taken. A graphical plot was obtained of particle size versus percentage concentration. Also values for D$_{10}$, D$_{50}$ and D$_{90}$ were quoted which represent the particle diameter below which 10%, 50% and 90% of the particles fall.

3.2.2 XPS Analysis of BFR Surface

XPS analysis was conducted using a VG ESCALAB Mark 1 machine by staff from Institute of Science and Technology (ISST) at Loughborough University. To avoid any possible contamination only non-plastic utensils and containers were used to collect and store the BFR. Samples were then mounted on metal stubs and places in the vacuum chamber of the XPS unit. The samples are then irradiated with X-rays from a AlKα source with energy 1486.6 eV, which excites the core electrons in the atoms in the surface of the sample to cause photoemission. These photoelectrons are collected and analysed. The energies of the photoelectrons emitted are a characteristic of the element from which they come.

Hence the data produced from the XPS analysis can be in the form of a broadscan spectrum of intensity against binding energy. From this spectrum the relative amounts of elements present on the surface of the sample are measured. Only photoelectrons near to the surface the sample are enough energy to escape. This method can be used to determine surface elements up to 5 to 10nm into the sample. From the scans obtained the percentage of each element present can be determined, although this method cannot detect hydrogen.

3.3 Compounding

Approximately 80 compounds dived into 9 sub groups were compounded. All compounding was carried out using an APV twin screw co-rotating extruder with Ktron, granule and powder feeders.

Before and after compounding both of the polymers used were dried to remove all moisture. The HIPS was dried at a temperature of 50°C [122] whilst for the PBT a higher temperature of 70°C [10] was used. After compounding and drying the formulations were stored, in sealed plastic bags, before being moulded.

3.3.1 Equipment Used

An APV MP30TC twin screw extruder, with a L/D ratio of 30:1, fitted with a four 1.5mm strand die, was used After exiting the die the compounded material was passed through a water bath before being granulated. Figure 3.1 shows the configuration of the screws used for all of the compounds, whilst Table 3.4 lists the barrel temperatures used for PBT and HIPS. The temperatures for HIPS were taken from [15]. Initially those for PBT were taken from [10], but these temperatures made the material un-processable after exiting the die, so they were reduced to those shown in Table 3.4. Screw speeds were kept constant for compounds of the same polymer but were different for each of the polymers used. For the HIPS a screw speed of 250rpm was used, whilst for PBT this was reduced to 200rpm. For both polymers, a constant output rate of 8kg/hour was maintained, so that all formulations could be compounded at a constant mass flow rate.

When processing PBT there were problems with air bubbles causing the stands to break in the water bath. To remove air and any other gases present a vacuum was applied at the open vent (shown in Figure 3.1). This removed most of the gases and reduced this problem. The vacuum was not needed for the HIPS compounds.

	1(Die)	2	3	4	5	6(Feed)
HIPS (°C)	200	200	200	200	200	200
Suggested PBT Temp. (°C)	270	265	260	250	245	240
PBT Temperatures Used (°C)	250	245	245	240	235	230

Table 3.4, Process Temperatures used for compounding HIPS and PBT
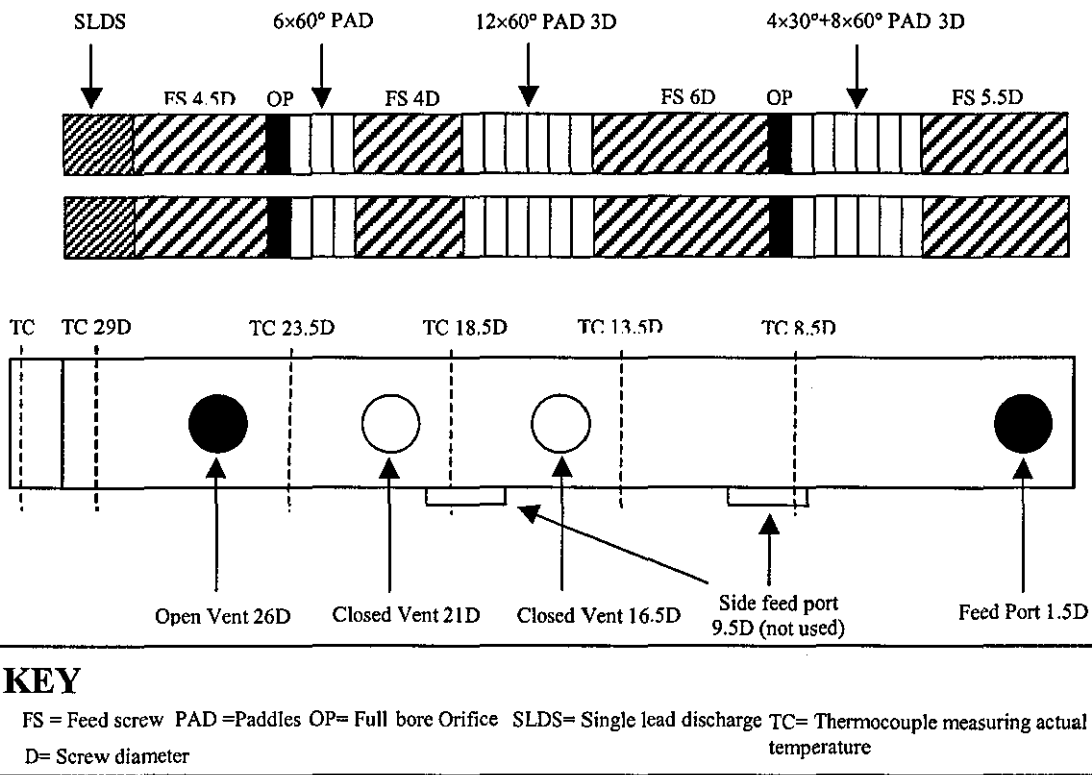
Figure. 3.1, Screw Configuration of APV.

Both polymers were supplied in a granule form and were fed using a Ktron Soder T20 volumetric feeder unit. This feeder was fitted with a long pitch double spiral feed screw, with a secondary rotor agitator blade, which stopped the materials from bridging over the screws. Calibration of the feeder was conducted immediately before compounding as large variations in feed rates have been reported in previous work [46,47] when master calibration charts were used. The same type of feeder was used for feeding powders expect that a long pitch twin concave profile screw was used.

Where either more than one type of granule or powder was used, they were pre-mixed and fed through the appropriate feeder. The only exception to this was when low levels of powders were used (<4wt.%) they were mixed with the polymer granules and fed through the granule feeders. This was due to the fact that the powder feeder would not operate at these low loading levels.

To avoid contamination of compounds and reduce cleaning time between compounding runs, formulations with similar or the same materials (with different loading levels) were processed consecutively. Also between runs a small amount of unfilled material was passed through the extruder to purge out the previous formulations.

HIPS series 7, detailed in Table 3.5, was processed using a different method. To obtain a low amount of mixing during the compounding stage, the raw materials were first weighed to the correct ratios, and then hand mixed before being fed directly into the injection moulder hopper, and being passed through the machine, and moulded. The process avoided the high shear mixing obtained during twin screw extrusion, and allowed any benefits of dispersion of the masterbatch material to be determined.

3.3.1 Compounds Formulated

Table 3.5 lists all HIPS and PBT compounds produced. They have been compounded at various times through the work, but the first number of each compound ID indicates at which time they were compounded.

The code for the compounds is as follows: The first two numbers of the sample ID detail the compound and sample number. The letters after the first forward slash detail the polymer resin used. The next set of letters details the filler type and aimed for weight percentage in the formulations.

All PBT compounds also included an antioxidant PP18, which was primarily to stop the bromine compounds from oxidising [8]. It was included in all formulations to reduce the total number needed. Its low loading level, of 0.1wt%, combined with a melting temperature of 50°C, meant that its affect on properties were minimal.

Formulation ID	Polymer	Bromine Compound		Antimony Trioxide Grade		Filler	
		Type	Loading	Type	Loading	Type	Loading
1-1/HIPS	HIPS						
1-2/HIPS/Az-3.95	HIPS			Az	3.95		
1-3/HIPS/RS-3.5	HIPS			AO5	3.5		
1-4/HIPS/AO5-3.5	HIPS			RS	3.5		
1-5/HIPS/RT-3.5	HIPS			RT	3.5		
1-6/HIPS/TT-3.5	HIPS			TT	3.5		
1-7/HIPS/Az-14.95	HIPS			Az	14.95		
1-8/HIPS/RS-14.5	HIPS			AO5	14.5		
1-9/HIPS/AO5-14.5	HIPS			RS	14.5		
1-10/HIPS/RT-14.5	HIPS			RT	14.5		
1-11/HIPS/TT-14.5	HIPS			TT	14.5		
2-1/PBT	PBT			Az	3.95		
2-2/PBT/AZ-3.95	PBT			AO5	3.5		
2-3/PBT/RS-3.5	PBT			RS	3.5		
2-5/PBT/RT-3.5	PBT			RT	3.5		
2-6/PBT/TT.3.5	PBT			TT	3.5		

3-1/HIPS	HIPS						
3-2/HIPS/CW-0.45	HIPS					Castor wax	0.45
3-3/HIPS/FF-4	HIPS					Impact mod	4
3-4/HIPS/DE83R-12	HIPS	DE83R	12				
3-5/HIPS/DE83R-12/FF-4	HIPS	DE83R	12			Impact mod	4
3-6/HIPS//DE83R-12/Az-3.95	HIPS	DE83R	12	Az	3.95		
3-7/HIPS/ DE83R-12/AO5-3.5	HIPS	DE83R	12	AO5	3.5		
3-8/HIPS/ DE83R-12/RS-3.5	HIPS	DE83R	12	RS	3.5		
3-9/HIPS/ DE83R-12/RT-3.5	HIPS	DE83R	12	RT	3.5		
3-10/HIPS/ DE83R-12/TT-3.5	HIPS	DE83R	12	TT	3.5		
3-11/HIPS/DE83R-12/RS-3.5/FF-4	HIPS	DE83R	12	RS	3.5	Impact mod	4
4-1/PBT	PBT						
4-2/PBT/CW-0.45	PBT					Castor wax	0.45
4-3/PBT/BC58-12	PBT	BC58	12				
4-4/PBT/BC52-12	PBT	BC52	12				
4-5/PBT/BC52HP-12	PBT	BC52HP	12				
4-6/PBT/BC58-12/RS-3.5	PBT	BC58	12	RS	3.5		
4-7/PBT/BC52-12/RS-3.5	PBT	BC52	12	RS	3.5		

4-8/PBT/BC52HP-12/RS-3.5	PBT	BC52HP	12	RS	3.5		
4-9/PBT/BC58-12/TT-3.5	PBT	BC52	12	TT	3.5		
4-10/PBT/BC52-12/TT-3.5	PBT	BC58	12	TT	3.5		
4-11/PBT/BC52HP-12/TT-3.5	PBT	BC52HP	12	TT	3.5		
5-1/HIPS	HIPS						
5-2/HIPS/PETS-1.6	HIPS					PETS wax	1.6
5-3/HIPS/DE83R-12/ RS-4	HIPS	DE83R	12	RS	4		
5-4/HIPS/DE83R-12/ RS-4/PETS-1.6	HIPS	DE83R	12	RS	4	PETS wax	1.6
5-5/HIPS/Fyre-18	HIPS	FyreBlock	18				
5-6/HIPS/PDBS80-14.4/RS-4	HIPS	PDBS80	14.4	RS	4		
5-7/HIPS/DE83R-4	HIPS	DE83R	4				
5-8/HIPS/DE83R-16	HIPS	DE83R	16				
5-9/HIPS/DE83R-32	HIPS	DE83R	32				
5-10/HIPS/DE83R-12/ RS-4/FF-10	HIPS	DE83R	12	RS	4	Impact Modifier	10
5-11/HIPS/DE83R-12/ RS-4/FF-20	HIPS	DE83R	12	RS	4	Impact Modifier	20

6-1/HIPS/RS-10	HIPS			RS	10		
6-2/HIPS/RS-20	HIPS			RS	20		
6-3/HIPS/RS-32	HIPS			RS	32		
6-4/HIPS/TT-10	HIPS			TT	10		
6-5/HIPS/TT-20	HIPS			TT	20		
6-6/HIPS/TT-32	HIPS			TT	32		
7-1/HIPS	HIPS						
7-2/HIPS/DE83R-12/ RS-	HIPS	DE83R	12	RS	4		
7-3/HIPS/BC52-9.3/RS-6.7	HIPS	BC52	9.3	RS	6.7		
7-4/HIPS/ DE83R-12/ RS-4/PETS-2	HIPS	DE83R	12	RS	4	PETS wax	2
7-5/HIPS/ BC52-9.3/ RS-6.7/PETS-2	HIPS	BC52	9.3	RS	6.7	PETS wax	2
7-6/HIPS//PDBS80-14.4/RS-4	HIPS	PDBS80	14.4	RS	4		
7-7/HIPS/Fyre211-18	HIPS					Fyre Bloc 210	17.6
7-8/HIPS/Fyre210-18	HIPS					Fyre Bloc 211	17.6
7-9/HIPS/Fyre510-18	HIPS					Fyre Bloc 510	17.6
7-10/HIPS/Fyre2DB-370S3-19.2	HIPS					Fyre Bloc 2DB-370S3	20.8

8-1/PBT	PBT						
8-2/PBT/BC58-20	PBT	BC58	20				
8-3/PBT/BC52-20	PBT	BC52	20				
8-4/PBT/BC52HP-20	PBT	BC52HP	20				
8-5/PBT/BC58-32	PBT	BC58	30				
8-6/PBT/BC52-32	PBT	BC52	30				
8-7/PBT/BC52HP-32	PBT	BC52HP	30				

Table 3.5, HIPS and PBT Compounds and there Aimed for Formulations

3.4 Injection Moulding

3.4.1 Equipment used

All tests specimens for mechanical, flammability and thermal analysis, were injection moulded. A Negri-Bossi NB62 machine was used, Table 3.6, lists the machine specification.

Screw diameter	28mm
Screw length to diameter ratio (L/D)	23:1
Maximum mould clamping force	620kN
Maximum injection rate	66cm^3/min

Table 3.6, NB 62 Injection Moulder Specifications.

The machine has three heated barrel zones, a separate heated nozzle and a heated spur were used. Similar temperature profiles to those used for compounding were employed. The exact temperatures are listed in Table 3.7.

	HIPS	PBT
Mould (°C)	10	40
Spure (°C)	220	280
Nozzle (°C)	200	240
Zone 1 (°C)	200	235
Zone 2 (°C)	200	230
Zone 3 (°C)	200	225

Table 3.7, Temperatures Used for Injection Moulding HIPS and PBT.

Three different moulds were used, the first manufacturing unnotched bars for impact and fracture toughness testing, the second manufacturing bars for UL94 and LOI testing and the last producing dumbbell bars for tensile testing. Both moulds had a single gate at one end of the mould. Where appropriate, care was taken when testing these moulding to make sure the gate end was always in the same position. Table 3.8 lists the remaining variables for each of the moulds used, and Table 3.9 lists the dimension of the samples produced.

	HIPS	PBT
Injection speed 1 (%)	60	80
Injection Speed 2 (%)	5	5
Hold on pressure (MPa)	30	30
Hold on pressure time (s)	10	10

Table 3.8, Injection Moulding Variables Used for PBT and HIPS

Although capable of continuous operation the injection moulder was set to produce one sample at a time, this was because in some cases full ejection of the sample did not take place. The gap between cycles was maintained as short as possible, with an average of about 3 seconds. Problems with the material freezing in the spur of the mould were encountered with both filled and unfilled PBT. This is a common problem with PBT, and a heated spur-cleaning tool was used to unblock the spur when necessary. An additional purge was used after this was done, as degraded material was left in the spur. Each formulation was passed thought the screw of the injection moulders to purge out the previous compound. Once this had been accomplished 10-15 samples were produced and discarded, to fully purge the material in the spur of the mould, before collection of the test samples began.

	Length (mm)	Width (mm)	Thickness (mm)
UL94	126	8	1.6
LOI	120	4	4
Impact	60	10	4
Fracture Toughness	85	20	10
Tensile (dumbbell)	195	10	4

Table 3.9, Dimensions of Test Specimens Produced

3.5 Analysis of Compounds Prior to Injection Moulding

3.5.1 Volumetric Titration Analysis of Sb_2O_3

The titration analysis was carried out according to [9]. This testing was conducted by Great Lakes staff, at both Wallsend Newcastle and West Lafayette USA. This method was primarily designed for antimony content of metal ores (typically greater that 80%), and thus the error on the results are $\pm 1\%$.

3.5.2 Bromine Content Analysis

Bromine content analysis was conducted according to [11], by Great Lakes technicians at West Lafayette. The results obtained gave broad agreement with those expected. Care had to be taken as the results obtained were for the bromine content, and the amount of bromine compound added needed to be calculated from this.

3.5.3 Molecular Weight Determination

Molecule weight determination was conducted using high temperature gel permeation chromatography (HTGPC) as detailed in [88], the testing was conducted at RAPRA Technology. Solutions were prepared by the addition of approximately 15ml of 1,3-cresol solvent and 30mg of each sample using a Polymer Laboratories SP-260 sample preparation unit. The solutions were then heated to 120°C for 30 minutes with continuous shaking. After which the samples were filtered at 120°C through a 2μm sinter into sample vials and placed in the test apparatus.

The equipment used was a Polymer Laboratories GPC210 apparatus, fitted with Plgel 2× mixed bed 30cm column and a 10 microns guard column, as appropriate for medium/high molecular weight polymers such as PBT. A flow rate of 1.0ml/min thought the column was used with a test temperature of 120°C. A refractive index detector was fitted. Data capture and subsequent handling was carried out using Viscotek Trisec 3.0 software. The setup was calibrated using polystyrene. The results obtained were therefore considered to be polystyrene equivalents. Two measurements for each sample were made, with both M_W and M_N calculated.

3.6 Impact Testing

3.6.1 Equipment

All impact testing was conducted on a Rosand type 5 Falling Weight Impact Test machine (Figure. 3.2), fitted with a 26.2Kg weight, and configured for the Charpy test method. Apart from the use of the falling weight machine, all remaining parameters were taken from BS EN ISO 179: 1997 for determination of Charpy impact strength [12].

In this machine a Kistler force transducer is positioned between the striker and the weight and, when released from a pre-determined height the weight falls towards the sample on two low friction guides. The impact velocity is calculated by the optical sensor, just before impact. The optical sensor also starts the recording of the force and displacement data.
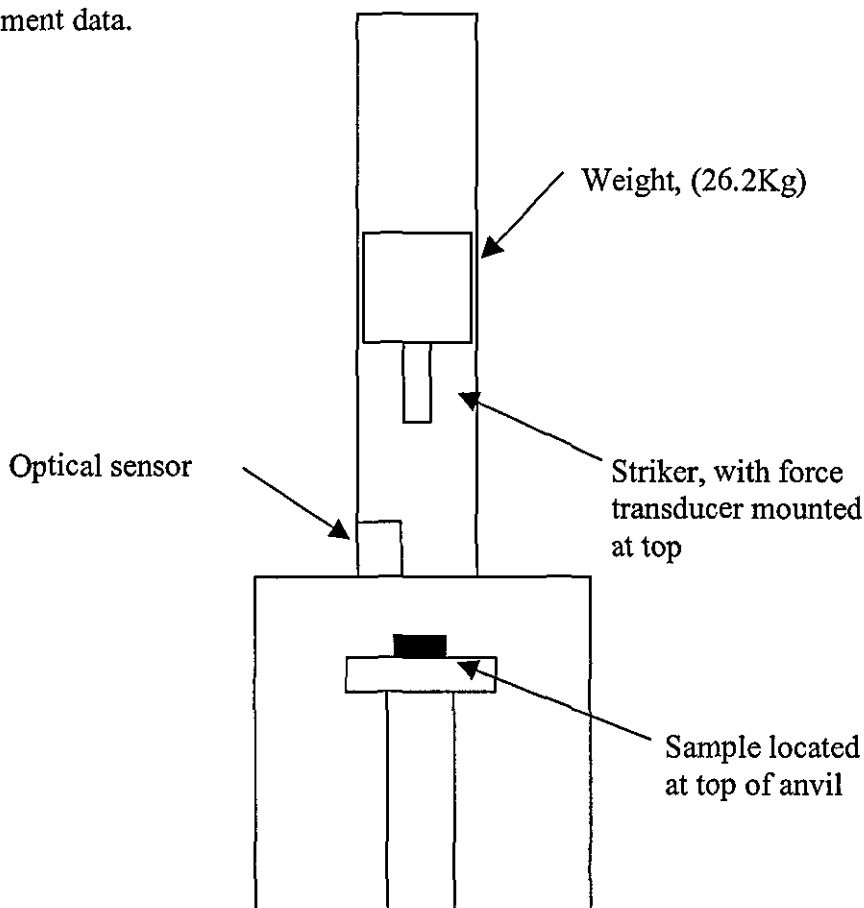
Figure 3.2, Diagram of Rosand Type 5 Falling Eight Impact Test Machine

A strike velocity of 3ms^{-1} was set, giving an impact energy of 118J. A span of 62mm was used to support the samples. The specimens used were as described in section 3.4. All impact testing was conducted at room temperature (23°C). The samples were placed with the notch (where needed) on the opposite face to the impact point.

Although the machine is of a substantial size and weight there were still substantial amounts of vibrations caused. These led to noise in the raw data. However, the computer program has a filter, which can be used to reduce the affect of this noise. If the filter is turned up too high then the results trace can be masked or lost, and the data collected will be incorrect. Several studies have looked at this [46,47], and determined the best level for the filter as 2.5KHz, which was used for all this work.

Impact testing was primarily conducted using unnotched specimens, although several sets of formulations were also tested with sharp V-notch samples. This was to determine the notch sensitivity of the polymer. Although un-notch samples tended to have a very large standard deviation they were more sensitive to filler effects such as size, shape and dispersion. The majority of results are therefore unnotched samples.

The notches were cut from unnotched bars, and conformed to BS EN ISO 179: 1997 for determination of Charpy impact strength [12]. The notches were sharp v-notches, and 2mm deep. When notched specimens were tested six samples were used together with ten unnotched samples. More samples were tested for the unnotched specimens, as the standard deviation was high for all these samples. In addition to the force/displacement traces, the following data was recorded: peak force and energy, and failure energy.

3.7 Fracture Toughness

Fracture toughness testing was conducted in accordance with linear elastic fracture mechanics (LEFM) standard for determining K_C and G_C for plastics [89]. Injection moulded samples were used as detailed in section 3.4. The samples initially had a notch cut with dimensions 5mm×1mm, before a razor blade was used to sharpen the notch. The cut made by the blade was approximately 0.5mm deep from the base of the notch.

The test was conducted as a three-point bend test and a force displacement graph obtained. The cut notch was always positioned on the tensile face of the bar. A Lloyds 2000R universal test machine was used for all fracture toughness testing, fitted with a 5KN load cell, and using a downward crosshead speed of 10mm/minute. Figure 3.3 illustrates the test set up and the cut notches.
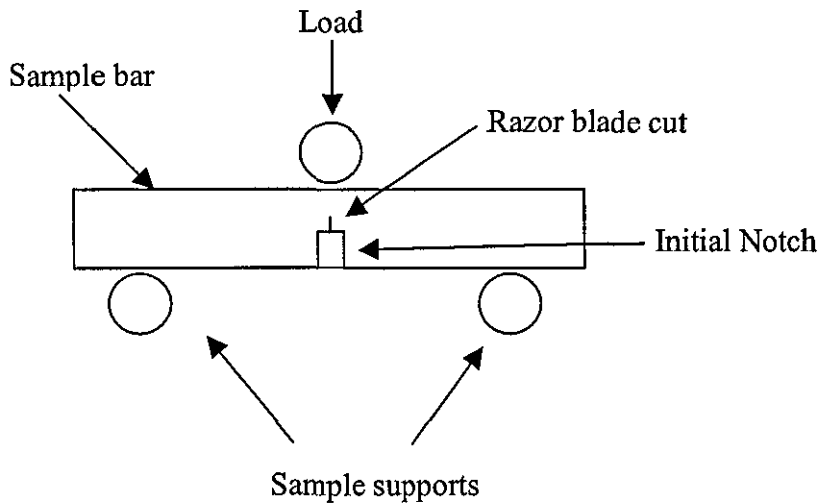
Figure. 3.3, Diagram of Test Set up for Fracture Toughness Testing

Equation 3.1 was used to calculate K_C, the critical stress intensity fracture. Values for f were obtained by creating a plot for a/w (where a is the starting crack length) verses ϕ, which is related to the size of the test samples, using values obtained from [89]. Figure. 3.4, shows how P_Q was determined for each sample, differences arose between HIPS and PBT as it was possible to take the maximum force value for PBT from the graph whilst for HIPS a 1° offset from the initial curve was taken, as the material exhibited some plastic deformation.

$$K_C = f \cdot \frac{P_Q}{BW^{0.5}} \qquad \textbf{Equation 3.1}$$

Where K_C = Critical Stress Intensity Factor (MN/m$^{3/2}$)

                 f = Calibration factor

                 P_Q = Force needed for crack initiation (MN)

                 B   = Breath of sample ($\approx$0.01m)

                 W   = Width of sample ($\approx$0.02m)
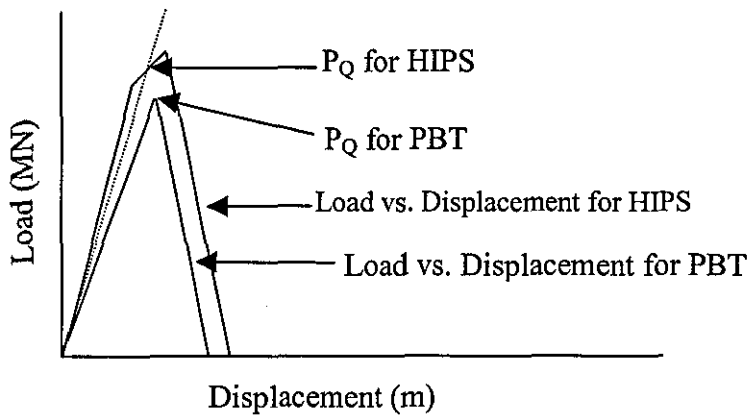
Figure. 3.4, Diagram of Load vs. Displacement Trace for PBT and HIPS,
Indicating How P_Q Was Calculated

3.8 Tensile Testing

All tensile testing was carried out on a Lloyds 2000R universal test machine. A 5kN load cell was fitted and a 100mm gauge length used. Dumbbell shaped specimens were used, as described in section 3.4. Although injection moulding conditions were keep constant, specimen dimensions did vary slightly, therefore all sample were measured to the nearest 0.1mm, before testing and these sizes used for calculations. BS 2782, Plastics, Method 321 Determination of Tensile Properties [90]. General Principles was used as a guide for test conditions and all testing was conducted at room temperature. A cross head speed of 50mm/min was used for HIPS, whilts a slower speed of 10mm/min was used for PBT.

3.9 Flame Testing

3.9.1 Underwriters Laboratory (UL-94) Vertical Burn Test

UL-94 vertical burn testing was conducted in accordance with [91]. Injection moulded samples were used as detailed in section 3.4. Figure 3.5 shows the basic test set up. A standardised gas flame of 19mm was applied to the bottom of the sample for 10 seconds at an angle of 45°, to prevent any drops from falling into the burner. If after removal the flame extinshished, it was reapplied for a further 10 seconds. Burning times, after glow, and any dripping, were recorded after each flame applications. This data was then applied to a criteria set down in [91], which gave a result of V0, V1, V2 or fail. V0 being the best result with little or no burning and no dripping at all. Six samples were tested, and depending on the results a further six samples were tested in accordance with [91]. By changing the sample thickness it is possible to change the results, the most common thicknesses used are 1.6 and 3.2mm. The thinner the sample the harder it for the material to obtain a V0 rating.
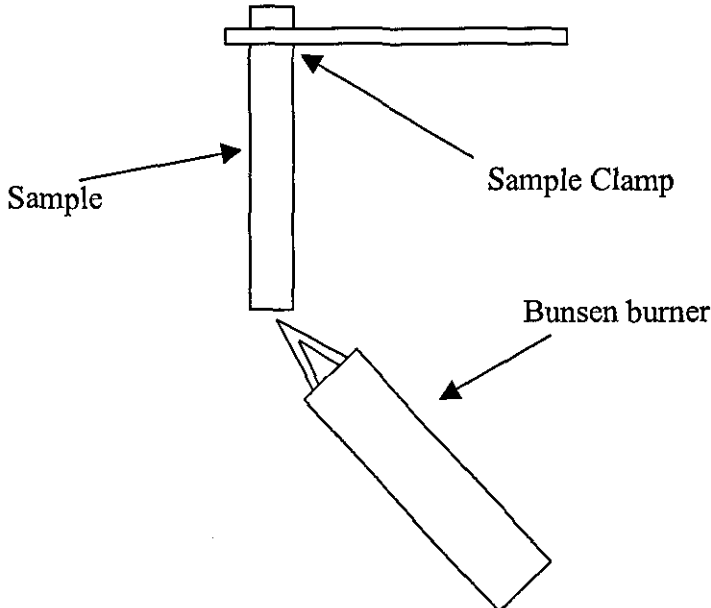
Figure 3.5, Test Set Up for UL94

3.9.2 Limiting Oxygen index

Limiting Oxygen index (LOI) determines the minimum amount of oxygen that is required for a polymer to just burn. A sample is clamped in a vertical position and a mix of oxygen and nitrogen gas passed along the chamber. The amount of oxygen that will just allow candle-like burning of the sample is the LOI value and this is quoted as a percentage. The test is inexpensive and easy to use, which has made it a popular choice in both research and industry. However, several studies [84] have questioned the correlations between LOI values and other flame testing.

Injection moulded samples were prepared as detailed in section 3.4. A diagram of the apparatus is shown in Figure 3.6, and testing was conducted using [92,93] as a guide. In the test a controlled flow of nitrogen and oxygen gives the desired oxygen concentration. A burner is placed to just ignite the top of the sample. The standard states that the burner should be applied for a total burn time of 30 seconds, in no more than 5 second bursts or until the sample has been ignited, which ever happens first. The flow rate of gas past the sample must be 18 1/min.

The LOI value quoted is the percentage of oxygen required to just sustain candle like combustion. A LOI value of 27 is considered to be self extinguishing. The Dixon up down method was used to more accurately determine the LOI value [92].

3.10 DSC

DSC was conducted on unfilled PBT, a range of the PBT compounds and on several of the BFR used. A TA instruments DSC machine was used, with liquid nitrogen used for cooling. PBT samples were taken from fracture toughness injection moulded bars, and to allow for any effect from the injection moulding process, both heating and cooling traces were obtained. Samples with masses between 10 and 15mg were cut from the bars. The samples were then placed in aluminium pans, before being placed in the DSC apparatus. A temperature range of 50°C to 300°C and back to 50°C was used for all polymer samples. For the BFR only the heating profile was used.
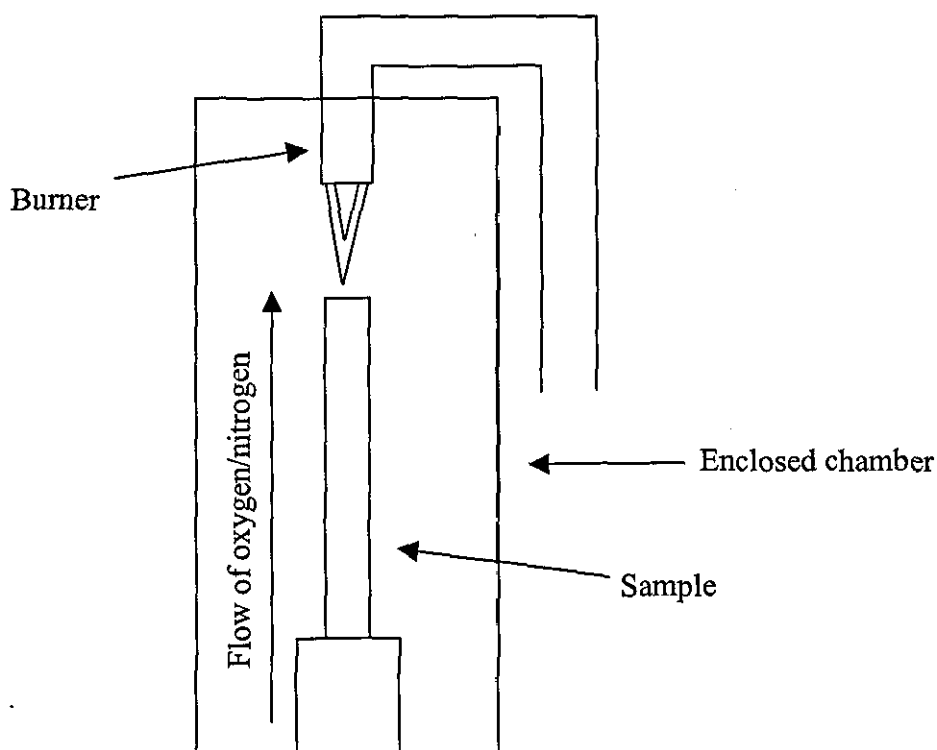
Figure 3.6, LOI Apparatus and Test Set Up

Glass transitions temperatures, melting temperature, recrystallisation temperature, onset of recrystallisation temperature, heat of fusion and heat of recrystallisation were recorded where relevant. Percentage crystallinity was calculated from both the heat of fusion and heat of recrystallisation, by dividing the values obtained by the theoretical 100% values which was obtained from [94].

3.11 SEM

3.11.1 Sample Preparation

Fracture surfaces from both unnotched and notched impact bars were used for this work. As polymers are not conducting material, a conductive layer of gold or carbon had to be applied to give a flow path to earth. This was approximately 10nm thick. All samples were mounted on aluminium stubs.

3.11.2 Equipment Used

A Cambridge/Leica Steroscan 360 instrument was used for all SEM work. When using the primary detectors for looking at fracture images, a low accelerating voltage of 10KeV was used. For the secondary back scattered images an accelerating voltage of 20KeV was needed to obtain clear images.

SEM images of both HIPS and PBT were obtained. For both polymers fracture surfaces were examined, and secondary backscattered electron images were taken of filled samples as these showed the filler particles. In most cases it was only possible to determine the dispersion and rough particle size of the fillers present but, with several of the HIPS samples, clear particle sizing and morphology could be determined. In all cases the bromines and antimony compounds could be located and identified as they had vastly different molecular weights.

3.12 TEM

Many previous reports [11,46,47,94,95] have shown that it is possible to stain both the secondary rubber phase and the fillers in polymers. The most common staining agent used is osmium tetroxide (OsO_4). An aqueous solution of OsO_4 was used to preferentially stain the double bonds in polybutadiene present in HIPS. Specimens were taken from either untested impact test bars, or from the stress whitened area of impact test specimens, to identify crazing and its effects. The HIPS samples were first cut to form an arrowhead shaped sample, before being immersed in a 2% OsO_4 solution for 72 hours. Once removed they were neutralised with sodium thoisulphate and rinsed with water.

Once stained the samples were sectioned using a Cambridge/Huxley Mark 2 single pass ultramicrotone. As a side effect the staining process hardens the polymer, which make sectioning possible at room temperature. The hardened layer was ultramicrotoned to an approximate size of 1mm×1mm×150nm using a glass knife and the section collected through distilled water and placed on a fine copper wire 200 mesh. Samples containing Sb_2O_3 were more difficult to section, as the Sb_2O_3 tended to damage the knife and cause the sections to rip very easily. These problems reduced the final image quality of samples containing Sb_2O_3.

A Jeol 100 CX TEM was used for all TEM to analyse the sectioned samples detailed above. This allowed all phases present to be identified as well as any particulate fillers present. Also the location of the Sb_2O_3 and other fillers could be determined compared to the styrene main phases and secondary polybudinene phases. Several sections were examined before photos were taken of representative parts of the samples.

3.13 Rheology of Compounds

Rheological studies were conducted using a Rosand RH7 Flowmaster capillary rheometer. This is a fully computer controlled twin bore rheometer. The twin bore design allows the simultaneous use of a capillary and orifice die, which allows the calculations of Bagley end correction using a zero length die. Figure 3.7 shows a diagram of the equipment used.

Table 3.10 lists the dimensions of both capillary and orifice dies used in this work. The capillary bore was fitted with a 15000 psi pressure transducer whilst the orifice bore had a 1500 psi pressure transducer fitted. It is possible to set a temperature profile along the bore length, but for both HIPS and PBT, a single test temperature was used, and these are shown in Table 3.11 After the dies had been inserted into the bores, the barrels where charged with samples that had been compounded and dried as described in previous sections. Once fully loaded the pistons were lowered until small pressure readings were obtained for both bores.

The control software can be programmed with pre test sequences, that consist of compression and heating cycles. Table 3.12 list the parameters used for both polymers, only one pre compression and heating stage was used for PBT due to its very sharp melting point and tendency to degraded.
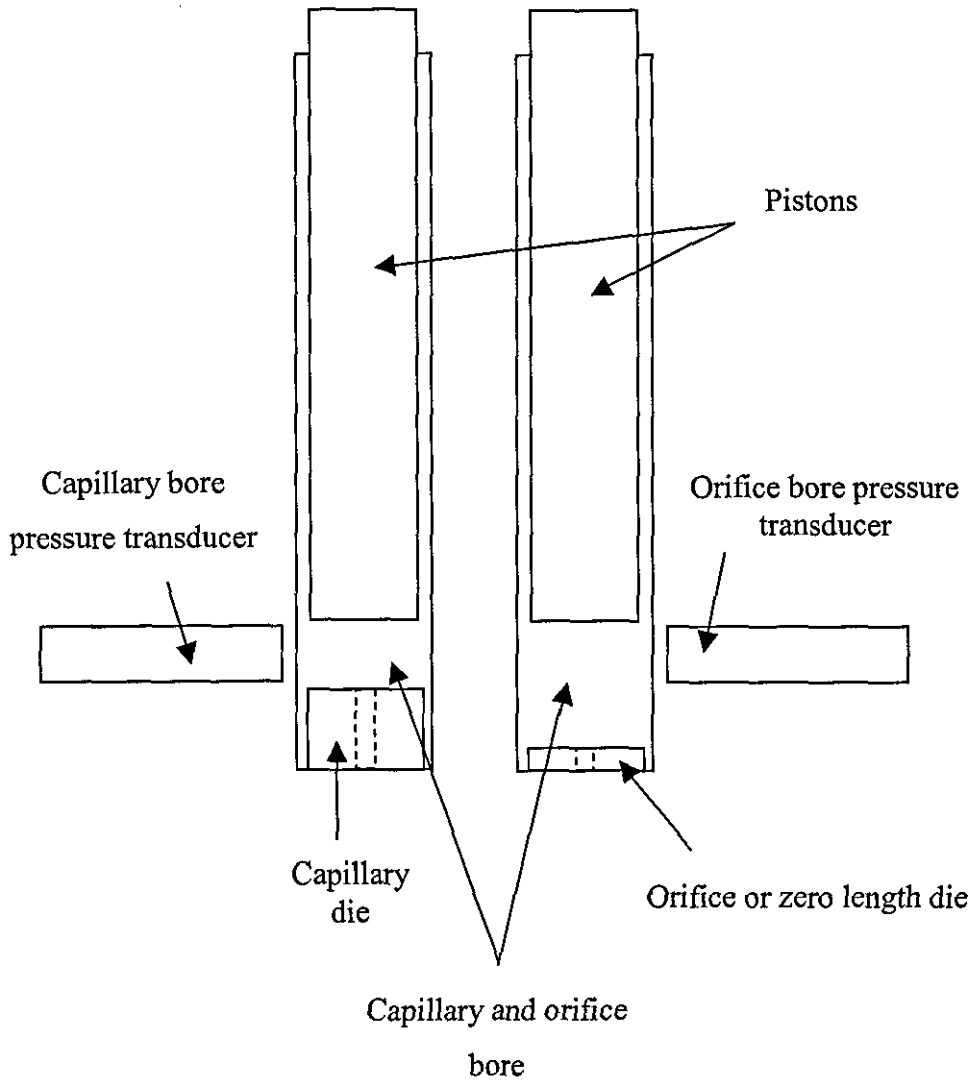
Figure 3.7, Diagram of Rosand RH7 Twin Bore Rheometer

	Capillary	Orifice
Length (mm)	16	0 (<0.2)
Radius (mm)	1	1
Entry (°)	180	180

Table 3.10, Dimensions of Capillary and Office Die

Rheometer Parameter	HIPS	PBT
Test Temperature (°C)	200	250
First pre Compression (MPa)	0.2	0.2
First pre heat time (s)	360	360
Second pre Compression (MPa)	0.2	Not used
Second pre heat time (s)	180	Not used

Table 3.11, Rheometer Test Temperatures and Pre tests Procedures

A large range of shear rates were used for both HIPS and PBT. For HIPS the range was $500s^{-1}$ to $10000s^{-1}$, whilst for PBT the range was used $150s^{-1}$ to $10000s^{-1}$. After each test the software was used to calculate shear rates using Equations 3.2, shear viscosity using Equation 3.3 and shear stress using Equation 3.4. Graphs of corrected shear rate against corrected shear stress, and viscosity, were then obtained. Both Bagley end correction and Rabinowitsch corrected shear rate were used on this data.

$$\dot{\gamma} = \frac{4 \cdot Q}{\pi \cdot R^3} \qquad \textbf{Equation 3.2}$$

Where $\dot{\gamma}$ =   apparent shear rate (/s)

Q =   volumetric output (mm^3)

R =   Die radius (mm)

$$\tau = \frac{(P_L - P_O) \cdot R}{2 \cdot L} \qquad \textbf{Equation 3.3}$$

Where τ =   Shear stress (KP.a)

P_L =   Pressure drop across the capillary die (MPa)

P_O =   Pressure drop across die due to end effects (MPa)

R =   Die radius (mm)

L =   Die length (mm)

$$\mu = \frac{\tau}{\dot{\gamma}} \qquad \textbf{Equation 3.4}$$

Where μ =   Shear viscosity (Pa.s)

Bagley correction accounts for the pressure drops at the entry and exit of a capillary die, as shown in Figure 3.7. The use of an office or zero length die will therefore give pressure readings that are only caused by entry and exit pressure drops from the die. It is not possible to obtain a zero length die, so a lower threshold is set. For these calculations it was assumed that the die is less than 0.2mm, and the Bagley end correction factor is seen in equation 3.3 as P_0.
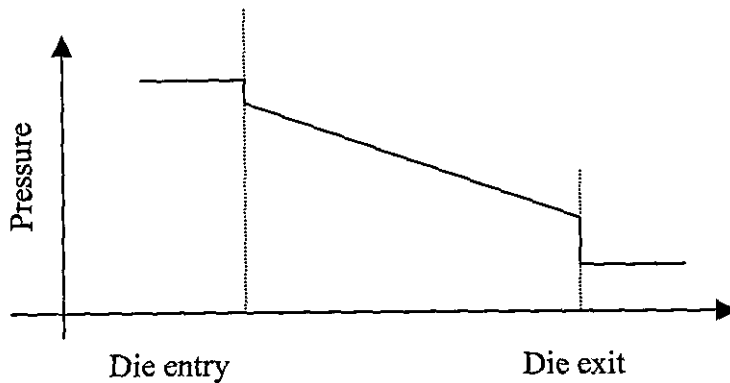
Figure 3.7, Diagram of Pressure Drop at Capillary Die Entrance and Exit

4.0 Results

4.1 Additive Particle Size

Particle size analysis was conducted on all the Sb_2O_3 grades and the BFR DBDPO. The particle size traces are given in Appendix 1, and Table 4.1 summarises the particle size distribution. The D values are the size at which X volume of the particles are under that values, where X is the subscript number. The average particle size values quoted from this point on will be the D_{50}.

Given its structure it was not possible to measure the Sb_2O_3 Azub particle size directly using laser particle sizing. However the Sb_2O_3 particle size was measured during the manufacturing process and was quoted at $0.08 \mu m$ [25].

Additive	D_{10} (μm)	D_{50} (μm)	D_{90} (μm)
DE83R (BFR)	0.90	4.87	20.28
Azub (Sb_2O_3)		0.08	
AO5 (Sb_2O_3)	0.14	0.41	1.54
Red Star (Sb_2O_3)	0.29	1.04	1.96
Trutint (Sb_2O_3)	1.15	4.99	11.09
Reduced Tint	2.78	10.94	30.02

Table 4.1, Particle Size Distribution of Additives.

4.2 XPS Analysis of BFR Surface

XPS analysis was conducted on all of the Tetrabromobisphenol A BFR. For all compounds tested, three elements were detected, oxygen, bromine and carbon (hydrogen cannot be detected). Table 4.2 summarises the percentage of each element detected.

Compound	Element		
	Carbon	**Oxygen**	**Bromine**
BC58	64	13	23
BC52	69	12	19
BC52HP	65	12	23

Table 4.2, Summary of XPS Data.

4.3 Bromine and Sb_2O_3 Content

The bromine contents of all BFRs used in the work are listed in Table 4.3. Also shown for each BFR are the theoretical bromine contents obtained from the manufactures [87]. The measured values in Table 4.3 have been used to determine the bromine compound loading level for the rest of the work. Also both the bromine and Sb_2O_3 contents of all the flame retardant masterbatches used in this work have been determined, these are shown in Table 4.4. The Sb_2O_3 data are direct results, but the bromine compound data is calculated from the information contained in Table 4.3. For the majority of the BFR the measured bromine contents were lower than the manufacturer's quoted values.

Additive	Br Content (wt.%)	Theoretical Values (wt.%)
BC-58	55.0	58.7
BC-52HP	49.8	53.9
BC-52	49.5	51.3
DE-83R	75.0	83.3

Table 4.3, Measured and Theoretical Bromine Content for the BFR Compounds

Additive	Br Content (wt.%)	Br Compound Content (wt.%)	Sb_2O_3 Content (wt.%)
Fyrebloc 2DB-370S3	47.0	55.0	22.8
Fyrebloc 510	31.5	46.6	31.1
Fyrebloc 210	53.6	63.2	18.9
Fyrebloc 211	54.8	64.1	27.6
PDBS 80	57.5	67.3	

Table 4.4, Bromine and Sb_2O_3 Content of Flame Retardant Masterbatches

Having determined the level of bromine and Sb_2O_3 in the additives the level of the BFR and Sb_2O_3 in the HIPS and PBT compounds produced was determined. As with previous results, Sb_2O_3 data was directly obtained, although, the bromine compound loading levels were calculated from data obtained in Table 4.3. The results for all compounds are shown in Table 4.5.

Formulation ID	wt.% Sb_2O_3	Br (wt.%)	Compound (wt.%)
1-2/HIPS/Az-3.95	3.4		
1-3/HIPS/RS-3.5	3.2		
1-4/HIPS/AO5-3.5	3.8		
1-5/HIPS/RT-3.5	2.5		
1-6/HIPS/TT-3.5	2.7		
1-7/HIPS/Az-14.95	14.1		
1-8/HIPS/RS-14.5	10.9		
1-9/HIPS/AO5-14.5	14.4		
1-10/HIPS/RT-14.5	12.6		
1-11/HIPS/TT-14.5	13.5		

Formulation ID	wt.% Sb_2O_3	Br (wt.%)	Compound (wt.%)
--			
2-2/PBT/Az-3.95	3.4		
2-3/PBT/AO5-3.5	3.3		
2-4/PBT/RS-3.5	3.9		
2-5/PBT/RT-3.5	2.8		
2-6/PBT/TT-3.5	4.3		
3-4/HIPS/DE83R-12		11.1	13.8
3-5/HIPS/ FF-4/DE83R-12		12.7	15.9
3-6/HIPS//DE83R-12/Az-3.95	4.2	10.9	13.6
3-7/HIPS/ DE83R-12/AO5-3.5	3.9	8.8	11.0
3-8/HIPS/ DE83R-12/RS-3.5	3.4	8.3	10.4
3-9/HIPS/ DE83R-12/RT-3.5	3.8	8.1	10.1
3-10/HIPS/ DE83R-12/TT-3.5	3.0	8.0	10.0
3-11/HIPS/FF-4/DE83R-12/RS-3.5	3.1	9.5	11.9
4-3/PBT/BC58-12		6.1	8.9
4-4/PBT/BC52-12		6.1	9.2
4-5/PBT/BC52HP-12		7.1	10.6
4-6/PBT/BC58-12/RS-3.5	3.9	7.9	11.4
4-7/PBT/BC52-12/RS-3.5	3.7	6.0	9.0
4-8/PBT/BC52HP-12/RS-3.5	4.5	5.7	8.6
4-9/PBT/BC58-12/TT-3.5	4.2	6.3	9.1
4-10/PBT/BC52-12/TT-3.5	4.8	7.8	11.7

Formulation ID	wt.% Sb_2O_3	Br (wt.%)	Compound (wt.%)
-------------------------------	---------	--------	-----------
4-11/PBT/BC52HP-12/TT-3.5	4.9	6.5	9.7
5-3/HIPS/DE83R-12/ RS-4	4.6	9.7	12.1
5-4/HIPS/DE83R-12/ RS-4/PETS-1.6	4.2	8.0	10.0
5-5/HIPS/Fyre-18	4.6	8.3	10.3
5-6/HIPS/PDBS80-14.4/RS-4	4.5	9.4	11.8
5-7/HIPS/DE83R-4		2.7	3.4
5-8/HIPS/DE83R-16		14.1	17.6
5-9/HIPS/DE83R-32		24.1	30.1
5-10/HIPS/FF-10/DE83R-12/ RS-4	4.6	9.3	11.6
5-11/HIPS/FF-20/DE83R-12/ RS-4	3.8	9.6	12.0
6-2/HIPS/RS-10	10.5		
6-3/HIPS/RS-20	24.2		
6-4/HIPS/RS-32	38.3		
6-5/HIPS/TT-10	13.4		
6-6/HIPS/TT-20	26.5		
6-7/HIPS/TT-32	38.3		
7-2/HIPS/DE83R-12/ RS-4	2.5	7.0	8.8
7-3/HIPS/ DE83R-12/ RS-4/PETS-1.6	3	6.0	7.5
7-4/HIPS/Fyre211-18	4.2	10.7	12.5
7-5/HIPS/Fyre210-18	4.0	10.5	12.3
7-6/HIPS/Fyre510-18	3.5	9.1	12.1

Formulation ID	wt.% Sb_2O_3	Br (wt.%)	Compound (wt.%)
7-7/HIPS/Fyre2DB-370S3-18	3.8	10.4	12.4
8-1/PBT/BC58-20		12.8	18.6
8-2/PBT/BC52-20		12.1	18.2
8-3/PBT/BC52HP-20		13.6	20.4
8-4/PBT/BC58-32		17.8	25.8
8-5/PBT/BC52-32		15.4	23.1
8-6/PBT/BC52HP-32		16.8	25.2
9-2/HIPS/Fyre210-18	3.5	5.7	8.5
9-3/HIPS/Fyre510-18	3.6	5.0	7.5
9-4/HIPS/Fyre211-18	4.6	8.3	10.4
9-5/HIPS/Fyre2DB-370S3-19.2	3.4	10.5	12.5

Table 4.5, Sb_2O_3, Bromine, and Bromine Compound Content Determined by Titration Analysis.

4.4 DSC

DSC analysis was conducted on all of the tetrabromobisphenol A based BFR's, to determine their thermal characteristics in the processing temperature range used. Graph 4.1 plots the traces obtained for all BFR compounds. From these traces the main point of interest is the T_g (marked on the graph), which is present for all three compounds. The T_g temperatures are summarised in Table 4.6.

BFR	T_g (°C)
BC52	161
BC58	187
BC52HP	193

Table 4.6, T_g of Tetrabromobisphenol A, Bromine Compounds.

DSC analysis was also conducted on a selection of the PBT compounds, to determine the effect of the additives on a range of thermal properties. Results for melt temperature (T_m), onset of melting (T_{OM}) recrystallisation temperature (T_c) and onset of recrystallisation (T_{sc}), are summarised in Table 4.7. Heat of fusion (ΔH_m), heat of recrystallisation (ΔH_c) and the percentage crystallinity values, for these PBT compounds, are summarised in Table 4.8. Percentage crystallinity was calculated using a melting enthalpy value of 140J.g^{-1} [1] for 100% crystallinity.
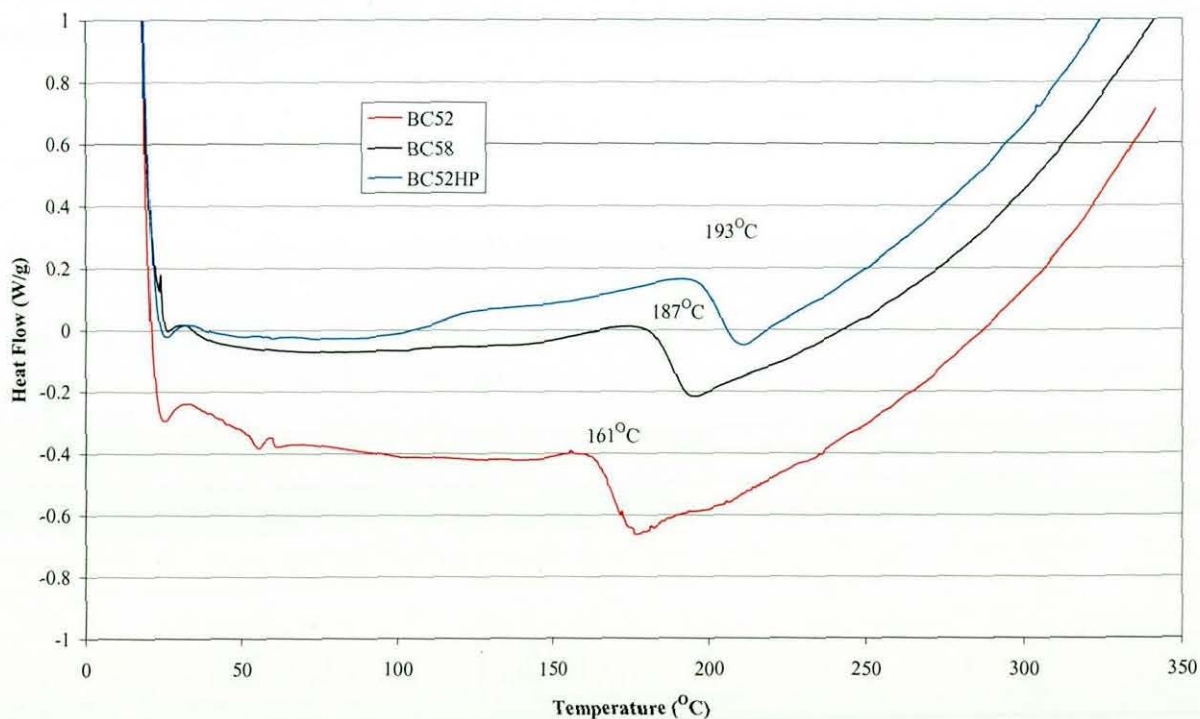
Graph 4.1, DSC Traces Obtained for Tetrabromobisphenol A Bromine Compounds

Corrections to all of these values have been made for the amount of filler in the compounds. From the data in Table 4.7, it would appear that there is a slightly higher crystallinity recorded during heating as compared to cooling, and that as the additive loading level increases the percentage crystallinity values decrease.

Compound ID	T_m (°C)	T_{om} (°C)	T_{sc} (°C)	T_c (°C)
2-1/PBT	226.2	215.1	193.8	189.2
2-2/PBT/Az-3.95	226.5	216.8	209.71	204.2
2-3/PBT/AO5-3.5	225.8	216.2	208.5	205.2
2-4/PBT/RS-3.5	226.7	216.69	208.8	202.9
2-5/PBT/RT-3.5	226.6	215.51	207.3	201.2
2-6/PBT/TT-3.5	226.5	215.7	208.5	202.9
4-3/PBT/BC58-12	224.3	212.7	191.0	184.1
4-4/PBT/BC52-12	225.1	213.0	191.0	185.4
4-5/PBT/BC52HP-12	224.2	213.42	191.2	185.6
4-6/PBT/BC58-12/RS-3.5	223.9	213.5	204.3	197.3
4-7/PBT/BC52-12/RS-3.5	224.5	213.6	202.9	195.1
4-8/PBT/BC52HP-12/RS-3.5	223.5	214.1	204.7	198.2
4-9/PBT/BC58-12/TT-3.5	223.9	213.4	200.6	194.0
4-10/PBT/BC52-12/TT-3.5	222.9	213.1	201.3	194.6
4-11/PBT/BC52HP-12/TT-3.5	223.9	214.0	202.7	195.2

Table 4.7, DSC Data for a Selection of PBT Compounds

Compound ID	ΔH_m J/g	% cryst (heating)	ΔH_c J/g	% Cryst (cooling)
2-1/PBT	45.6	32.6	46.4	33.1
2-2/PBT/Az-3.95	37.6	26.9	42.2	30.1
2-3/PBT/AO5-3.5	36.2	25.9	39.9	28.5
2-4/PBT/RS-3.5	38.3	27.4	43.1	30.8
2-5/PBT/RT-3.5	38.2	27.3	41.5	29.6
2-6/PBT/TT-3.5	41.7	29.8	42.9	30.6
4-3/PBT/BC58-12	34.3	24.5	35.3	25.2
4-4/PBT/BC52-12	36.6	26.1	37.2	26.6
4-5/PBT/BC52HP-12	33.2	23.7	33.9	24.2
4-6/PBT/BC58-12/RS-3.5	25.4	18.1	27.5	19.6
4-7/PBT/BC52-12/RS-3.5	24.9	17.8	25.4	18.1
4-8/PBT/BC52HP-12/RS-3.5	28.2	20.1	28.4	20.3
4-9/PBT/BC58-12/TT-3.5	26.1	18.6	26.5	18.9
4-10/PBT/BC52-12/TT-3.5	26.9	19.2	29.7	21.2
4-11/PBT/BC52HP-12/TT-3.5	27.2	19.4	29.1	20.8

Table 4.8, Heat of Fusion and Recrystallisation, and Corresponding Percentage Crystallinity Values for a Selection of PBT Compounds

4.5 GPC

GPC analysis was conducted on a selection of the PBT compounds, processed unfilled PBT, and PBT as supplied by the manufacturer. This was undertaken to determine the effect, if any, of the twin screw compounding on the PBT. Other tests were conducted to determine the effect that loading level and type of BFR had on PBT. The formulations tested, and the results obtained for them, are shown in Table 4.9. The traces obtained are shown in Appendix 2.

Formulation	M_W (g/mol)	M_N (g/mol)	Molecule weight Distribution (M_W/M_N)
Virgin PBT	84400	51500	1.6
	82200	49700	1.7
Processed unfilled PBT	80200	51100	1.7
	79500	53700	1.6
4-4/PBT/BC52-12	86300	52300	1.7
	86100	52700	1.6
8-5/PBT/BC58-30	85500	51100	1.7
	86100	53700	1.6
8-6/PBT/BC52-30	83400	51300	1.6
	83800	50400	1.7
8-7/PBT/BC52HP-30	85900	52900	1.6
	84700	52500	1.6

Table 4.9, Molecular Weight for a Selection of Unfilled and Filled PBT Compounds

4.6 Capillary Rheology

Capillary Rheology measurements were conducted on a selection of filled and unfilled PBT and HIPS compounds. The formulations tested where chosen to determine the effect produced by the majority of the additives used. Table 4.10 lists the formulations tested. Shear flow curves, where shear rate was plotted against corrected shear stress, were produced for all the compounds tested. A shear range of $150s^{-1}$ to $10000s^{-1}$ was used for both polymers, however, at low shear rates it was difficult to obtain positive pressures, which effectively determined the lower shear rate limit.

Formulations	Additive Type	Loading Level (wt.%)
8-1/PBT	-	-
4-4/PBT/BC52-12	BC52	12
8-3/PBT/BC52-20	BC52	20
8-6/PBT/BC52-30	BC52	30
8-5/PBT/BC58-30	BC58	30
8-7/PBT/BC52HP-30	BC52HP	30
5-1/HIPS	-	-
5-9/HIPS/DE83R-32	DE83R	32
6-7/HIPS/TT-32	TT	32

Table 4.10, Compounds Used in Rheology Tests

4.6.1 PBT Compounds

The selection of PBT compounds tested were selected to determine the effect of varying the grade of tetrabromobisphenol A and the effect of loading level. Graph 4.2 shows how varying the loading level of BC52 affects the corrected shear viscosity of the PBT compounds at a large range of shear rates. For all compounds, as the shear rate increased, the corrected shear stress values increased. As the filler loading level increased the corrected shear stress, at any given shear rate, decreased and became closer to that of unfilled PBT.
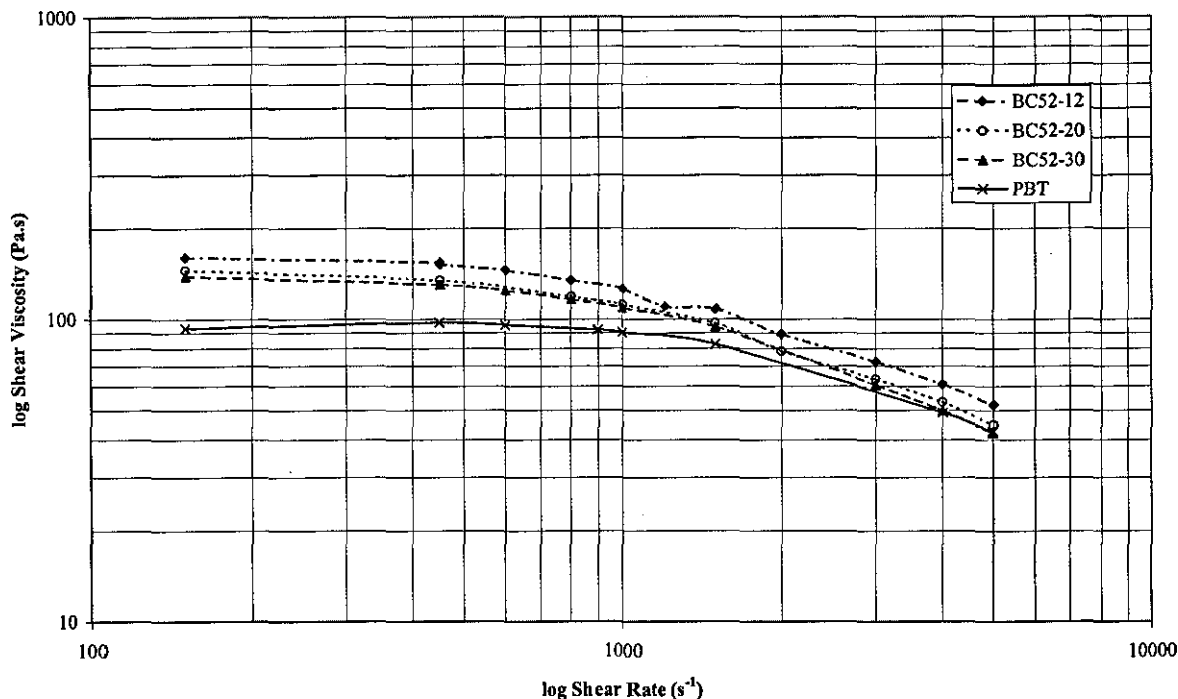
Graph 4.2, Effect of Tetrabromobisphenol A BC52 Loading Level on Shear Viscosity of PBT.

Graph 4.3 shows how varying the grade of Tetrabromobisphenol A at a constant loading level of approximately 30wt.% affected shear viscosity over the shear rate range used. As the shear rate increased the differences between the filled and unfilled PBT compounds was reduced. Filled compounds had a higher shear viscosity value than unfilled PBT. Differences were also seen between the different grades of Tetrabromobisphenol A, with those containing BC52HP having the highest values, followed by BC58. Compounds containing BC52 were closest to unfilled PBT

4.6.2 HIPS Compounds

Graph 4.4 shows the effect of DE83R, TT and RS on the corrected shear stress of HIPS. Compounds containing the highest loading level were used to increase the visibility of any effects caused by the additives. The effect of the FR additives on the rheological properties of HIPS was less than that seen for PBT.
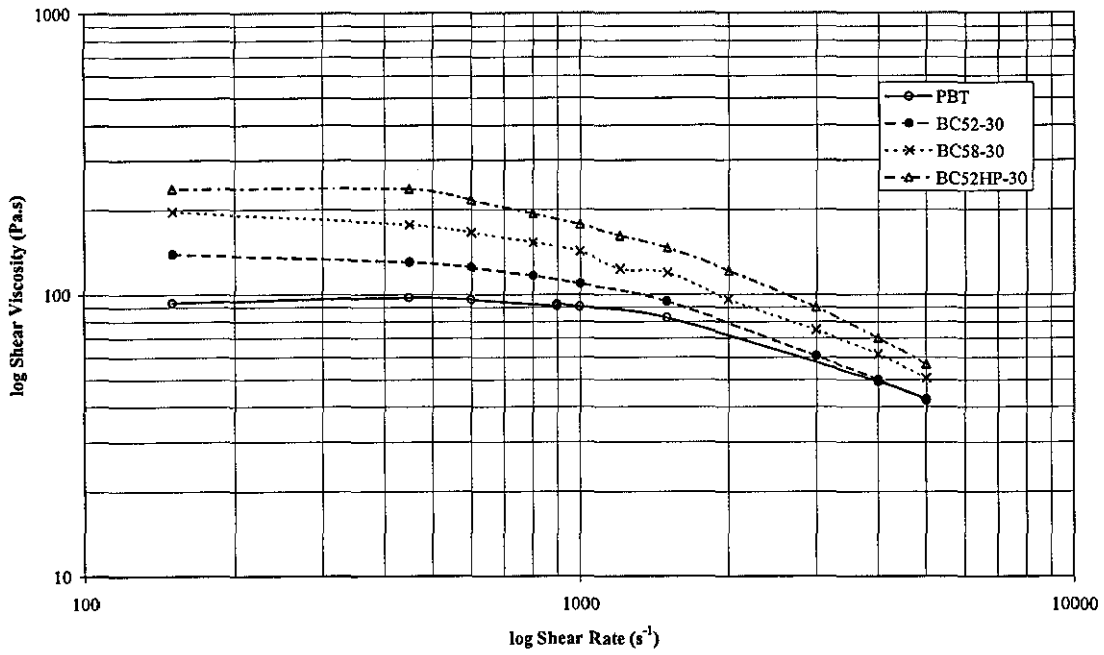
Graph 4.3, Effect of 30 wt.% Tetrabromobisphenol A BC52, BC58 and BC52HP on Shear Viscosity of PBT
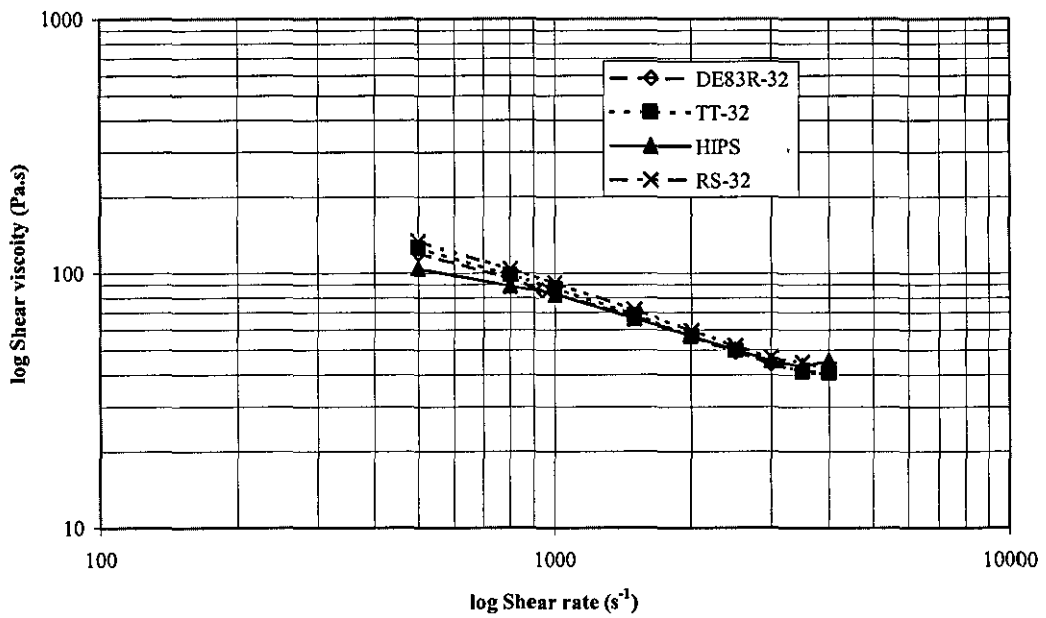
Graph 4.4 Effect of 30wt.% DE83R, TT and RS at on Shear Viscosity of HIPS

4.7 Impact

Impact testing made up the largest part of the characterisation procedure for all compounds. It was conducted as detailed in section 3.5. The results shown here are peak and failure energy, and peak force. Deflection at peak and failure were also recorded, although differences seen were smaller than for the energy values or duplicated trends seen for energy values, so the energy values were concentrated on.

4.7.1 Particle size

When added at low levels, filler particle size can have the greatest effect on impact properties. The data shown in this section is for a range of Sb_2O_3 grades, which had a particle size range from $0.08\mu m$ to $10\mu m$. Graphs 4.5 and 4.6 show peak and failure energy, for HIPS and PBT respectfully, for un-notched specimens, at a range of Sb_2O_3 particle sizes. The standard deviations are high, at between 20 and 40% of mean values. Despite the high standard deviations, trends for both HIPS and PBT can be seen from these graphs.

	HIPS	0.08	0.5	1.2	4	10
☐ Peak	1.8	1.8	1.3	1.5	3.4	2.3
☐ Failure	4.1	4.2	3.1	3.2	5.0	5.0

Particle Size of Antimony Trioxide (µm)
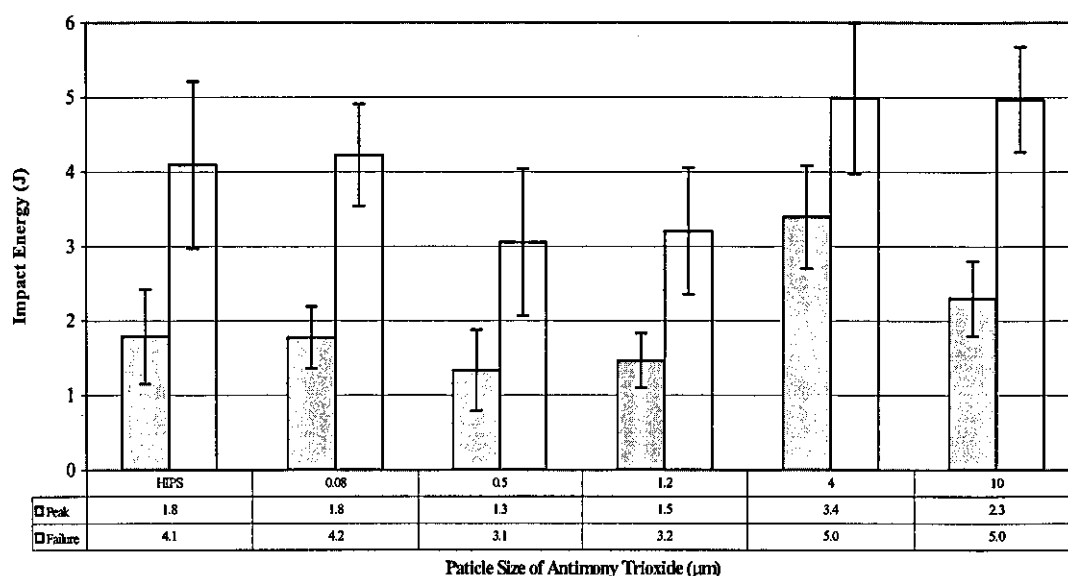
Graph 4.5, Influence of Sb_2O_3 Particle Size on Peak and Failure Energy of HIPS

Particle Size of Antimony Trioxide (μm)	PBT	0.08	0.5	1.2	4	10
□ Peak	2.3	0.4	1.6	1.8	2.0	2.5
□ Failure	6.5	0.9	3.1	3.5	4.3	5.4
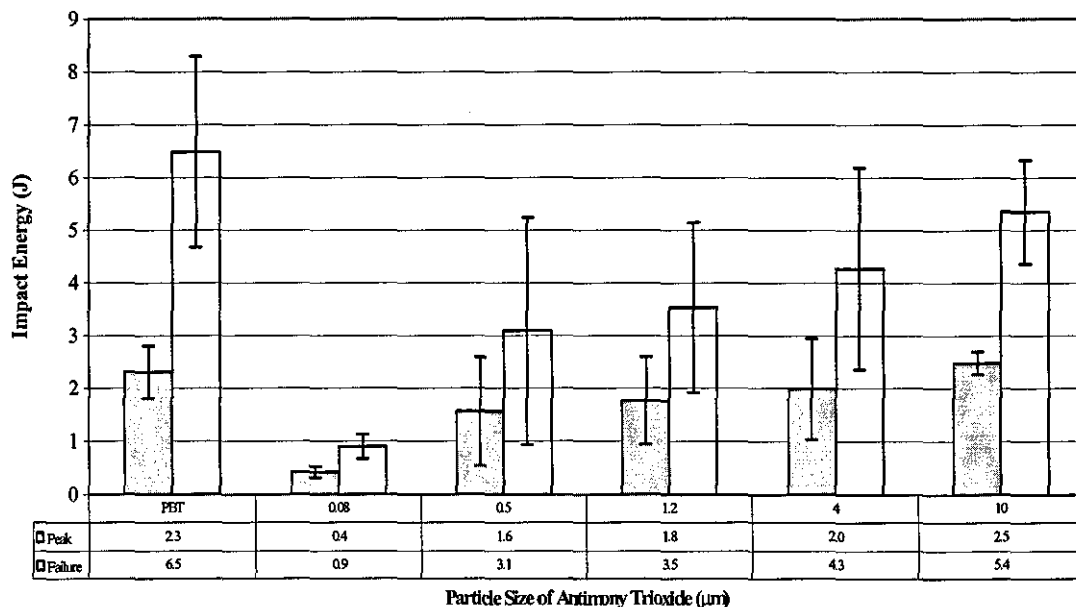
Graph 4.6, Influence of Sb$_2$O$_3$ Particle Size on Peak and Failure Energy of PBT

4.7.2 Loading level

A variety of the Sb$_2$O$_3$ and bromine compounds were compounded into both HIPS and PBT, at a range of loading levels, up to 32wt%. Table 4.11 summarises the additive, polymer and loading level ranges they have been used at. All loading levels used were chosen because they have a use in HIPS or PBT at these loading levels, or as a comparison between the BFR and other additive used in HIPS and PBT.

Filler	Polymer	Loading level range (wt.%)
RS	HIPS	0-32
TT	HIPS	0-32
DBDPO	HIPS	0-32
Impact Modifier	HIPS	0-20
BC52	PBT	0-32
BC52HP	PBT	0-32
BC58	PBT	0-32

Table 4.11, Summary of Fillers and Loading Level Range Used.

Graphs 4.7 to 4.13 summarise the peak and failure energy for the fillers and loading levels described above. All of the fillers had significant effects on both the HIPS and PBT. Increasing the loading level of particulate fillers decreased both peak and failure energy, although the biggest effects were seen for failure energy. For the impact modifier increasing loading level increased failure energy, but an overall decrease in peak energy was observed. Standard deviations were between 10 and 20 % for failure energy and less than 10 % for peak energy values. Graph 4.14 shows the force displacement graphs obtained directly from the Rosand IFWI machine. From this it can be seen that as the level of impact modifier increases, peak force values decrease. This accounts for the decrease in peak energy as it is calculated from the area under this section of the curve. Graph 4.15 shows the force displacement data obtained for unfilled PBT and PBT compounds containing 32wt.% BC52.

	6-1/HIPS	1-4/HIPS/RS-3.5	6-2/HIPS/RS-10	1-9/HIPS/RS-14.5	6-3/HIPS/RS-20	6-4/HIPS/RS-32
Peak	1.5	1.5	1.3	1.0	0.9	0.5
Failure	4.0	3.2	2.1	1.7	1.5	1.0
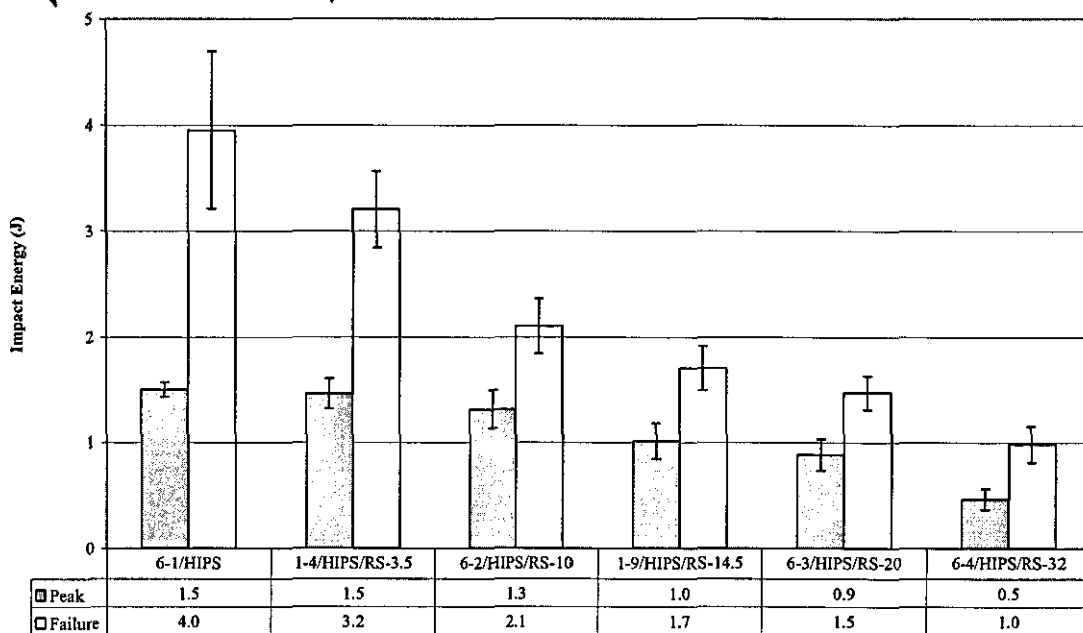
Graph 4.7, Effect of RS Loading Level on Impact Peak and Failure Energy of HIPS

	6-1/HIPS	1-5/HIPS/TT-3.5	6-5/HIPS/TT-10	1-9/HIPS/TT-14.5	6-6/HIPS/TT-20	6-7/HIPS/TT-32
☐ Peak	1.5	1.6	1.2	1.3	1.2	0.9
☐ Failure	4.0	4.1	1.9	1.8	1.7	1.2
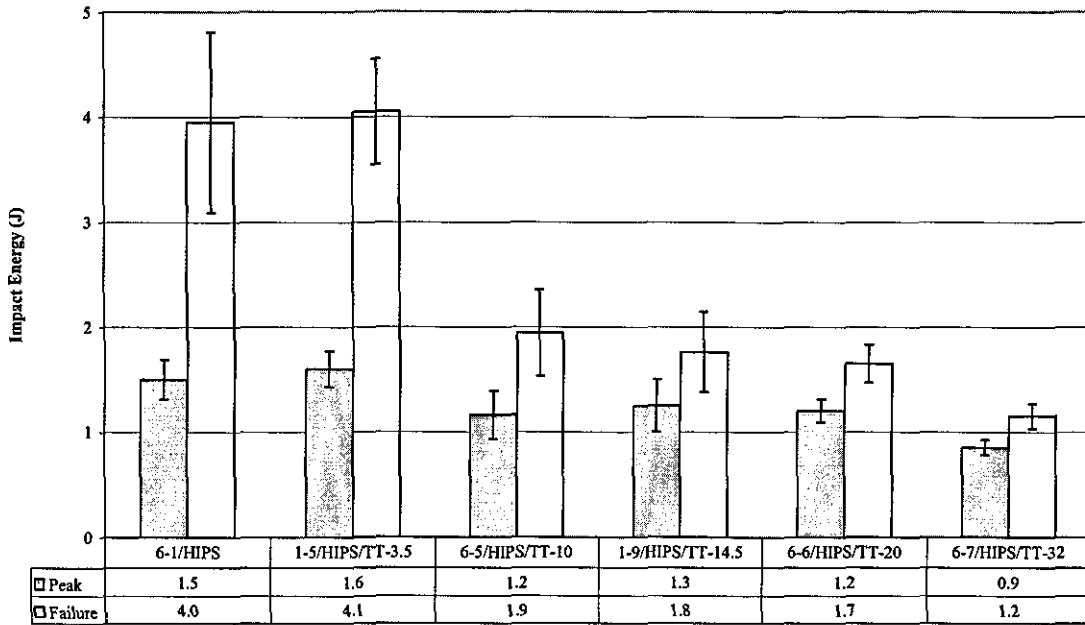
Graph 4.8, Effect of TT Loading Level on Impact Peak and Failure Energy of HIPS

	5-1/HIPS	5-7/HIPS/DE83R-4	3-4/HIPS/DE83R-12	5-8/HIPS/DE83R-16	5-9/HIPS/DE83R-32
☐ Peak	1.8	1.7	1.1	1.2	0.4
☐ Failure	3.8	3.8	2.1	1.7	0.8
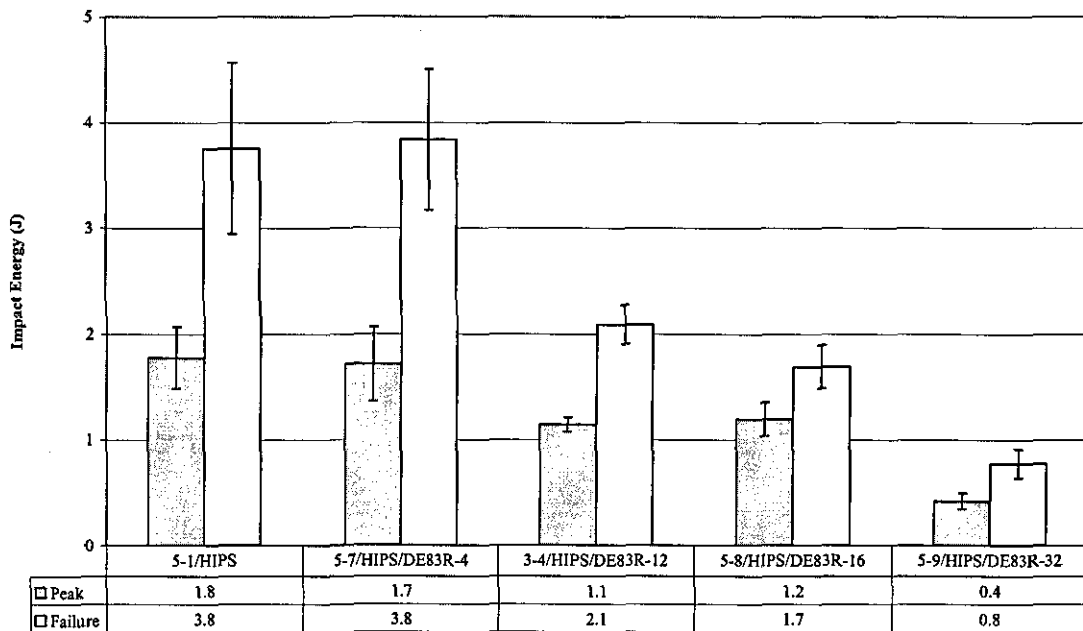
Graph 4.9, Effect of DE83R Loading Level on Impact Peak and Failure Energy of HIPS

	5-1/HIPS	3-8/HIPS/ DE83R-12/RS-3.5	3-11/HIPS/FF-4/DE83R-12/RS-3.5	5-10/HIPS/FF-10/DE83R-12/ RS-4	5-11/HIPS/FF-20/DE83R-12/ RS-4
☐ Peak	1.8	1.2	1.4	1.7	1.1
☐ Force	3.8	2.3	2.5	3.8	4.7

Graph 4.10, Effect of Stereon 840 Impact Modifier Loading Level on Impact Peak and Failure Energy of HIPS, Containing DE83R (12%) and RS (4%)

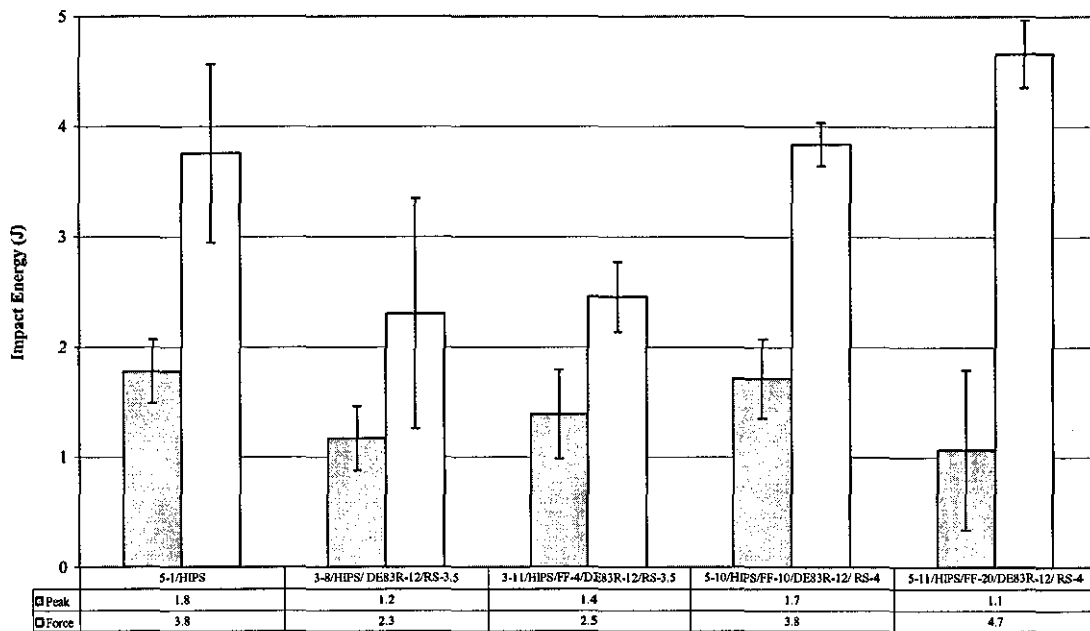|	8-1/PBT	4-3/PBTBC58-12	8-2/PBT/BC58-20	8-5/PBT/BC58-32
☐ Peak	2.3	1.5	1.2	0.9
☐ Failure	6.5	3.5	1.9	1.4
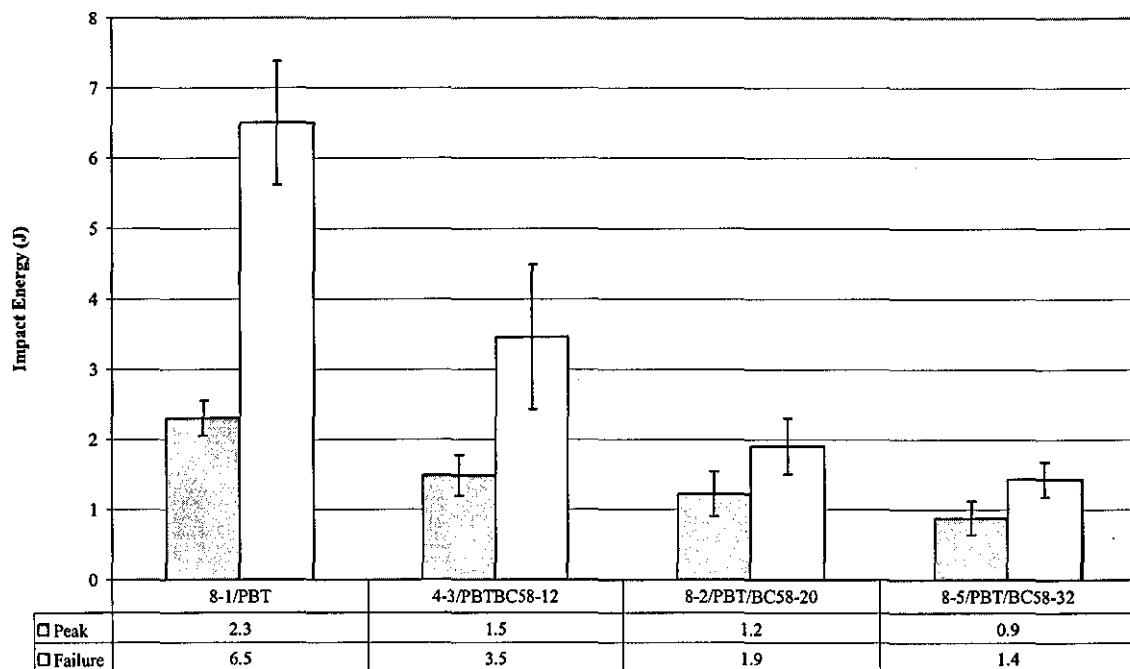
Graph 4.11, Effect of BC58 Loading Level On Peak and Failure Energy of PBT
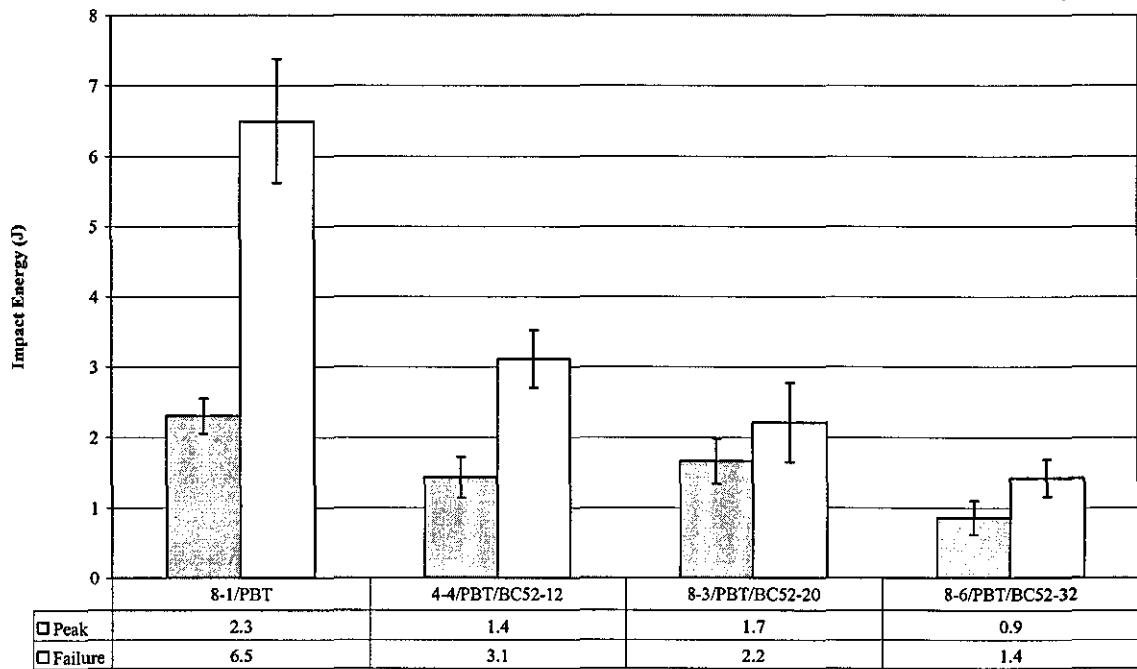
Graph 4.12, Effect of BC52 Loading Level On Peak and Failure Energy of PBT

	8-1/PBT	4-4/PBT/BC52-12	8-3/PBT/BC52-20	8-6/PBT/BC52-32
▢ Peak	2.3	1.4	1.7	0.9
▢ Failure	6.5	3.1	2.2	1.4

	8-1/PBT	4-5/PBT/BC52HP-12	8-4/PBT/BC52HP-20	8-7/PBT/BC52HP-32
▢ Peak	2.30	0.99	0.61	0.48
▢ Failure	6.50	2.73	0.97	0.76
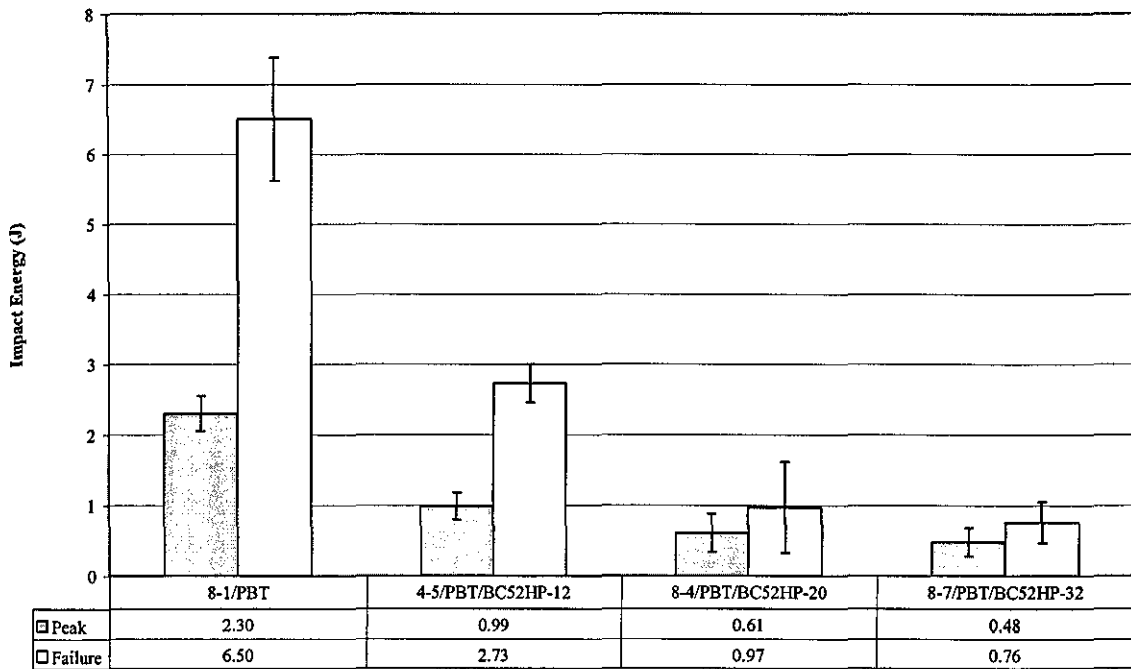
Graph 4.13, Effect of BC52HP Loading Level On Peak and Failure Energy of PBT
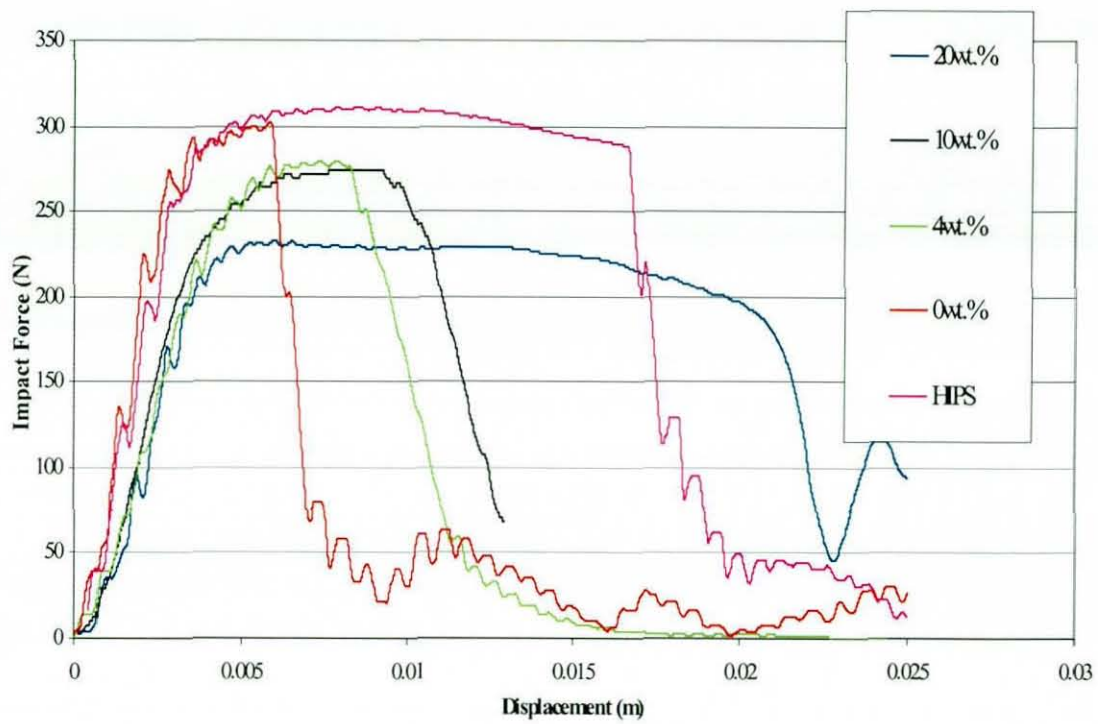
Graph 4.14, Force Displacement Data for HIPS Compounds Containing Stereon Impact Modifier
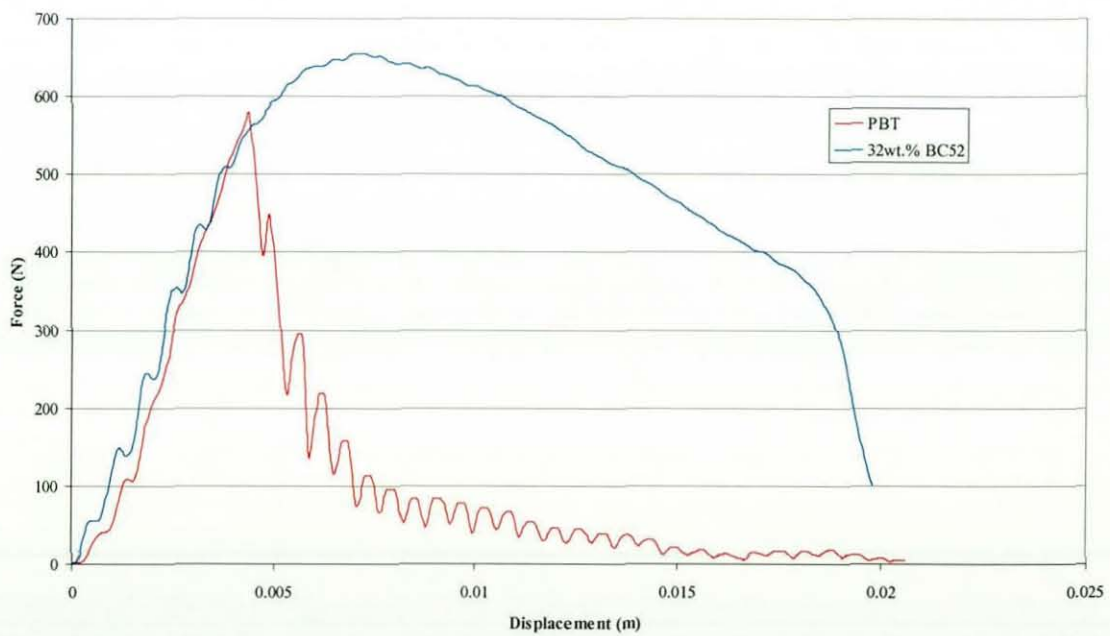
Graph 4.15, Force Displacement Data for Unfilled PBT and 32wt.% Filled PBT

4.7.3 Combined Effect of BFR and Sb$_2$O$_3$

A series of formulations in both HIPS and PBT were compounded using a selection of BFRs and Sb$_2$O$_3$. The additives used for each polymer were chosen because of their compatibility and/or current use in commercial FR grades. Graph 4.16 shows the effect of varying Sb$_2$O$_3$ particle size with DBDPO in HIPS. All of the filled compounds had lower peak and failure energy than unfilled HIPS. Graph 4.17 shows the effect on peak and failure energy of all of the Tetrabromobisphenol A BFRs with RS and TT Sb$_2$O$_3$ in PBT compounds. Large reductions in both peak and failure energy were seen for all of the filled compounds. Differences between the compounds were observed, and mirrored those seen for the BFR and Sb$_2$O$_3$ used individually.

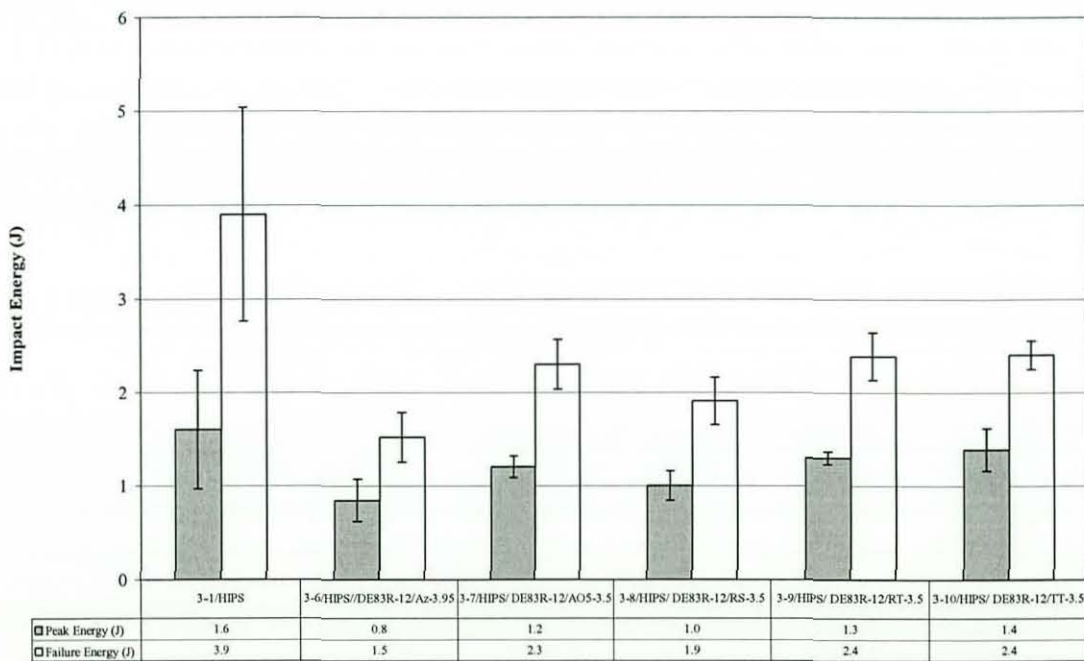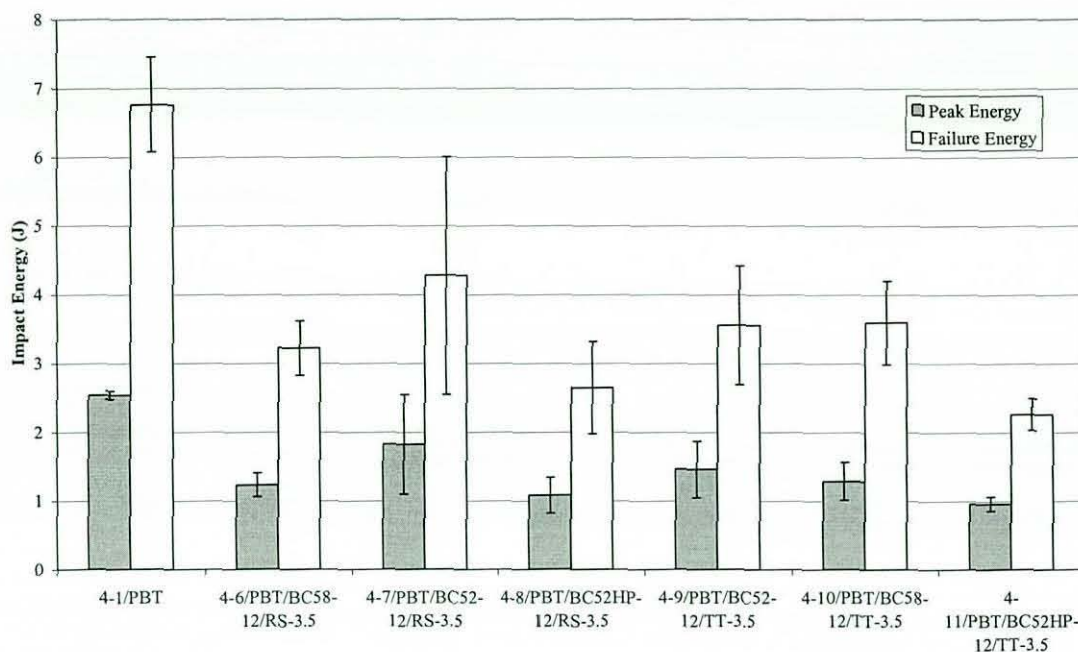|	3-1/HIPS	3-6/HIPS//DE83R-12/Az-3.95	3-7/HIPS/ DE83R-12/AO5-3.5	3-8/HIPS/ DE83R-12/RS-3.5	3-9/HIPS/ DE83R-12/RT-3.5	3-10/HIPS/ DE83R-12/TT-3.5
☐ Peak Energy (J)	1.6	0.8	1.2	1.0	1.3	1.4
☐ Failure Energy (J)	3.9	1.5	2.3	1.9	2.4	2.4

Graph 4.16, Effect of DBDPO and Sb$_2$O$_3$ with Varying Particle Size on Peak and Failure Energy of HIPS

Graph 4.17, Effect of BRF and Sb₂O₃ (RS and TT) on Peak and Failure Energy of PBT

The Fyrebloc materials were compounded in HIPS using a twin screw extruder and also by feeding directly into the injection moulder. This was done to determine any benefits that the Fyrebloc materials might have on dispersion and hence impact properties. Table 4.12 summarises peak and failure energy for the formulations compounded both by twin screw extrusion and through the injection moulder. Also given are the values for the BFR/Sb₂O₃ added directly as powders. The values given in brackets are the standard deviations for each set of results. From the data in Table 4.12 it would appear that the method of manufacture does not affect impact properties

Compound	Peak Energy (J)		Failure Energy (J)	
	APV	Injection Moulder	APV	Injection Moulder
HIPS	1.6 (0.1)	1.2 (0.1)	3.9 (0.4)	3.5 (0.5)
DE83R (12)+RS (4)	1.2 (0.2)	0.7 (0.1)	2.3 (0.1)	1.4 (0.2)
DE83R (12)+RS (4)+PETS (2)	1.4 (0.1)	1.1 (0.1)	2.6 (0.2)	1.8 (0.2)
Fyrebloc 210	1.1 (0.1)	0.8 (0.1)	1.8 (0.3)	1.5 (0.3)
Fyrebloc 211	0.7 (0.1)	1.0 (0.1)	1.5 (0.4)	1.8 (0.3)
Fyrebloc 510	0.6 (0.2)	0.9 (0.1)	1.2 (0.3)	1.4 (0.2)
Fyrebloc 2DB-370S3	0.7 (0.1)	1.0 (0.1)	1.5 (0.2)	2.0 (0.4)

Table 4.12, Comparison of Twin Screw Extrusion and Injection Moulding Fyrebloc Materbatches and Controls in HIPS.

4.7.4 Effect of Carriers on Impact Properties of HIPS

The effect that the carrier waxes have on HIPS has been determined. This was done to determine any effect that they may have on the impact performance of HIPS. Table 4.13, summarises the effect of the carry waxes (Castor and PETS wax) at the loading levels that they have been used at in HIPS. Neither of the two waxes appears to have any effect on the impact performance of HIPS.

Compound ID	Peak Energy (J)	Failure Energy (J)
5-1/HIPS	1.8 (0.1)	3.8 (0.7)
5-2/PETS-2	1.9 (0.2)	3.6 (0.5)
3-2/CW-0.45	1.8 (0.2)	3.7 (0.5)

**Table 4.13 Effect of Carry Waxes On Peak and Failure Energy of HIPS**

4.8 Fracture Toughness

Fracture toughness testing was conducted on a selection of HIPS and PBT compounds to determine the effect of Sb_2O_3 particle size and additive loading level. For the majority of compounds six samples were tested and the standard deviations are shown for all compounds. For each sample tested the initial crack length and P_Q were recorded, and K_C calculate from this, using equation 3.1. The standard deviation was generally between 20 and 30% of the overall value obtained.

In all the fracture toughness tests on HIPS compounds there were concerns about the amount of plastic deformation. The test [75] set limits for the amount of plastic deformation at the crack tip, and for the HIPS compounds this was on the limit. Several of the compounds (those containing impact modifier) did not meet the criteria and so the data obtained could not be used. The majority of results given in this section are within these limits, but this point must be taken into account when analysing them.

4.8.1 Sb_2O_3 Particle Size

The effect of Sb_2O_3 particle size on the fracture toughness of HIPS and PBT compounds has been evaluated. Compounds containing Sb_2O_3 with a particle size range of 0.08µm to 10µm have been tested, at an approximate loading level of 3.5wt.% Sb_2O_3. Graph 4.18 shows the effect of Sb_2O_3 on HIPS whilst 4.19 shows the effect on PBT.
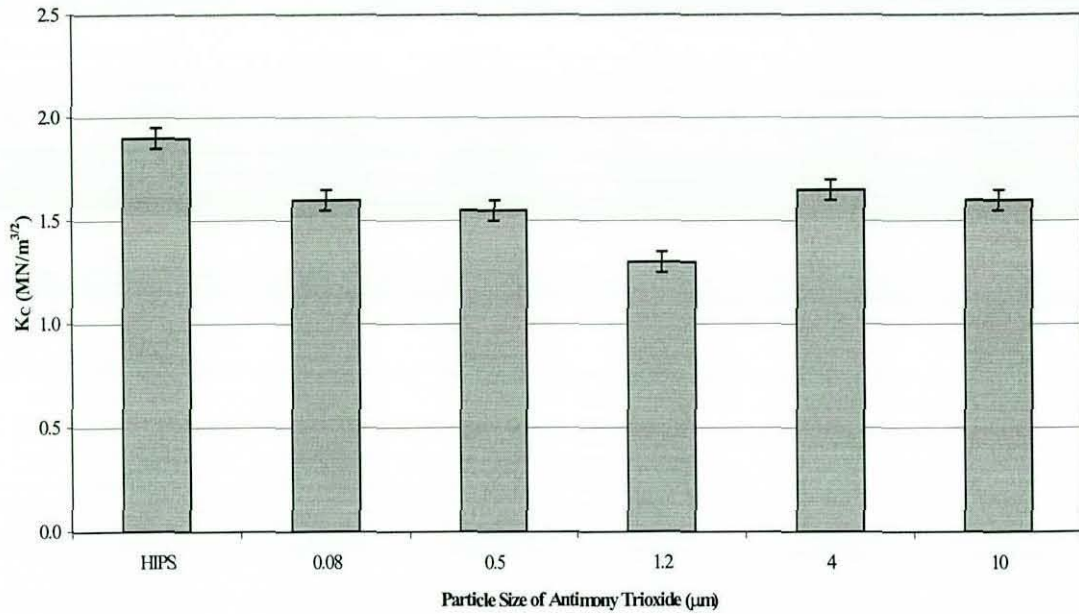
Graph 4.18, Effect of Sb$_2$O$_3$ Particle Size on Fracture Toughness (K$_C$) of HIPS
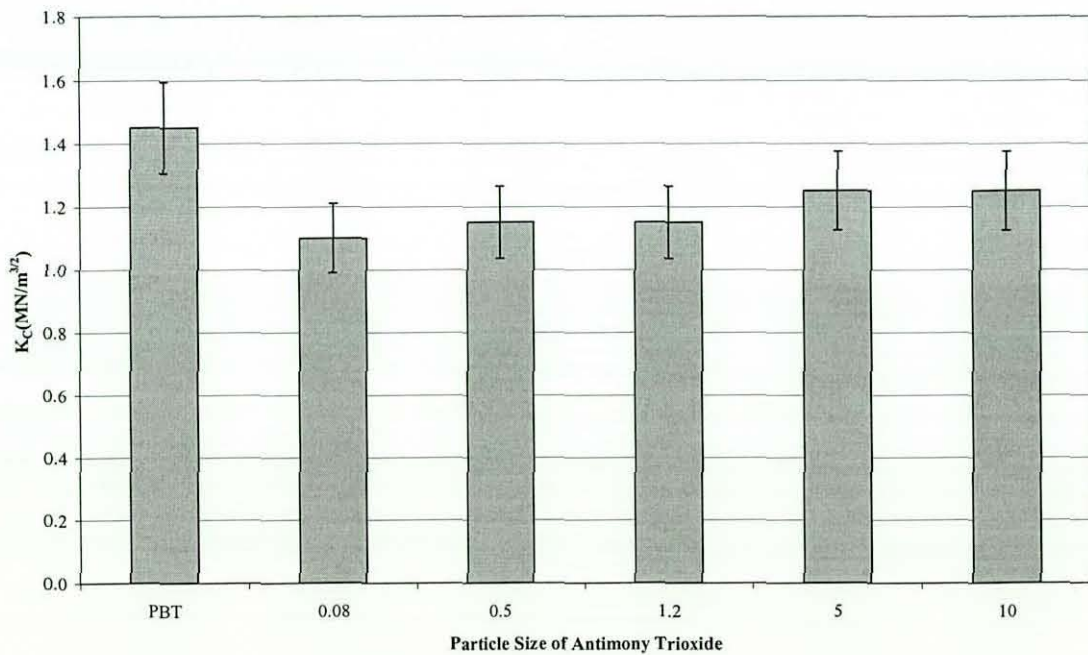
Graph 4.19, Effect of Sb$_2$O$_3$ Particle Size on Fracture Toughness (K$_C$) of PBT

4.8.2 Additive Loading Level

The effect of additive loading level on the fracture toughness K_C values of both HIPS and PBT have been determined. Graphs 4.20 to 4.22 summarise the results obtained from the testing.
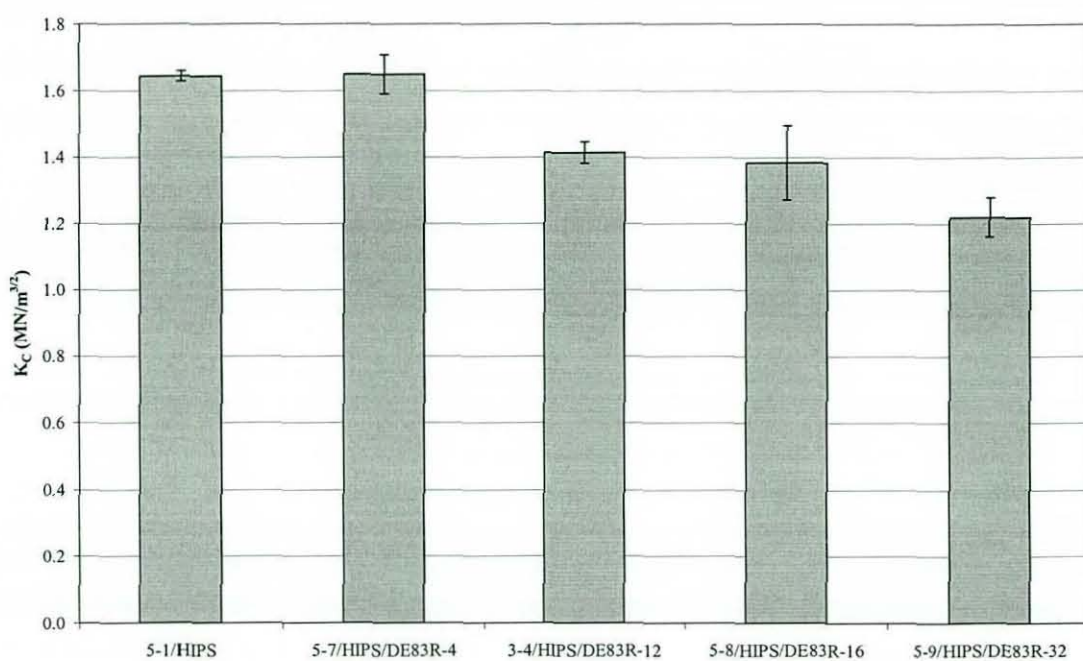
Graph 4.20, Effect of DBDPO Loading Level on Fracture Toughness K_C Values of HIPS
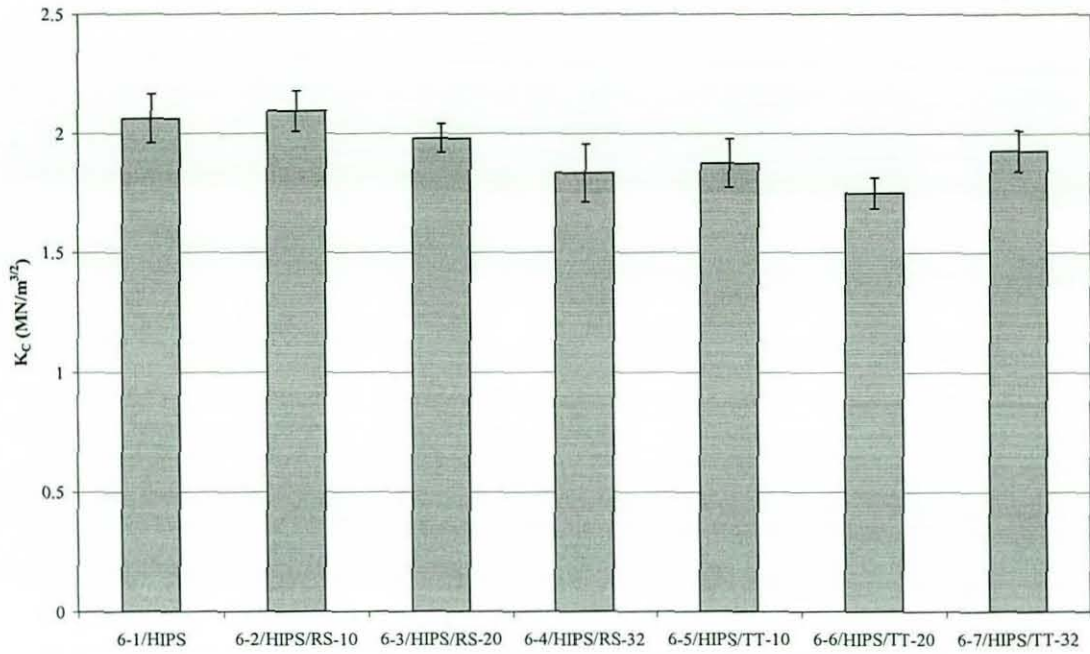
Graph 4.21, Effect of Sb₂O₃ Loading Level on Fracture Toughness K_C Values of HIPS
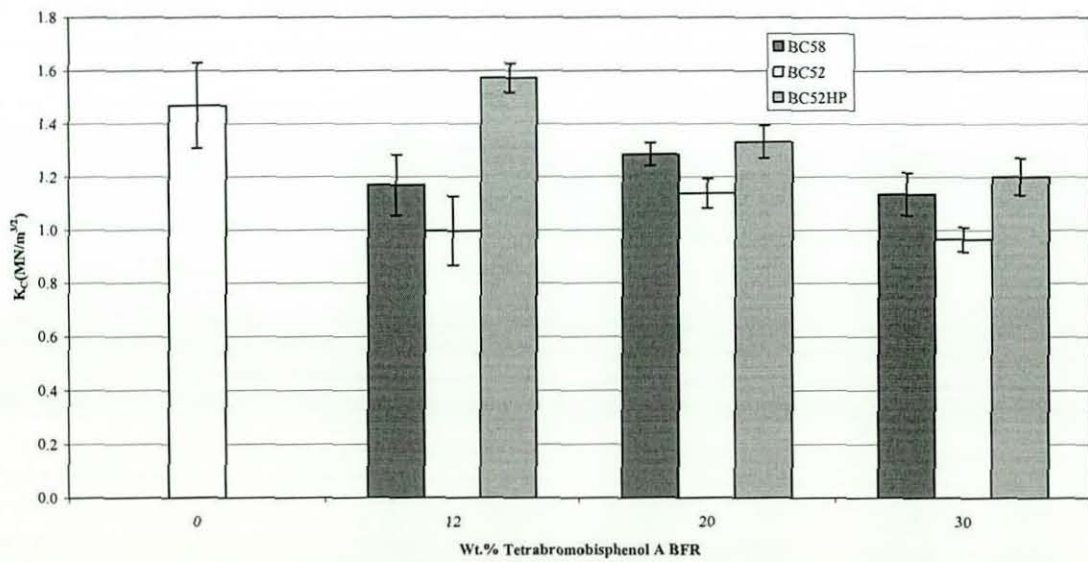
Graph 4.22, Effect of Tetrabromobisphenol A Loading Level on Fracture Toughness K_C Values of PBT

4.8.3 Combined Effect of Sb_2O_3 and BFR

Fracture toughness (K_C) values for a selection of HIPS and PBT compounds containing both Sb_2O_3 and BFR were determined. The results obtained are shown in Graphs 4.23 and 4.24.
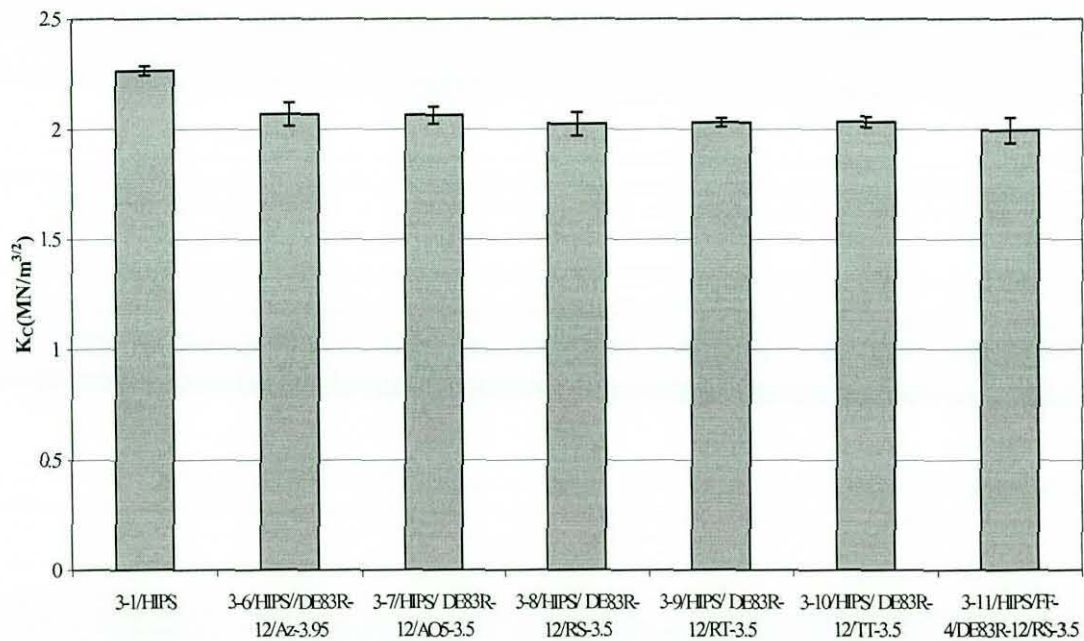
Graph 4.23, Effect of Sb_2O_3 and DBDPO on Fracture Toughness K_C Values of HIPS
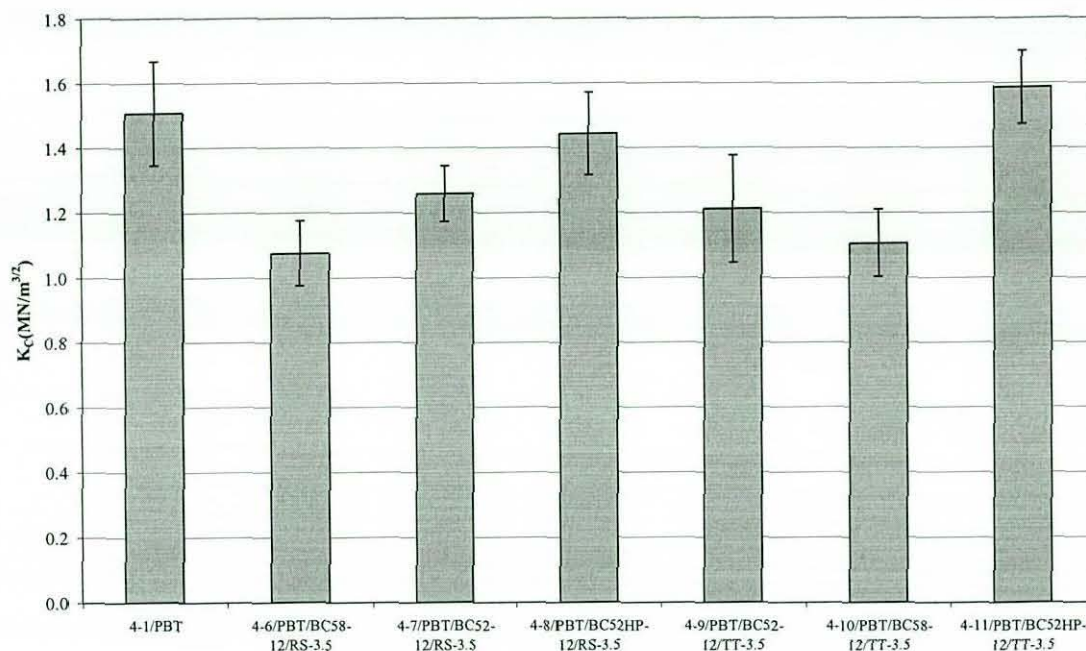
Graph 4.24, Effect of Sb$_2$O$_3$ and Tetrabromobisphenol A on Fracture Toughness K$_C$ Values of PBT

4.9 Tensile Properties

Three different tensile properties of both unfilled and compounds containing FR additives are grouped together in this section, these are strain at break, tensile strength and Young's modulus. The following tables summarise the average values obtained for both HIPS and PBT compounds. The effect of the FR additives was generally smaller than that for impact properties, therefore a selection of compounds have been tested. The majority of the results are presented in tabular form, the numbers in brackets are the standard deviations of each set of compounds. For tensile strength and Young's modulus these values were quite small, from 5 to 20%, but for strain at break they were up to 50%.

4.9.1 Sb_2O_3 Particle Size

The effect of Sb_2O_3 particle size, at 3.5wt.% loading level, on tensile properties was minimal. Tables 4.14 and 4.15 summarise the effect of Sb_2O_3 on strain at break, tensile strength and Young's modulus for HIPS and PBT.

Compound ID	Strain at Break (%)	Maximum Stress (MPa)	Young's Modulus (MPa)
1-1/HIPS	38.0 (1.2)	24.9 (1.8)	1567 (45)
1-2/HIPS/Az-4.14	30.0 (1.0)	22.6 (1.7)	1534 (67)
1-3/HIPS/AO5-3.6	27.9 (1.8)	23.6 (1.5)	1599 (23)
1-4/HIPS/RS-3.6	25.1 (1.8)	22.7 (1.3)	1508 (78)
1-5/HIPS/RT-3.6	34.0 (1.3)	23.5 (1.6)	1499 (89)
1-6/HIPS/TT-3.6	32.0 (1.4)	22.9 (1.3)	1634 (47)

Table 4.14, Effect of Sb_2O_3 Particle Size on the Tensile Properties of HIPS

Compound ID	Strain at Break (%)	Maximum Stress (MPa)	Young's Modulus (MPa)
2-1/PBT	14.2 (1.5)	60.1 (1.2)	1850 (35)
2-2/PBT/Az-3.95	9.6 (1.0)	64.4 (1.5)	1865 (58)
2-3/PBT/AO5-3.5	10.9 (0.8)	65.6 (1.8)	1872 (65)
2-4/PBT/RS-3.5	10.6 (2.0)	63.0 (1.3)	1855 (34)
2-5/PBT/RT-3.5	11.8 (1.4)	62.4 (1.9)	1878 (78)
2-6/PBT/TT-3.5	12.5 (1.8)	65.2 (1.3)	1868 (56)

Table 4.15, Effect of Sb_2O_3 Particle Size on the Tensile Properties of PBT

4.9.2 Loading Level

The effect of increasing loading levels of several additives on tensile properties was determined. The results for tensile strength, Young's modulus, and strain at break are summarised for this section in Tables 4.16 to 4.19. Graph 4.25 shows a typical stress/strain curve for HIPS, and HIPS compounds containing varying Sb_2O_3 TT loading levels. Graph 4.26 shows a typical stress/strain curve for PBT and PBT compounds containing varying BC52 loading levels.

Compound ID	Strain at Break (%)	Maximum Stress (MPa)	Young's Modulus (MPa)
5-1/HIPS	35.0 (1.2)	24.1 (1.8)	1500 (55)
5-7/HIPS/DE83R-4	34.8 (1.9)	23.7 (1.2)	1589 (49)
3-4/HIPS/DE83R-12	30.4 (1.2)	22.1 (0.9)	1552 (34)
5-8/HIPS/DE83R-16	24.3 (1.7)	21.6 (2.0)	1608 (67)
5-9/HIPS/DE83R-32	13.2 (1.9)	22.8 (1.6)	1548 (29)

Table 4.16, Effect of DBDPO loading Level on Tensile Properties of HIPS

| Compound ID	Strain at Break (%)	Maximum Stress (MPa)	Young's Modulus (MPa)
5-1/HIPS	35.0 (1.6)	23.9 (1.5)	1545 (55)
3-11/HIPS/FF-4/DE83R-12/RS-3.5	28.4 (1.8)	23.5 (1.3)	1516 (46)
5-10/HIPS/FF-10/DE83R-12/ RS-4	27.4 (2.5)	22.1 (1.8)	1589 (26)
5-11/HIPS/FF-20/DE83R-12/ RS-4	27.9 (2.3)	21.9 (1.5)	1601 (59)

Table 4.17, Effect of Stereon 840 Impact Modifier loading Level on Tensile Properties of FR HIPS

Compound ID	Strain at Break (%)	Maximum Stress (MPa)	Young's Modulus (MPa)
8-1/PBT	12.9 (0.8)	59.9 (0.4)	1739 (44)
4-3/PBT/BC58-12	9.5 (1.5)	61.7 (0.9)	1841 (50)
4-4/PBT/BC52-12	10.2 (2.0)	62.0 (05)	1867 (51)
4-5/PBT/BC52HP-12	9.0 (1.0)	60.9 (0.2)	1818 (85)
8-2/PBT/BC58-20	6.8 (0.5)	64.0 (1.2)	1837 (39)
8-3/PBT/BC52-20	5.3 (0.1)	63.4 (0.5)	1876 (58)
8-4/PBT/BC52HP-20	4.9 (0.4)	54.2 (4.2)	1896 (93)
8-5/PBT/BC58-32	5.3 (0.5)	56.6 (5.2)	1769 (59)
8-6/PBT/BC52-32	5.4 (0.3)	54.2 (3.5)	1786 (41)
8-7/PBT/BC52HP-32	5.8 (0.3)	55.2 (1.2)	1772 (63)

Table 4.18, Effect of Tetrabromobisphenol A Loading Level and Type on Tensile Properties of PBT

Compound ID	Strain at Break (%)	Maximum Stress (MPa)	Young's Modulus (MPa)
6-1/HIPS	35.3(1.2)	23.7(1.5)	1450 (105)
6-2/HIPS/RS-10	23.3 (2.1)	24.0 (1.8)	1549 (45)
6-3/HIPS/RS-20	18.6 (1.5)	23.2 (1.6)	1525 (67)
6-4/HIPS/RS-32	11.6 (1.2)	23.3 (0.9)	1780 (45)
6-5/HIPS/TT-10	24.6 (1.7)	23.0 (2.0)	1465 (78)
6-6/HIPS/TT-20	18.7(1.4)	22.9 (1.3)	1628 (89)
6-7/HIPS/TT-32	13.2(1.8)	21.5 (1.1)	1682 (45)

Table 4.19, Effect of Sb_2O_3 Loading Level and Type on Tensile Properties of FR HIPS
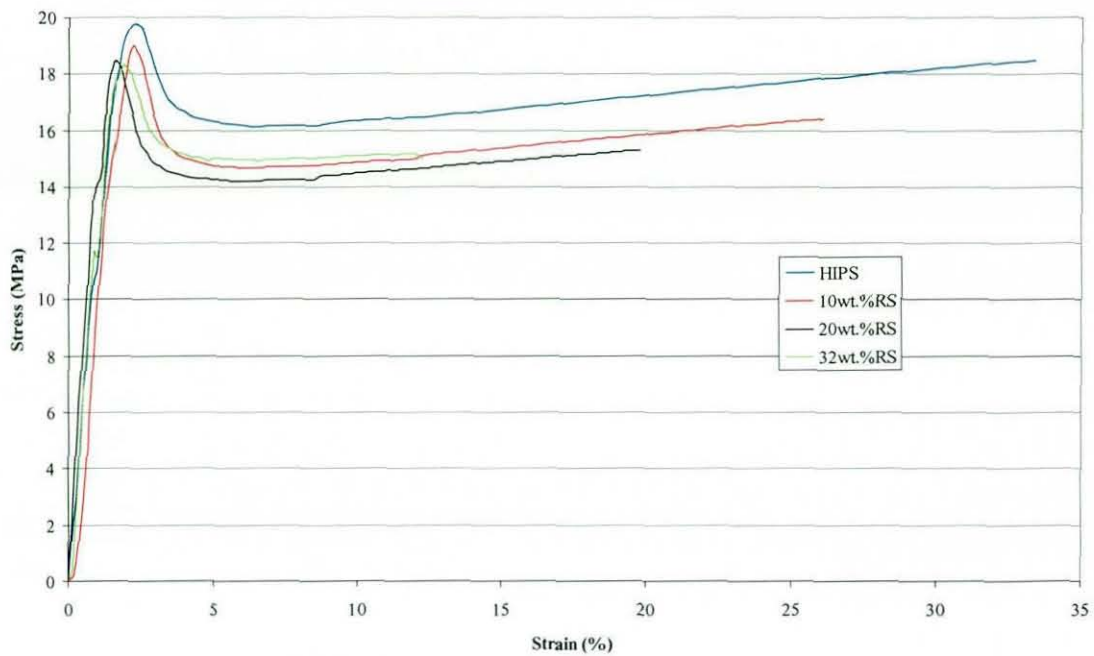
Graph 4.25, Stress/Strain Curves for HIPS Compounds with Varying Loading Levels of RS
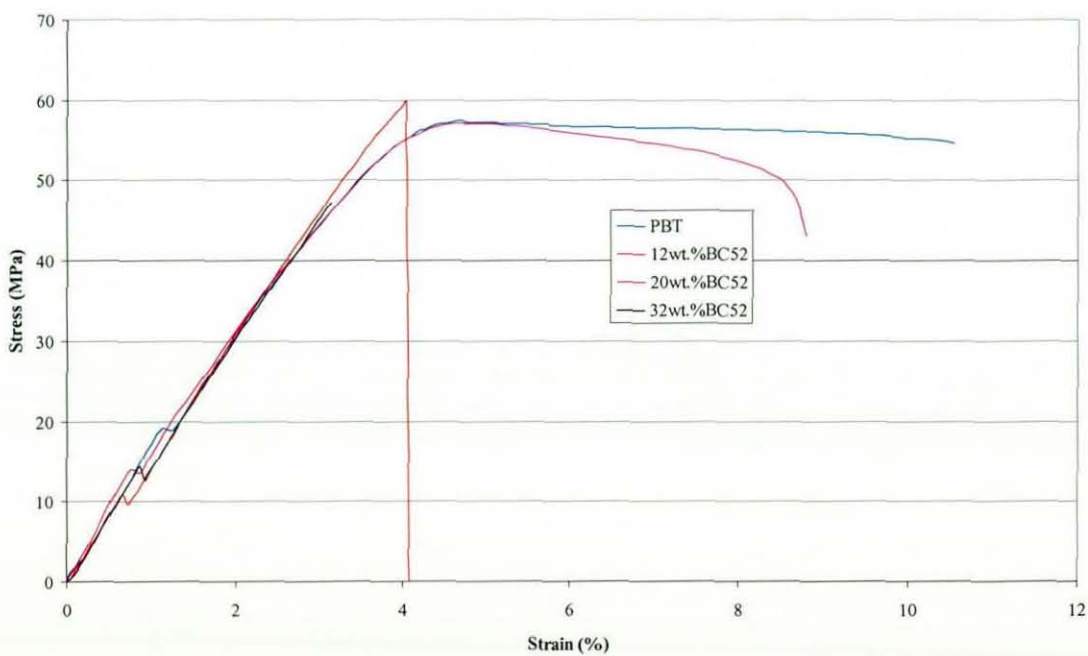
Graph 4.26, Stress/Strain Curves for PBT Compounds with Varying Loading Levels of BC52

4.10 Flame Retardancy

Flame testing has been conducted on unfilled PBT and HIPS, and compounds containing both Sb_2O_3 and BFR at loading levels required to produce high levels of flame retardancy. The results in this section summarise those obtained for UL94 and LOI for both HIPS and PBT. For the LOI data a single number has been quoted, for the UL94 results other observation such as burn times and dripping are given as well as the UL94 value that this equates to.

4.10.1 HIPS

LOI and UL94 testing, on HIPS compounds can be divided into three groups, HIPS compounds containing traditional FR formulations, Fyrebloc compounds, and those containing impact modifier. LOI testing was not conducted on the Fyrebloc compounds, as this testing was done to determine the effect of additive dispersion, and LOI was not sensitive to this variable. The results obtained are summerised in Tables 4.20 to 4.22.

Compound ID	LOI (%)	UL94		
		Rating	Total Burn Time (s)	Comments
3-1/HIPS	17	Fail	<300	Flaming Drip
3-6/HIPS//DE83R-12/Az-3.95	25.8	V-0	6	-
3-7/HIPS/ DE83R-12/AO5-3.5	25.1	V-0	8	-
3-8/HIPS/ DE83R-12/RS-3.5	25.9	V-0	77	Non Flaming
3-9/HIPS/ DE83R-12/RT-3.5	25.8	V-2	45	Flaming Drip
3-10/HIPS/ DE83R-12/TT-3.5	25.5	V-0	115	-

Table 4.20, LOI and UL94 Results for Flame Retardant HIPS Compounds.

Compound ID	LOI (%)	UL94		
		Rating	Total Burn Time (s)	Comments
5-1/HIPS	17	V-2	<300	Flaming drips
3-8/HIPS/ DE83R-12/RS-3.5	25.8	V-0	44	Non flaming drips
5-10/HIPS/FF-10/DE83R-12/ RS-4	24.8	V-0	77	Non Flaming drips
5-11/HIPS/FF-20/DE83R-12/ RS-4	26.1	V-2	115	flaming drips

Table 4.21, Effect of Impact Modifier On FR Properties of HIPS

Compound ID	UL94		
	Rating	Total Burn Time (s)	Comments
7-1/HIPS	Fail	<300	Flaming drips
7-2/HIPS/DE83R-12/ RS-4	Fail	150	Flaming drips
7-3/HIPS/ DE83R-12/ RS-4/PETS-1.6	Fail	100	Flaming drips
7-4/HIPS/Fyre211-18	V-0	58	
7-5/HIPS/Fyre210-18	V-0	63	Non flaming drips
7-6/HIPS/Fyre510-18	V-0	47	
7-7/HIPS/Fyre2DB-370S3-18	V-0	103	Non flaming drips
9-2/HIPS/Fyre210-18	Fail	152	Flaming drips
9-3/HIPS/Fyre510-18	Fail	281	Flaming drips
9-4/HIPS/Fyre211-18	V-0	58	
9-5/HIPS/Fyre2DB-370S3-19.2	V-0	87	Non flaming drips

Table 4.22, Effect of Fyrebloc Masterbatches and Compounding Method on UL94 Results of HIPS

4.10.2 PBT

Flammability of PBT compounds has consisted of LOI and UL94 testing of compounds 4-1 and 4-6 to 4-11. This data is summarised in Table 2.23.

Compound ID	LOI (%)	UL94		
		Rating	Total Burn Time (s)	Comments
4-1/PBT	21.4	V-2	<300	Flaming drips
4-6/PBT/BC58-12/RS-3.5	30.0	V-0	0	Non flaming drips
4-7/PBT/BC52-12/RS-3.5	29.8	V-0	0	Non flaming drips
4-8/PBT/BC52HP-12/RS-3.5	29.6	V-0	0	Non flaming drips
4-9/PBT/BC58-12/TT-3.5	29.6	V-2	0	Non flaming drips
4-10/PBT/BC52-12/TT-3.5	30.2	V-0	0	Non flaming drips
4-11/PBT/BC52HP-12/TT-3.5	29.4	V-0	0	Non flaming drips

Table 4.23, LOI and UL94 Results for PBT Compounds.

4.11 Additive Morphology

Both SEM and STEM analysis has been used to primarily determine the additive morphology but also to confirm the particle size data obtained from the laser particle results. Plates 4.1 to 4.10 are either SEM or STEM images of the additives used in this work, a scale in μm has been attached to each plate. The magnification has been chosen to show the greatest detail for each filler, this means it varies vary for several of the plates.

This analysis was conducted to allow both the size and morphology of the additives to be determined before being compounded into the polymers matrix, which would allow any aggregate or agglomerate formed during processing to be identified. Also it helped in allowing the particles to be identified once they had been processed, by relating particles present in the final compounds to those shown in this section. As the Azub material used did not contain individual Sb_2O_3 particles, but a more complicated structure both a high and low magnification have been shown (Plates 4.1 and 4.2). For the majority of the samples it has been possible to obtain clear images, which allows the particles to be identified.
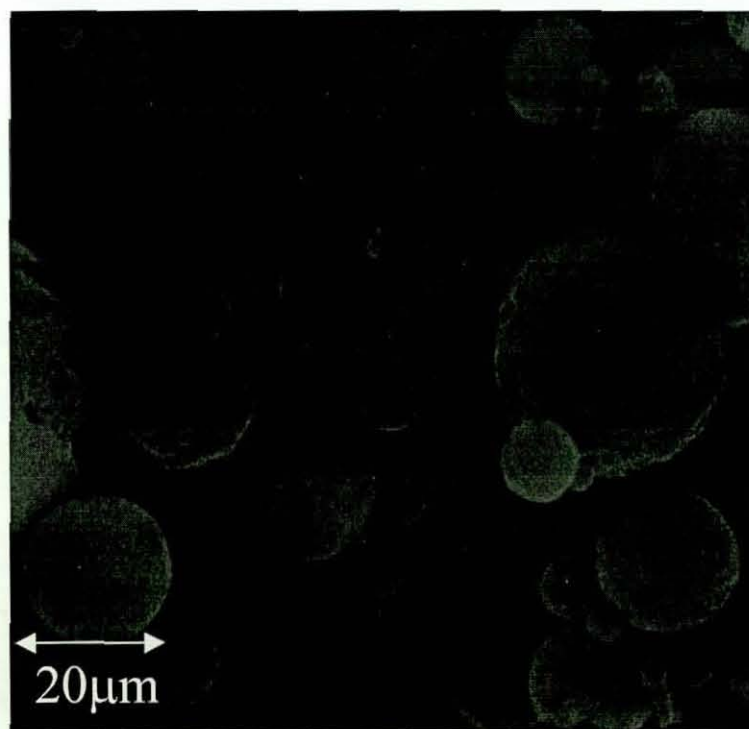

Plate 4.1, STEM Image of Azub Sb_2O_3 material.
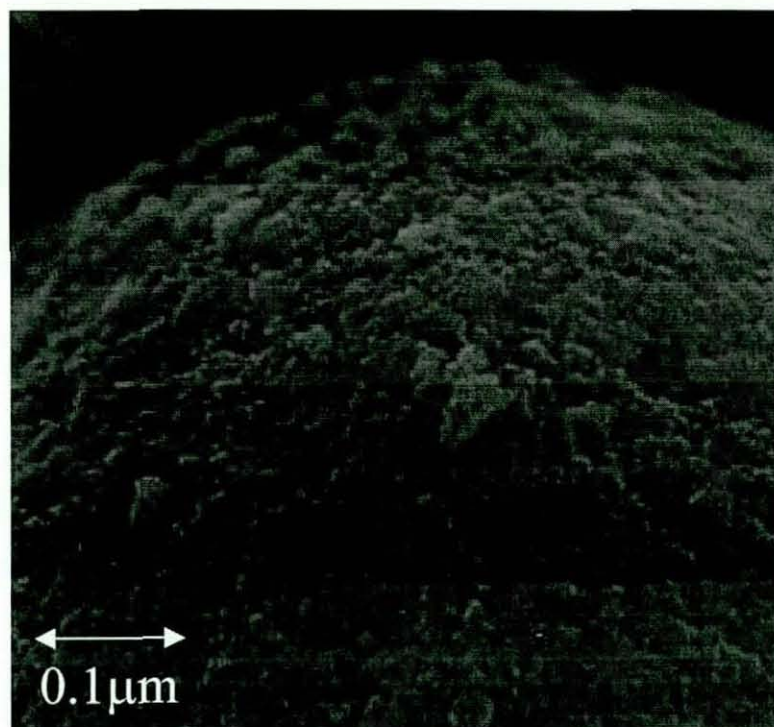
Plate 4.2, STEM Image of Azub Sb$_2$O$_3$ Surface.
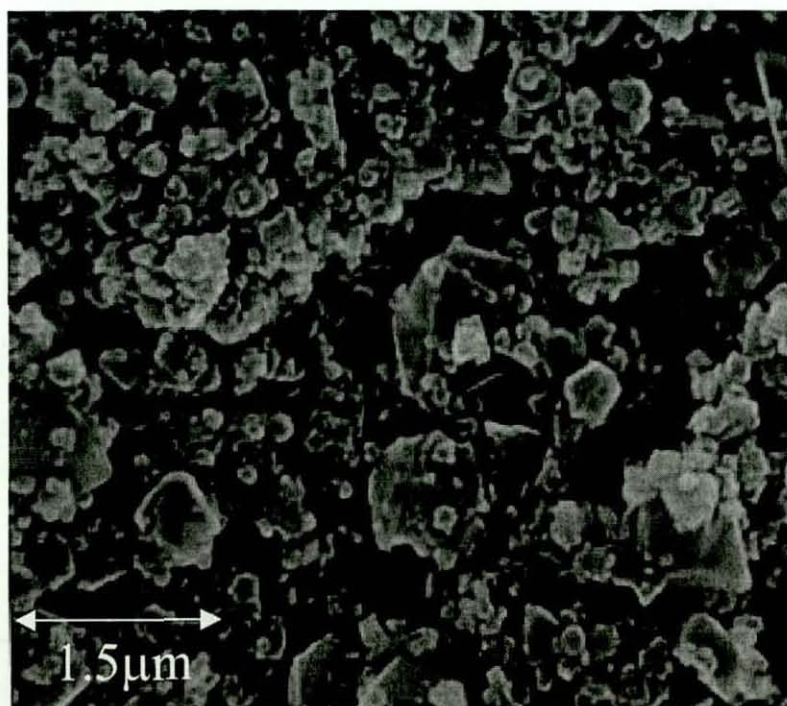
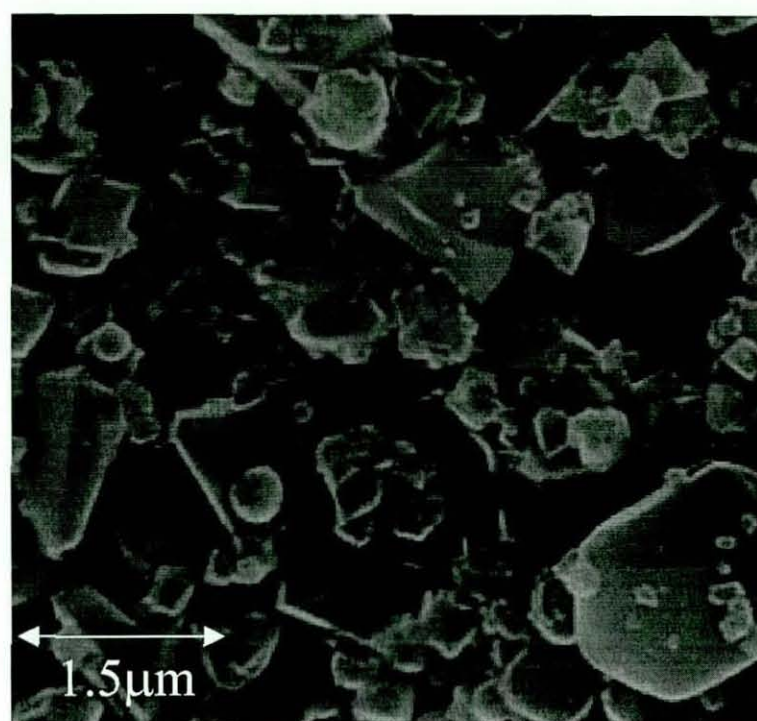**Plate 4.3, STEM Image of A05 Grade of Sb$_2$O$_3$**

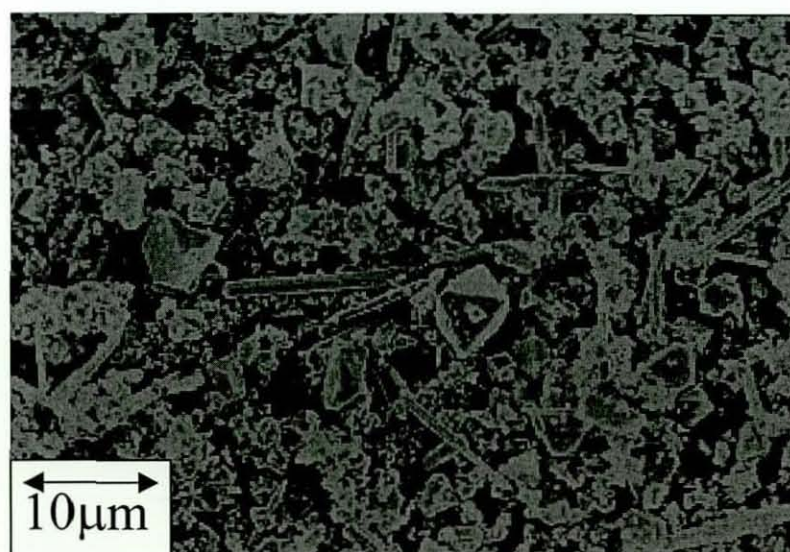**Plate 4.4, STEM Image of RS Grade of Sb$_2$O$_3$**

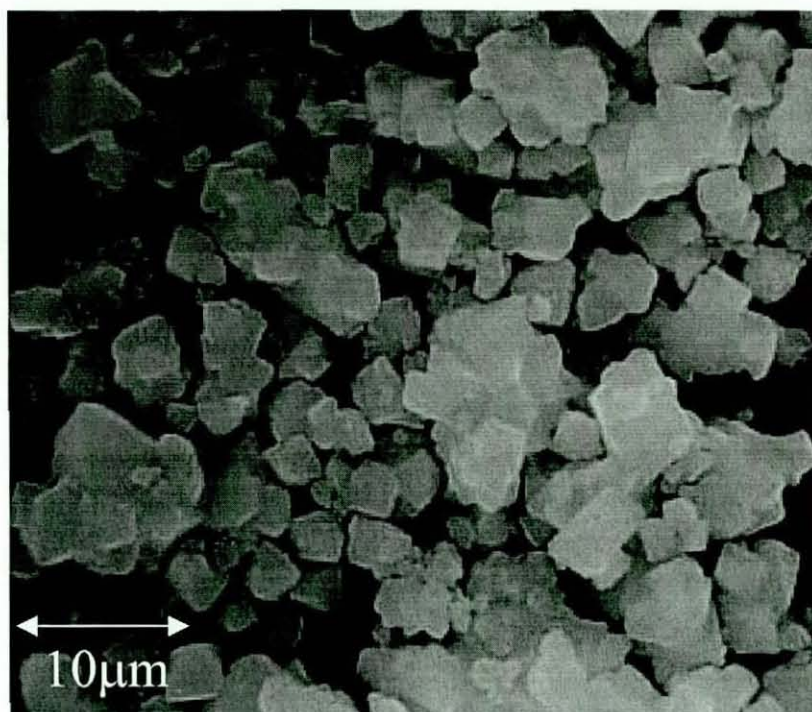**Plate 4.5, SEM Image of TT Grade of Sb$_2$O$_3$**

Plate 4.6, STEM Image of RT Grade of Sb_2O_3

Plate 4.7, SEM Image of BC52 Grade of Tetrabromobisphenol A
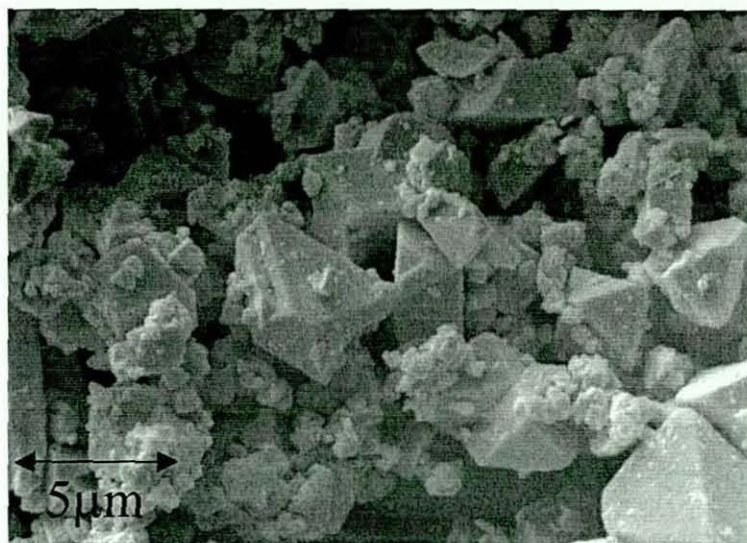
Plate 4.8, SEM Image of BC58 Grade of Tetrabromobisphenol A
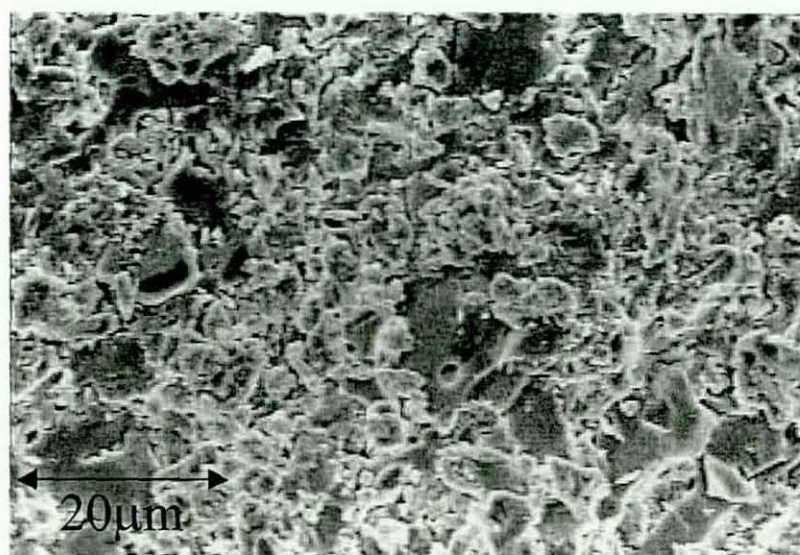
Plate 4.9, SEM Image of BC52HP Grade of Tetrabromobisphenol A
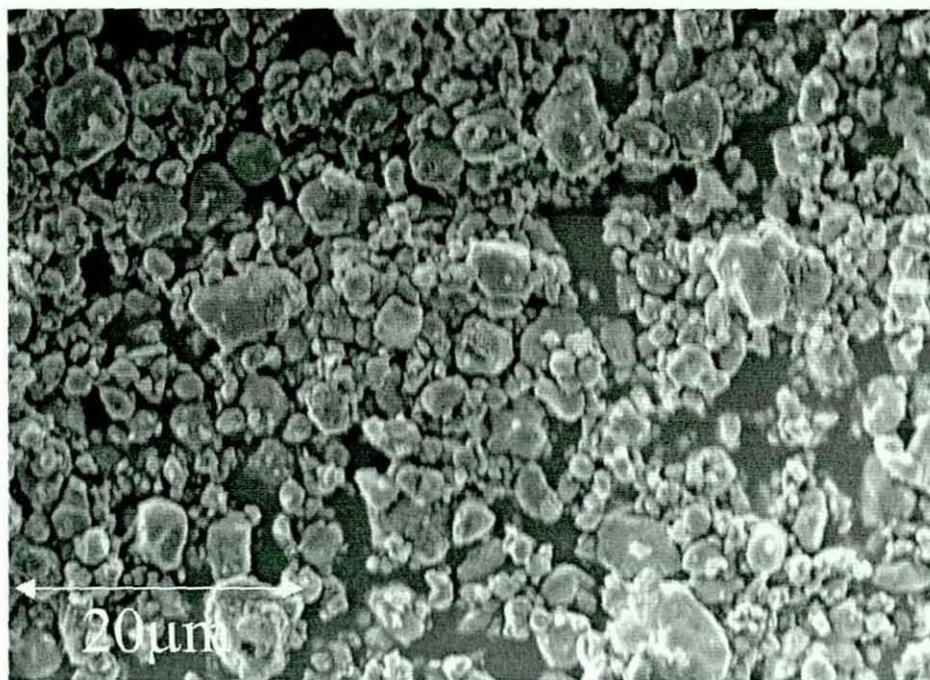
Plate 4.10, SEM Image of DBDPO BFR.

4.12 SEM Examination of Polymer Compounds

A SEM examination has been conducted of both HIPS and PBT compounds impact fracture surfaces. This was primarily to determine the additive dispersion, but the effect of additives on fracture surfaces has also been determined for the HIPS compounds. To determine additive dispersion and morphology in the polymers matrix, the SEM was used in back scattered mode, which showed the additives as bright white areas whilst the polymer matrix was a grey colour. A selection of HIPS and PBT compounds have been examined using this method. The plates shown in this section summarise the results. Plates 4.11 to 4.17 show examples of HIPS and PBT compounds containing Sb_2O_3 or BFR.
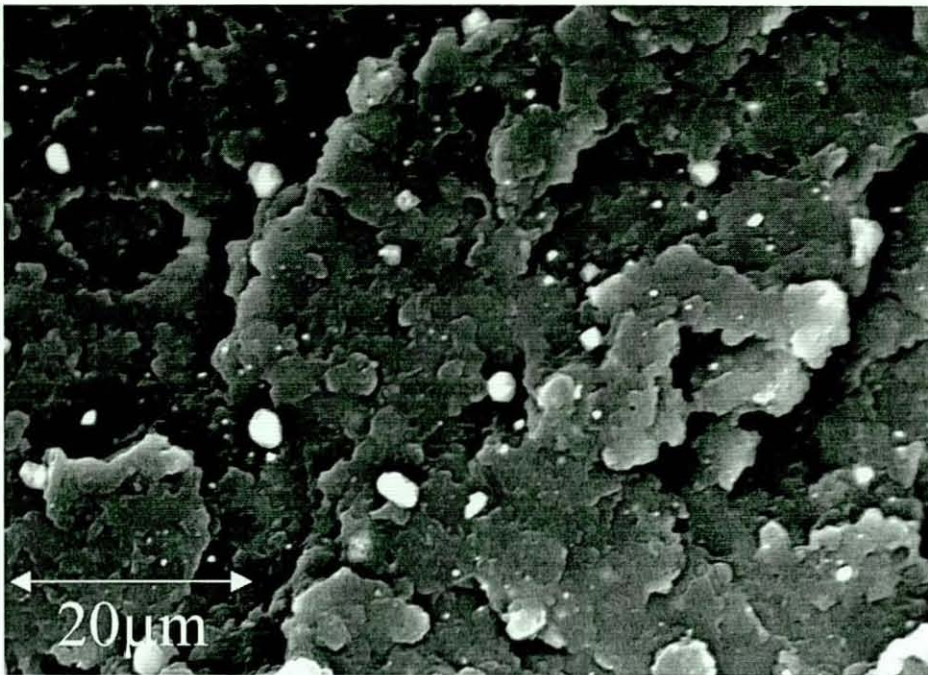
Plate 4.11, Back Scattered SEM Image of HIPS Containing 4wt.% RS.
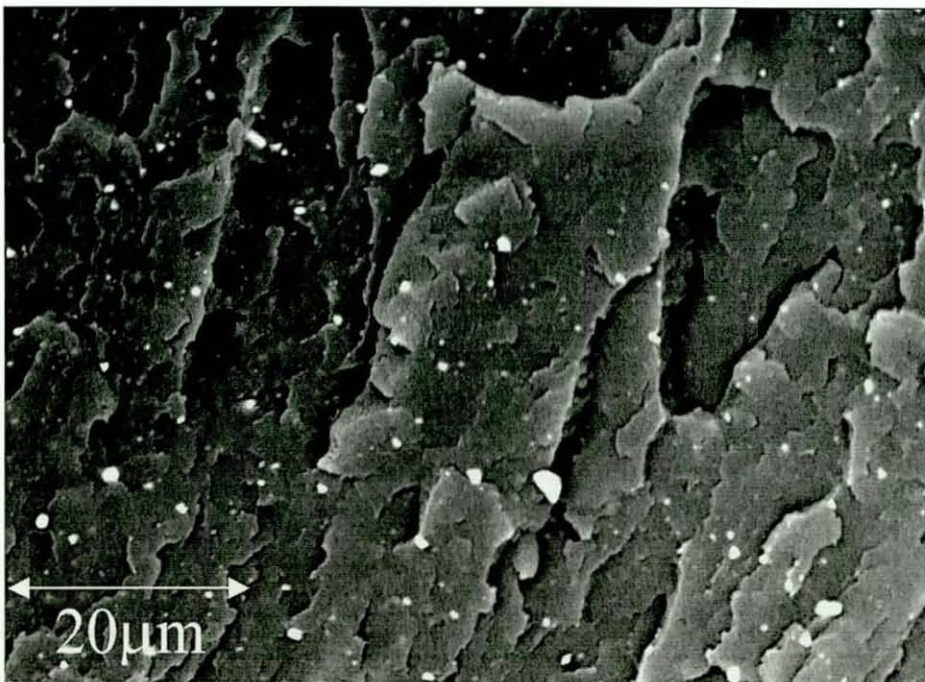
Plate 4.12, Back Scattered SEM Image of PBT Containing 4wt.% RS.
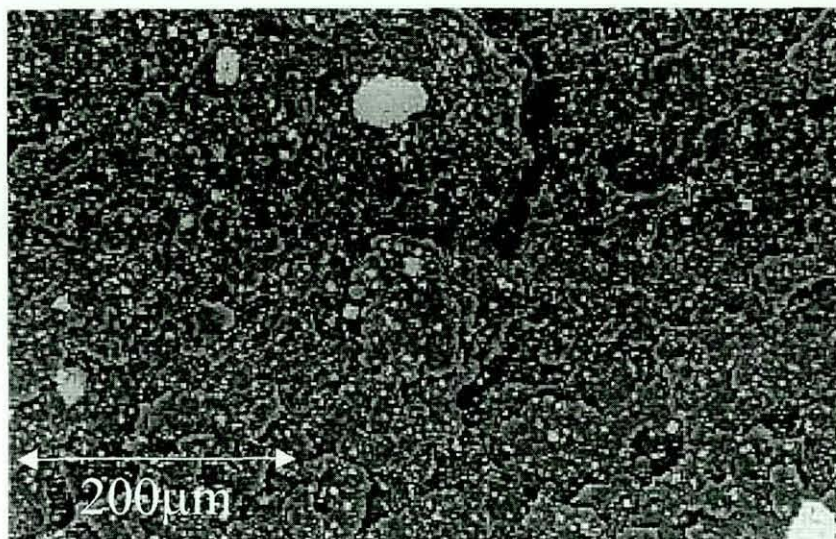
Plate 4.13, Back Scattered SEM Image of HIPS Containing 12wt.% DBDPO
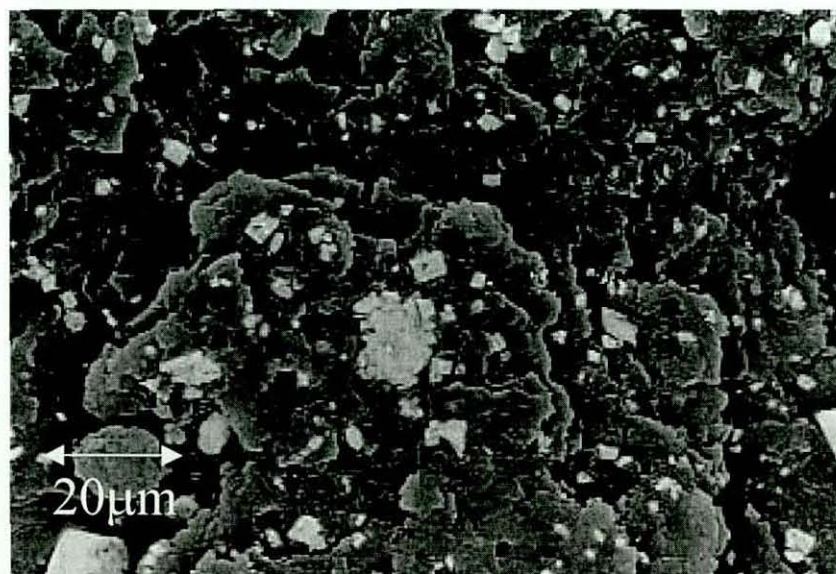
Plate 4.14, Back Scattered SEM Image of HIPS Containing 12wt.% DBDPO
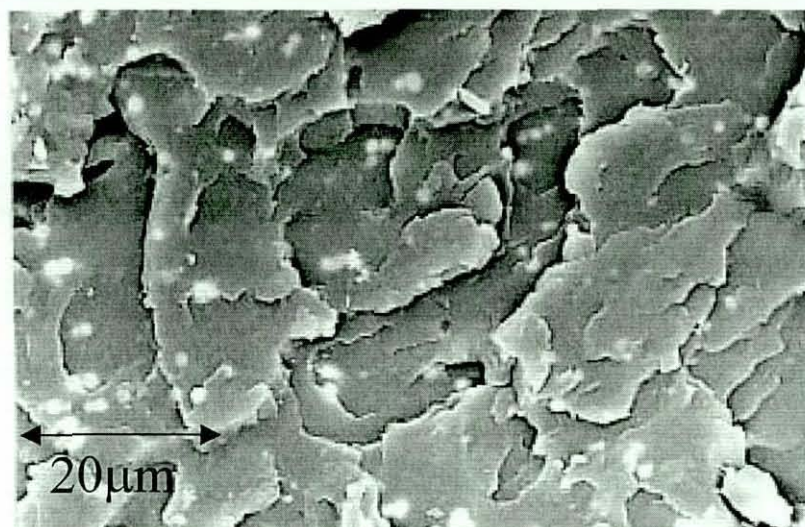
Plate 4.15, Back Scattered SEM Image of PBT Containing 12wt.% BC52
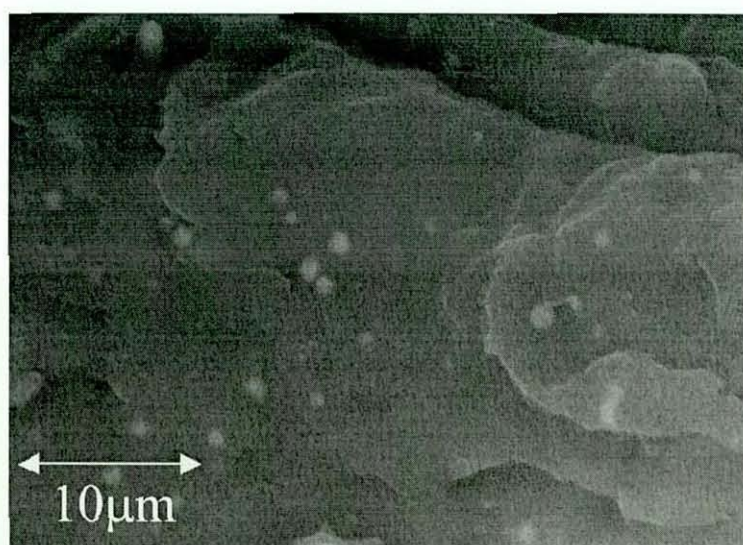
Plate 4.16, Back Scattered SEM Image of PBT Containing 12wt.% BC58
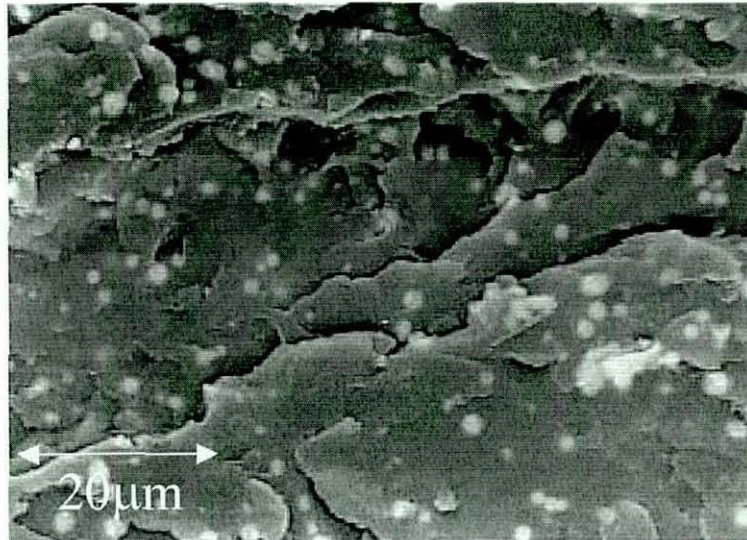
Plate 4.17, Back Scattered SEM Image of PBT Containing 12wt.% BC52HP

Plates 4.18 and 4.19 are PBT compounds containing both Sb_2O_3 and Tetrabromobisphenol A based BFRs. It was possible to determine both the Sb_2O_3 and BFR using this method for the vast majority of the PBT compounds. In the PBT compounds in Plates 4.11 to 4.19 the Sb_2O_3 shows up as brighter white region than the Tetrabromobisphenol A compounds. The additives used have been labelled in Plates 4.18 and 4.19.
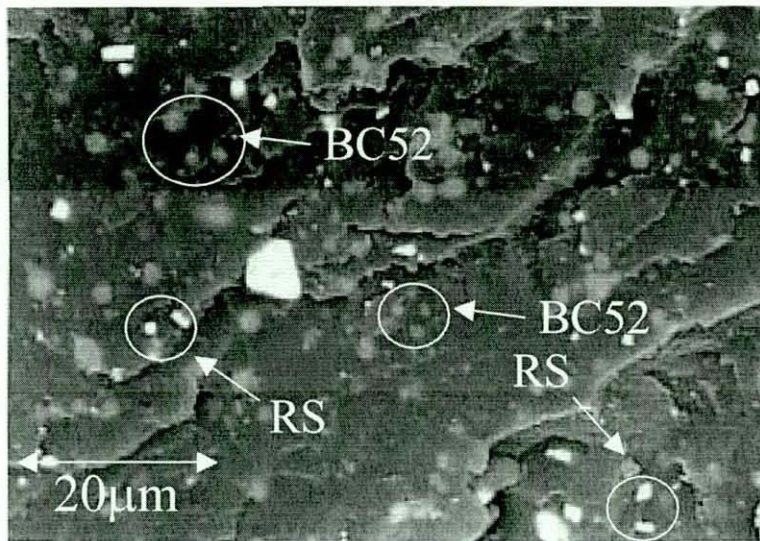
Plate 4.18, Back Scattered SEM Image of PBT Containing 12wt.% BC52 and 4wt.%RS
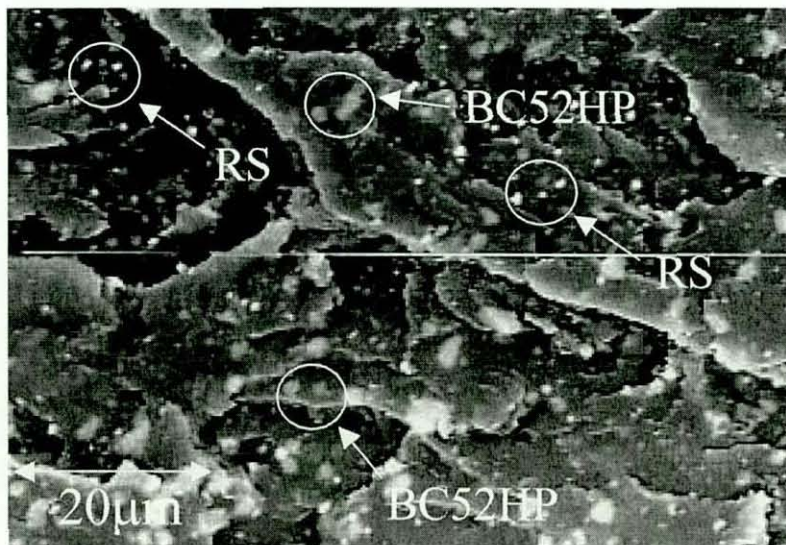
Plate 4.19, Back Scattered SEM Image of PBT Containing 12wt.% BC52HP and 4wt.%RS

Plates 4.20 to 4.27 show a selection of HIPS formulations containing Sb_2O_3 RS and DBDPO BFR based formulations. The plates shown, show the effect of processing and use of masterbatches on additive dispersion. Both low magnification images, to evaluate dispersion, and high magnification images, to identify any agglomerates or aggregates present, have been shown of each of these compounds.
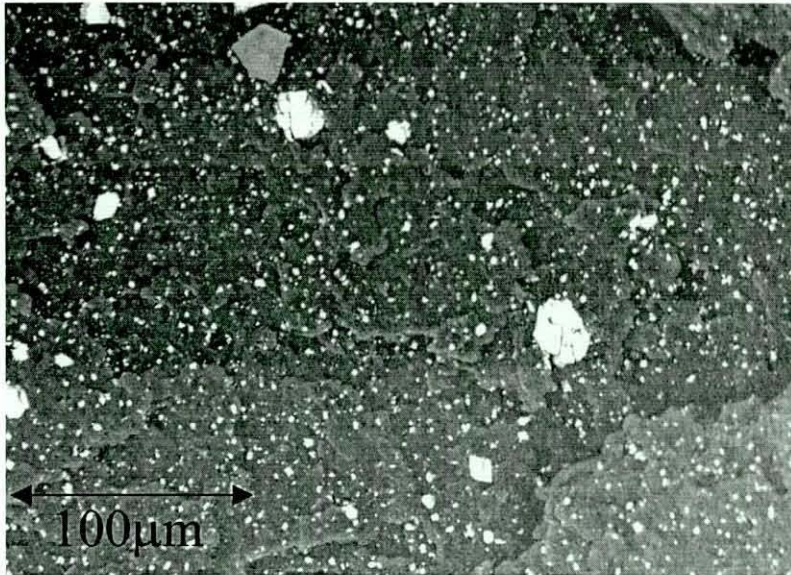
Plate 4.20, Back Scattered SEM Image of HIPS Containing 12wt.% DBDPO and 4wt.% RS Compounded Using A Twin Screw Extruder

Plate 4.21, Back Scattered SEM Image of HIPS Containing 12wt.% DBDPO and 4wt.% RS Compounded Using An Twin Screw Extruder
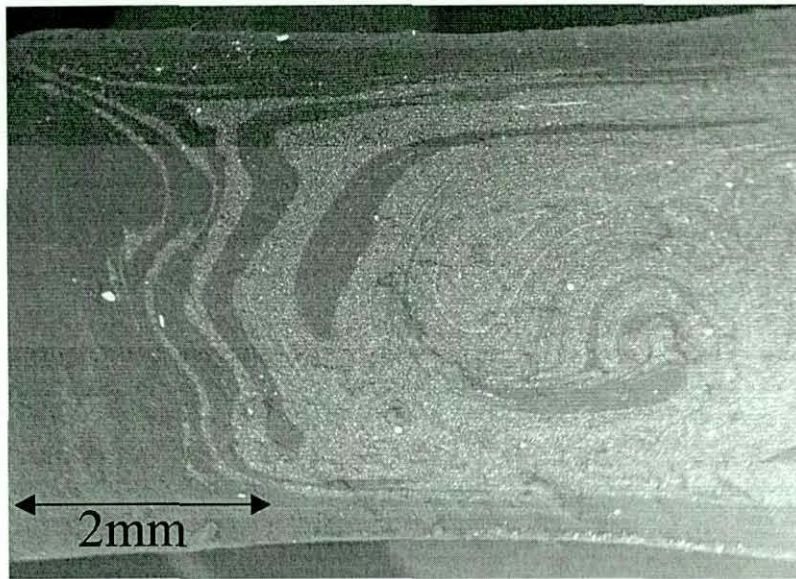
Plate 4.22, Back Scattered SEM Image of HIPS Containing 12wt.% DBDPO and 4wt.% RS Compounded Using An Injection Moulder
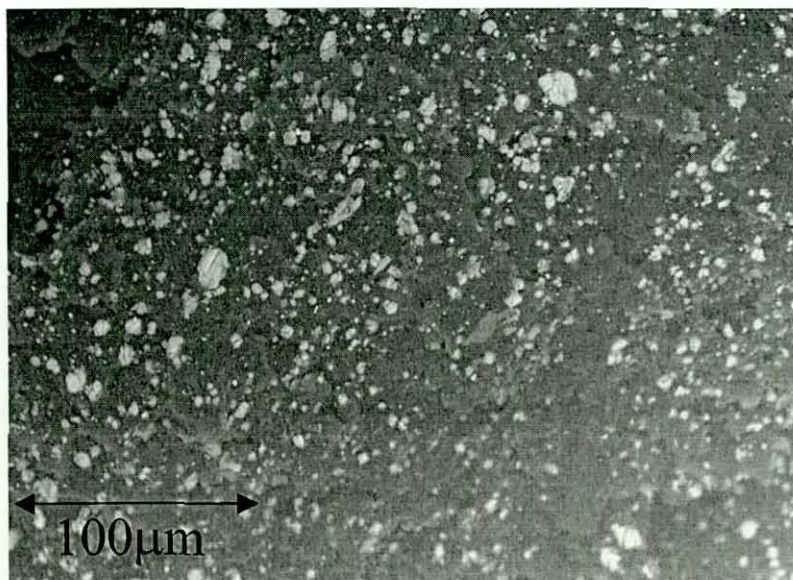
Plate 4.23, Back Scattered SEM Image of HIPS Containing 12wt.% DBDPO and 4wt.% RS Compounded Using An Injection Moulder
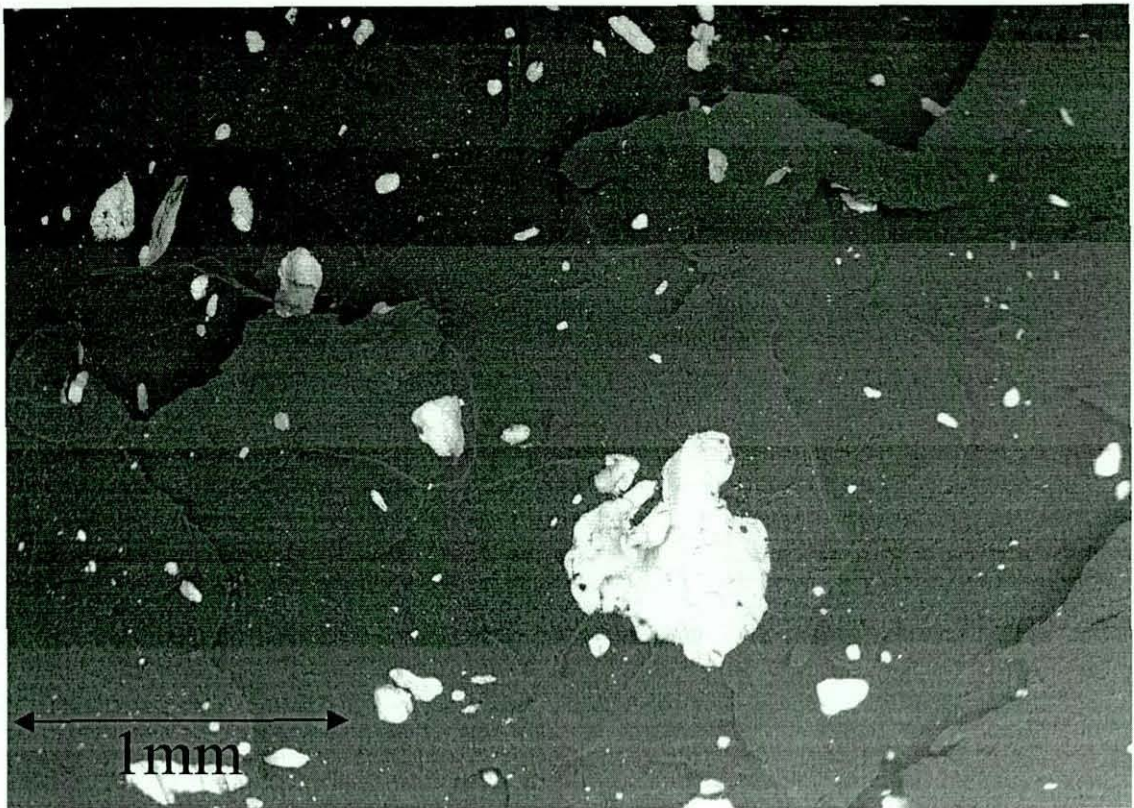
Plate 4.24, Back Scattered SEM Image of HIPS Containing 18wt.% Fyrebloc 210, Compounded Using A Twin Screw Extruder
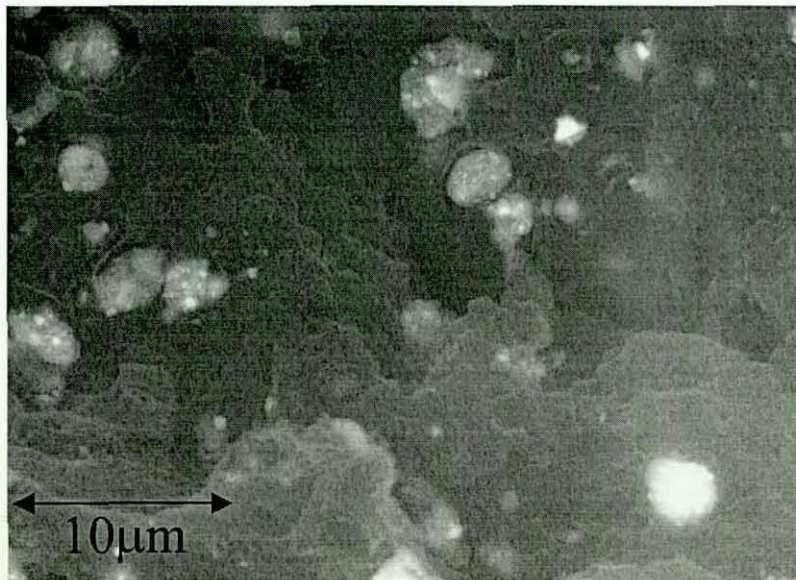
Plate 4.25, Back Scattered SEM Image of HIPS Containing 18wt.% Fyrebloc 210, Compounded Using A Twin Screw Extruder
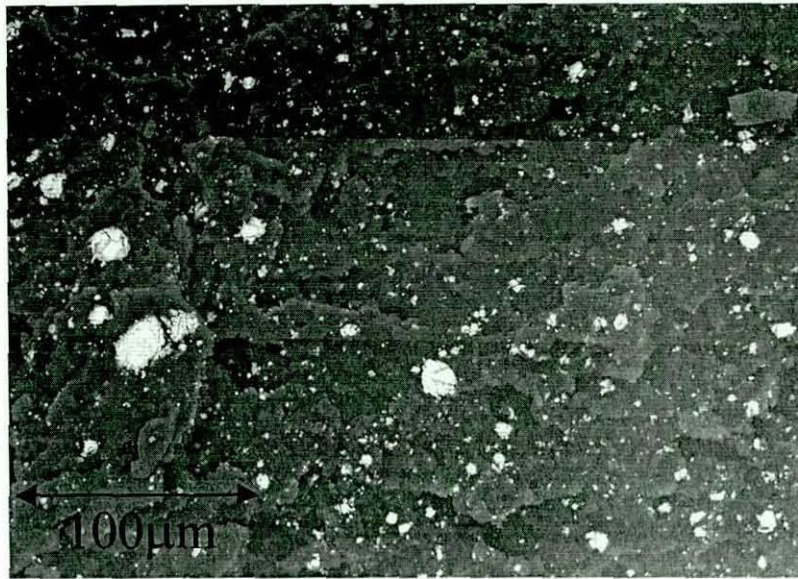
**Plate 4.26, Back Scattered SEM Image of HIPS Containing 18wt.% Fyrebloc
210, Compounded Using An Injection Moulder**
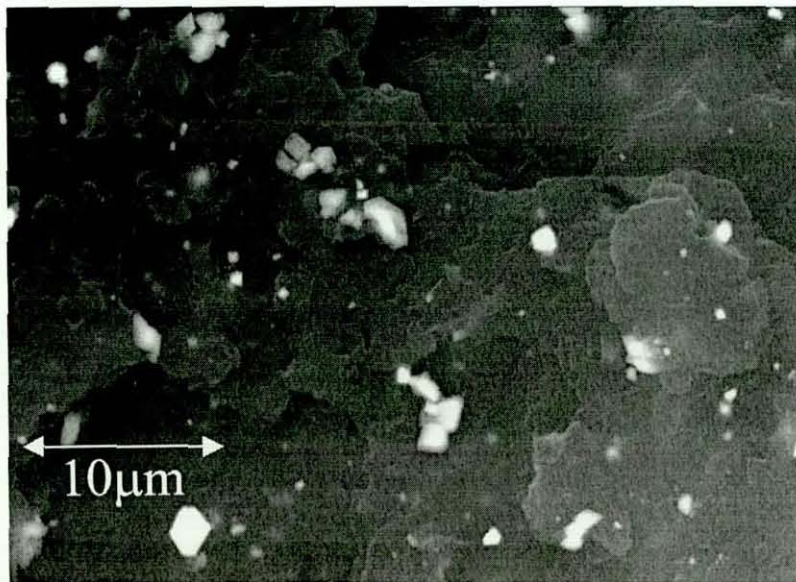
**Plate 4.27, Back Scattered SEM Image of HIPS Containing 18wt.% Fyrebloc
210, Compounded Using An Injection Moulder**

A SEM examination has been conducted on the impact fracture surfaces of HIPS and HIPS compounds containing various loading level of FR additives. Plate 4.28 show unfilled HIPS, and Plates 4.29 to 4.32 are HIPS compounds containing various loading levels of DBDPO. These are very low magnification images which has led to some distortion of them.
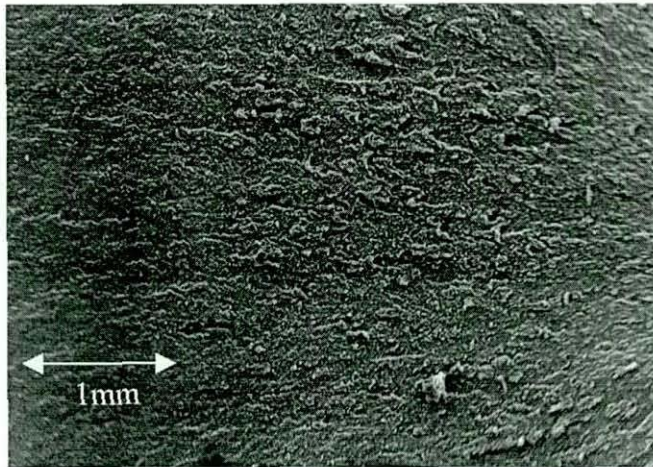
Plate 4.28, SEM Image of HIPS Impact Fracture Surface
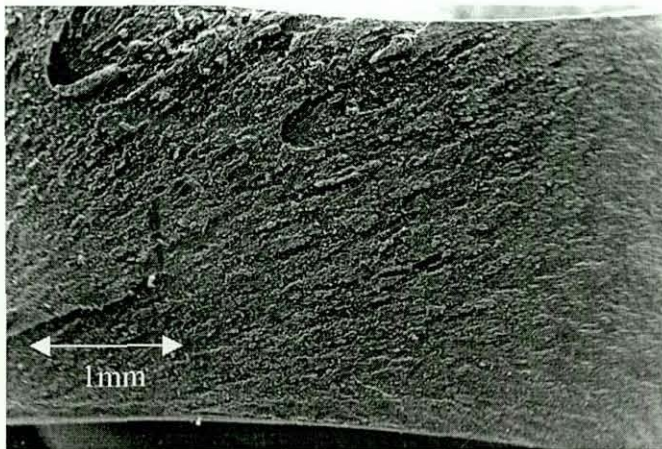
Plate 4.29, SEM Image of HIPS Containing 4wt. % DBDPO, Impact Fracture Surface
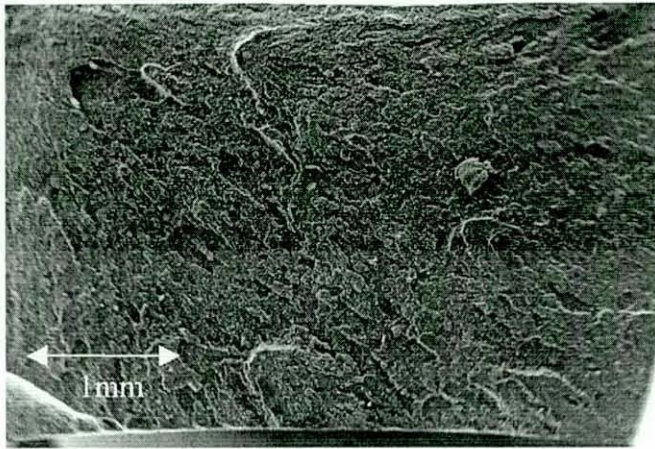
Plate 4.30, SEM Image of HIPS Containing 12wt. % DBDPO, Impact Fracture Surface
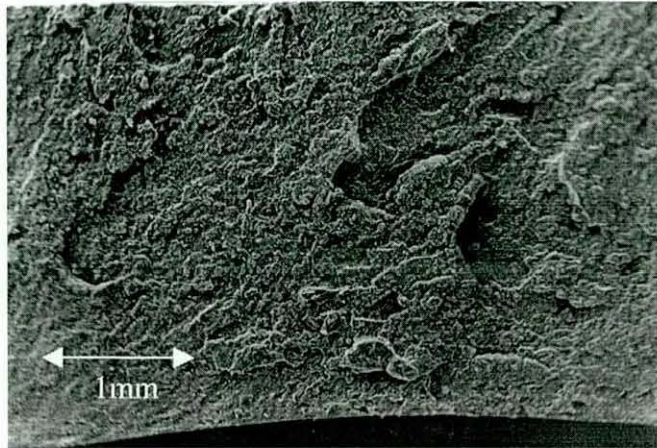
Plate 4.31, SEM Image of HIPS Containing 20wt. % DBDPO, Impact Fracture Surface
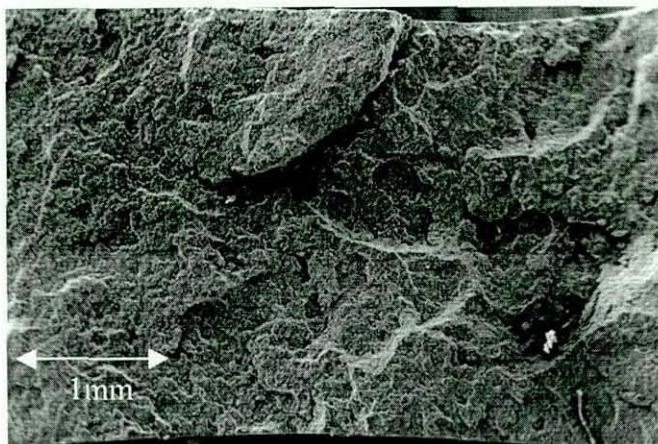
Plate 4.32, SEM Image of HIPS Containing 32wt. % DBDPO, Impact Fracture Surface

4.13 TEM Examination of HIPS Compounds

TEM examinations have only been conducted on unfilled HIPS and a selection of filled HIPS compounds. Plate 4.33 shows a TEM image of unfilled HIPS. From this image the primary rubber phase, (that added during manufacture), can be seen, with polystyrene inclusion. Plates 4.34 and 4.35 show TEM images of HIPS containing DBDPO BRF and RS Sb_2O_3 respectively. Both of these FR additives are shown as dark black particles which makes them easily identifiable. They always located themselves in the polystyrene matrix. Problems were encountered when sectioning samples containing any grade of Sb_2O_3, as the Sb_2O_3 damaged the glass knife used, which led to relatively poor sections. This meant that obtaining high quality images containing Sb_2O_3, and using this method to determine Sb_2O_3 particle size and morphology, was difficult.
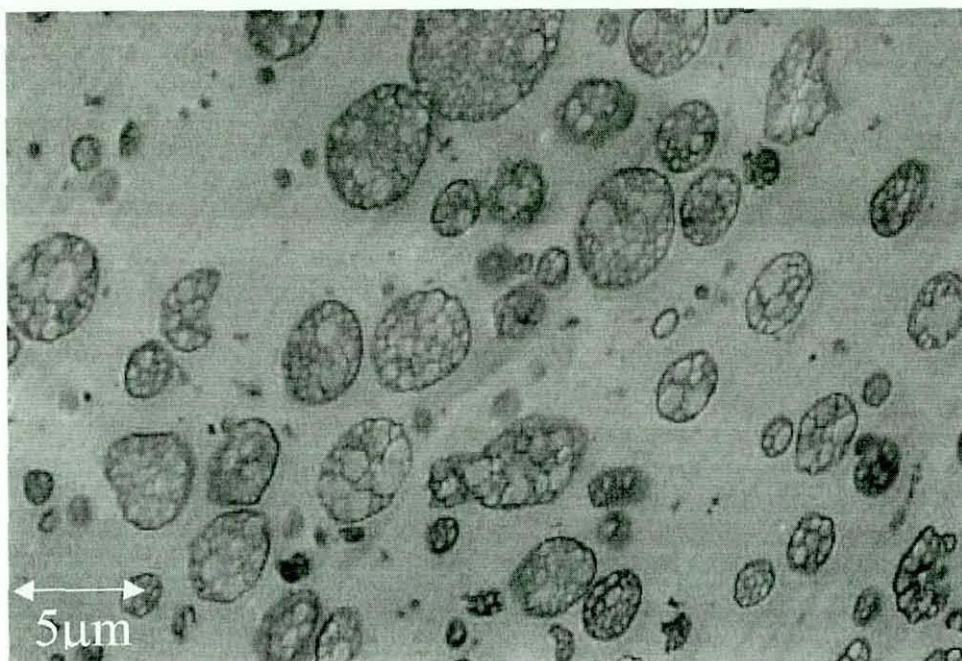
Plate 4.33, TEM Image of Unfilled HIPS
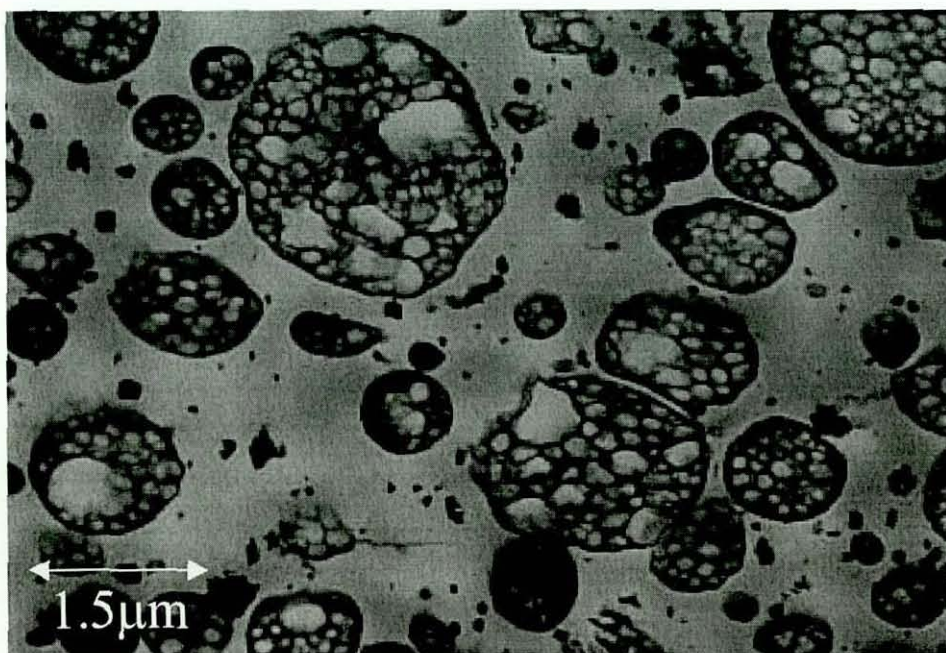
Plate 4.34, TEM Image of HIPS Containing 4 wt.% RS Sb$_2$O$_3$
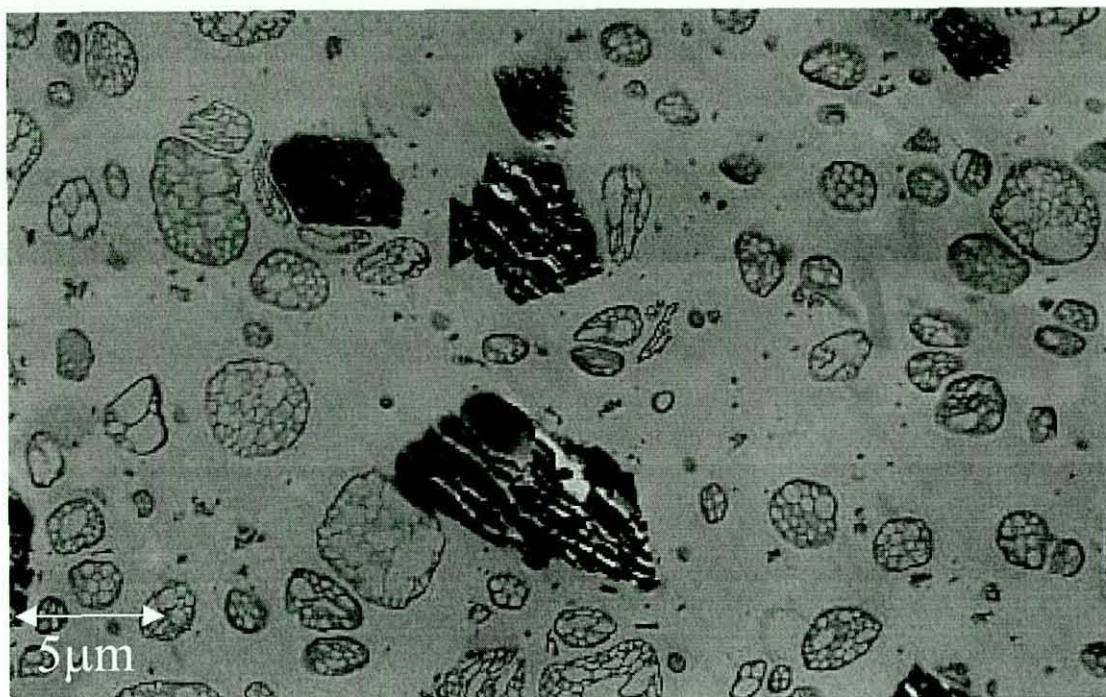
Plate 4.35, TEM Image of HIPS Containing 12 wt.% DBDPO BFR

Extensive TEM examination of HIPS compounds containing the impact modifier has been conducted. Plates 4.36 to 4.41 summaries the findings, for each of the loading levels of impact modifier used. For each loading level a high magnification image is shown to identify the morphology of the impact modifier. Plate 4.36, shows a HIPS compound containing RS, DBDPO and Stereon 840 impact modifier at 4wt.%, each of the additives and the main parts of HIPS have been labelled.
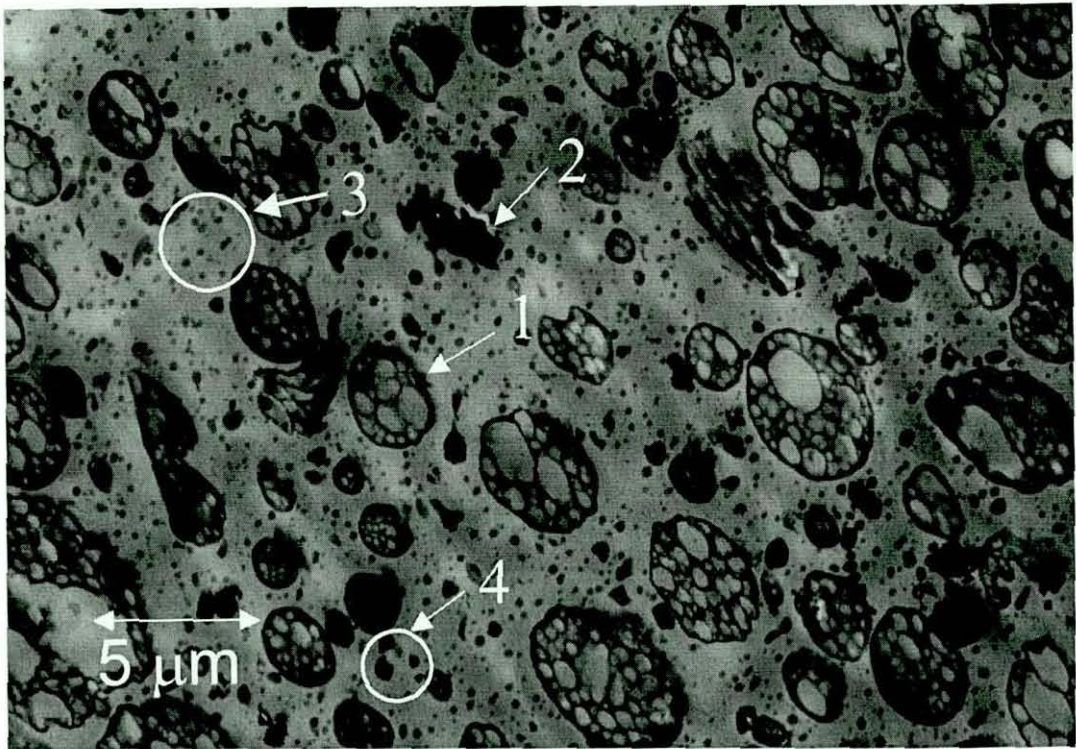
Key

1 → Primary Rubber Phase With Styrene Inclusions

2 → DBDPO

3 → Secondary Rubber Phases (Impact Modifier)

4 → Sb_2O_3

Plate 4.36, TEM Image of HIPS Containing RS (4wt.%), DBDPO (12wt.%) and Stereon 840 (4wt.%)
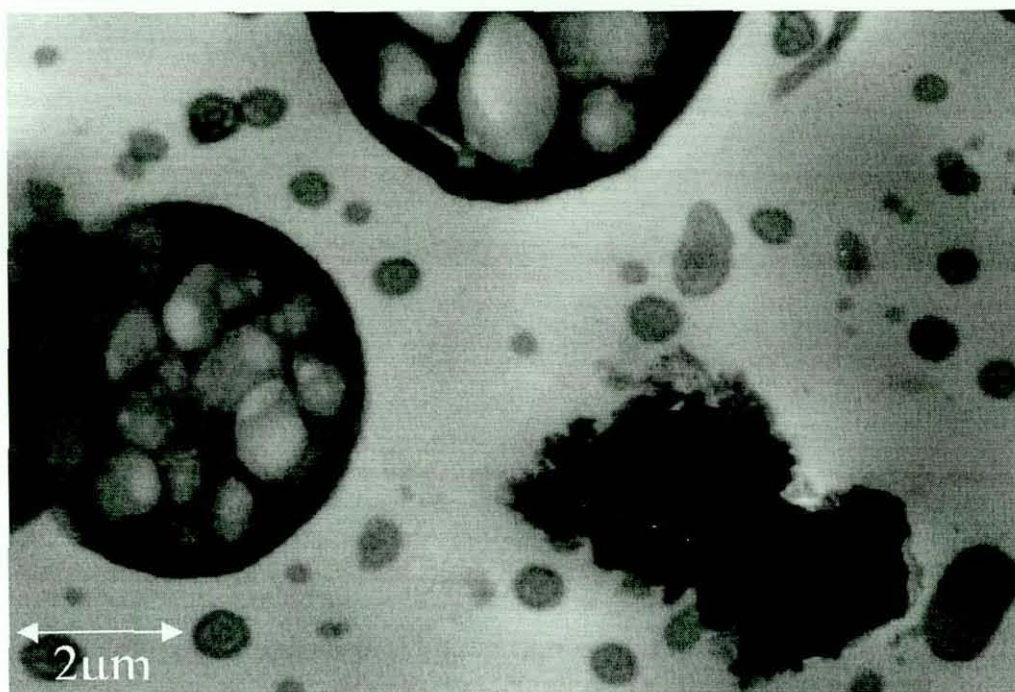
Plate 4.37, TEM Image of HIPS Containing RS (4wt.%), DBDPO (12wt.%) and Stereon 840 (4wt.%)
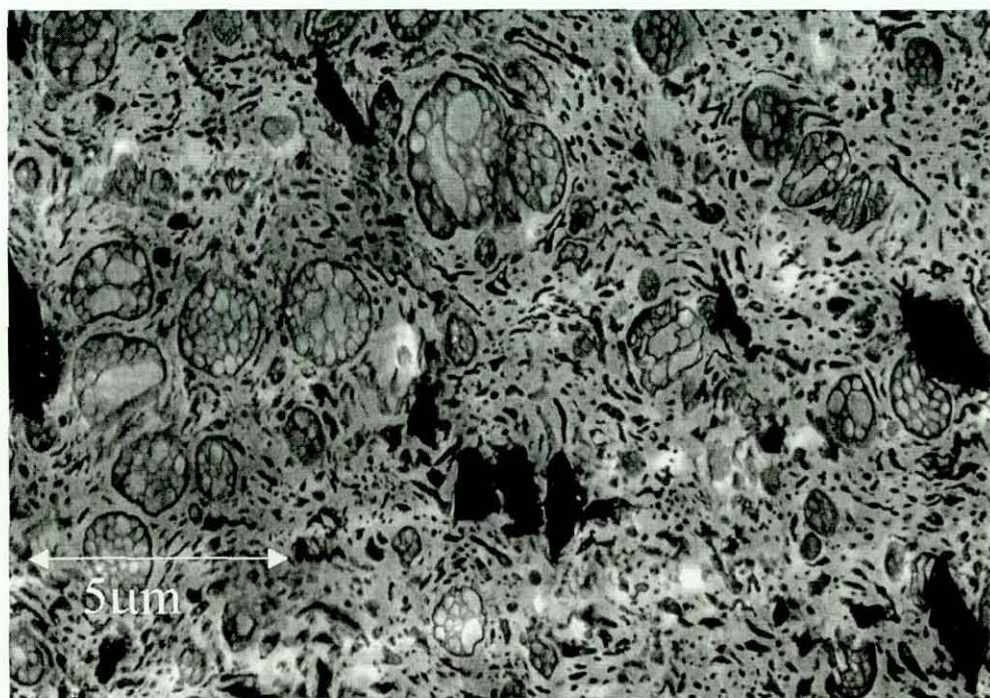
Plate 4.38, TEM Image of HIPS Containing RS (4wt.%), DBDPO (12wt.%) and Stereon 840 (10wt.%)
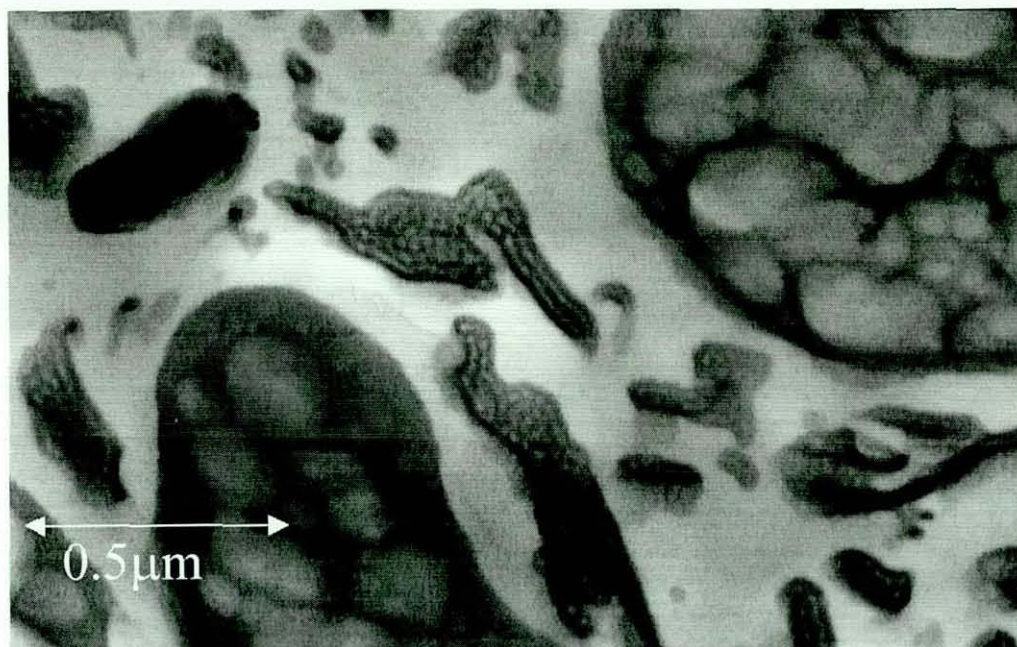
Plate 4.39, TEM Image of HIPS Containing RS (4wt.%), DBDPO (12wt.%) and Stereon 840 (10wt.%)
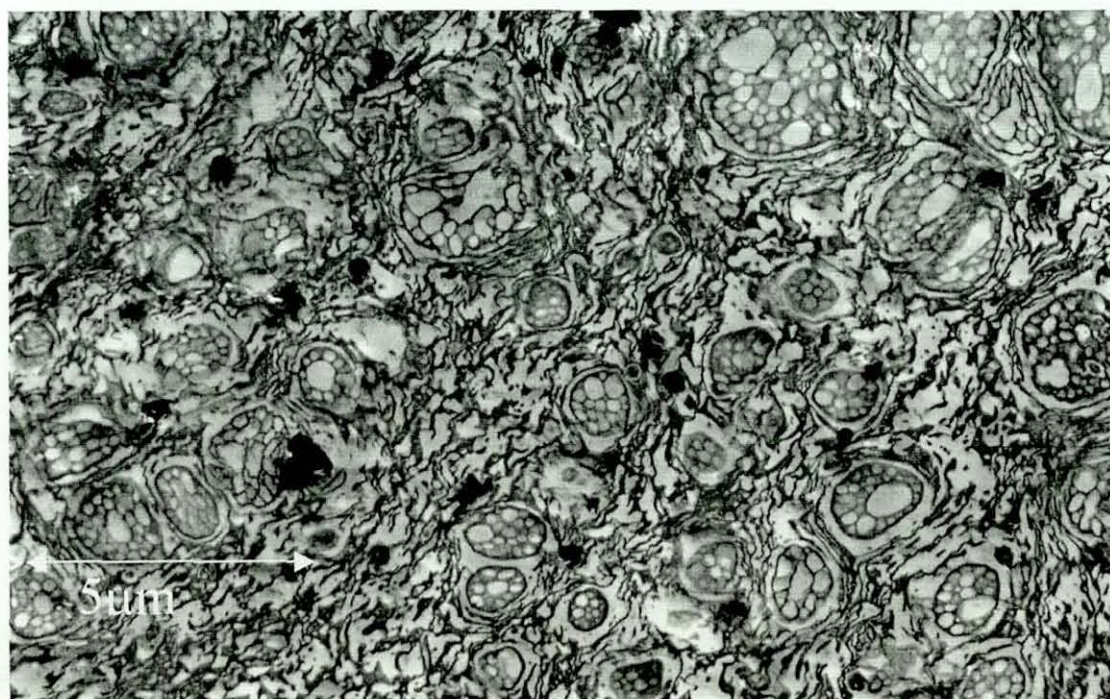
Plate 4.40, TEM Image of HIPS Containing RS (4wt.%), DBDPO (12wt.%) and Stereon 840 (20wt.%)
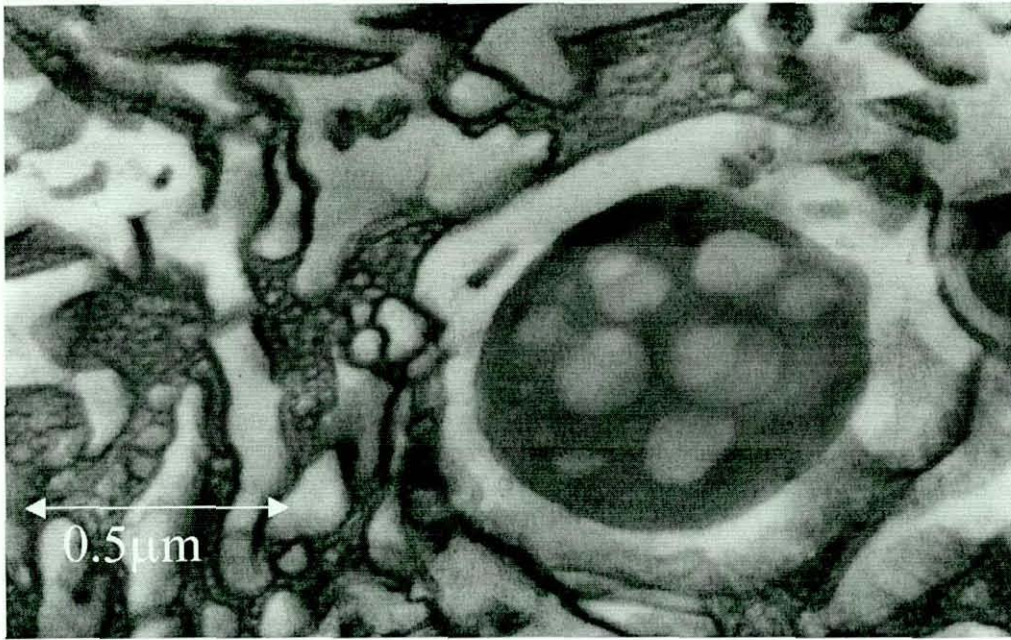
Plate 4.41, TEM Image of HIPS Containing RS (4wt.%), DBDPO (12wt.%) and Stereon 840 (20wt.%)

TEM examinations have also been conducted on sections taken from just under the fracture surfaces of impact test bars. This was done to determine if crazes were present in this grade of HIPS and to observe any interactions between the additives used and crazes in the HIPS samples. A selection of samples was choosen for examinination to determine the effect, if any, of each additive on crazes in the HIPS matrix. It was difficult to obtain hard copies of the images, as the intensity of the beam destroyed the samples during imaging, plates 4.42 to 4.46 summarise the results obtained.
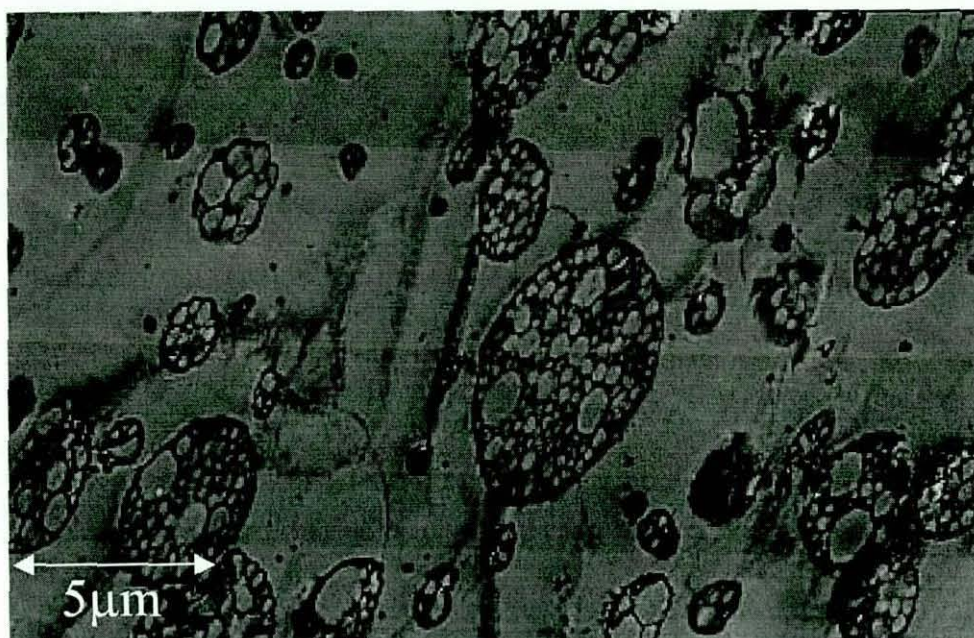
Plate 4.42, TEM Image of Crazes Present In Unfilled HIPS
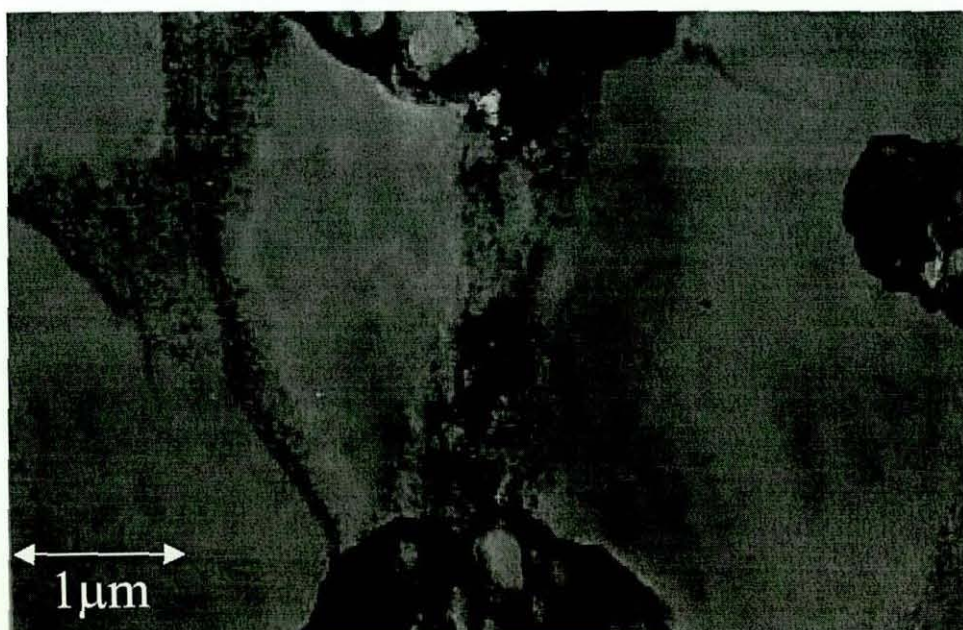
Plate 4.43, TEM Image of Crazes Present In Unfilled HIPS
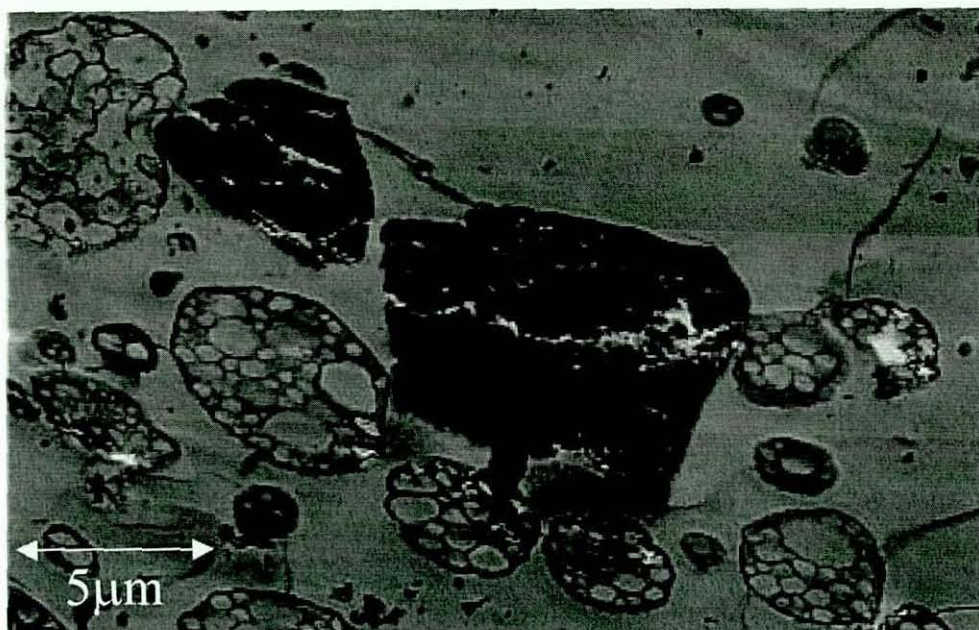
Plate 4.44, TEM Image of Crazing in HIPS Compound Containing DBDPO (12wt.%)
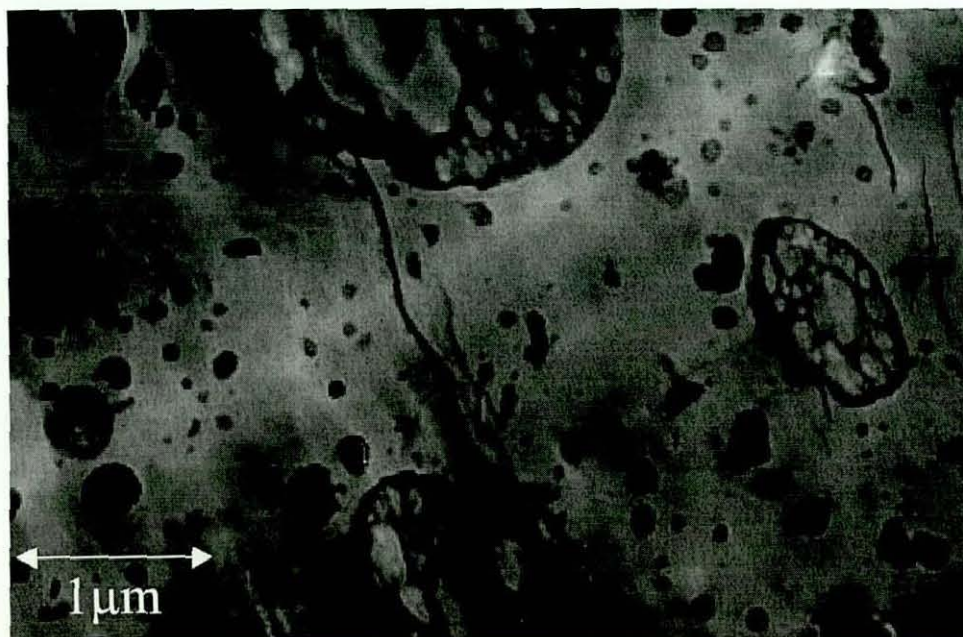
Plate 4.45, TEM Image of Crazing in HIPS Compounds Containing DBDPO (12wt.%), RS (4wt.%)and Stereon 840 (4wt.%)
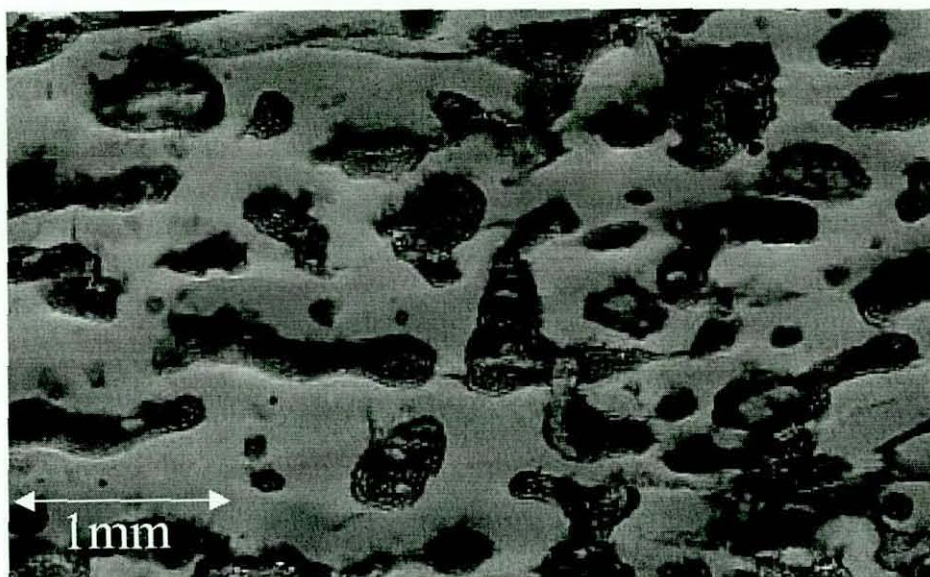
Plate 4.46, TEM Image of Crazing in HIPS Compounds Containing DBDPO (12wt.%), RS (4wt.%)and Stereon 840 (10wt.%)

5.0 Discussion

This chapter discusses the results given in the previous chapter and where possible develops models based on these results. Also in this chapter the results and observations made on them are related to available literature.

The chapter has been divided into several sub sections, each one deals with one of the major additives used in the work, a final section deals with formulations that provide a fully flame retardant effect. Each section covers all results relating to those compounds and where relevant compares them to results in other sections.

5.1 Antimony Trioxide

This section discusses the results obtained for both HIPS and PBT compounds containing Sb_2O_3. This mainly consists of compounds containing Sb_2O_3 of varying particle sizes, and also includes loading levels of RS and TT in HIPS with loading levels up to 32wt.%. Several of the results revealed little or no difference when compared to the unfilled polymer, or between the grades of Sb_2O_3 used. These results have been included for completeness in the results section and are discussed here.

5.1.1 Particle Size and Morphology

5.1.1.1 Powders

For the four grades of Sb_2O_3 where particle size was directly measured, there was broad agreement with the manufacture's data [86,110], for this form of analysis. Generally the Sb_2O_3 was regularly shaped, with square or rectangular shaped particles. This indicated that they are in the crystal form Senarmontite. The other crystal form of Sb_2O_3, Valentinte, has been reported in Sb_2O_3 grades RS and TT. There was no evidence of any Valentinte in either the RS powder or compounds studied (Plate 4.4 and 4.11 to 4.12). In the TT powder there was a significant proportion of Valentinte present (Plate 4.5), this was identified as the long thin needle like particles.

Apart from the A05 grade of Sb_2O_3 all had a monomodal distribution about their D_{50} value. The A05 had a bi-modal distribution, with a main peak at $0.41\mu m$, the quoted D_{50}, and smaller peak at $1\mu m$. This was most likely caused by contamination with RS during the collection stage of the manufacturing process [130]. Plates 4.1 and 4.2 show the Azub material used. This has a more complex structure than the other Sb_2O_3 grades. From Plate 4.1, it can be seen that large particles of castor wax, approximately $20\mu m$, make up the structure with Sb_2O_3 particles on the surface. Plate 4.2 shows a high magnification image of the surface, showing the Sb_2O_3 particles to be less than $0.1\mu m$. The layer of Sb_2O_3 particles are approximately $2\mu m$ thick, covering the whole of the castor wax sphere's surface [133].

5.1.1.2 Dispersion in Polymer Matrix

From the backscattered SEM images for both HIPS and PBT, Plates 4.11 and 4.12, containing only Sb_2O_3, it would appear that the twin screw extrusion processing used, dispersed the Sb_2O_3 well in both HIPS and PBT, with few or no aggregates or agglomerates present. From these plates, the Sb_2O_3 morphology is the same as the raw powders, with regular rectangle and square shape particles. There is no evidence that there is any adhesion between any of the grades of Sb_2O_3 and polymer matrixes, this is in agreement with observations by other authors [33,34]. Seddon [34] reported that voids formed around Sb_2O_3 particles present in ABS polymers. There is evidence in both the HIPS and PBT that this is also occurring, and will act to reduce many mechanical properties.

For the HIPS compounds the Sb_2O_3 particles always located themselves in the PS matrix and not the rubber phase, or the PS inclusion within the rubber phases. This can clearly be seen in Plate 4.33, but there is also evidence in Plates 4.34, 4.36 and 4.37. There are several reasons for this, including the fact that Sb_2O_3 might be more compatible with the PS, or the Sb_2O_3 particles cannot penetrate the rubber phases during processing. This second explanation is more likely as there is no Sb_2O_3 in the PS inclusions in the rubber phase.

5.1.1.3 Rheology

Graph 4.4 shows the effect of Sb_2O_3, grades RS and TT, at a loading level of 32wt.% on the shear viscosity of HIPS. At the lower shear rates used small differences were observed, as the shear rate increased the values of shear viscosity converged with that for unfilled HIPS. It has been reported that the shear viscosity of rubber toughened polymer does not increase with the addition of fillers till a loading level of 40wt% [17]. This has been attributed to the rubber phases dominating shear viscosity.

5.1.2 Particle Size

5.1.2.1 Impact Properties

All grades of Sb_2O_3 had significant detrimental effect on impact properties when added to PBT at 3.5wt%. This effect can be explained by several mechanisms, such as the dilution effect. When the filler is added less polymer is present to absorb the impact energy reducing impact performance. The particles can also act as stress concentrators, as there appears to be no bonding between the particles and the PBT. As a consequence voids will form under an applied load, as discussed in section 5.3.2. This can affect the fracture mechanism of the polymer and reduce the impact properties.

A reason for the largest particles having the highest impact properties is due to them having the lowest surface area to react with the polymer. In this section all grades of Sb_2O_3 were added at 3.5wt%. As the particles increase in size, the total surface area that they have decreases compared to grades with smaller particle size, this would reduce the area that can react between the Sb_2O_3 and PBT polymer. The term react does not refer to the Sb_2O_3 bonding or bridging with the PBT. It has been shown above that there is no bonding between Sb_2O_3 and PBT. Sb_2O_3 may act as a catalysis, in a similar manor to PET, which would cause reductions in molecule weigh, affecting many properties.

Sb_2O_3 is used in polyethylene terephthalate (PET) at low loading levels during the manufacturing process as a catalyst [24,23], this does not allow the use of Sb_2O_3 in PET as a flame retardant as it breaks down the molecule structure. Sb_2O_3 is the main fire retardant antimony synergist used in PBT, so it might cause reductions in the molecular weight [112]. Which will affect mechanical properties such as impact and facture toughness [113]. Unfortunately molecule weight determination was conducted for PBT compounds containing Tetrabromobisphenol A, discussed in section 5.2, but was not conducted for PBT compounds containing Sb_2O_3. However, any reductions in molecular weight are likely to be small, given that no noticeable effects were seen on processing, and Sb_2O_3 is commonly used in PBT.

Graph 5.1 shows a plot of log Sb_2O_3 particle size against impact failure energy for PBT. From this graph it can be seen that a logarithmic relationship between particle size and impact failure energy exists. Equation 5.1 derived from Graph 5.1 shows the numerical relationship between Sb_2O_3 particle size and impact failure energy.
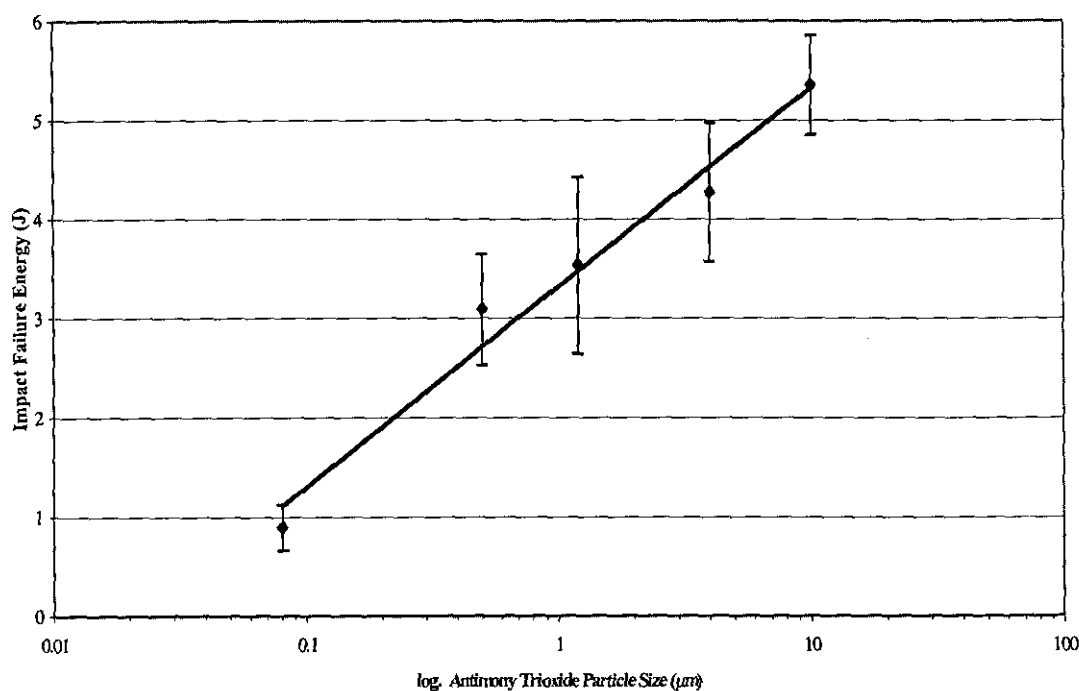
Graph 5.1, Particle Size Effect of Sb_2O_3 on PBT

Impact Failure energy (J) = 0.87log S+3.31   **Equation 5.1**

Where S is the particle size in μm

The effect of particle size on the impact properties of HIPS is more complex. The smallest particle sized material used, had no effect on either peak or failure energy compared to unfilled HIPS. Previous work [34] indicated that use of a nanometre sized Sb_2O_3 has little or even a reinforcement effect on styrene based polymers such as ABS. The reinforcement effect was attributed to the castor wax and not the Sb_2O_3 particles. The castor wax, which is present at approximately 15wt.%, is present to stop the Sb_2O_3 particles forming agglomerates and aggregates during the manufacturing processing. From Table 4.12 it can be seen, that unlike ABS, castor wax gives no improvements in HIPS. This shows that formulations containing only Sb_2O_3 with a particle size of less than 0.1μm exhibit no decrease in impact properties, compared to unfilled HIPS.

Compound containing grades of Sb_2O_3 with quoted particle sizes of 0.5μm (AO5) and 1.2μm (RS) had similar peak and failure energy values, which were less than unfilled HIPS. The reasons for this can be seen from the particle size traces (Appendix 1). Although AO5 has a D_{50} of 0.5μm the particle size trace showed that it is bi-modal and that a second peak is present at 1.2μm, which is similar to RS. These results indicate that a small number of particles 1-2μm can reduce impact properties even when the majority of the particles are fine.

The formulations with TT (5μm) and RT (10μm) had improved peak and failure energies. TEM examination of HIPS (Plates 4.33 to 4.36) showed that the polybutadiene regions were approximately 5μm. It would appear that when particles with a similar size are added a small improvement in impact properties is observed. Although it has both different chemistry and particle morphology, DBDPO has a similar D_{50} (≈5μm) and particle size distribution to that of TT and showed similar impact results, (Graph 4.5 and 4.9) when added to HIPS at 3.5 to 4wt%.

The reasons for particles with a D_{50} of 5µm giving a reinforcement effect at low loading is associated with both their size and the inter-particle distance. Many authors [100,19,18,17] have reported that rubber particles have to be bigger than a critical size in order to provide toughness enhancements to PS. Both Sb_2O_3 TT and DBDPO are of a similar size to the rubber phase present in the HIPS compounds. This would indicate that particles with a size similar to that of the rubber reinforcement act like rubber particles at low loading levels. They allows stable craze growth, and due to their inter particle distance allows craze termination before they develop into large cracks which would cause premature failure. Plate 4.44 shows a craze terminating at DBDPO particles, but there was no evidence of other sized particles acting as craze termination sites. Bucknall [17] proposed that the impact absorption of rubber-reinforced polymers is directly linked to the amount of crazing within the sample during failure. Therefore if the TT and DBDPO increases the amount of crazing accruing during failure, a reinforcement effects may be seen if compared to unfilled HIPS.

Although many particles, such as Sb_2O_3 and DBDPO have the potential to act as both craze initiators and terminators, they are not as efficient as rubber particles as they only give a reinforcement effect at low loading levels. Several authors have shown [47,50] that given the same particle size and inter-particle distance, particles with some adhesion (not perfect or near perfect) to the PS matrix will create a better reinforcement effect. Both Sb_2O_3 and DBDPO have little or no bonding with the HIPS compound, so they will not be as efficient as craze initiation and termination sites.

The trends discussed above primarily explain the failure energy values, although they also apply to the majority of peak values. Although the trends are the same, the amount of variation is smaller. This would indicate that the Sb_2O_3 is affecting the ability of both HIPS and PBT to plastically deform (permanent deformation) to a greater extent than elastic deformation (recoverable). This will be caused by the Sb_2O_3 particles acting as rigid sites within the compounds, reducing the ability of the polymers to deform around them.

5.1.2.2 Fracture Toughness

Fracture toughness K_C values for all compounds containing only Sb_2O_3 were lower than for unfilled HIPS and PBT (Graphs 4.18 and 4.19). This means that the Sb_2O_3 is increasing the stress at the crack tip in both polymers. For HIPS there was no significant difference between the different grades of Sb_2O_3 used. Fracture toughness results were the same for PBT, with a reduction seen for all of the Sb_2O_3 grades, but no difference between them. In both HIPS and PBT compounds, Sb_2O_3 particles act as sites of failure initiations by either being points of increased stress within the compounds, or by creating voids around them. This will reduce the fracture toughness of the compounds, as failure will occur at low loading levels. This effect may also cause some of the reduction seen in impact properties as it will allow cracks to travel faster through the compounds, reducing the amount of energy absorbed during failure.

5.1.2.3 Tensile Properties

In HIPS, Sb_2O_3, at a constant loading level, had little effect on the tensile properties measured. The most significant effect however, was on strain at break values, where decreases up to 29% compared to unfilled HIPS were observed. Values for both maximum stress and Young's modulus were unaffected by Sb_2O_3 at these particle sizes and loading level. From Table 4.13 the trend for strain at break values is similar to that for impact and fracture toughness properties. This shows that the Sb_2O_3 particles, even at these loading levels, reduces the ability of the HIPS polymer to plastically deform. However, they have little effect on the elastic deformation or load bearing ability of HIPS.

Similar trends were seen for PBT. Strain at break values decreased by up to 30% of the unfilled value, for all of the Sb_2O_3 filled compounds. As with impact properties the compounds containing the largest particles exhibited the smallest reduction in strain at break values, compared to unfilled PBT. This shows that the Sb_2O_3 is reducing the ability of the PBT to plastically deform and that Sb_2O_3 particle size has a small effect, which is a similar trend to that seen for HIPS. The effect on maximum stress and Young's modulus values were small when compared to unfilled PBT.

5.1.2.4 Crystallinity

A loading level of 3.5wt.% Sb_2O_3, did not effect the onset or melting temperatures of PBT, however it did cause an increase in the onset and solidification temperatures. There was no apparent effect due to Sb_2O_3 particles size, with only small differences present. All grades of Sb_2O_3 decreased the percentage crystallinity values, for both heating and cooling, compared to unfilled PBT. There was a slight trend that the smaller the Sb_2O_3 the large the reduction in crystallinity but this was small.

These results show that the Sb_2O_3 is making crystallisation easier, as the Sb_2O_3 particles can be used as points for crystal growth to start. The fact that no effects were seen during heating is due to the samples being taken from injection mouldings. Injection moulding is known to effect crystallisation properties, as both high shear rates and rapid cooling profiles are used, compared to the controlled cooling of the DSC. Therefore the settings used during injection moulding will control these properties instead of the Sb_2O_3 particles. During cooling however any affects from injection moulding will have been lost.

Maiti [117] used Ni powder in polypropylene, using both DSC and X-ray diffraction, found that as the volume percentage of Ni powder increased the corrected crystallization percentage decreased. This was attributed to the Ni particles creating more nucleating sites, but forming smaller spherulites causing a reduction in the total crystalline percentage. Also the Ni powder decreased both the nucleation rate and growth of the crystal structure. It is possible that Sb_2O_3 is acting in a simile manor in PBT.

5.1.3 Sb_2O_3 Loading Level

The effect of increasing Sb_2O_3 loading levels in HIPS was determined. Of the five Sb_2O_3 grades used, RS and TT were chosen to investigate this effect. This was because RS is the most common commercial grade used, and TT gave good impact properties from the previous section, and also had a similar particle size to DBDPO. This allowed other variables to be studied such as the effect of particle morphology and any interaction between the additives and the matrix.

5.1.3.1 Impact

Graph 5.2 combines data from Table 4.4 (Sb_2O_3 contents) and Graphs 4.7 and 4.8 (impact data) to show the effect of Sb_2O_3 loading level on impact peak energy for HIPS. Graph 5.3 uses data from the same sources to show the effect of Sb_2O_3 on the failure impact energy of HIPS. Trend lines are shown for each set of data on the graphs. For the peak values linear trends lines were used, whilst for failure energy polynomial trend lines were used. The equations for these lines are shown in Equations 5.2 to 5.5, where L is the Sb_2O_3 loading level. These equations have been used later in this section to taken account of variations in Sb_2O_3 loading levels of compounds containing Sb_2O_3/DBDPO mixes.

From Graphs 5.2 and 5.3 it can be seen that increasing the loading level of RS and TT decreases both the peak and failure energies of HIPS compounds. The reduction in failure energy is bigger than that for peak energy, for example, at loading level of 38wt.%, the reductions in peak values were ≈65%, for failure values this was ≈75%, compared to unfilled HIPS. As discussed for Sb_2O_3 particle size, this indicates that the increasing addition of the Sb_2O_3 makes the failure more brittle, by reducing the ability of the HIPS to plastically deform after failure has started.

There are many reasons why increased loading levels reduce impact value. Crazing can initiate at Sb_2O_3 particles, but they are not as efficient as the rubber phase at acting as sites for craze initiate and termination. Therefore less crazes will form to absorb energy during impact [17,44]. Also as the loading level increases, effects such as dilution of the polymer and void formation, will increase, as more Sb_2O_3 particles are present.

From the trend lines it can be seen that both peak and failure energy values, were higher for TT than RS, at all loading levels. For failure energy, the trend line diverged up to a loading level of ≈25wt.% at which point they remained constant at ≈0.2J. However for peak values the difference in trend lines increased as the loading level increases. Bigg's [44] observed a similar effect in ABS filled with talc.

He noted a rapid decrease in impact strength at low loading levels before it levelled of at high loading levels. Impact failure is due to rapid crack propagation through material. Compounds with better impact resistant will absorb more of the impact energy and propagate a crack very slowly. One mechanism of slowing crack growth is craze formation at the crack tip. These crazes form perpendicular to the direction of the crack and impact energy is required for their creation (discussed in section 2.1.4). There is evidence that crazes are more likely to from at TT particles than RS (section 5.1.2.1), which explains why TT compounds had high peak and failure energy values than RS compounds

From Graphs 5.2 and 5.3 and those in 4.5 it can be seen that both Sb_2O_3 particle size and loading level affect peak and failure energy of HIPS. Graphs 5.2 and 5.3, show that although Sb_2O_3 particle size and loading level do affect impact properties neither dominate or control failure. It can be seen that as the loading level increases impact value decrease, but that results for RS and TT are also different at all loading levels.
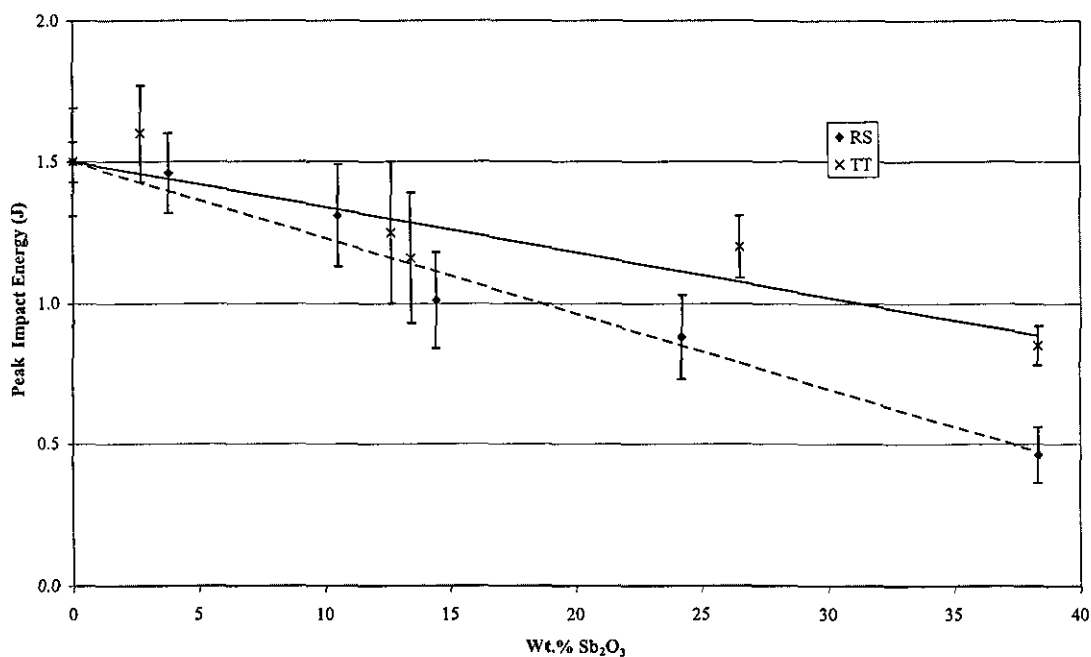
Graph 5.2, Sb_2O_3 Loading Level and Particle Size Effects on Peak Impact Energy Values of HIPS Compounds
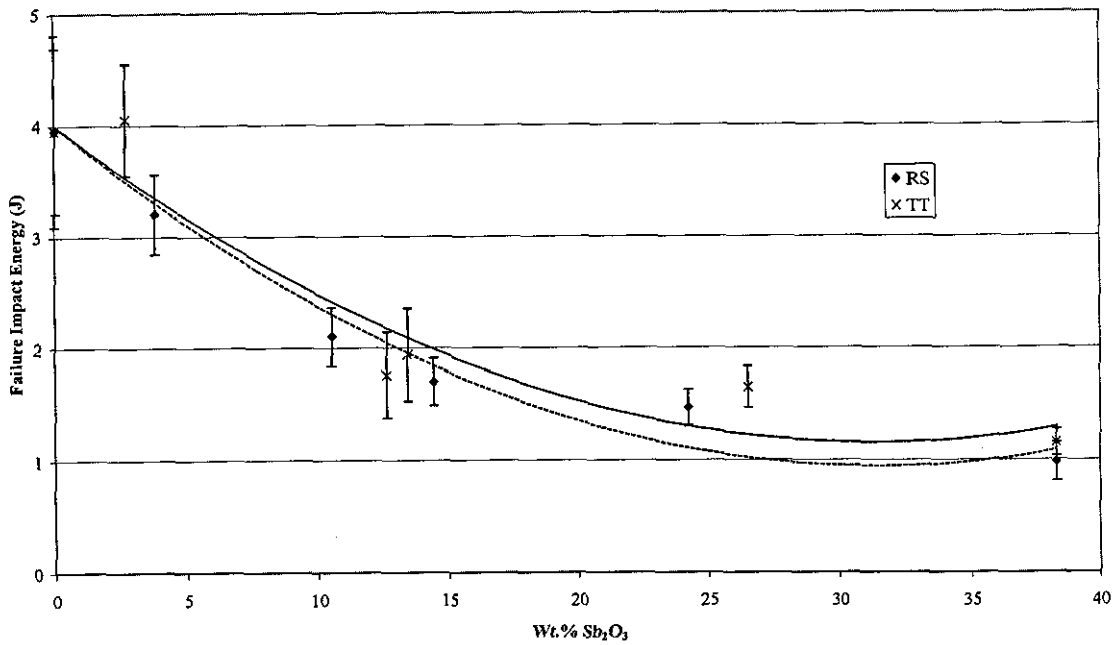
Graph 5.3, Sb$_2$O$_3$ Loading Level and Particle Size Effects on Failure Impact Energy Values of HIPS Compounds

Peak Impact energy for HIPS containing RS = -0.027L+1.5

Equation 5.2

Peak Impact energy for HIPS containing TT = -0.016L+1.5

Equation 5.3

Failure Impact energy for HIPS containing RS = $0.003L^2$-0.18L+4.0

Equation 5.4

Failure Impact energy for HIPS containing TT = $0.003L^2$-0.2L+4.0

Equation 5.4

5.1.3.2 Fracture Toughness

The effect of Sb_2O_3, (grades RS and TT), loading level on the fracture toughness properties of HIPS is summarised in Graph 4.21. The actual values do not agree with several other sets of results obtained for HIPS compounds, the reasons for this are detailed in section 4.8. However, even if the results are valid, the effects of Sb_2O_3 loading level on the K_C values of HIPS are small. There is no direct relationship between K_C values and TT loading level, although as the loading level of RS increased the K_C decreased, the differences between HIPS and the other compounds are small however.

Friedrich [55], whose work has been discussed in section 2.5.2, suggested that the polymer carries the entire load during failure, and at a critical loading level of 10wt.% additive the fracture toughness is reduced as the particles act as sites of failure, and cause the polymer to cease to be a continuous phase that can support the applied load. If the critical loading level of additive is lower for Sb_2O_3 in HIPS is lower than this critical value (<4%) then this may account for the results seen.

5.1.3.3 Tensile

The Sb_2O_3 loading levels had various effects on the tensile properties calculated, although the biggest effect was on strain at break values. Table 4.18 summarises the data collected, and Graph 4.25 shows a typical stress/strain curve obtained for HIPS.

Graph 5.4 combines data for actual RS and TT loading levels. It indicates that a linear relationship exists between Sb_2O_3 loading level and strain at break values. Equations 5.5 and 5.6 model the trends seen. The effect of loading level is greater than the effect of Sb_2O_3 particle size. At increasing loading levels the values for strain at break converge. The reduction in strain at break values is in broad agreement with that finding of other authors [55,44,56,107] for various filled polymers systems. This data indicates that the Sb_2O_3 is affecting the ability of the HIPS polymer matrix to plastically deform. This was also observed for the impact testing results discussed early.
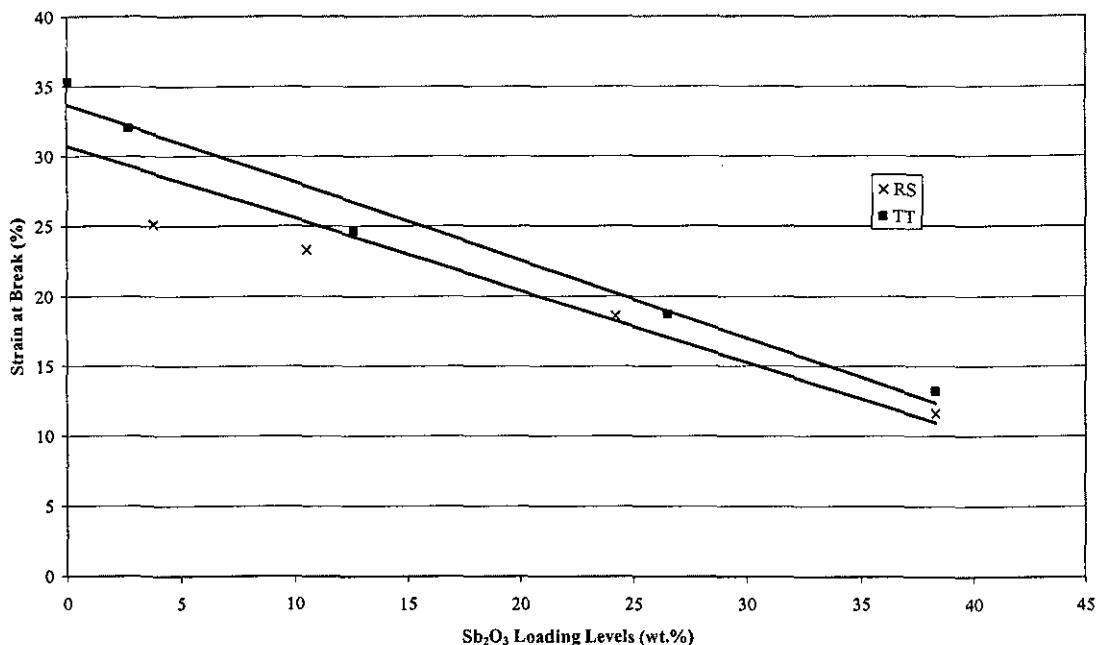
Graph 5.4, Effect of Sb$_2$O$_3$ Loading Level, and Type, on Strain at Break of HIPS Compounds

Strain at break values for HIPS containing RS = 30.7 - 0.52L **Equation 5.5**

Strain at break values for HIPS containing TT = 33.7 - 0.55L

Equation 5.6

Where L = Sb$_2$O$_3$ loading level

Overall an increase in Young's Modulus was observed as the Sb$_2$O$_3$ loading level increased, although no direct relationship between loading level and Young's modulus was observed as for strain at break values. As with strain at break values, this is in broad agreement with many published papers, which report that fillers and additives increase Young's modulus [32, 44,55,56,107], by increasing the stiffness of the compound, due to the Sb$_2$O$_3$ particles being more rigid than HIPS.

There was little or no effect of Sb_2O_3 loading level on the maximum tensile stress of HIPS, as can be seen from Table 4.18 and Graph 25. This is in agreement with the data for impact testing where there was only a small effect on peak values (maximum stress values). Thus the addition of Sb_2O_3 does not significantly affect the load bearing capabilities and elastic properties of HIPS, although plastic and final failure properties are dramatically affected.

5.2 Tetrabromobisphenol A

Tetrabromobisphenol A bromine compounds were predominantly used in PBT. Both the loading level and type of Tetrabromobisphenol A used affected the majority of the properties tested. This section discusses both the analysis of the raw powders, and the final PBT compounds containing Tetrabromobisphenol A compounds.

5.2.1 Analysis of Tetrabromobisphenol A Powders

Analysis of the Tetrabromobisphenol A compounds (by the method described in section 3.5.2) showed that the bromine contents where all lower than values obtained from the literature [125,126,127]. As stated in the results section the actual values obtained were used to calculate the wt.% of Tetrabromobisphenol A present in relevant compounds. The reasons for these variations are unclear. There are no major impurities present (discussed later), but they could be caused by minor changes in manufacturing methods, or variations in raw materials.

Results for XPS analysis of the Tetrabromobisphenol A surfaces are shown in Table 4.2. These show that there are no major impurities present in quantities greater than 1% (the resolution of the method) in any of the Tetrabromobisphenol A compounds. Direct comparisons cannot be made with the bromine contents of the bulk compounds, as hydrogen is not detected. However the bromine level at the surface would appear to be significantly lower than that in the bulk of the Tetrabromobisphenol A powders. This could reduce the effectiveness of the Tetrabromobisphenol A compounds as a fire retardant, as it's the bromine that creates the flame retardant effect.

The only variation in the data was between BC52 and the other compounds. BC52 had a lower bromine content and higher carbon level than the others. The influence this had on the PBT compounds properties, such as impact and tensile, however appeared minimal.

5.2.2 Particle Size and Morphology

Plates 4.7 to 4.9 are SEM images of the grades of Tetrabromobisphenol A used in this work. From these plates, it can be seen that all of the Tetrabromobisphenol As had particles in the size range 1 to 8µm. The majority of the particles present were regular shaped rectangular particles.

Manufacture's data indicated that all the grades of Tetrabromobisphenol A used should be completely melt blendable in PBT. However using back scattered SEM images it was possible to identify Tetrabromobisphenol A particles from all three grades that remained as secondary phases after processing. This can primarily be seen from Plates 4.15 to 4.17, which are back scattered SEM images of PBT compounds containing only Tetrabromobisphenol A. For all three grades the particles appear as translucent white regions. This was different from the images seen for Sb_2O_3 and may indicate that the Tetrabromobisphenol A compounds are at least partially melt/chemically compatible with the PBT polymer matrix. The sizes of the Tetrabromobisphenol A particles in the PBT was different to that of the raw powders. The Tetrabromobisphenol A had a particle size of ≈ 1 to 4µm, in the PBT, and appeared smaller than seen in the SEM images of the raw powders.

Unlike Sb_2O_3 there appears to be some degree of bonding between the Tetrabromobisphenol A and the PBT polymer. Fracture and crack propagation appear to have travelled thought the PBT matrix and additives, with no sign of debonding of the Tetrabromobisphenol A from the PBT matrix. The Tetrabromobisphenol A particles appear to be embedded in the polymer, unlike all the Sb_2O_3 grades. The bonding is most likely due to polar or hydrogen bonding between phenol end groups on the Tetrabromobisphenol A and negatively charged oxygen atoms on the PBT polymer chains.

5.2.3 DSC

5.2.3.1 Powders

DSC analysis showed that all of the Tetrabromobisphenol A compounds had different T_g temperatures. The heat flow rates involved are small, but the differences in temperatures are significant. The differences between BC52 (the lowest value) and BC52HP (the highest) was over 30°C. These effects are caused by differences in the chemical structure of the compounds, primarily concerned with the end groups. All three DSC curves rapidly increased after the T_g points. This was not caused by oxidation as the testing was conducted in a nitrogen atmosphere but is due to base line drift for each of the compounds [128]. The differences in the initial base lines are most likely not caused by differences in the Tetrabromobisphenol A, but small differences in the weight of the pans, used in the testing.

From Table 3.1 (manufacturers data) and Table 4.6 (DSC data) large differences can be seen in the thermal properties of Tetrabromobisphenol A compounds. There was no evidence of melting endotherms, from the DSC data, although all of the Tetrabromobisphenol A compounds have melting ranges according to the literature. From the DSC traces T_g temperatures were present. This explains why Tetrabromobisphenol A was seen as a secondary phase in the PBT polymers as discussed in section 5.2.1, and why there were significant effects on mechanical properties. The variations in T_g temperatures may also explain some of the differences seen in other properties such as impact strength and shear viscosity, discussed later in this section.

5.2.3.2 PBT Compounds

In all cases the additions of FR additives reduced the crystallinity of PBT compounds, for both heating and cooling, as can be seen from Table 4.8. There was little different in effect between the different grades of additives used, with loading level controlling any differences seen. This is is most likely caused by the FR additives interfering with the ability of the PBT to crystallise.

For the Tetrabromobisphenol A compounds this interference with the crystallization of PBT can be attributed to bonding between the Tetrabromobisphenol A compounds and PBT. The affects on crystallinity are related to the total amount (wt.%) of FR additives present in the compounds.

The addition of all of the FR additives reduced the melting temperatures and increased the re- crystallization temperatures. Many authors have reported similar results [117,119], and the main reason is attributed to the additives acting as nucleating sites, which makes crystallisation easier to start. From these results it would seem that the FR additives used makes crystallisation of PBT easier but once started hinders crystallization reducing the total percentage in the solid polymer.

5.2.4 Rheological Properties

Effects were seen on shear viscosity at increasing shear rates due to both loading level and type of Tetrabromobisphenol A compound in PBT, as can be seen from Graphs 4.2 and 4.3. All of the filled compounds and unfilled PBT exhibited a linear or near linear relationship between log shear rate and log shear viscosity up to a shear rate of $450s^{-1}$. For this range of shear rates the n value is 1, which means the compounds are behaving in a Newtonian manner. After this the gradient of the line and hence the n value decreases with increasing shear rate, indicating a pseudoplastic flow.

The greatest differences between compounds were seen at the lower shear rates, as have been reported by several other authors [114,115,116] for various filled polymer systems. As the shear rates increased the differences between the filled compounds and unfilled PBT decreased, with the values of shear stress for the unfilled PBT and compounds containing varying BC52 loading levels converging (Graph 4.2)

All Tetrabromobisphenol A compounds had higher shear viscosities, at the lower shear rates used, than unfilled PBT. As the shear rate increased the differences between the filled compounds and PBT decreased. Several authors have attributed this to the additives aligning into a orientation more favourable to flow [114].

Clear trends were seen between the three Tetrabromobisphenol A compound, as shown in Graph 4.3. BC52 had the lowest values of viscosity, followed by BC58, and then BC52HP, at all shear rates. This effect could be caused by several factors, the primary one being difference degrees of bonding between the Tetrabromobisphenol A compounds and the PBT. The BC52 has the weakest bonding and the BC52HP the strongest which would cause the effects seen. This also explains why the differences get smaller at higher shear rates, as the bonding between the PBT and Tetrabromobisphenol A compounds is overcome by the shear forces acting on the compounds reducing the viscosity of the compounds.

Also the differences in T_g temperatures could affect the melt properties of the Tetrabromobisphenol A compounds. The order of the differences in the T_g corresponds to the increases in the shear viscosity of the relevant filled compounds. The different Tetrabromobisphenol A grades would be at different softness at the test temperature of 250°C, corresponding to the T_g values, and thus having the effects seen in Graph 4.3.

The effects of BC52 loading level on shear viscosity were also determined. The results are shown in Graph 4.2. Trends were seen for BC52 loading levels but the differences were smaller than those seen for the other two Tetrabromobisphenol As. The lower the loading levels the higher the shear viscosity values. This disagrees with finding by many authors [116]. The exact causes for these results are unclear but are most likely related to interactions between the PBT and Tetrabromobisphenol A BFR or the relative viscosities of the polymer and additives at the test temperature.

5.2.5 Molecular Weight

The effect of processing, Tetrabromobisphenol A compound type, and loading level, on the molecular weight of PBT was determined. Table 4.9 summaries the data. This was done as there were concerns over the Tetrabromobisphenol A compounds reducing molecule weight, through impurities present in them [121]. From Table 4.9, it would seem that there is no molecular weight reduction caused by the high shear from twin screw extrusion compounding.

Loading level and Tetrabromobisphenol A compound type also had little or no effect on molecular weight of PBT. Theses results also indicate that adequate drying was performed, before and after compounding to remove water, to stop any molecular weight breakdown during processing. This was concluded as the virgin PBT had similar values to that of unfilled PBT that had been passed thought the APV.

5.2.6 Impact

Effects were seen for all the Tetrabromobisphenol A compounds, at various loading levels, on both peak and failure energy of PBT Compounds, as shown in Graphs 4.11 to 4.13. Standard deviations were high. For peak energy they ranged from 8% (for unfilled PBT) to 45% of the mean values. For failure energy the standard deviations varied from 10% (for unfilled PBT) to 40% of the mean values. The additions of the Tetrabromobisphenol A compounds increased the percentage standard deviations.

Graphs 5.5 and 5.6, combine data from Table 4.5 and Graphs 4.11 to 4.13 to produce plots for actual Tetrabromobisphenol A loading level against peak and failure energy for the three compounds. Trend lines have been fitted to each set of data. For failure energy a polynomial was found to give the best fit with the data, whilst for peak energy exponential trend lines gave the best fit to the data.

From Graphs 4.11 to 4.13 and 5.5 and 5.6 it t can be seen that the addition of all three grades of Tetrabromobisphenol A reduces both peak and failure energy substantially at all loading levels used. Using the trend lines from Graph 5.6, at loading levels of ≈10wt.%, a reduction of between 47 and 54%, compared to unfilled PBT, was preducted for peak energy. The decreases continued for all Tetrabromobisphenol A compounds and at the highest loading levels reductions from 70 to 85% compared to unfilled PBT were seen.

For failure energy similar trends were seen. Using the trends lines from Graph 5.5, at loading levels of 10wt.%, reductions of between 45 and 68% compared to unfilled PBT were observed. At 23wt.% Tetrabromobisphenol A reductions of between 80 and 91% compared to unfilled PBT were seen.

From this data the effects on failure energy are greater than for peak energy. As with Sb_2O_3 particle size in PBT, it would seem that the addition of Tetrabromobisphenol A has a greater effect on the ability of PBT to absorb energy after crack initiation. This is most likely caused by reducing the ability of the PBT to plastically deform.
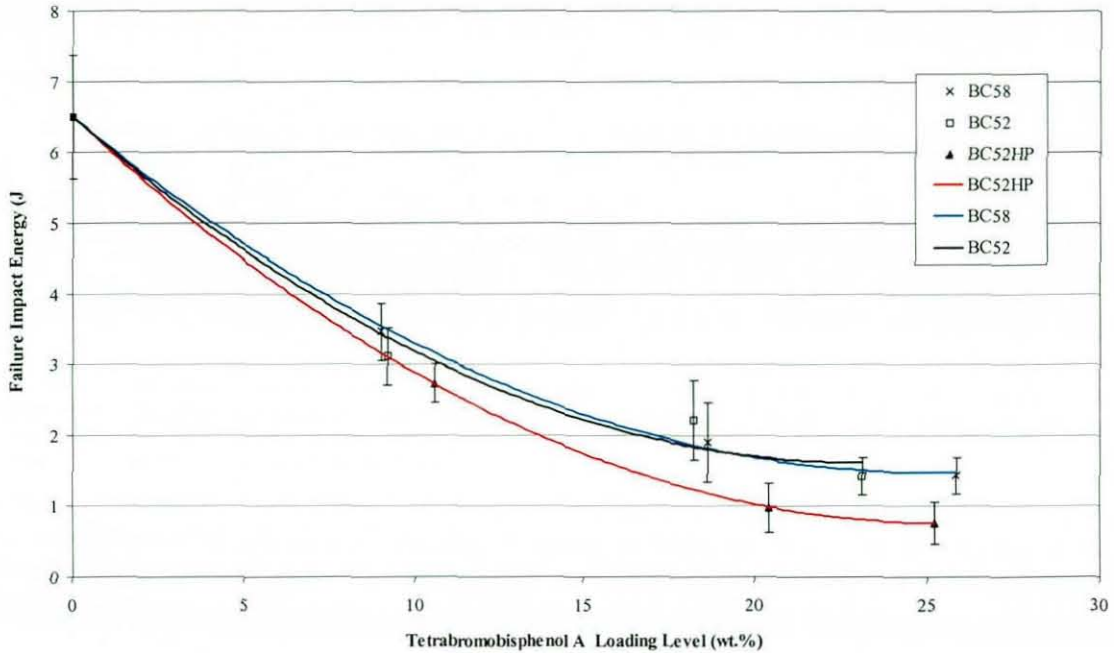
Graph 5.5, Effect of Tetrabromobisphenol A Type and Loading Level On Impact Failure Energy of PBT

This is also seen in Graph 4.15, which shows two traces, one for PBT and another for PBT containing ≈32wt.% BC52. The main difference between the two is the large reduction in deflection before failure after peak load. The total areas under the curve, which correlate to failure energy, are substantially less. It can also be seen that the force required to initiate failure and the energy associated with this are lower for the filled compounds, compared to unfilled PBT.
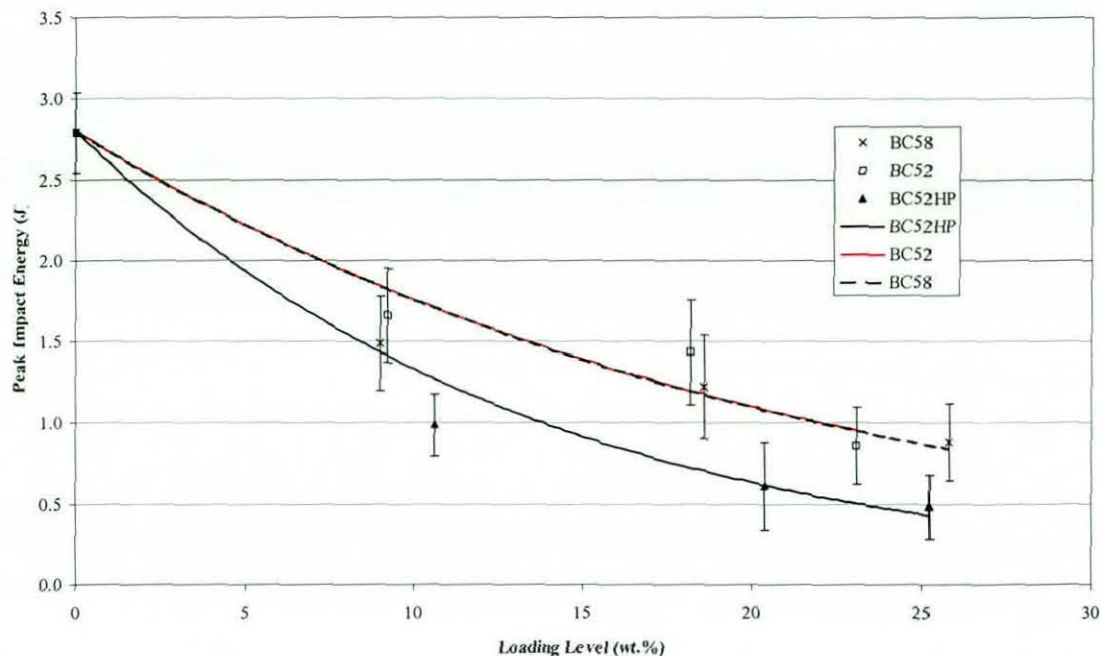
Graph 5.6, Effect of Tetrabromobisphenol A Type and Loading Level On Impact Peak Energy of PBT

For both peak and failure energy, BC52 and BC58, had very similar results at all loading levels, and were higher than those for BC52HP. From Graphs 5.5 and 5.6, it can be seen that the differences between BC52HP and the other Tetrabromobisphenol A compounds increases as the loading level increases. From Graph 5.6 the trend lines for BC52 and Bc58 lei on top of each other. This was the case for both peak and failure energy. Similar trends have been seen for other properties such as shear viscosities, fracture toughness (discussed in section 5.3) and T_g temperature of the powders. These various property changes, are discussed elsewhere in this section, but have primarily been caused by the Tetrabromobisphenol A compounds bonding with the PBT in varying degrees.

Other factors may also have caused the reductions in impact properties seen as the Tetrabromobisphenol A levels increased. Unfilled PBT is a tough material, which can absorb large amounts of impact energy. Dilution of the PBT, by additives such as Tetrabromobisphenol A that can absorb less impact energy, will decrease impact properties. However, this cannot be the only reason for the reductions noted, as they are too great and varied for the grade of Tetrabromobisphenol A used.

The main difference between the BC52HP and the other Tetrabromobisphenol A compounds, are the end groups. Both BC52 and BC58 have phenol end groups, although BC52 has a higher molecule weight which is more significant. BC52HP has Tribromophenol end groups, which would appear less likely to bond with PBT. The different end groups caused differing degrees of bonding between the PBT and Tetrabromobisphenol A compounds, causing the effect seen in Graphs 5.5 and 5.6.

Many authors have reported that better bonding between additives and the polymer matrix can increase impact properties of filled polymers [28,122,123]. There have been several explanations given for these effects. Firstly, better load transfer from the polymer matrix to the additive present, which allows the additive to bear some of the load and absorb energy. Secondly, if the additive is bonded to the polymer, void formation around the particles is less likely to happen or will happen at a later stage in the failure process, both of which can improve impact properties. Lastly, de-bonding of the additive particles from the polymer matrix itself can act as an energy absorbing mechanism. From the SEM images of the impact fracture surfaces there is no evidence of matrix/additive de-bonding, which means that the variations in impact properties most likely caused by the first two reasons.

5.2.7 Fracture Toughness

Fracture toughness of PBT compounds containing Tetrabromobisphenol A varied for both loading level and type. Graph 5.7 combines data from Table 4.5 and Graph 4.22, to produce a plot, for the three Tetrabromobisphenol A compounds, of actual loading level against K_C values. Lines have not been fitted to this data because there were no obvious trend between points for similar Tetrabromobisphenol A compounds. However the values of K_C for each of the compounds were always in the same relative positions. Standard deviations were small, and varied from 3 to 11% of the mean values.
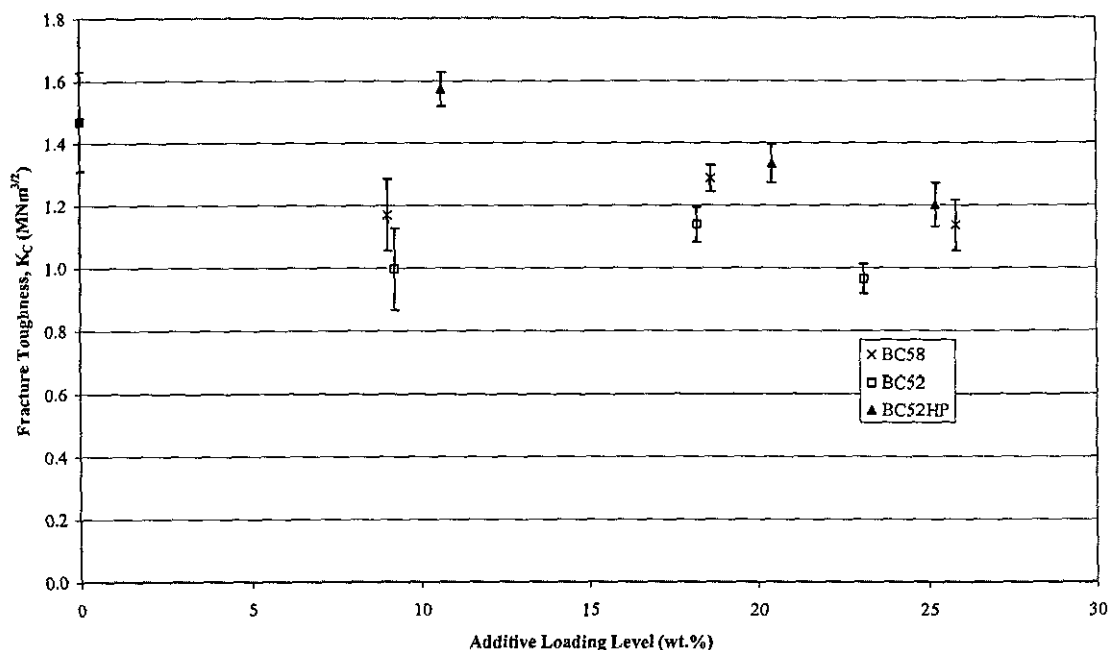
Graph 5.7, Effect of Tetrabromobisphenol A Type and Actual Loading Level on Fracture Toughness of PBT.

From Graphs 5.7 and Graph 4.22, the most noticeable effect was caused by Tetrabromobisphenol A compound type. At all loading levels BC52HP had the highest results, followed by BC58 and then BC52. This is the direct opposite of the results seen for impact testing. The trends for impact testing were associated with the degree of bonding between the Tetrabromobisphenol A compound and PBT, these results would indicate that the better the bounding between the additive and PBT the bigger the reduction in K_C values.

At the maximum loading levels reductions of between 20 and 33 % were seen compared to unfilled PBT. This is substantially less than the reductions both peak and failure impact energy for these compounds.

5.2.8 Tensile Properties

The effect of both type and loading level of Tetrabromobisphenol A on strain at break, maximum stress and Young's modulus are listed in Table 4.17. Graph 4.26, shows the range of stress strain curves used to generate some of the data in table 4.17. The graph only shows curves for BC52, at all loading levels used, as little variations were seen between the three Tetrabromobisphenol A compounds. Although all of the Tetrabromobisphenol A compounds did cause effects on these properties, they were generally small compared to other properties such as impact and fracture toughness. Also unlike other properties, there was little difference between the different grades of Tetrabromobisphenol A.

Although the differences between the compounds were small, so were all of the standard deviations. For strain at break the standard deviations were between 3% and 20% of the total values. For maximum stress, the standard deviations ranged from <1% to 8%, whilst for Young's modulus standard deviations varied from 2% to 5%. These values are much smaller than those seen for impact and fracture toughness testing, but similar to those for other tensile testing, for both PBT and HIPS.

The main effect seen was in strain at break values. As the loading level increased strain at break values decreased. There was little effect seen between the various Tetrabromobisphenol A compounds used. Significant decreases were seen for loading levels up to ≈20wt.%, after which the values levelled of. This can also be seen in the stress/strain curves shown in Graph 4.26, for PBT compounds containing various BC52 loading levels. Significant reductions can be seen in strain at break values at both 12 and 20 wt.% BC52. At a loading level of 20wt.% BC52, the stress strain curve for PBT is typical of a brittle polymer such as PS, with no plastic deformation after the maximum stress is reached. Unfilled and 12wt.% BC52 compounds had similar curves through the elastic region, but then under went significant plastic deformation prior to failure.

It is not completely clear if there is a critical additive loading level at which the PBT changes from a ductile to brittle polymer, or if a gradual decreases in plastic deformation occurs as the loading level increases. However, given the gradual change from unfilled to 12wt.% BC52, it is likely that it continues to gradually decrease as the loading level increases. The decreases in maximum stress values at high loading levels are caused by reduction in the ability of these compounds to elastically deform. A transition from ductile to brittle failure seen in strain at break properties has been reported by a several authors [107, 122,119]. Bazhenov [107] showed that at a critical loading level, a co-polyester based polymer filled with calcium carbonate changed from a ductile to brittle failure. Similar trends were seen for PBT filled with Tetrabromobisphenol A.

The effect was caused by the filler reducing the ability of the polymer to strain harden. PBT will strain harden when a load is applied so this explanation can be used for the results seen in Table 4.17 and Graph 4.26 As the Tetrabromobisphenol A loading level increases it reduces the ability of the PBT to strain harden. At a critical value the mode of failure changes from ductile to brittle failure. The polymer matrix primarily determines this value, although additive properties such as particle size and polymer/additive adhesion can affect the values [55,107, 116-119]. The degree of bonding between PBT and the Tetrabromobisphenol A BFR did not affect the critical loading level values for the PBT compounds.

Maximum stress values only varied slightly across the entire Tetrabromobisphenol A loading level range tested. As with other tensile properties there was no effect due to Tetrabromobisphenol A type. For loading levels between 0 and 12wt.% there was no variation in maximum stress values. At a loading level of 20wt.% there was a small increase, this increase coincided with the change from ductile to brittle seen in the strain at break values. As the loading level increased further the maximum stress values decreased compared to both unfilled values and those for 20wt.%. This seems to be caused by the fact that there is a linear relationship between stress and strain at this point, so as the additives reduce the ability of the PBT to deform further, with constant Young's modulus (discussed later) a reduction in the maximum load will happen.

There was minimal effect on Young's modulus due to either Tetrabromobisphenol A loading level or type, as can be seen from Table 4.17 and Graph 4.26. The major effect seen is an increase for all the filled compounds compared to unfilled PBT. This is in agreement with most available literature [119,28,129], and can be attributed to the Tetrabromobisphenol A compounds bonding with the PBT matrix. This will reduce the ability to the PBT to deform under an applied load. It has also been shown that after an initial increase in Young's modulus the effect of additional additives is minimal [29,129].

5.3 DBDPO

DBDPO was used exclusively in HIPS, and its effects have been characterised at loading levels from 4 to 32wt.%. This section discusses both the results for DBDPO and where relevant compares then to HIPS compounds containing Sb_2O_3 at similar loading levels.

The effect of DBDPO at 32wt.% on the shear viscosity of HIPS compounds is shown, in Graph 4.4. There is a small increase in shear viscosity at low shear rates but as the shear rate is increased the values converge with unfilled HIPS. Similar trends were seen for Sb_2O_3 at the same loading levels, and reasons have been discussed in section 5.1 and are the same for DBDPO filled compounds.

5.3.1 Particle Size and Morphology

Both SEM and laser diffraction data gave good agreement for the particle size of the DBDPO powder; giving average sizes up to 5μm. However the laser diffraction data in Table 4.1 and Appendix 1, shows that there was a small number of much larger particles, between 20 and 50μm present. From Plates 4.13 and 4.14 and 4.35 to 4.40 there was good dispersion of the DBDPO and no or little evidence of aggregate or agglomeration formation of the DBDPO in the HIPS matrix. Plate 4.13 is a back scattered SEM image of HIPS containing 12wt.% DBDPO. The larger DBDPO particles can be seen from this image.

Plate 4.13, shows a high magnification of the same compound, and shows that the majority of the particles present are ≈5μm or smaller and are oblong in shape. It would appear that there was no interaction between the DBDPO and the HIPS matrix. The DBDPO particles appeared to sit on the fracture surfaces, and there was evidence that voids had formed around several of the particles during failure, these voids will reduce many mechanical properties such as impact strength, and strain at break. This was similar to the finding for Sb_2O_3 in both HIPS and PBT.

Several possible mechanisms for failure in filled polymer systems have been proposed, including, failure through the polymer matrix, which is typical of good polymer additive bonding, failure at the additive/polymer interface, and failure through both polymer matrix and additive, where there is good adhesion. As with Sb_2O_3 in HIPS it would seem that failure occurred by starting at the DBDPO/HIPS interface. This creates voids around the DBDPO particles, which will significantly reduce mechanical properties.

Plate 4.35 is a stained TEM image of a HIPS compound containing 12wt.% DBDPO. From this plate it can be seen that the DBDPO resides in the PS main phase, this is the same as for all the Sb_2O_3 grades used, and previous work in other rubber reinforced styrene polymers [33,34]. There is evidence of the DBDPO particles affecting the morphology of the rubber phase, which could influence properties. The size and morphology seems to agree with the SEM images of compounds and data for the raw powders.

5.3.2 Impact

Graph 5.9 combines data from Table 4.4 and Graph 4.9 and shows the effect of DBDPO loading level on HIPS up to 32wt% (this is the amount needed to achieve a UL94 V-0 rating with no synergist present). Trend lines have been fitted to this data. For peak energy a linear line was found to give the best fit, and for failure energy a polynomial line was found to give the best correlation with the data. For both peak and failure energies the trend lines fit the data well, in all cases being within the standard deviations for the data points.

The graph shows that as the loading level increases there is initially little change from unfilled HIPS. From 5wt.% to 32wt.% DBDPO both peak and failure energies decrease. Failure energy decreased overall by 80% and peak energy by 70%, which is also shown in Equations 5.7 and 5.8. A linear model was used for peak energy but polynomial for failure energy. This data shows that the DBDPO is causing the HIPS to fail in a more brittle mode, by having a greater effect on the failure energy, reducing the ability of HIPS to plastically deform, whilst it has only a small effect on elastic deformation and maximum load bearing capability.
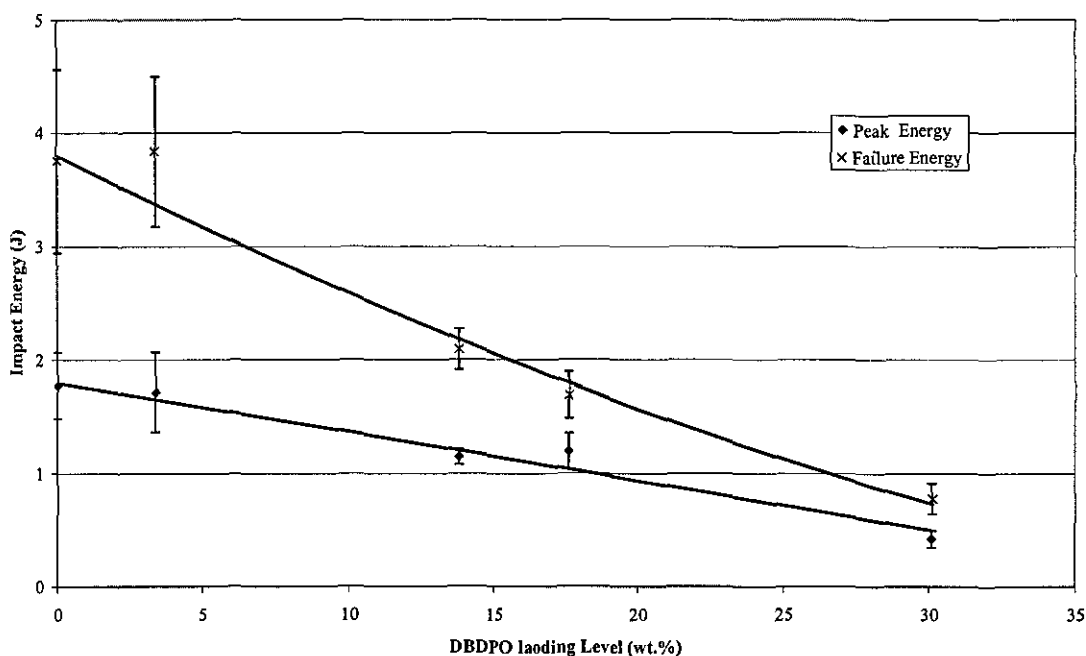
Graph 5.8, Influence of DBDPO Loading Level on Impact Properties of HIPS.

Failure Impact energy (J) = $-0.0009L^2 - 0.12L + 3.8$ **Equation 5.7**

Peak Energy (J) = $-0.043L + 1.8$ **Equation 5.8**

Where L= Loading level of DBDPO in HIPS (wt.%)

Trends shown in Graph 5.8 are similar to those in Graph 5.2 and 5.3 for Sb_2O_3. The data for failure energy, for RS, TT and DBDPO have been combined in Graph 5.9. Up to loading levels of 20wt.% the trend lines for TT and DBDPO are very similar. After this point DBDPO continues to drop whilst values for TT level of. From this data it is likely that the curve for DBDPO will level of at a higher loading level than for both TT and RS.
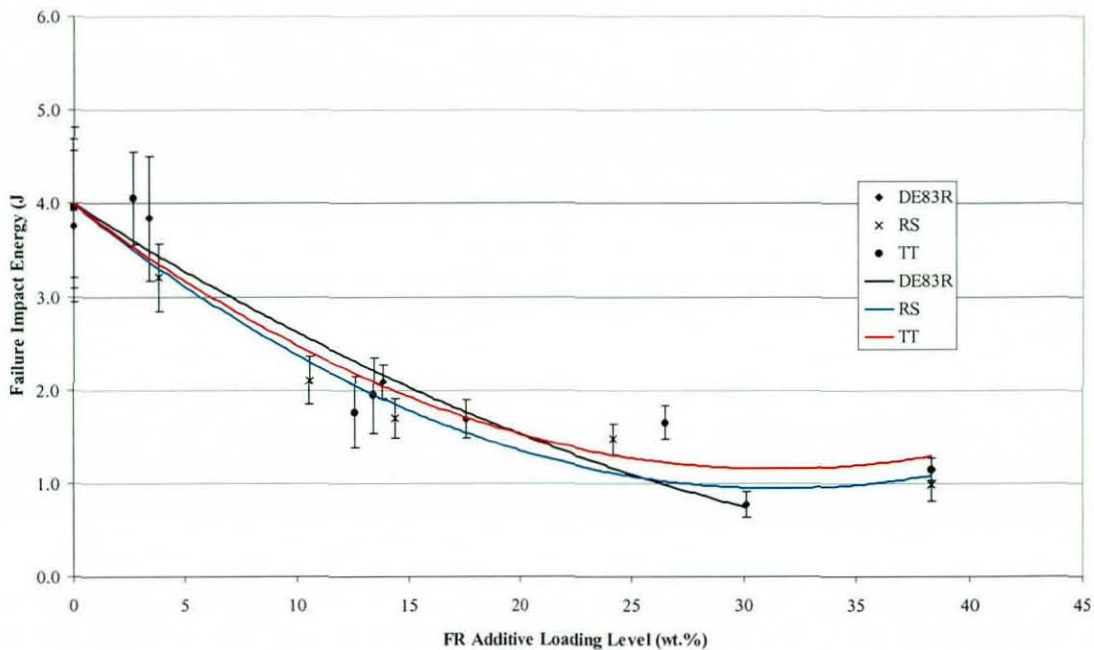
Graph 5.9, Impact Failure Energy Versus Loading Level of TT, RS and DBDPO.

Friedrich [55] divided void formation into three stages. Firstly poor bonding between the additive and matrix allowing the polymer to detach from the additive creating a series of voids on both sides of the particles, perpendicular to the applied load. During the second stage the voids grow in the same direction, to a length, which is related to the size of the particles present. In the final stage the holes around the particles linked up and cause the polymer compounds to fail. Friedrich stated that as the additive loading level increased, the amount of energy required for stages 1 and 2 would continue to decrease whilst stage 3 will be unaffected.

This eventually causes a transformation from ductile fracture to a microscopically brittle fracture. In the ductile mode the polymer is not restricted in its ability to deform and absorb energy. In the brittle mode the fracture is dominated by the voids around the particles, which control crack formation, and reduce the amount of energy that is required for failure in the compound. This method can be applied to void formation in many of the PBT and HIPS compounds including DBDPO in HIP. For silicon oxide in polypropylene Friedrich found that a critical loading level of 15% existed where the failure mode changed from ductile to brittle. For DBDPO in HIPS this value is <10wt.%.

Plates 4.28 to 4.32 show low magnification SEM images of the HIPS fracture surface, for the compounds containing up to 32wt.% DPDPO. From the images of the fracture surfaces a clear trend can be seen from unfilled HIPS (Plate 4.28) up to the most highly filled DBDPO HIPS compound (Plate 4.32). As the level of DBDPO increases there is a change in topology as the surface roughness increases. The change in topology can be correlated with impact values. As the impact values decrease the amount of surface roughness increased. Similar trends have been observed for other HIPS compounds used in this work with varying loading levels of bromine and Sb_2O_3.

From these plates it can be concluded that the FR additives used have a noticeable effect on the fracture surfaces, which can be related to the amount of additive present. As the loading level of DDBPO increases the number of particles will increase, which will affect crack propagation through the sample. From Plates 4.13 and 4.14 cracks appear to propagate from one particle to another. For samples containing a larger number of particles the crack will be diverted more often creating a rougher surface topology. Similar results and causes were seen by Maita [119] using polypropylene filled with various loading levels of Kalolin.

Owen [33] and Seddon [34] observed similar trends for Sb_2O_3 and BFR in ABS. Their results concluded that unfilled ABS had a smooth facture surface, and that as impact energy was reduced due to the presence of FR additives, the fracture mechanism changed, and a rougher fracture surface was seen.

This would indicate that reductions in the impact properties of rubber toughened styrene based polymers are accompanied by an increase in the fracture surface roughness. Also the change in fracture surfaces is independent of FR additive loading level and type, but related to the effects they have on impact properties.

5.3.3 Fracture Toughness

Fracture toughness K_C values are shown for various DE83R loading levels in Graph 4.20. Unlike some of the fracture toughness results for HIPS clear trends were seen as the DBDPO loading level increased. The standard deviations varied from <1% to 9% of the mean values. These were much smaller than for the impact test data. Increased loading levels reduced K_C. The effect was smaller, compared to impact testing, with only a 25% reduction at the maximum loading level, compared to 70% for peak impact energy.

As with other results a plot for actual loading level against K_C is shown in Graph 5.10. A linear trend was found to give the best fit to the data points, fitting the data very well. As with the vast majority of filled HIPS compounds the K_C values were all lower than for unfilled HIPS. As with Sb_2O_3 the DBDPO particles increased stress at the crack tip, which caused a reduction in K_C values. The trend seen for DBDPO loadings levels is different to that for Sb_2O_3 where no trend was clear.

5.3.4 Tensile Properties

The effect of DBDPO on the tensile properties was similar to that for Sb_2O_3. The biggest effect seen was for strain at break, were reductions of up to 63% at the maximum loading level, were recorded compared to unfilled HIPS. The standard deviations varied from 5% to 20% of the mean values, which was less than for impact results for DBFDPO filled compounds. The reasons for this significant decrease are similar to those discussed for Sb_2O_3 loading level (section 5.1.3.3).

Young's modulus values for the filled compounds increased slightly over unfilled HIPS. Although the numbers are large, as a percentage of the mean, they only varied from 2% to 4 % o. The increases seen were small, especially if the standard deviations were considered, and there were no trends related to the DBDPO loading level. As with Sb_2O_3 in HIPS, DBDPO had no effect on the maximum stress values. The standard deviations were also small varying from 4% to 9% of the mean values.

5.4 Combined Affect of Sb_2O_3 and BFR

This section discusses compounds that contain both BFR and Sb_2O_3 at levels required to achieve a high degree of flame retardancy. For PBT the direct addition of Tetrabromobisphenol A compounds and RS grades of Sb_2O_3 only were considered. For the HIPS compounds direct additions were complemented by the use of an impact modifier, and the use of new grades of BFR and Sb_2O_3 masterbatches named 'Fyrebloc'.

5.4.1 BFR and Sb_2O_3 in HIPS

5.4.1.1 Impact

Results for both peak and failure energy are given in Graph 4.17 for compounds containing only DBDPO and Sb_2O_3 with varying particle sizes. Differences between all of the compounds can be seen, and they all have significantly lower peak and failure energy values than unfilled HIPS. As with compounds containing only DBDPO or Sb_2O_3 reductions in failure energy were greater than that for peak energy. Failure energy was reduced by between 40 and 50% compared to unfilled HIPS, whilst for peak energy reductions of between 12 and 50 % of unfilled HIPS were recorded.

In the majority of cases, the trends seen followed those for shown in Graph 4.5, which shows the effect of varying Sb_2O_3 particle size on peak and failure energy of HIPS. The DBDPO also appeared to control the impact properties of these HIPS compounds.

In Graph 4.17 the effects of Sb_2O_3 particle size were much smaller, than those in Graph 4.5. It was not possible to relate the effect seen for Sb_2O_3 and DBDPO individually to compounds containing both. The result seen in Graph 4.17, are higher than would be indicated by simply adding the effect for the individual components the individual additives.

From the individual effects, the DBDPO caused the biggest reduction, therefore it is likely that this would also be seen for the combined data. Both Owen [33] and Seddon [34] also found that the BFR used dominated failure in ABS compounds containing both Sb_2O_3 and BFRs. This was attributed to the BFR being used at higher loading levels, and similar fracture patterns between compounds containing only BFR and those with both BFR and Sb_2O_3. However the fact that trends seen in Graph 4.17 follow those seen for Sb_2O_3 particle size in HIPS (Graph 4.5) would indicate that Sb_2O_3 particle size is having some effect on failure, although effects caused by DBDPO are still dominate failure.

The reasons for the reductions not being as large as indicated by the individual data can be accounted for by several factors. Firstly the loading levels were generally lower than aimed for. From Graphs 5.3 and 5.8 plotting loading level against failure impact energy, it can be seen that small variations in loading level can have significant differences on impact properties. Also, these results may indicate that the DBDPO is dominating fracture and impact properties. Lastly these results show that the reductions seen in impact properties are not solely due to the dilution effect of the FR additives on the HIPS matrix.

The only results that did not fit those previously seen were for the compounds containing Azub, this was lower than would have been predicted from the additives used separately. This is most likely due to either the high loading level of Azub and DBDPO present in this compound (Table 4.5), or due to grades of Azub easily forming agglomerates during processing, which can substantially reduce impact properties.

5.4.1.2 Flame Properties

Table 4.19 shows LOI and UL94 results for compounds containing DBDPO and Sb_2O_3 with varying particle size. From this table it can be seen that the DBDPO/Sb_2O_3 additions increase LOI value from 17 to ≈26%. Many authors have reported that this increase changes HIPS from a non-flame retarded polymer to one that is considered to be flame retarded [14,15,120]. There was no variation between the different grades of Sb_2O_3 used, indicating that the particle size of Sb_2O_3 has no affect on LOI values.

Variations in both UL94 rating and the observations made during testing, varied between unfilled and filled HIPS and the grades of Sb_2O_3 used. For the majority of compounds, the use of DBDPO and Sb_2O_3 increased the UL94 rating from fail to V-0, the highest possible. This was achieved by a reduction in both burn time and by reducing the type and amount of dripping. Generally the compounds with the smallest particle size Sb_2O_3 gave the highest flame retardant effect. Also the filled compounds that gave the lowest results had slightly lower DBDPO and Sb_2O_3 levels. These results show that if either the Sb_2O_3 or DBDPO loading level is lower than 3.5 and 12 wt.% respectfully, then the flame retardant effect that they achieve in HIPS is significantly lower. Therefore a critical loading level for both Sb_2O_3 and DBDPO exists when used in HIPS. If the loading levels are above this, high levels of flame retardancy will be achieved, below this only small improvements will be seen.

5.4.2 BFR and Sb_2O_3 in PBT

The effect on impact properties of both the Tetrabromobisphenol A and Sb_2O_3 grade RS and TT are given in Graph 4.17. Standard deviations ranged from 10 to 40 % of the mean value for failure and 20 to 40% of the mean value for peak. Small trends were seen for Tetrabromobisphenol A type, although the Sb_2O_3 grade had little effect. The trends were the same as seen when the Tetrabromobisphenol A compounds were used on their own, with BC52 and BC58 having similar results, and BC52HP giving slightly lower results than the others.

The reduction in both peak and failure energy are not as large as would be predicted from when Sb_2O_3 and the Tetrabromobisphenol A compounds were used separately. Similar trends were seen for DBDPO and Sb_2O_3 in HIPS. Given that the trends follow those for the Tetrabromobisphenol A compound, it would indicate that it is the Tetrabromobisphenol A compounds which control impact properties when combined with Sb_2O_3.

Table 4.22 summaries LOI and UL94 data for all PBT compounds that have been flame tested. All of the filled PBT compounds had significantly higher LOI and UL94 results than unfilled PBT. LOI values increased by ≈30% for each of the compounds, whilst UL94 results changed from a fail for unfilled PBT to V-0 for all of the filled compound. This was due to a reduced burn time and a change in dripping type from burning to non burning. All of the filled compounds still had a significant amounts of dripping, This can be controlled by the use of Teflon compounds as anti drip agents [90]. The bromine and Sb_2O_3 contents varied for each of the compounds, and were generally lower than aimed for. Unlike HIPS this did not seem to affect either UL94 or LOI properties.

5.4.3 Effect of Impact Modifier on Properties of FR HIPS

This section details the effect of the impact modifier used in FR HIPS. The impact modifier was only used in compounds that contained 12wt.% DE83R and 4wt.%RS, at loading levels of 0 to 20wt.%. Effects were seen on several properties including impact and flame properties. As with other HIPS compounds the Sb_2O_3 and DE83R particles located themselves in the PS matrix, and never in either the primary or Stereon rubber phase.

5.4.3.1 Rubber Morphology

Plates 4.36 to 4.41 are TEM images of HIPS compounds with varying amounts of Stereon impact modifier. These plates show both high and low magnification images of each loading level used.

As the loading level increases, there are changes in the morphology of the Stereon rubber phase. At a loading level of 4wt.%, the Stereon impact modifier formed a combination of spheres and irregular shaped particles of $\approx$0.5 μm (Plates 4.36 and 4.37), these were all separate with no interaction between either the Stereon particles or the primary rubber phases.

As the loading level increased the morphology of the rubber also changed, the particles became larger, and all highly irregular in shape. As with 4wt.% loading level the Stereon particles remained independent of each other, with significant inter-particle distance between them. The irregular shaped Stereon particles seen in all relevant compounds are typical of the results obtained for the mechanical blending of rubber, as opposed to the primary rubber phase, which are regular shaped and typical of rubber added during manufacture [33,34,17]. At 20wt.% Stereon impact modifier the morphology changed from that seen in the other loading levels. The main difference was that the particles joined to from a network within the PS matrix (Plates 4.40 and 4.41), although they still did not interact with the primary rubber phase.

As with the primary rubber phases an internal structure can be seen for the Stereon impact modifier. The Stereon impact modifier contains small PS inclusion. These are smaller than those for the primary rubber phases, at $\approx$0.025μm in size, compared to $\approx$0.5 μm for the primarily rubber phase, this is due to the Stereon impact modifier forming smaller particles than are present for the primary rubber phase.

5.4.3.2 Impact

Unsurprisingly the impact properties of HIPS were affected by the addition of the impact modifier at all loading levels used. Graph 5.10 plots the percentage impact modifier as aimed for, against peak and failure energy. Compound 5-3/HIPS/DE83R-12/ RS-4 was used as the control, instead of an unfilled compound, as this had a similar Sb_2O_3 and DE83R content to the remaining compounds.

As can be seen from Graphs 4.10 and 5.10, at all of the loading levels used, the Stereon impact modifier increases failure energy, but overall decreases in peak energy occur. Graph 4.13, shows representative force displacement graphs as obtained from the impact tests. As the amount of Stereon increases, failure initiation occurs at lower forces, but there is more deformation before eventual failure, giving higher failure and lower peak energies. This may indicate one way in which the Stereon impact modifier increases failure impact properties, which is by increasing the amount of deformation that the polymer can undergo before total failure. It has been reported by many authors that toughening of polymers can be achieved by rubber phases deforming within the polymer, absorbing energy as they do so [17,1,55]. From Graphs 4.13 and 5.10 it can be seen that the Stereon impact modifier reduces the force (and hence energy) required to initiate failure. These reductions increase as the loading level of Stereon increases from 0 to 20wt%. When using Stereon impact modifier it is a trade-off, between overall increase in failure energy, and a slight reduction in peak energy with a more distinct reduction in force required to initiate failure.

As discussed in section 2.1.4 rubber toughness enhancement is primarily caused by crazes formed in the polymer, and secondly deformation of the rubber phases within the PS matrix. Both of these methods can absorb significant amounts of energy during failure. It has been shown above that the second of these methods occurs. The size of the rubber is also critical in determining its effective in craze iniation and termination. The particles formed by Stereon, are much smaller than the primary rubber phase, which may explain why they are not as effective as the primary rubber phase.

From Plate 4.46, a TEM image of a HIPS compound containing Stereon impact modifiers, it can be seen that both craze formation and termination are occurring at the Stereon impact modifier particles. Manufacturers recommend 4wt.% to obtain a noticeable increase in impact properties. From this data, this loading level only gives minimal improvements, over similar compounds with out it. To achieve noticeable increases in failure energy 10wt.% is required, which amount returns failure energies close to that for unfilled HIPS. Also the reduction in peak force and energy is no more than that for 4wt.%.
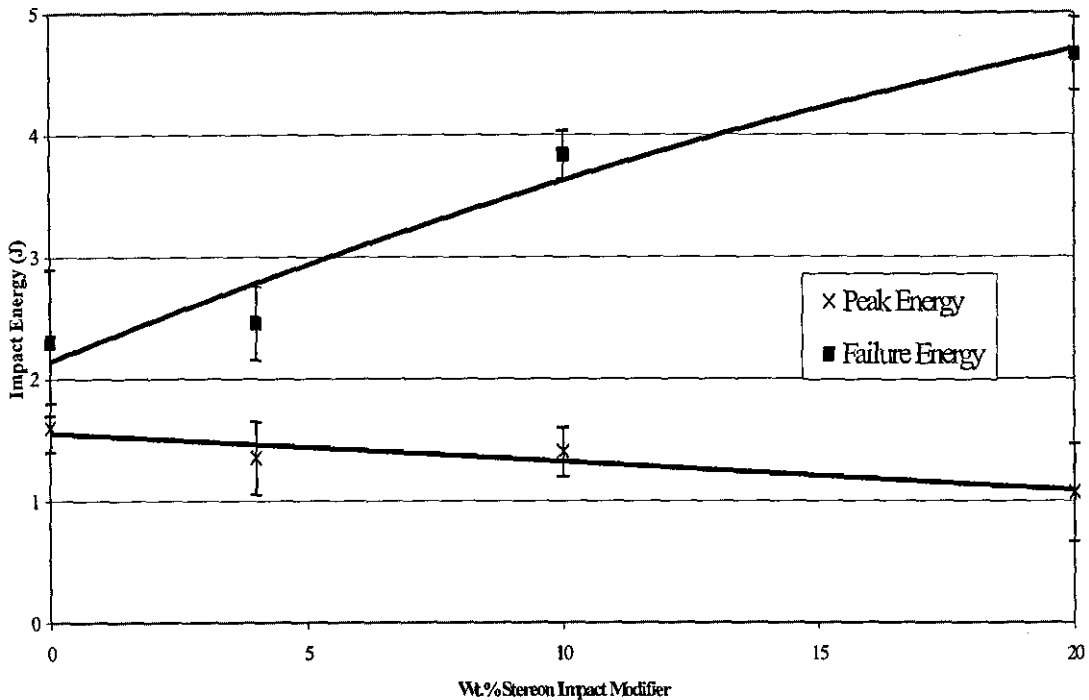
Graph 5.10, Effect of Stereon Impact Modifier on Peak and Failure Energy of FR HIPS.

5.4.3.3 Tensile

Table 4.16 summaries the data for strain at break, Young's modulus and maximum stress for all compounds containing Stereon impact modifier. From this table it can be seen that additions of the impact modifier have no noticeable effect on these properties. Given the data for impact testing, increases in strain at break values and possible reductions in maximum stress values were required. These would correspond with increases in deflection at break and reductions in peak force/energy in the impact tests

The fact that no differences were observed may be due to the tensile testing not being sensitive to the effects that the Stereon impact modifier has on HIPS. Other effects, such as Sb_2O_3 particle size, did not significantly affect these tensile properties. This has also been reported by several other authors [33,34]. The deformation of the added rubber may be restrained by the surrounding PS, which may mean it will deform without affecting strain at break.

5.4.3.4 Flammability

The addition of the Stereon impact modifier affected UL94 results, although no effect was seen on LOI results. Similar trends have been seen for impact modifiers added to other polymers [27,34,31]. As the loading level of Stereon increased the burn time, after the removal of the Bunsen burner, increased from 0 to 115s, also the type of dripping increased from non-flaming drips to flaming. Although all of the HIPS compounds dripped the flaming drips were mainly caused by the increased burn times. The addition of rubber into thermoplastics has been shown to increase the flaming time and amount of dripping [34,90].

5.4.4 Fyrebloc Masterbatches in HIPS

5.4.4.1 Additive Content

Table 4.4 summaries the bromine and Sb_2O_3 contents of all the Fyrebloc material used, and Table 3.3 gives the manufacture's data for BFR, Sb_2O_3 and carrier loading levels. The loading level of the Sb_2O_3 and BFR in the Fyrebloc materials was generally different from those aimed for. Also the dispersions of the Sb_2O_3 and BFR in the Fyrebloc materials were bad. From the results discussed in this section, it would appear that big localised variations in the FR additives existed.

The percentage bromine in three of the Fyrebloc masterbatches were either equal to or lower than shown in Table 3.3, with 2DB-370S3 having a higher value. The shortfalls were between 5 and 25% of the aimed for contents. 2DB-370S3 used HIPS as the carry rather than PETS as the other did, it also had a higher Sb_2O_3 content than indicated by the literature. For all but Fyrebloc 510, the Sb_2O_3 levels of the Fyrebloc materials were approximately equal to or higher than the manufactures data, the increases were between 5 and 23% of the manufactures data. The increases seen for Sb_2O_3 were not equal to the decreases in BFR, which indicates more PETS wax must have been present than stated by the manufactures (Table 3.3).

The exact reason for the discrepancies between the aimed for values and measured BFR and Sb_2O_3 levels are unclear, but some of the most likely causes are, poor dispersion, caused by inadequate mixing of the FR additives and carrier, leading to localised differences in composition, errors in the ratios of the constituent components used prior to mixing, variations in the amount of bromine present in the BFR used in the manufacture of the Fyrebloc materials, preferential feeding of one of the FR additives, or the test methods giving incorrect values.

Variations in BFR and Sb_2O_3 were also seen in both the formulations compounded thought the APV and then injection moulded. The two dry powder additions, added directly to the injection moulder, had significantly less DBDPO and RS than aimed for. In fact up to 35% total FR additive less than aimed for. This was due to large amounts of the powder adhering to the hopper and other parts of the feeding mechanism prior to entering the injection moulder. This problem was not encountered with the Fyrebloc materials as they were a relatively dust free pellets, which made the feeding method used easier. This can be seen in that both the BFR and Sb_2O_3 are much closer to the levels aimed for, with only small increases of $\approx 4\%$ measured.

Variations were also seen with the formulations containing Fyrebloc materials that were compounded through the APV before injection moulding (series 9). All of the Sb_2O_3 contents varied from the aimed for levels by ≈ 10 to 15%. The bromine contents varied from ≈ 4 to 40% of the aimed for values. The main variations in loading levels were in the BFR, which are significantly lower than the $\approx 12wt.\%$ aimed for. However, these can be matched to the lower BFR found in the raw Fyrebloc materials.

5.4.4.2 Dispersion

The use of the Fyrebloc masterbatches affected the dispersion of both the BFR and Sb_2O_3 in HIPS, this also caused agglomerates/aggregates to be formed in several of the HIPS compounds containing Fyrebloc masterbatches. Plates 4.20 to 4.27 show the effect of Fyrebloc masterbatches and processing condition on the dispersion of FR additives within HIPS.

The dry powders processed through the APV first, then injection moulded, showed that both the DBDPO and Sb_2O_3 were well dispersed. It was not possible to determine the DBDPO and Sb_2O_3 particles apart in these images. As with formulations containing only DBDPO, large particles were present, these, were not agglomerates or aggregates but large DBDPO particles.

The dispersion of both the DBDPO and Sb_2O_3 was different when formulated directly through the injection moulder. Plate 4.22 and 4.23 show the effect. At high magnification there appears to be little difference when compared with formulations compounded using the APV prior to injection moulding. At low magnification (Plate 4.22) there are differences. The FR additives appear to have followed the flow lines of the HIPS polymer during injection. This is seen for both dry powder formulations used.

The Fyrebloc masterbatches appeared to form agglomerates or aggregates within the HIPS compounds. Plates 4.24 and 4.25 show repsentive images of the dispersion of DBDPO and Sb_2O_3 in HIPS. From these images the FR additives appear to be well dispersed through the HIPS. From the higher magnification image (Plate 4.25), it can be seen that the Fyrebloc materials do not appear to have broken down to the unit particles. Using the SEM, elemental analysis was conducted on the particles, the main large particles were found to be bromine, with the smaller particles being antimony.

When processed by the direct injection moulding method, differences were seen with the dry powder additions. The Fyrebloc materials did not disperse along the injection flow lines, as did the dry powders. This may suggest better mixing with the HIPS, however they did form large aggregates or agglomerates. These are shown in Plate 4.25 and were both numerous and significant in size. These particles were seen in all of the Fyrebloc materials, elemental analysis showed that they were a mix of bromine and antimony, and would indicate that although the Fyrebloc materials mix better than dry powder additions they are unable to disperse down to their unit particles.

The Fyrebloc masterbatches made initial breakdown and dispersion of the FR additives easier, but aggregates formed during manufacture of them did not break down during either processing through a twin screw extruder or during the injection moulding process. It must also be noted that it was much easier to handle the Fyrebloc materials, especially using the direct injection route, as they were relatively dust free.

5.4.4.3 Impact Properties

Table 4.12 summaries the peak and failure energies for the Fyrebloc materials in HIPS, using both directly injection moulding and APV processing routes. When evaluating the results in Table 4.12, effects caused by the state of dispersion and especially the loading level of each of the additives must be considered, which makes direct comparisons difficult. Standard deviations for both peak and failure energy were consistence at between 5 and 20 % of the mean values for peak energy and 10 to 20% of the mean values for failure energy.

For HIPS compounds containing dry powder additions of Sb_2O_3 and DBDPO there seemed to be no differences between the APV and injection moulding method. However, the loading levels in the compounds produced by the injection moulding method were significantly lower than aimed for. This was due to difficulties feeding the powder into the injection moulding machine. Using Graphs 5.3 and 5.8 And corresponding equations 5.2, 5.13 and 5.14, for the effect of loading level Sb_2O_3 and DBDPO, it can be seen that if the loading levels were similar then a much lower peak and failure impact energy would have results. Therefore it can be concluded that the bad dispersion discussed in section 5.4.4.2 causes lower impact results. Bad dispersion of additives has been reported to lower many mechanical properties including impact [63,118]. This is attributed to the badly dispersed additives causing localised areas of weakness within the polymer matrix.

Analysing the HIPS compounds containing the Fyrebloc materials is difficult because both the loading levels of Sb_2O_3 and DBDPO and ratios present are different for the majority of the compounds.

For the majority of HIPS compounds containing Fyrebloc materials, there was little difference between the APV route and direct injection moulding. Using the APV route all of the Fyrebloc compounds had lower peak and failure energy compared to the dry powder additions. It has been shown in section 5.4.4.2 that large aggregates and agglomerates were present in the Fyrebloc compound, which caused these lower results. The fact that they were not broken down during twin screw extrusion means that they are more likely to be agglomerates and not loose groups of aggregates.

A consideration of the injection moulding route, showed that the majority of Fyrebloc compounds gave better peak and failure energy results than the dry powder additions. From section 5.4.4.2 it can be seen that the Fyrebloc compounds had a more uniform dispersion than the dry powder additions, but both still had aggregates and agglomerates present. When consideration is taken of the fact that the loading level of the dry powder addition was lower than aimed for, it would appear that the more uniform dispersion gained by using the Fyrebloc materials, is measurably beneficial to the peak and failure energy of these HIPS compounds.

5.4.4.4 Flame Properties

Table 4.21 summarise UL94 data for HIPS compounds containing Fyrebloc masterbatches, for both processing routes used. This was done to determine the effect of dispersion of the BFR and Sb_2O_3 additives on their flame retardant effect. Although variations in dispersion were seen (see section 5.4.4.1), from Table 4.21 these have not directly affected UL94 data. The effects seen are caused by variations in the BFR and Sb_2O_3 loading levels in the Fyrebloc and final HIPS compounds. The compounds that did not achieve V-0 rating had either lower Sb_2O_3 or BFR than aimed for. This is in agreement with results seen in section 5.4.1.2, and shows that if either small reduction in Sb_2O_3 or BFR occur then significant reductions in flame retardancy will be achieved.

5.5 Comparison Between HIPS and PBT Compounds

This section compares and contrasts results for HIPS and PBT compounds, and details the major differences seen between them. Where possible explanations are given for the results and differences observed.

5.5.1 Impact

The impact values for unfilled PBT were 50% higher than for unfilled HIPS. The reduction caused by the majority of the FR additions used was greater for the PBT compounds than HIPS compounds. This meant that for HIPS and PBT compounds containing similar loading levels, peak and failure energy values were closer than unfilled HIPS and PBT. This effect was due to a reduction in plastic deformation caused by the additives, which was much larger for filled PBTR compounds compared to filled HIPS compounds.

The influence of Sb_2O_3 particle size was similar for both PBT and HIPS compounds. The major differences in effect seen were for the smallest Sb_2O_3, which had no effect on HIPS but caused the greatest reduction in PBT. Although effects caused by dilution and void formation were significant for both polymers, the major energy absorbing mechanism in HIPS was by crazing. The influence of FR additive size and morphology on the ability of HIPS to form crazes was the causes of many of the differences seen between additives at similar loading levels. PBT does not craze during failure, which also explains many of the differences seen between the two types of compounds.

The effects of FR additive loading level on both peak and failure energy of HIPS and PBT compounds, were similar, with large initial reductions in peak and failure energy, and further smaller reductions with loading levels beyond 20wt.%. However, the reduction in peak and failure energy caused by the FR additives was greater for PBT than HIPS. For unfilled PBT the failure energy was $\approx6J$ compared to HIPS at $\approx4.5J$. At the highest loading levels, values for failure energy were between 1 and 2J for both HIPS and PBT compounds.

These results show that although the trends are the same for the FR additives used they have a greater effect on PBT, over the loading level range used than on HIPS. Authors have shown [33,34,55] that the dilution of tough polymers by less tough additives will reduce impact properties and PBT is more sensitive to this than HIPS. Also as stated early HIPS absorbs energy during failure by crazing. It has been shown that some of the FR additives can increase crazing within HIPS, or are less detrimental than other additives. Therefore the ability of HIPS to craze and the effect of FR additives on crazing means it is less sensitive under impact loads to the FR additives.

5.5.2 Tensile

For both HIPS and PBT compounds, the major effect seen when FR are added is in the strain at break values. For both HIPS and PBT compounds, as the loading level increased, the strain to break decreased. In PBT this was a much more significant effect than for HIPS. For PBT compounds at the highest loading levels used there was no plastic deformation observed before failure. For HIPS compounds, although reductions were seen, it did not affect the yield properties seen. Several authors have reported that in rubber toughened polymers such as HIPS the amount of filler or additive required to cause a ductile to brittle transition is higher than in other non-rubber toughened polymers [107,117,119]. It is therefore likely that if the loading level were increased further in HIPS a transition from ductile to brittle failure would be seen, similar to that for PBT.

For both HIPS and PBT compounds the effect on both Young's modulus and maximum stress were minimal. Small increases in Young's modulus were seen for the filled compounds, but this seemed independent of loading level or the type of additive used. The reductions at high loading levels for maximum tensile stress values, seen for PBT compounds, were cause by a transition from ductile to brittle fracture (discussed in section 5.2.8), which did not happen in the HIPS compounds at the loading levels used.

5.5.4 Flame Retardancy

With no FR additives present both HIPS and PBT fail UL94 tests and have low LOI values. The addition of BFR and Sb_2O_3 increases UL94 results to V0 and causes large increases in LOI. Although similar amounts of both Sb_2O_3 and BFR compounds were used in HIPS and PBT, the difference in bromine contents between the DBDPO used in HIPS and the Tetrabromobisphenol A compounds used in PBT means that a 3:1 ratio of Br/Sb_2O_3 was required in HIPS, but only 2:1 in PBT. Also HIPS was sensitive to small variations in either Sb_2O_3 or DBDPO loading level, which caused significant reductions in UL94 results. The PBT compounds did not seem to be affected as significantly by small variation in the FR additives as HIPS. This is most likely caused by PBT being more naturally flame retardant than HIPS, which is evidenced by the higher LOI value.

6.0 Conclusions

The following conclusions can be made from this work: -

- The bromine content of all the BFRs was lower than the literature indicted. The Tetrabromobisphenol A compounds had lower amounts of bromine on the surface than the bulk. From DSC analysis no evidence of melting was seen for any the Tetrabromobisphenol A compounds although T_g temperatures were present.

- Using a twin screw extruder all of the dry powder additions of the FR additives were well dispersed within both the HIPS and PBT matrixes. The FR additives always located themselves in the PS phases of the HIPS compounds.

- The shear viscosity of the HIPS compounds was not affected by the addition of either Sb_2O_3 or BFR at loading levels from 0 to 32wt.%.

- The shear viscosity of PBT was affected by both Tetrabromobisphenol A loading level and compound type. All the filled compounds had higher shear viscosities than unfilled PBT, and these differences were greater at low shear rates. The Tetrabromobisphenol A compounds with either more end groups, or those with more polar end groups, had most influence on the viscosity increase.

- The molecular weight of the PBT compounds was unaffected by either Tetrabromobisphenol A loading level or compound type.

- As Sb_2O_3 particle size decreased it caused was increasing reduction in impact properties of PBT. There was a logarithmic relationship between Sb_2O_3 particle size and impact failure energy.

- In HIPS the effects of FR additives on impact properties at loading levels below 5wt.% were mixed. Above this loading levels reductions compared to unfilled HIPS were seen for all the FR additives used. The additives with the larger particles sizes caused less of a reduction at comparable loading levels than smaller particles.

- As the loading level of all the FR additives used, increased from ≈5 to ≈20wt.%, in both HIPS and PBT impact properties decreased significantly. Above this loading level there was little further change.

- The Fracture toughness (K_c) of both PBT and HIPS was reduced for all loading levels of FR additives used. There was no correlation between loading level or Sb_2O_3 type and these reductions.

- The addition of FR additives significantly reduced the ability of both HIPS and PBT to plastically deform, whilst having little or no effect on elastic deformation.

- The addition of FR additives to both HIPS and PBT caused a reduction in the tensile strain at break. As the loading level increased so did the reductions. For PBT compounds a transition from ductile to brittle failure type occurred. At the loading levels used this was not seen in the HIPS compounds.

- None of the additives used caused a significant change in Young's modulus or maximum tensile stress at the loading level used.

- Both the unfilled HIPS and PBT ignited and burnt with ease, and exhibited substantial dripping once ignited. The additions of BFR/Sb_2O_3 combinations at loading levels of ≈15wt.% substantially increased the flame retardancy, with both HIPS and PBT obtaining UL94 V0 rating and much higher LOI values. The fire performance of HIPS was sensitive to small variations in both Sb_2O_3 and BFR. content caused by feeding during processing. This effect was not seen in PBT.

- The FR additives caused changes in the topology of HIPS fracture surfaces. As the loading level of the FR increased the surface roughness of the fracture surfaces increased.

- The use of Stereon impact modifier in HIPS compounds containing DBDPO and Sb_2O_3 increased impact failure energy at all loading levels used, but reduced peak energy, which was greatest at high loading levels. Stereon impact modifier caused a reduction in flame retardancy as the loading level increased, primarily due to increased dripping.

- The morphology of the Stereon changed, from small discreet particles to a continuous phase within the PS, as the loading level increased. There appeared to be no blending between the Stereon impact modifier and the primary rubber phase.

- The dispersion of the Sb_2O_3 and BFR in the Fyrebloc masterbatches was poor, with large local variations present.

- The use of Fyrebloc masterbatches in HIPS compounds aided dispersion when using the direct injection moulding route. This caused improvements in impact properties, compared to direct BFR/Sb_2O_3 additions, but did not affect the UL94 results.

- Both the BFR and Sb_2O_3 caused greater reductions in properties including impact and tensile strain at break in PBT than HIPS. Typically, at loading levels of ≈ 30wt.% FR additive, reductions of 80% were seen for PBT and 65% for HIPS, for impact properties. Therefore it is important to experimentally evaluate the effects for each polymer system, using BFR and Sb_2O_3, to determine and interactions.

7.0 Future Work

There are several areas of interest, which would justify further work. The formulations using the Fyrebloc materials in HIPS could be re-compound, after obtaining new Fyrebloc materials with more consistent Sb_2O_3 and BFR loading levels. This would allow for better comparison between the use of twin screw extrusion and the direct injection moulding route and to determine any beneficial affects due to better dispersion from the use of the Fyrebloc materials.

The use of masterbatched BFR/Sb_2O_3 could also be investigated in PBT formulations. These could use carriers such as Dupont Elvaloy® PTW which is an ethylene copolymer. This material is designed as an impact modifier and should aid dispersion of fillers and additives within polymers such as PBT. Also the possible use of other suitable Fyrebloc material in PBT could be investigated. These would include using Fyrebloc 510, as this has BC52 as the bromine compound, but possibly also new mixtures using other grades of BFR and Sb_2O_3.

None of the Tetrabromobisphenol A compounds were melt belendable in PBT. Therefore other BFR could be experimented with to determine if any of these are melt blendable and any possible benefits that this may have on properties of PBT compared to the non-melt blenable grades.

Flame retardant PBT is often glass fibre reinforced, the effects that the glass fibres have on fracture properties when used with the FR additives could be determined. The use of BFR and antimony compounds could be investigated in other polymers systems such as PET, this would be an obvious choice as it is chemically very similar to PBT.

References

1   G.L. Nelson, Fire and polymers II, 1995, ISBN 0-8412-3231-8

2   Protecting Lives & Property, The case for flame retardants, March 1997, The european flame retardants association.

3   D. Bliss, Fire Performance of IT equipment studied in the furniture calorimeter, Interflam 2001.

4   An open letter from the national association of state fire marshals to those who make, sell and buy computer equipment, USA.

5   I.C. Van Nuffel and R.Vaneeckhoutte, Influence of moulded in stresses in on buring behaviour of HIPS, Flame Retardants 94, pp 143-154.

6   J. Hietaniemi, Fires originating from electric household appliances: an experimental and simulations study, Interflam 2001, pp977-988

7   Bromine frequently asked questions, produced by Bromine science and environmental forum (BSEF)

8   Notes from PhD Review Meeting Minutes Held on 11-2-00

9   G. Smith, Determination of antimony in antimony ores

10   GE Plastics, Product Information, Valox 325F

11   Watson, L.K., O'Callaghan, M.P., Halogenated Organic Compounds Determination of Total Bromine (Schoniger Flask Method), Great Lakes Chemical Corporation Analytical Method, p1-5 (1982)

12   British standard BS EN ISO 179 1997: Plastics- determination of Charpy impact strength

13   C.B. Bucknall, Toughened Plastics, London Applied science publishers 1977, ISBN 08533469x.

14   Enter a new crop of enhanced HIPS, Plastics Technology, Vol. 6, 1993, pp 25-27

15   M.DE.Poortere, C. Schonbach and M. Simonson, The fire safety of TV set enclosure materials a survey of european statistics, Fire and materials 24, 2000, pp 53-60.

16   M. Ahmed, Colouring of Plastics, Van nostrand reinhold co., New York, 1979.

17   L. Bottenbruch, Polycarbonates polyacetals polyesters cellulose esters, Hanser

Publishers 1996, ISBN 3-44-6-17473-7.

18   O. Olabisi, The handbook of thermoplastics, Marcel Dekker 1997, ISBN 0824797973.

19   Polybutylene terephthalate, applications abound in PBT, but capacity steadies price, Modern Plastics International, 1999, Vol 1, pp 59.

20   Michell. E.W.J, Morley J.C, Antimony Oxide and its Derivatives

21   Principles of flame-retardancy and test methods, Anzon technical memorandum 1&2

22   J. Brydon, Plastics Materials, London Butterworth scientific, Sixth Edition, 1995, ISBN 0750618647.

23   T.C. Bouton and D.V. Brock, Impact modifiers for the flame retardant HIPS, ANTEC producing, 1981, pp 826-828

24   P. Svec, L. Rosik, Z. Horak, F. Veceka, Styrene-based plastics and their modification, 1989, ISBN 0-13-682485-4

25   A.M. Donald, E.J. Kramer, Internal structure of rubber particles and craze break-down in high impact polystyrene (HIPS), Journal of Materials Science,1982, pp 2351-2358.

26   S. Wu, Phase structure and adhesion in polymer blends: A criterion for rubber toughening, Polymer, vol. 26, pp1855-1862.

27   M. Parvin and J.G. Williams, The effect of temperature on the fracture of rubber modified polystyrene, Journal of Material Science, 1976 vol. 2045-2050.

28   M. Baer, Studies on heterogeneous polymeric systems. I. Influence of morphology on mechanical properties, Journal of Applied Polymer Science, 1972, vol. 16, pp 1109-1123.

29   H. Keskkula, M. Schwarz and D.R. Paul, Examination of failure in rubber toughened polystyrene, Polymer 1986, vol 27 pp 221-215,

30   A. M. da Silva and R. Borggreve, The effect of rubber properties on the mode of deformation in rubber modified polystyrene, Polymer 1976, vol 17 pp 107-112,

31   T.T. Wang, M. Matsuo and T.K. Kwei, Criteria of craze initiation in glassy polymer, Journal of Applies Physics, October 1971,vol. 42, pp 4188-4196.

32   O.K. Spurr, and W.D Niegisch, Stress crazing of some amorphous thermoplastics, Journal of Applied Polymer Science, 1962, vol. 11, pp585-599.

33   M. Matsuo, T.T. Wang and T.K. Kwei, Crazing of polystyrene containing two rubber ball: A model for ABS plastics, Journal of Polymer Science: part A, 1972 vol. 10, pp 1085-1095

34   S. Wu, Impact fracture mechanisms in polymer blends: Rubber-toughened nylon, Journal of Polymer Science, 1983, vol. 21, pp 699-716.

35   C.B. Bucknall and R.R Smith, Stress-whitening in high-impact polystyrenes, Polymer Vol. 6, 1965, pp 437-446.

36   A.V. Antonov, R.M. Gitna and S.N. Novikov, The action of high molecular weight bromine containing flame retardants in styrene plastics. Polymer science 1990, vol 32, no 9 pp 1809-1815

37   J.C. Gill, Brominated polystyrene flame retardants: A step forward. Plastics compounding September/October 1989.

38   PhD Review meeting minutes held on 11-2-00, Loughborough university.

39   GE Plastics product information, 2000, Valox 325F.

40   Anzon Ltd. Technical memorandum 3 –10, 1995

41   C.B. Bucknall, C.A. Correa, V.L.P Soares and X.C. Zhang, Role of rubber particles in toughened polystyrene, Polymer Science 1981, vol 25, no 9 pp 107-112

42   Anzon Ltd. Technical memorandum 3 –10, 1995

43   D.L. Mcallister, Brominated flame retardants: current issues and future prospects. Journal of Material Science, 1986, pp 1956-1962.

44   I. Narisawa, Fracture toughness of crystalline polymer solids, Polymer Engineering and Science, January 1987, Vol. 27, No 1, pp 41-45.

45   F.A Pettigrew, J.S. Reed and L. Van Wabeeke, Ethyl Corporation, Flame Retardants 94, pp 155-161

46   S.R. Owen, Antimony trioxide compounds for flame retardant ABS polymers, Loughborough university PhD thesis, 1998.

47   R. Seddon, Influence of flame retardant additives on the processing

characteristics and physical properties of ABS, Loughborough university thesis, 2000.

48   E.B. Rabinovitch, E. Lacatus and J.W. Summers, The Lubrication mechanism of calcium stearate/paraffin wax systems in PVC compounds, vol. 6, September 1984, pp 98-103

49   S. White and A. Docherty, Flame Retardants technical service report, ref AD 2316. The effect of particle size of Sb_2O_3 on the flammability and impact of UPVC, HIPS and ABS, GLCC internal report, February 1994.

50   B.V. Smith, D.K. Wiseman and E.H. Crook, Development of impact modified flame retardant PBT formulations, Journal of Vinyl & Additive Technology, March 1995, vol 1 no. 1.

51   M.Y. Boluk, and H.P Schreiber, Interfacial interactions and properties of filled polymers II: Dispersion of filler particles, Polymer Composites, august 1989, vol 10, No 4.

52   B. Turcanyi, B. Pukanszky, F. Tudos, Compostion dependence of tensile yield stress in filled polymers, Journal of Materials Science letters 7, 1998 pp 160-162

53   G. Pritchard, Plastics additives, Chapman & Hall publisher, 1998, ISBN 0-412-72720-X.

54   J. Murphy, Additives for plastics handbook, Elsevier science Ltd publisher, 1996, ISBN 185617 281 3.

55   G. Wypych, Fillers, Chemtec publishing, 1983, ISBN 1-895198-02-X.

56   D.M. Bigg, Interrelation among feedstock form product requirements, equipment type, and operating parameters in polymers mixing processes, Polymer Plastics and engineering 23, 1984, pp. 134-167.

57   Y. Suestsugu, State of dispersion-Mechanical properties correlation in small particle filled polymer composites, International Polymer Processing, 1990, pp. 184-190.

58   L. E. Nielsen, Simple theory of stress-strain properties of filled polymers, Journal of Applied Polymer Science, 1966, Vol 10 pp 97-103.

59   M. Bramuzzo, A. Savadori and D. Bacci, Polypropylene composites: fracture analysis of impact strength, Polymer Composites, January 1985 vol. 6, pp 1-7.

60   D.m. Bigg, Mechanical properties of particulate filled polymers, Polymer

Composites, April 1987 vol. 8 pp115-122.

61   T.J. Hutley and M.W. Darlington, Impact strength-d.s.c. correlation in mineral filled polypropylene, Polymer Communications August 1984 Vol. 25.

62   T.J. Hutley and M.W. Darlington, Further observations on impact strength-d.s.c. correlation in mineral filled polypropylene, Polymer Communications September 1985 Vol. 26.

63   S. Miyata, T. Imanashi and H. Anabuki, Fire-Retarding polypropylene with magnesium hydroxide, Journal of Applied Polymer Science, 1980 Vol 25, pp 415-425.

64   Q. Fu and G. Wang, Polyethylene toughened by rigid inorganic particles, Polymer Engineering and Science, January 1992 vol 32, pp94-97.

65   M. Rink, T. Ricco, W. Lubert and A Pavan, Force- displacement evaluation of macromoleclar materials in flexural impact tests. Influence of rubber content, degree of grafting and temperature on the impact behaviour of ABS resins, Journal of Applied Polymer Science, 1978, Vol 22 pp 429-443.

66   C.L. Raymond, Coatings for magnesium hydroxide fillers in polyethylene compounds, Loughborough university PhD thesis 1997.

67   R.J. Young, Failure of brittle polymer by slow crack growth, Journal of Material Science 12, 1977, pp 684-692.

68   J. Lee, A.F. Yee, role of inherent matrix toughness on fracture of glass bead filled epoxies, Polymer 41, 2000, pp 8375-8385

69   S.F. Mudrich, J.W. Wilchester, the influence of molecular weight on crack growth resistance in polycarbonate resin, Antec 94, pp 3251-3254

70   K. Friedrich and U.A. Karsch, Failure processes in particulate filled polypropylene, Journal of Materials Science, vol. 16, 1981, pp 2167-2175.

71   G.C. Richardson and J.A. Sauer, Effect of reinforcement type on the mechanical properties of polypropylene composites, Polymer Engineering and Science, vol. 16, April 1976, pp 252-256.

73   F. Ramsteiner and R. Theysohn, On the tensile behaviour of filled composites, Composites, vol. 15, no. 2, April 1984.

74   J. Jancar, J. Kucera and P. Vesely, Peculiarties of mechanical response of heavily filled polypropylene composites part 1 elastic modulus, Journal of

Material Science 26, 1991, pp 4878-4882.

75   J. Jancar, J. Kucera and P. Vesely, Peculiarties of mechanical response of heavily filled polypropylene composites part 2, dynamic mechanical moduli, Journal of Material Science 26, 1991, pp 4883-4887.

76   J. Jancar, Influence of filler particle shape on elastic moduli of PP/CaCO$_3$ and PP/Mg(OH)$_2$ composites, Journal of Material Science 24, 1989, pp 3947-3955.

77   M. Sumita, Y.Tsukumo, K. Miyasaka and K. Ishikawa, Tensile yield stress of polypropylene composites filled with ultrafine particles, Journal of Materials Science 18, 1983, pp 1758-1764.

78   L. Nicolais and M. Narkis, Stress-strain of styrene-acrylonitrile/glass bead composites in the glassy region, Polymer Engineering and Science, May 1971, vol 11, no 3.

79   F. Danusso and G. Tieghi, Strenght versus composition of rigid matrix particulate composites, Polymer, 1986 vol 27, pp 1385-1390.

80   J.P. trotignon, L. Demdoum and J. Verdu, Effect of mineral fillers in low concentrations on the mechanical properties of polymeric materials. Part 1, Composites vol 23 September 1992, pp 313-318

81   J.P. trotignon, L. Demdoum and J. Verdu, Effect of mineral fillers in low concentrations on the mechanical properties of polymeric materials. Part 2, Composites vol 23 September 1992, pp 319-325.

82   M. Sumita, Y. Tsukumo, K. Miyasaka and K. Ishikawa, Tensile yield stress of polypropylene composites filled with ultrafine particles, Journal of Material Science, 1983 vol 18, pp 1758-1764.

83   K. Mitsuishi, S.Ueno, S. Kodama and H. Kawasaki, Crystallization behaviour of polypropylene filled with surface-modified calcium carbonate, Journal of Applied Polymer Science, vol. 43, 1991, pp 2043-2049.

84   J. Troitzsch, Plastics flammability handbook, 1982, ISBN 3-446-13571-5

85   C.P. Yang and B.S. Sheen, Effect of tetrabromobisphenol A didllyl ether on the flame retardnacy of high impact polystyrene, Journal of Applied Polymer Science, 1989, vol 37, pp 3185-3194.

86   R.L. Markezich, R. Mundhenke and D.G. Aschbacher. Use of chlorinated flame retardants in combination with other flame retardants, Flame retardants

94, pp 203-211.

87   GLCC, Interoffice Memorandum, DE-83R Controls in HCC-333 HIPS

88   Personnel report on tilted `Report on high temperature gel permeation chromatography (HTGPC)`, carried out by RAPRA, April 2002.

89   Williams, J.G, A Linear Elastic Fracture Mechanics (LEFM) Standard For Determining K_C And G_C For Plastics (1990).

90   BS 2782, Plastics, Method 321 Determination of Tensile Properties. General Principles.

91   UL94, Standard for Flammability of Plastics Materials for Parts in Devices and Appliances, January 24, 1980.

92   Plastics Determination of Burning behaviour by Oxygen Index- Party 1: Guidance.

93   Plastics Determination of Burning behaviour by Oxygen Index- Party 2: Ambient temperature test.

94   H. Keskkula, M. Schwarz and D.R. Paul, Examination of failure in rubber toughened polystyrene, Polymer, February 1986 Vol. 27, pp 211-216.

95   C.B Bucknall, P. Davies and I.K. Partridge, Part 10 Effect of rubber particle volume fraction on the kinetics of yielding in HIPS, Journal of Materials Science 21 (1986) pp 307-313.

96   Minutes of PhD review Meeting Held at Loughborough University on 11-2-00

97   S. Devine, Internal Anzon company report `sturure of dry powder Azub`, 1998.

98   Miller, S., Donovan, J., MacKnight, W., Kambour, R., Toughness Enhancement Through Conversion of Cyclic Polybutylene Terephalate to Linear PBT, Journal of Applied Polymer Science vol 47, 1999 pp 779-790.

99   Notes from PhD Review Meeting Minutes Held on 31-7-01

100   S.N.Maiti and P.K.Mahapatro, Crystallization of PP in PP/Ni composites and its correlation with Tensile Properties, Journal of Applied Polymer Science vol 37, 1989 pp 1889-18899.

101   Great Lakes Chemical Corporation, Technical Information for Tetrabromobisphenol A BC52, www.greatlakeschem.com

102   Great Lakes Chemical Corporation, Technical Information for Tetrabromobisphenol A BC52HP, www.greatlakeschem.com

103   Great Lakes Chemical Corporation, Technical Information for Tetrabromobisphenol A BC58, www.greatlakeschem.com

104   Personnel communication with S. Warrington, 8-6-02

105   S.N.Maiti and B.H.Lopez, Tensile properties of polypropylene/Kaolin composites, Journal of Applied Polymer Science, Vol 44, 1992, pp 353-360

106   P.R. Hornsby and A. Mthupha, Rheological characterization of polypropylene filled with magnesium hydroxide, Journal of Material Science 29, 1994, pp 5293-5301.

107   F.N. Cogswell, Polymer Melt Rheology, A guide for industrial practice, 1981, ISBN 1855731983

108   A.V. Shenoy, Rheology of filled polymer systems, 1999, ISBN 0412831007

109   Personnel email from Greatlakes Chemical corporation,

110   P. Bajaj, N.K. Jha and R.K. Jha, effect of titanate coupling agent on mechanical properties of mica filled polypropylene, Polymer Engineering and Science, April 1989 vol 29, pp 557-563

111   T.L Wong, C.M.F. Barry and S.A Orroth, The effects of filler size on the properties of thermoplastics polyolefin blends, Journal of vinyl & additives technology, December 1999, vol 5, pp 235-240.

112   L. Jilken, The effect of mineral fillers on impact and tensile properties of polypropylene, Polymer Testing 10, 1991, pp 329-344.

113   Ampacet-Flame retardants, company information, www.ampact.com

114   N.S.Enikolopyan, M.L.Fridman, I.O. Stalnova, V.L. Popov, Filled polymers: mechanical properties and processability, Advances in polymer science 1996, Filled Polymers I, Springer-verlaig Berloin 1990.

115   C.B Bucknall, P. Davies and I.K. Partridge, Part 9 Effect of rubber particle volume fraction on deformation in HIPS, Journal of Materials Science 21 (1986) pp 301-306.

116   H.J Ludwig and P. Eyerer, Influence of the processing conditions on morphology and deformation behaviour of poly(butylene terephthalate) (PBT), Polymer Engineering and Science, February 1988, Vol. 28, No 3, pp 143-146.

117   I. Pillin, S. Pimbert, J.F. Feller and G. Levesque, Crystallization Kinetics of poly(butylene terephthalate) (PBT): Influence of additives and free carboxylic

acid chain ends, Polymer Engineering and Science, February 2001, Vol. 41, No 2, pp 178-191.

118   K. Bouma and R.J. Gaymans, Crystallisation of poly(ethylene terephthalate) and poly(butylene terephthalate) modified by diamides, Polymer Engineering and Science, March 2001, Vol. 41, No 3, pp 466-474.

119   C.D. Han, Van Den Weghe, P. Shete and J.R. Haw, Effects of coupling agents on the Rheological properties, processability, and mechanical properties of filled polypropylene.

120   K. Mitsuishi, S. Kodama and H. Kawasaki, Mechanical properties of polypropylene filled with calcium carbonate, Polymer Engineering and Science, 1985, pp 1069-1073.

121   G. Levita, A. Marchetti and A. Lazzeri, fracture of ultrafine calcium carbonate/polypropylene composites, polymer composites, 1989, pp 39-43

122   GLCC, Interoffice Memorandum, DE-83R Controls in HCC-333 HIPS

Appendix 1

COULTER LS   9:30 19 Dec 2000
File name: LIMS2987.S01

Group ID: LIMS2987
Sample ID: 4241-30-20 (DE83R)
Operator: AJA
Comments: DE83R
Comments: MSTOKES

From   0.375
To   2000
Volume 100.0
Mean: 6.062
Median: 4.873
D(3,2): 2.513
Mode: 5.878
S.D.:   4.778
C.V.:   78.82
% <
10   0.904
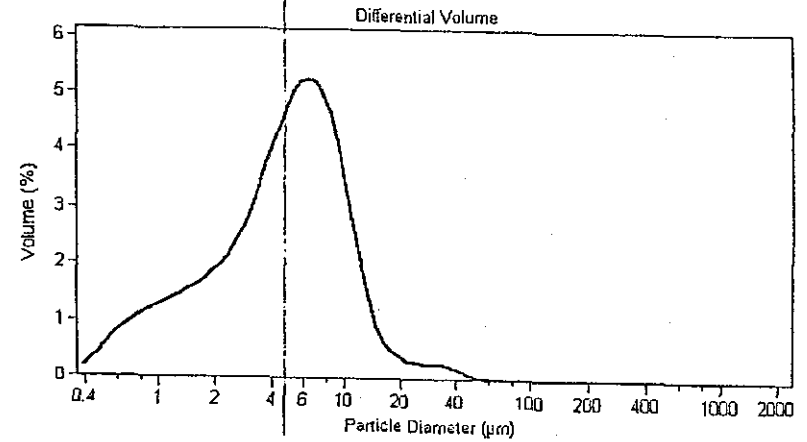50   4.873
90   13.09
99   20.28
99.9   24.54
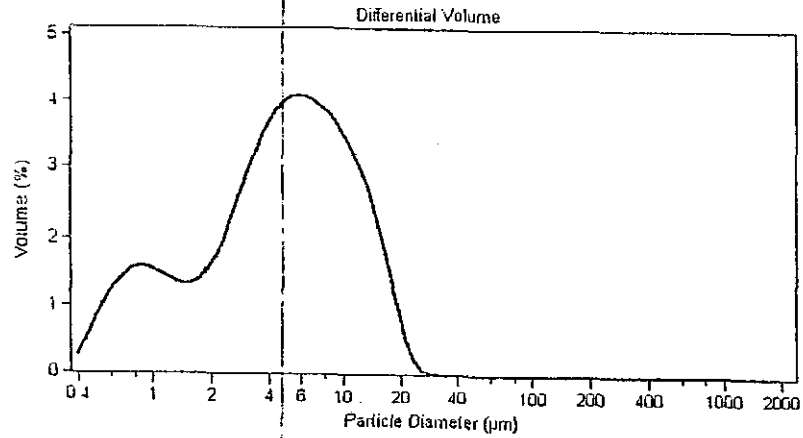
Unable to create OLE Object

COULTER LS   9:25 20 Dec 2000
File name: lims2989.S02

Group ID: LIMS2989
Sample ID: 4241-30-22. (Treatint. TT)
Operator: AJA
Comments: AO5
Comments: MSTOKES

From   0.375
To   2000
Volume 100.0
Mean: 5.993
Median: 4.988
D(3,2): 2.817
Mode: 6.452
S.D.:   5.269
C.V.:   87.92
% <
10   1.152
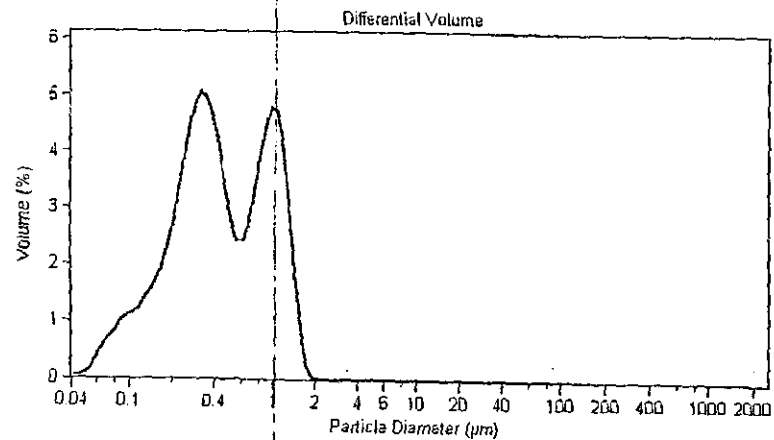50   4.988
90   11.09
99   29.88
99.9   45.31

Unable to create OLE Object

COULTER LS   9:26   9 Jan 2001
File name: lims2994.$01

Group ID: LIMS2994
Sample ID: 4241-30-27   (AOS (2))
Operator: AJA
Comments: AOS
Comments: MSTOKES

From   0.0400
To   2000
Volume 100.0
Mean: 0.554
Median: 0.407
D(3,2): 0.303
Mode: 0.326
S.D.:   0.391
C.V.:   70.51
% <
10   0.143
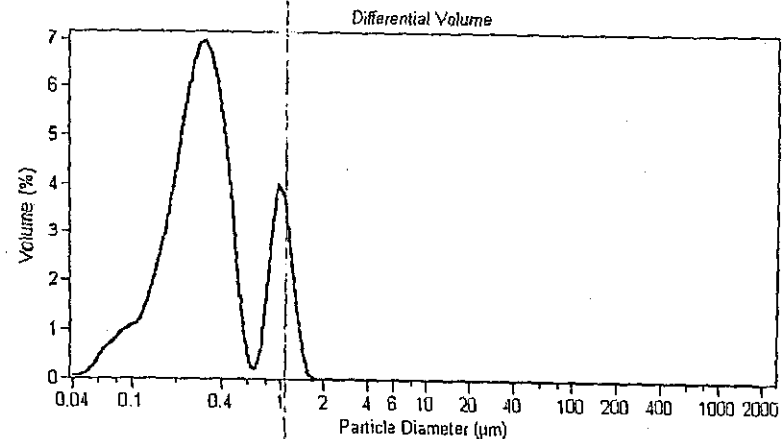50   0.407
90   1.156
99   1.544
99.9   1.793

Differential Volume

Unable to create OLE Object

COULTER LS   14:48   19 Dec 2000
File name: LIMS2993.$01

Group ID: LIMS2993
Sample ID: 4241-30-26   (AOS (1))
Operator: AJA
Comments: AOS
Comments: MSTOKES

From   0.0400
To   2000
Volume 100.0
Mean: 0.424
Median: 0.315
D(3,2): 0.258
Mode: 0.326
S.D.:   0.323
C.V.:   76.25
% <
10   0.139
50   0.315
90   1.012
99   1.353
99.9   1.528

Differential Volume

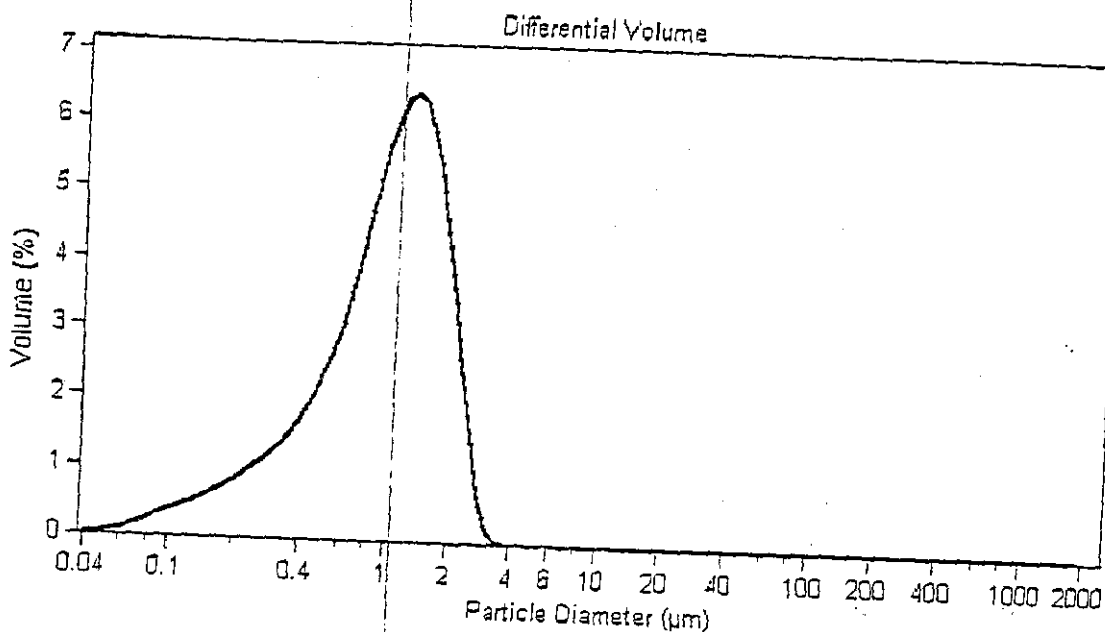Unable to create OLE Object

Great Lakes Chemical Corporation

COULTER LS   15:47 19 Dec 2000
File name: LIMS2990.S01

Group ID: LIMS2990
Sample ID: 4241-30-23 _(Racl Star)_
Operator: AJA
Comments: AO5
Comments: MSTOKES

From	0.0400
To	2000
Volume	100.0
Mean:	1.094
Median:	1.041
D(3,2):	0.607
Mode:	1.322
S.D.:	0.622
C.V.:	56.83

% <	
10	0.293
50	1.041
90	1.956
99	2.659
99.9	3.132

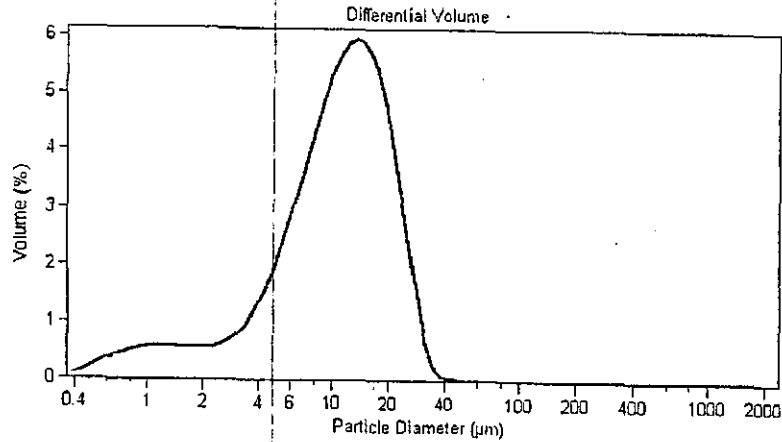Differential Volume

Unable to create OLE Object

COULTER LS   9:32 20 Dec 2000
File name: lims2991.$02

Group ID: LIMS2991
Sample ID: 4241-30-24 (RT (2))
Operator: AJA
Comments: AOS
Comments: MSTOKES

From   0.375
To   2000
Volume 100.0
Mean: 11.75
Median: 10.94
D(3,2): 5.371
Mode: 13.61
S.D.:   7.028
C.V.:   59.81
% <
10   2.796
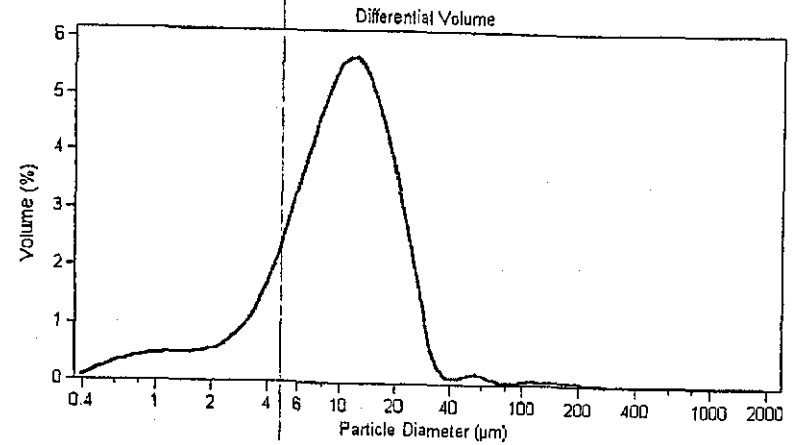50   10.94
90   21.59
99   30.02
99.9   35.63

Differential Volume

Unable to create OLE Object

COULTER LS   9:33 20 Dec 2000
File name: lims2992.$02

Group ID: LIMS2992
Sample ID: 4241-30-25
Operator: AJA
Comments: AOS (RT (1))
Comments: MSTOKES

From   0.375
To   2000
Volume 100.0
Mean: 11.94
Median: 10.12
D(3,2): 5.485
Mode: 12.40
S.D.:   11.36
C.V.:   95.19
% <
10   3.038
50   10.12
90   21.33
99   48.49
99.9   164.9

Differential Volume

Unable to create OLE Object

Appendix 2

Sample	Run No.	Mw	Mn	Polydispersity
PBT 8 - 6	D0927	83,400	51,300	1.6
(RTL0430 / 5)	D0930	83,800	50,400	1.7
PBT 8 - 7	D0928	85,900	52,900	1.6
(RTL0430 / 6)	D0931	84,700	52,500	1.6

Figure 1 below shows an overlay of the computed molecular weight distributions for duplicate runs of the six samples provided. Figures 2 to 6 compare sample "PBT 1-1" with the five remaining samples individually. The plots are all normalised with respect to area, the y-axis being a function of weight fraction.
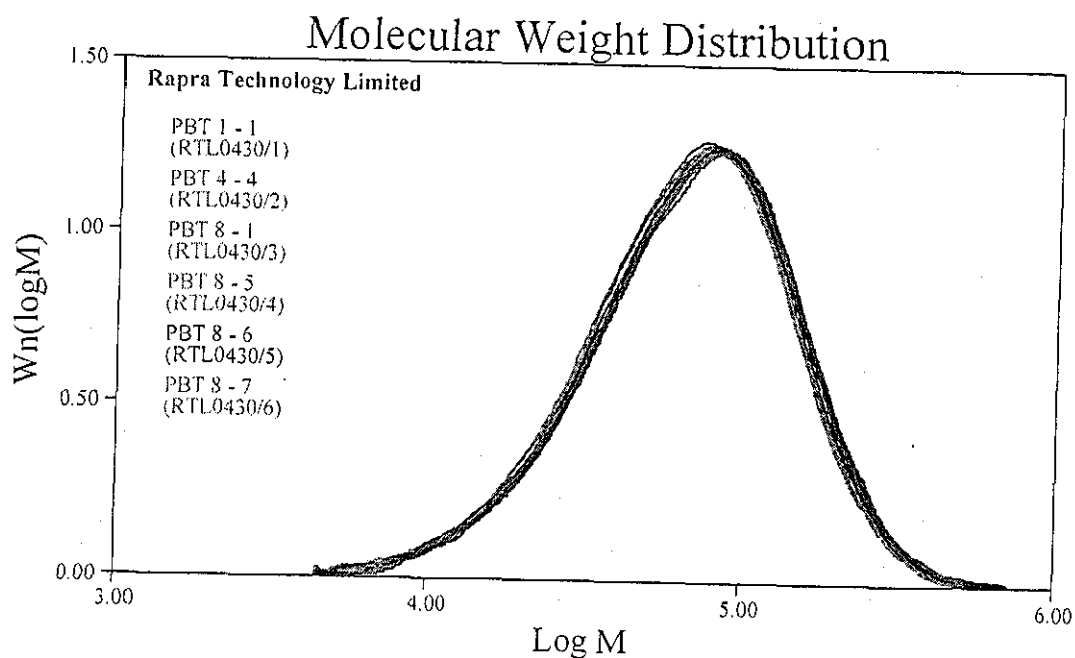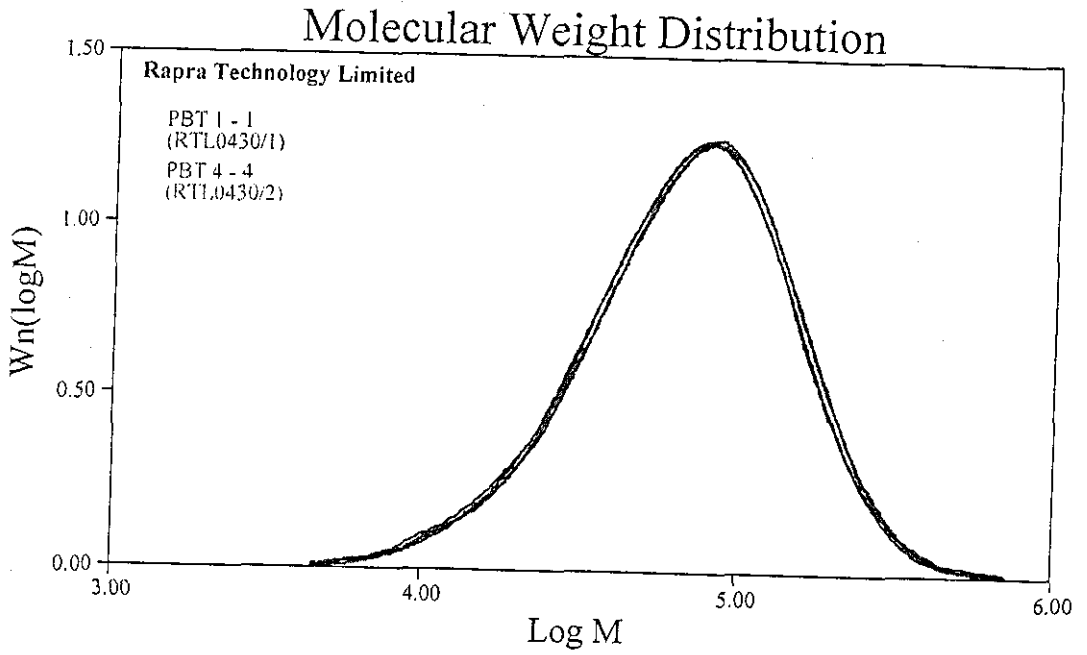

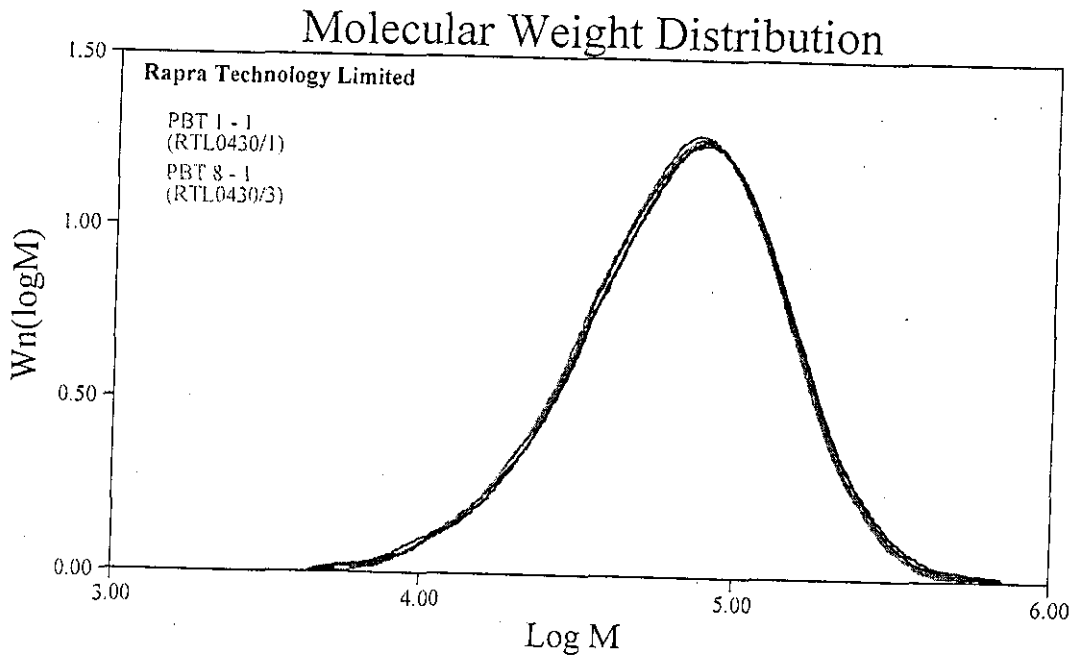## Molecular Weight Distribution

Rapra Technology Limited

PBT 1 - 1
(RTL0430/1)
PBT 4 - 4
(RTL0430/2)
PBT 8 - 1
(RTL0430/3)
PBT 8 - 3
(RTL0430/4)
PBT 8 - 6
(RTL0430/5)
PBT 8 - 7
(RTL0430/6)

Wn(logM)

Log M

Figure 1

Molecular Weight Distribution

Rapra Technology Limited

PBT 1 - 1
(RTL0430/1)
PBT 4 - 4
(RTL0430/2)

Figure 2

Molecular Weight Distribution

Rapra Technology Limited

PBT 1 - 1
(RTL0430/1)
PBT 8 - 1
(RTL0430/3)

Figure 3

Molecular Weight Distribution

Rapra Technology Limited

PBT 1 - 1
(RTL0430/1)
PBT 8 - 5
(RTL0430/4)

Figure 4

Molecular Weight Distribution

Rapra Technology Limited

PBT 1 - 1
(RTL0430/1)
PBT 8 - 6
(RTL0430/5)

Figure 5

Molecular Weight Distribution

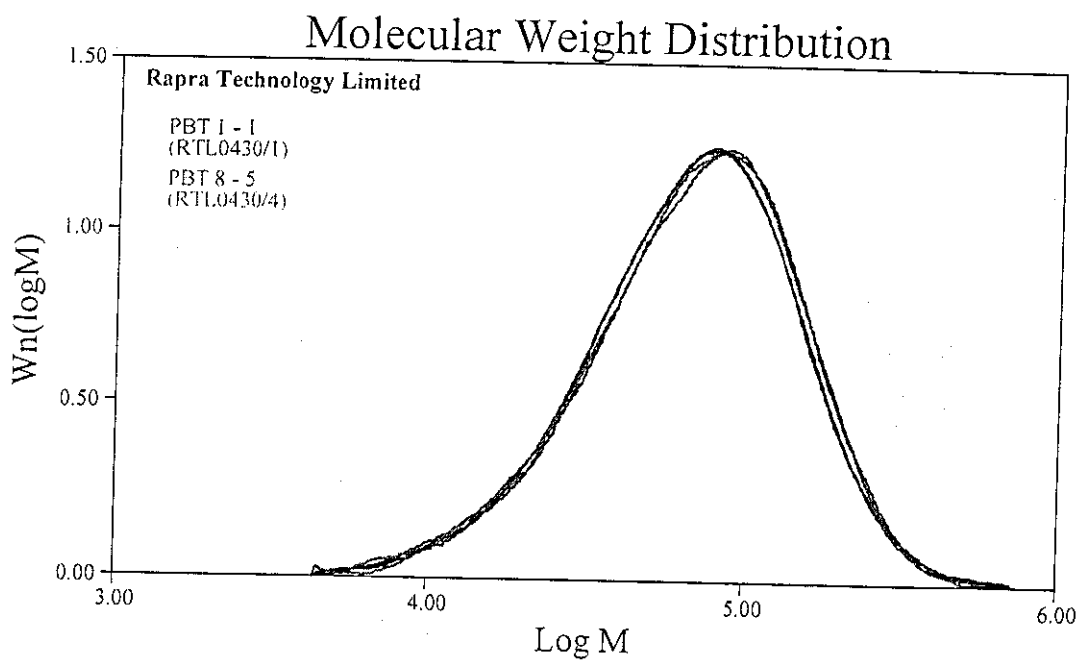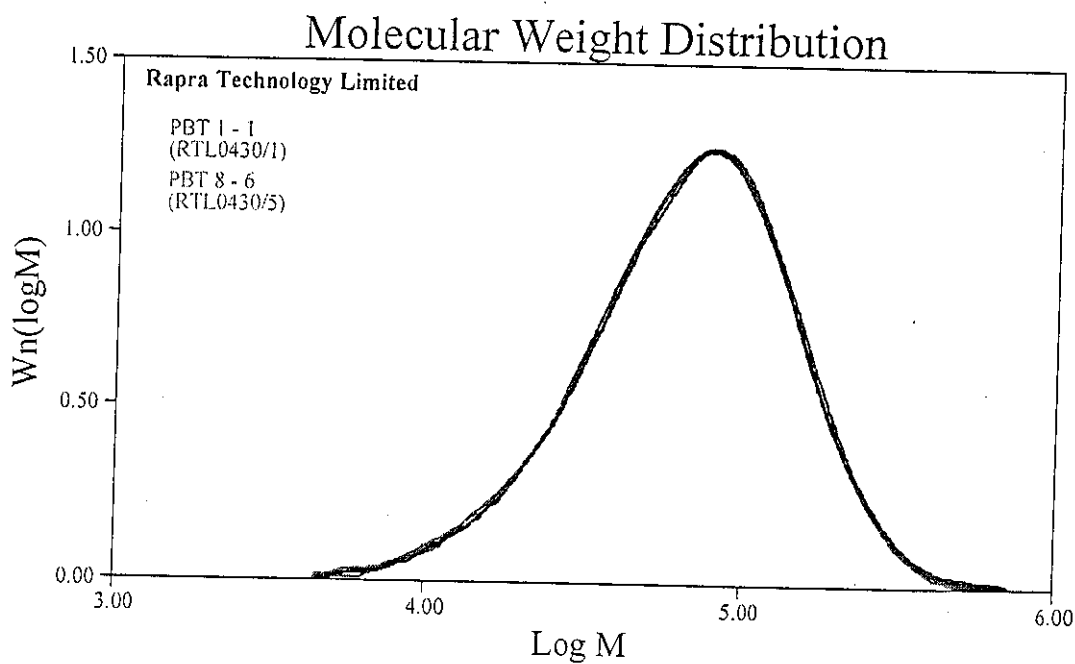Rapra Technology Limited
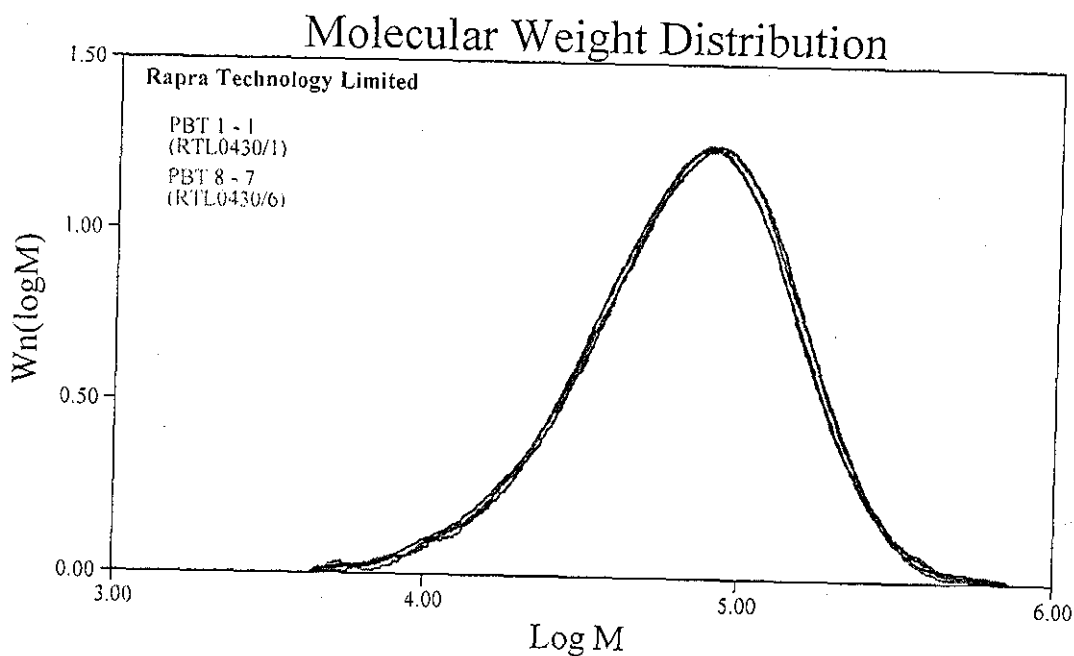
PBT 1 - 1
(RTL0430/1)
PBT 8 - 7
(RTL0430/6)

Figure 6

Comments

The molecular weight distributions of all six samples are very similar. Only small differences in the distributions and the calculated weight and number molecular weight averages can be seen.

The long-term reproducibility of a particular GPC system may not be good, so the technique is best regarded in a comparative manner, with the emphasis being placed on any observed differences between the samples and not simply on the numerical values of the results themselves.

Stephen Jones   Steve Holding
10th April 2002